STUDIES ON MECHANICS OF CHISEL TYPE SHARES IN DRY CLAY SOIL IN RELATION TO DESIGN OF DEEP TILLAGE TOOL

Thesis submitted inpart fulfilment of the requirements for the degree of Doctor of Philosophy (Agricultural Engineering) to the Tamil Nadu Agricultural University Coimbatore

by

D. MANOHAR JESUDAS M.Tech

DEPARTMENT OF FARM MACHINERY
COLLEGE OF AGRICULTURAL ENGINEERING
TAMIL NADU AGRICULTURAL UNIVERSITY
COIMBATORE - 641 003
1994

CERTIFICATE

This is to certify that the thesis entitled **STUDIES ON MECHANICS OF CHISEL TYPE SHARES IN DRY CLAY SOIL IN RELATION TO DESIGN OF DEEP TILLAGE TOOL** submitted in part fulfilment of the requirements for the award of the degree of **DOCTOR OF PHILOSOPHY** in **AGRICULTURAL ENGINEERING** to the Tamil Nadu Agricultural University, Coimbatore is a record of bona fide research work carrried out by Thiru. **D. MANOHAR JESUDAS** under my supervision and guidance and that no part of this thesis has been submitted for the award of any other degree, diploma, fellowship or similar titles or prizes and that the work has not been published in part or full in any scientific or popular journal or magazine.

Place: Coimbatore
Date : 20-7-1994

(Dr. M. BALASUBRAMANIAN)
CHAIRMAN

Approved by:

CHAIRMAN:

(Dr. M. BALASUBRAMANIAN)

MEMBERS:

7/12/94
(Prof. K.R. SWAMINATHAN)

(Dr. V.V. SREENARAYANAN)

(Dr. L. GOTHANDAPANI)

Date: 7.12.94

External Examiner:

7.12.94
(Dr.T.GURUSWAMY)

ACKNOWLEDGEMENTS

ACKNOWLEDGEMENTS

I feel extremely happy and priviieged to express my deep sense of sincere gratitude and indebtedness to Dr. M. Balasubramanian, Head, College of Agricultural Engineering and Chairman of the Advisory Committee for his valuable guidance, Constructive criticism, learned counsel, cordial treatment and constant encouragement throughout the course of this investigation and in the preparation of the thesis.

I am extremely grateful and record my indeptedness and thanks to Prof. K.R. Swaminathan, Professor of farm machinery and former Dean, College of Agricultural Engineering for his constant encouragement throughout the course of this investigation and valuable guidance as member of the Advisory Committee.

My sincere and warm thanks are due to Dr. V.V. Sreenarayanan and Dr. L. Gothandapani, members of Advisory Committee for their constant guidance.

My sincere thanks are due to Mr. T.V. Job and K. Rengasamy, Professors, Department of farm machinery. My sincere thanks are also due to colleagues C. Divakar Durairaj, V.J.F. Kumar and A. Surendra Kumar for their kind help during this study.

I owe immense thanks to all the staff of farm machinery workshop. The valuable help rendered by Mr. G. Samuel, Mr. A. Deivaraj, Mr. A. Balasundararaj, Mr. Paulraj, Mr. C.N. Muthuselvan, Mr. A. Subramanian and Mr. K. Arunachalam, shall always be remembered by me.

My thankful acknowledgement is due to the Tamil Nadu Agricultural University for permitting me to pursue the studies as a part-time student and providing necessary facilities required during the course of the investigation.

Grateful acknowledgements are made to Mr. S. Venkatesan, draftsman, for preparing all the drawings. My sincere thanks are due to M/s. STAPLES for formatting and printing the thesis.

I wish to thank Dr. P. Radhakrishnan, Professor, CAD/CAM centre, PSG College of Technology for valuable help in stress analysis work.

Thanks are due to Mr. M. Shankaranarayanan and other staff of Computer Centre for their help in data analysis and simulation.

I am happy to record the kind assistance provided by my friend Mr. R. Kalaimani in data analysis and computer graphics.

Finally I wish to place on record the prayers and encouragements of my wife A. Vanathi and children Nithia and Immanuel during the study period.

D. Ramakar Jouda

ABSTRACT

ABSTRACT

STUDIES ON MECHANICS OF CHISEL TYPE SHARES IN DRY CLAY SOIL IN RELATION TO DESIGN OF DEEP TILLAGE TOOL

By

D. MANOHAR JESUDAS

Degree : Ph.D. (Agricultural Engineering)

Chairman : Dr. M. Balasubramanian
Professor and Head
Department of Farm Machinery
Tamil Nadu Agricultural University
COIMBATORE - 641 003.

1994

Performance of shares of different geometries at different depths and speeds of operation were measured under dry clay loam soil conditions similar to those encountered during summer fallow tillage in Tamil Nadu. The experiments were conducted using instruments specially designed for the study. The behaviour of deep tillage tools under the same soil conditions was also predicted by using existing models. A tillage tool was designed and fabricated based on the results of the above study and its performance tested under field conditions.

A tractor mounted cone penetrometer, tillage dynamometer and furrow profile meter were specially developed for evaluating the performance of deep tillage tools and used for the experiments.

Fifteen shares with five levels of share width (20, 25, 30, 40 and 50 mm) and three levels of share length (100, 150 and 200 mm) were fabricated with a share lift angle of 20° and tested at five levels of depth and five levels of speeds. The forces on tool and furrow geometry created were measured. The physical properties of the experimental field was also measured.

The results of the field experiments showed that the longitudinal reaction of most shares at a depth of 35 cm and speed of 1 m/s varied between 778 kg and 1065 kg. The longitudinal reaction - depth relation was quadratic with the slope increasing from 22 kg/ cm at 12.5 cm depth to 45 kg/cm at 37.5 cm depth. The vertical reaction - depth relation was almost linear in the range of 15 to 25 cm depth of operation. The horizontal reaction-speed relation was almost linear with the slope varying from 115 kg/m/s, at 0.25-0.5 m/ s range, to 118 kg/m/s at 1.0 to 1.25 m/s range. The vertical reaction showed minimum variation with speed. The share width had significant influence on horizontal reaction only at depths greater than 35 cm and the horizontal reaction increased with share width. The horizontal reaction- share length relation favoured the selection of 150 mm long share to ensure minimum draft. The orientation and location of the resultant reaction showed similar pattern for almost all shares.

The influence of depth on furrow width was observed to be linear and the depth-furrow area relation was quadratic. Generalized equations relating dimensionless horizontal reaction, furrow width and furrow area terms with the share aspect ratio were developed. The generalized equations yielded good fit for the experimental data of all share geometries. From these equations the draft requirement per unit width of furrow for a 2 cm wide share working at a depth of 40 cm was predicted to be 13 kg/cm. The unit draft for the same conditions was 0.74 kg/cm^2.

The performance of shares were predicted through four different models viz., Godwin and Spoor (1977), McKyes and Ali (1977), Perumpral (1983) and Swick and Perumpral (1988) by using soil properties measured from experimental field. The predicted soil reaction - depth relation was similar to experimentally observed results. However, the models slightly under predicted the horizontal reaction. The predicted results showed that a share with 20° lift angle would perform with minimum draft requirement and would have sufficient penetration ability. The models considerably over predicted the furrow cross sectional area.

The geometry of share was optimised with width of 25 mm, length of 150 mm and share lift angle of 20°. A prototype chisel plough for deep tillage was designed based on the results of the study. A three dimensional framed structure with rectangular hollow sections was designed using ANSYS structural analysis package. The prototype was fabricated and tested under red soil and black soil conditions. The soft top soil under both field conditions resulted in excessive slippage of drive wheels. Under black soil conditions, the implement was operated up to a depth of 40 cm under III gear and under red soil conditions speeds up to IV gear were used by limiting the depth to 35 cm. The chisel plough developed would cost about Rs.5000/-. The cost of deep tillage would be Rs.265 per ha.

CONTENTS

LIST OF ANNEXURES

LIST OF TABLES

LIST OF FIGURES

LIST OF PLATES

INTRODUCTION

CHAPTER I
INTRODUCTION

Tillage is of vital importance to agriculture. It is as ancient as civilization and reference to tillage tools are found in Sumerian cuneiform writings dating back to 1700 B.C.

In tropical zones where rain-fed agriculture is practiced, tillage requirements are critical for ensuring a successful crop. The tillage operations must not only ensure proper soil environment for crop establishment and growth but also ensure conservation of moisture and prevention of soil loss. Hence sustainable agricultural production under tropical rain-fed conditions is possible only through adoption of scientific tillage practices.

1.1 Scenario of dry farming in India

India has a predominantly tropical climate and 93.13 million ha are rain-fed. These areas constitute 68.4 per cent of net area sown and they contribute 40 per cent of total food grain production. Tamil Nadu has 5.7 million ha of net area sown, of which 3.1 million ha are under rain-fed agriculture. Increase in food production from the present level of 177 million tonnes (1992-93) could be achieved only by significantly improving productivity under rain-fed areas. Hence evolving suitable cultivation practices for rain-fed areas will be of prime importance in the coming decade.

One of the reasons for the low yields in the existing system of dry farming is the failure to adopt scientific tillage practices. Earliest research works made during 1930s have recommended deep ploughing (> 25 cm) once in three years for improving intake and storage of precipitation in the dry lands (Kanitkar *et al.* 1968). Subsequent research works under All India Coordinated Research on Dry land Agriculture and by International Crop Research Institute for Semi Arid Tropics have proved that with proper tillage and other improved practices, there is scope for increasing productivity even to eight times the existing levels.

1.2 Summer fallow Tillage in Tamil Nadu

Tamil Nadu has large areas under medium to heavy clay soils which are generally classified as Red soils (Alfisols) and Black soils (Vertisols). These soils are susceptible to subsoil compaction. Deep tillage of these soils is done preferably when they are dry so that the compacted layers are shattered without any risk of compaction. These soils are usually clod forming soils with high draught requirement and are similar to those investigated by Hillel *et al* (1969) and Wolf and Luth (1979). The working loads on tillage elements is higher and narrower tools are required. The high draft requirement is the major constraint in adoption of deep tillage inthesеareas. The tractors popularly used in this region are in the 35-45 HP range and are unsuitable for operating existing deep tillage tools. Hence for adoption of deep tillage practices for summer fallow tillage in Tamil Nadu, suitable deep tillage tools with reduced draft requirement has to be developed.

1.3 Present status of Deep Tillage Research

Considerable research had been done to investigate the soil- machine-plant relationship under deep tillage systems. The investigations relating to soil-machine interaction have been mainly focused on the effect of tool geometry and operational parameters on soil reaction forces and soil disturbance under different soil conditions. The investigations under soil bin conditions have mainly focused on establishment of mechanism of soil failure by deep tillage tools. The field investigations using different designs of dynamometers were aimed at quantifying the tool forces for application in the design of the implements. The soil disturbance pattern also had been investigated in detail since the effect of the tillage operation would be significant, only if the tool can produce appreciable changes in the soil structure. Since most of the studies relate to temperate regions, the investigations have been done in soils that were tilled at higher moisture levels. Very little information is available regarding the performance of deep tillage tools operating in dry compacted clay soils similar to those encountered in Tamil Nadu during summer fallow tillage.

1.4 Present study

In this study, detailed investigations were done to determine the soil reaction and furrow geometry due to a deep tillage tool when tilling heavy clay soils at low moisture content. A clear understanding of thisphenomenonis essential to design an efficient tillage tool. However these soil specific informations are not available at present. Hence the following study was undertaken. Soil reaction and furrow geometry were measured for deep tillage tools of different geometries by varying the depth and speed of operation.

The soil reaction on the tool was measured and recorded using a specially constructed tractor mounted dynamometer with hydraulic force sensors. The initial soil condition was measured using a tractor mounted cone penetrometer designed to operate up to 0.5 m depth. The furrow profile was recorded by using a suitably designed furrow profilemeter.

The soil reaction on tools was also theoretically computed by using different models of soil-tool interaction proposed by Godwin and Spoor (1977), McKyes and Ali (1977), Perumpral *et al* (1983) and Swick and Perumpral (1988). The mechanical properties of soil under given field conditions were measured and used for the simulation.

The results of the investigations were used to optimise the configuration and design of a chisel type deep tillage tool. The prototype implement was fabricated. The performance of tractor-implement system during deep tillage using the implement was evaluated through suitable instrumentation. Based on these field performance results, the cost of operation for deep tillage using chisel plough was calculated and compared with conventional summer fallow tillage system.

1.5 Objectives

The following were the specific objectives of this study.

* Development of instrumentation for performance evaluation of deep tillage tools.
* To determine the effect of tool geometry and operational parameters on the effectiveness of deep working chisel type tools.
* Prediction of performance of chisel type deep tillage tools as influenced by tool geometry and operational parameters under given soil conditions.
* Design and fabrication of a deep tillage tool based on the results of the above investigations.
* Evaluation of performance of prototype implement under field conditions.

REVIEW OF LITERATURE

CHAPTER II
REVIEW OF LITERATURE

The soil-machine-plant interaction under deep tillage system had been investigated in detail by many researchers. However only limited investigations have been done regarding deep tillage of clay soils under semi-arid climate. The literatures related to development of a deep tillage tool for rain-fed agriculture are reviewed and presented in this chapter.

2.1 Deep Tillage under Rainfed Agriculture

Deep tillage which loosens the subsoil is mostly aimed at improving the performance of crop by improving the water intake, retention and transmission characteristics of the soil. As reported by Chaudhary *et al.* (1985) considerable variations exist in the desirable aspects of the soil due to subsoiling. These variations need to be viewed in the light of the statement by Professor Kuipers (1980) that "Tillage problems are very much dependent upon specific circumstances just as the research approaches for solving them".

2.1.1. Tillage under rain-fed agriculture

Nearly one-third of the worlds 1.4 billion cultivated hectares are semi-arid lands. According to Venkateswarlu (1987), about 70 per cent of the 143.8 million hectares of arable land in India depend entirely on natural precipitation.

Kanitker *et al*, (1968) while reviewing earlier efforts towards improved crop management in drylands described the Madras/Bombay/Deccan dry farming methods which among others included deep tillage (> 25 cm) once in three years for better intake and storage of precipitation. Venkateswarlu (1987) reviewed earlier works that recommended shallow tillage in light textured soils and deep tillage for heavy clay soils with hard pan, for improving crop yield under dry farming situations.

Wolf and Luth (1979) investigated the problem of tillage of clod-forming soils under semi-arid climate. According to him, 250 million hectares of land have potential clod-forming soils. The clod-forming soils were observed to have low organic content and thus were susceptible to compaction while wet during the previous crop season by tillage, planting, cultivating, spraying and harvesting activities. After being intensively dried during summer season, these soils were found to form large hard blocks of clods bounded by cracks. The strength of the soil mass was non uniform due to the presence of the cracks. These soils required deep tillage to break the hard pan and thereby improve water infiltration and storage and improve root penetration. Deep tillage also helped to mix soil, control weeds and control salinity. It was observed that primary tillage was frequently done when the moisture content was in the range of 4 to 10 per cent.They also observedthat since large portion of the clod-forming soils were in less developed countries, little research on tillage has been expended in these areas. Jones *et al* (1990) reportedthat dry land tillage practices should be aimed at conserving maximum amount of water during the non crop period and creating a seedbed that allows the crop to establish at the optimum time and use the available water supply effectively.They also enumerated the features of existing dry land tillage systems and factors that influence their selection.

2.1.2. Deep Tillage for moisture conservation

Experiments by Saveson and Lund (1958) showed that deep tillage by using mould board plough and sweeps had positive effect on soil water retention. In studies by Jensen and Sletten (1965) deep tillage increased the water intake during the period from 0.33 to 7.3 hr after beginning of water application by 103 per cent in Pullman clay loam. Musick and Dusek (1975) studied the effect of deep tillage in Pullman clay loam and found that deep tillage to 40 cm, increased storage efficiencies from 46.5 to 61.9 per cent. However, deep tillage to 60 and 80 cm decreased water storage efficiency due to deep percolation loss. Studies by Doty and Reicosky (1978) showed that chiseled plots retained more moisture in the root zone compared to conventionally ploughed plots. Negi

et al. (1980) observed that the amount of water available to plants at 0.3 m depth was twice as large in the subsoiled and rototilled plots as against the compacted untilled, ploughed and chiseled plots.

2.1.3. Effect of deep tillage on crop growth

Jones (1939) discussed the theory and practice of deep tillage and advocated deep tillage with increased application of humus to increase depth of root zone. He observed 100 per cent increase in yield of potato due to deep tillage Savesen and Lund (1958) concluded that yield response to deep tillage can be expected on light textured soils during moisture deficit years. Musick and Dusek (1975) observed that average yield of grain sorghum was increased from 3390 kg/ha to 5650 kg/ha by deep tillage. The yield response was higher at limiting water availability levels. The yield of sugarbeet was found to increase by 27 per cent by deep tillage to a depth of 40 cm. Doty and Reicosky (1978) studied the effect of chiseling to 38 cm depth as compared to the conventional ploughing to 15 cm depth on drought resistance under rain-fed and artificially imposed drought situations. When there was no water stress, chiseling increased the yield by about five per cent. However after 10, 20 and 30 consecutive days without rain, the yield difference were 25, 34 and 30 per cent,respectively. The moisture available in the chiseled soil was sufficient to supply water for atleast 8 to 24 days longer than conventionally ploughed soil. In experiments reported by Adeoye (1982) the yield of maize and cotton were found to increase by 10 per cent by deep tillage under tropical climate. Ide *et al.* (1984) observed that the removal of high resistance plough sole by subsoiling improved the yield of barley. This was associated with increased rooting depth, root density and enlargement of root zone. However, Rawitz *et al.* (1983) observed that basin tillage would be advantageous as compared to deep tillage to reduce runoff and improve infiltration. Chaudhary *et al.* (1987) observed that yield of maize was increased by 35 per cent at low and high levels of irrigation for an early sown crop and the yield increase was 47 per cent under low irrigation and 27 per cent under high irrigation for a late sown

crop. In a four season semi-arid tillage study by Willcocks (1981), mould board plough, sweeps, chisel, disc and precision strip tillage were compared. The yield from shallow tilled plots (0.1 m) were generally lower than that from deep tilled plots (0.2-0.3 m). Vittal *et al.* (1983) studied the effect of deep tillage to 23.3 cm using disc plough against shallow tillage to 15.5 cm using country plough in red soil of Andra Pradesh and found that the advantage due to deep tillage was dependent on rainfall pattern and plant type. Deep tillage was found to be beneficial for deep rooted crops when the rainfall was normal or above normal. Negi *et al.* (1980) investigated tillage by subsoilers, chisels and mould board ploughs under different levels of wheel traffic. Subsoiled plots were found to yield better than other tilled or compacted plots. Barber and Diaz (1992) studied soya yield over seven cropping seasons, 1985-1989. The percentage yield increase for subsoiling in 1985, disc ploughing in 1985 and annual subsoiling were compared with conventionally tilled plots and found to be 14, 19 and 25 per cent respectively. Wild *et al.* (1992) observed that in vertisols, structural degradation could be ameliorated by deep ripping and application of gypsum.

2.2 Instrumentation for deep Tillage Studies

The penetration resistance as measured by different designs of cone penetrometers had been extensively used by researchers to quantify the initial soil conditions and degree of loosening obtained by deep tillage tools. The forces encountered by tillage tools have been investigated by many designs of dynamometers under laboratory and field conditions. The cross section of the furrow loosened by deep tillage tools had been investigated by different designs of furrow profile meters and by other techniques that measure the deformation of soil or reduction in bulk density. These instruments require special design provisions to make them suitable for deep tillage studies. Some researchers have developed special equipments for deep tillage studies (Owen, 1987).

2.2.1 Cone Penetrometer

According to Perumpral (1987) penetrometers have been in use as early as 1816. Considering the simplicity involved in the construction and use of penetrometers for successful evaluation of soil properties, the cone penetrometer was developed for predicting the trafficability of vehicles, (Knight and Freitag 1962). McClelland (1956) developed a horizontally penetrating conical probe to evaluate variations in the soil strength and correlated them with draft of mould board plough. Terry and Wilson (1952) developed a mechanically recording soil penetrometer that used movement of a vertical rod and the deflection of a compression spring to provide a continuous mechanical recording of cone index against depth on a small x-y chart. Carter (1967) developed a penetrometer with a recording string depth indicator.

Osburn *et al.* (1970) developed an electronic hand operated recording pènetrometer. It employed a small x-y plotter to record the soil strength profile. Wilford *et al.* (1972) developed a tractor mounted penetrometer for penetration tests. A hydraulic cylinder was used to force the penetrometer into the soil. A x-y plotter recorded the soil strength profile. A similar but electrically operated penetrometer was developed by Smith and Dumas (1978). The unit was capable of measuring penetration resistance in the range of 0-14 MPa. Anderson *et al.* (1980) developed a solid state recording hand-held penetrometer. The unit had provision for electronic readout and statistical analysis using programmable calculator. Wells *et al.* (1982) developed a cone penetrometer capable of remote acquisition of soil cone index. The unit was portable and could be operated by single operator. Riethmuller *et al.* (1983) developed a microcomputer system for cone index measurements. This provided for quick analysis and interpretation of results. The unit was later mounted to a tractor and forced hydraulically. Morrison and Bartek (1987) developed a hand pushed digital soil penetrometer. Data were logged in a data logger and later transferred to a host computer. Rawitz and Margolin (1991) developed another electronic hand-held penetrometer using which an operator can make 150 penetrations per hour. Olsen (1989) developed an electronic penetrometer mounted to a wheelbarrow

Table 2.1 Specification of cone penetrometers developed

S.No.	Name and Year	Cone Geometry Tip angle deg.	base area mm²	Load sensing & range kg	Depth range mm	Drive & speed cm/s
1.	WES 1948	30	322	proving ring		3.04
2.	Terry and Wilson 1952	30	129	spring		Hand pushed
3.	Knight and Freitag 1962	30	322	proving ring		Hand pushed
4.	Carter 1967	30	129		122	Hand pushed
5.	Hendrick 1969	30	129	55	360	Hand pushed
6.	Osburn et al.1970	30	129	Load cell	610	Hand pushed
7.	Smith and Dumas, 1978	30	323	Load cell 440	800	Electric Motor 3.05
8.	Anderson et al. 1978	30		50	150	Hand pushed
9.	Wells et al. 1982 (ASAE S131.1)	30	131	Load cell 89	361	Hand pushed
10.	Riethmuller et al. 1983	30		Load cell 330	600	Hydraulic
11.	Morrison and Bartek 1987		129	Load cell	1000	Hand pushed
12.	Rawwitz and Margolin 1987			Load cell 100	1000	Hand pushed
13.	Olsen, 1989		500	Load cell	700 5 - 3.0	Motorised
14.	Ohmiya et al. 1993	30	323 200	Load cell	860 3.5	AC motor

like structure and driven by electric motor. Data acquisition was by a microcomputer interfaced through a microprocessor. Ohmiya *et al.* (1993) developed a system to generate cone resistance distribution maps. The unit was capable of measuring the penetration resistance over an area of 1.5 m by 2 m and to a depth of 0.6 m. Salient features of some of the penetrometers developed are tabulated in Table 2.1.

2.2.2 Tillage Dynamometers

Numerous designs of dynamometers have been developed for tillage studies. This could be classified based on application as soil-bin or field measurement system, or as drawbar dynamometers, three point linkage dynamometer and multicomponent dynamometers.

Complete system of forces that hold a tillage tool in equilibrium against translation and rotation about the three orthogonal axes could be evaluated only by measuring the six force parameters that hold the tool in equilibrium (Kepner *et al.* 1972). Pioneering works in the measurement, representation and interpretation of forces on soil engaging tools under field conditions was done by Clyde (Clyde 1936, 1937, 1939 and 1961).

Measurement of tillage tool forces under field condition adopt any one of the following principles.

1. Instrumented hitch links
2. Three point linkage dynamometer
3. Support reaction on the sub frame
4. Instrumentation to measure forces on any component or support member

Mounted implements can be hitched through free or restrained link hitch systems. In either situation the forces on the hitch linkages could be used to calculate soil reaction encountered by the tool using principles outlined by Heitshu 1952 and Kepner *et al.* 19 72.Roges and Johnston 1953, replaced the tractor hitch linkages with hydraulic cylinders and recorded the indicated pressure photographically. This was later modified using strain

gauges driving pen recorders (Radhey Lal 1959). Radhey Lal (1959) developed the prerunner of the present day three point hitch dynamometers. The draft and vertical force were sensed by measuring the torsion and bending moment on the instrumented cross shaft. The top link was also instrumented to measure the force transmitted through the top link. The accuracy of mounted implement draft prediction using strain gauges mounted directly on the hitch linkages was investigated by Upadhayaya *et al.* (1985) both by computer simulation and experimentation.

Three point linkage dynamometers were developed to measure the forces between tractor and implement. They were highly adoptable to any design of implement and hitch system. Jensen (1954) used cantilever beam mounted with strain gages to measure the forces transmitted through the hitch points. Johnson and Voorhees (1979) developed the first three point hitch linkage dynamometer which could be easily mounted between tractor and implement. It employed an aluminium transducer tube to measure the draft vertical force and moment. The dynamometer developed by Carter (1981) was similar to that described by Jensen (1954). The instrument measured the average draft by using bridge excitation from a ground wheel driven generator. Wolf *et al.* (1981) developed a system for evaluating energy input in tillage. This consisted of a three point linkage dynamometer with cantilevered flat steel bars mounted with strain gauges. The dynamometer developed by Smith and Barker (1982) employed two frames connected with commercial load cells using special flexure elements. The unit was used to monitor field energy requirement. Reid *et al*(1985) described a three point hitch dynamometer. The unit was similar to that reported by Carter (1981) and used cantilevered aluminium beam as sensing element. Garner *et al* (1988) developed a three point linkage dynamometer based on the design by Johnson and Voorhees (1979). The loads were sensed by transducers mounted on a tubular cross shaft. The three point hitch dynamometer developed by Thomson and Shinners (1989) was specially designed for deep tillage studies and could measure draft forces upto 6000 kg. The load was sensed by commercial clevis pin load cells. The three point linkage dynamometer developed by Palmer (1992) consisted of an inverted U shaped frame and the load was sensed by six dynamometers.

Harrison (1975) developed a dynamometer for field operation. It consisted of an active frame that carried the toolbar. The active frame was isolated from the main frame through six commercial load cells and the data were recorded by a computer based system. The concept of using a trailed carriage on which the tool was mounted using dynamometers was used by McKyes and Desir (1984). The forces were sensed through hydraulic cylinders fitted with pressure gauges. This instrument was used mainly for draft measurement of deep tillage tools. Own *et al* (1987) developed an instrumentation system specially for deep tillage research. The system was designed to investigate the soil tool interaction when working to depths of 1.0 m. A triaxial force and moment measurement transducer for tillage implements was developed by Godwin *et al* (1993) by employing two extended octagonal ring transducer mounted with their axis at right angles and a torque tube. The instrument was designed for soil bin and field investigation and could measure draft forces upto 10000 kg and torque up to 10000 kg-m

2.2.3 Furrow Profile Meter

The geometry of the furrow formed by the passage of a tillage tool through the soil could be evaluated by excavation of the loosened soil and measurement of the furrow geometry using the furrow profile meter.

The geometry of the three dimensional failure envelop created by shares of different geometry was visualised by Payne and Tanner (1959) by measuring the surface upheavel pattern using a template. A simple profile meter to measure the surface profile of soil was described by Ram and Zwerman (1960), they used 0.6 cm diameter and 60 cm long measuring pins mounted at an interval of 2.5 cm. The profile was marked by running a pencil over the top of the pins. This device was further modified by Willat and Willis (1965), to measure furrow profile created by deep tillage tools. The equipment consisted of 36 rods spaced at 2.5 cm interval on a cross beam. The rods slid inside guides and were held in the raised position by friction between a pressure pad. Ouwerkerk and Schakel (1965) developed an integrating reliefmeter for soil tillage studies. The vertical

measuring pins were filled with water and connected with a measuring reservoir. Currence and Lovely (1970) used mechanised probes to measure surface profiles over an area of 152 cm by 204 cm. Curtis and Cole (1972) used photographic method to record surface profile measured by a mechanical profile meter. Mitchell and Jones (1973) developed a profile measuring system employing electro mechanical probe. Spoor and Godwin (1978) used a furrow profile meter to measure the furrow geometry created by deep working rigid tines. The profile meter had a series of vertical pins freely sliding through a wooden board. This device was later used by Godwin *et al.* (1981) to measure soil disturbance by mole ploughs. Spoor and Fry (1983) measured the furrow profile created by trenchless drainage tines by using a vertical rigid rule and a horizontally positioned surveying staff.

2.3 Factors influencing soil reaction

Gill and Vanden Berg (1967) identified the factors that determine the tool forces as tool shape, manner of tool movement and initial soil condition.

2.3.1 Influence of soil type and condition on soil reaction

The soil reaction on deep tillage tools operating under varied soil types and conditions have been investigated by many researchers. Bowers (1985) recommended that draft energy requirements for various tillage operations be classified and reported based on soil textural classification and implement system used. The reported data on draft and energy requirement for deep tillage under various soil conditions are presented in Table 2.2. The table clearly indicates the variations in soil reaction force due to changes in soil and tool parameters.

2.3.2 Operational Parameters

The depth of operation and forward speed are the key operational parameters having dominant influence on soil reaction force on a deep tillage tool.

Table 2.2 Draft requirement of deep tillage tools under different soil conditions

Sl. No.	Authour(s) & Year	Soil type	Soil Con. M.C %	Soil Con. C.I KPa	Oper. Values Depth mm	Oper. Values Speed m/s	Draft Kg	Tool Values
1.	Dowding et al. 1967	Light sandy loam			216	0.64	1766	50 mm wide share
2.	Fornstrom and Becker, 1977	Light sandy loam			150	1.23	192	50 mm wide share
3.	McKyes et al. 1977	Loose sand to medium clay			150		200-600	27°, 300 mm wide share; 50x 100mm.std
4.	Wildman et al. 1978	sandy loam					1090	Straight std.
		sandy loam					940	Curved std.
		Clay loam	14.4	775	308		2080	Straight std.
		Clay loam	14.4	775	308		1700	Curved std.
5.	Frisby and Summers, 1979	Clay	29.0		307	1.70	105	
		Silt loam	16.0		307	1.50	81	Chisel plough
		Sand	6.0		307	1.90	90	
		Clay	29.0		410	1.80	588	
		Silt loam	16.0		410	1.90	846	Ripper
		Sand	6.0		410	1.90	1468	
6.	Wolf et al.1981	Sandy loam	5.85-10.5		280	1.63	252	Share 32/ 70 mm
					380	1.63	462	wing 200 mm Std. St.
					440	1.48	620	45°,32x 102 mm
7.	Upadhyaya et al. 1984	Loamy sand	5.66-6.27		356	1.80	559	38.1 mm width
					356	2.00	663	308 mm long share
					356	2.60	785	25.4 mm curved std.
8.	Bowrers, 1985 (Compilation)	Clay loam		1411	203	0.50	268	Chisel plough
					356	1.00	1200	
					356	1.40	1600	Subsoiler 25 mm wide
					356	1.80	1900	
					356	2.20	2100	
		Sandy clay loam	13.38		178	1.54	254	
		Silt loam	14.00	1214	180	1.53	153	
					130	1.97	96	
		Sandy loam	7.00	2694	150-180	1.83	217	
			10.82		254	1.45	210	
			5.82	2855	203	0.50	206	

Sl. No.	Authour(s) & Year	Soil type	Soil Con. M.C %	C.I KPa	Oper. Values Depth mm	Speed m/s	Draft Kg	Tool Values
					356	1.00	700	
					356	1.40	880	
					356	1.80	800	
					356	2.20	950	
			8.60		97	1.79	229	
			8.96		292	1.63	209	
		Sandy soil	5.00	2140	150-120	2.14	101	
9.	Summers et al. 1986	Clay loam	21.50		10xd/s	3.60	(9.25+0.579s)d	Chisel plough
		Clay loam	13.50		10xd/s	3.60	(8.92+0.494s)d	
		Silt loam	14.50		10xd/s	3.60	(11.37+0.834s)d	
		Clay loam (ASAE)			10xd/s	3.60	(5.81+0.582s)d	
10.	Garner et al. 1987	Sandy loam			300	1.5-1.7	1520	Subsoiler
					360	"	1980	
					460	"	2760	
		Sand			300	"	980	
					360	"	1300	
					460	"	1820	
		Sandy loam			300	"	960	
					360	"	1360	
					460	"	2030	
					d		120d-190d	ASAE standard
		Clay loam			d		175d-280d	for subsoilers
11.	McKyes and Desir 1987	Clay	40.20	150	1.40		250	Lift angle = 20°
			40.20	250	1.40		483	Width of
			44.40	150	1.40		257	share = 63
			44.40	250	1.40		443	
		Loam	21.99	150	1.40		43	
			21.99	250	1.40		148	
			30.10	150	1.40		47	
			30.10	250	1.40		180	
12.	Chaplin et al. 1988	Loamy sand	8.20	250	1.90		310	Width of share = 62.5
13.	Khalilian et al. 1988	Loamy sand		250	2.00		445	Subsoiler
				350	1.90		625	Subsoiler
				250	1.80		268	Chisel
				250	2.00		421	Subsoiler
				350	1.80		670	Subsoiler
				250	1.90		225	Chisel
14.	Owen, 1988	Clay laom	22.60-19	450/s			17.37+0.87s²	Subsoile 20°share, 40 mm wide shank, 75mm

Sl. No.	Authour(s) & Year	Soil type	Soil Con. M.C %	Soil Con. C.I KPa	Oper. Values Depth mm	Oper. Values Speed m/s	Draft Kg	Tool Values
		Sandy loam	30.50-16.7		450/s		20.6+0.87s²	share with wings=260
15.	Smith and Williford 1988	Silty clay loam	10.80		520 520 540 540	0.89 1.30 0.95 1.44	2960 2905 2490 2510	
16.	Owen , 1989	Clay laom	30-25		1000d	0.416	0.4+0.416dw +117.3d²	90°, 40 mm std share 26°,40 mm length =182 mm wing width=260.

a. Depth of Operation

O'Callaghan and Farrelly (1964) measured draft of vertical tines under three soil conditions. The slope of the draft-depth relation line exhibited a transition at the point where the mechanism of failure changed from shallow to deep mode. This transition occurred at a share aspect ratio, d/w = 0.6. The above mechanism of failure was extended to model failure of soil by angled blades. The transition from shallow to deep mode of cleavage for angled blades was investigated by O'Callaghan and McCullen (1965). The critical aspect ratio and rake angle were observed to have an exponential relation. Luth and Wismer (1971) observed a linear draft-depth relation for infinite width of blade and a curvilinear relation for a finite blade width. Godwin and Spoor (1977) reported work by Kostritsyn (1956) which investigated the transition from shallow to deep mode of failure for angled blades. They developed a model to predict forces on deep tillage tool which assumed a crescent failure above critical depth and lateral flow failure below critical depth. McKyes and Ali (1977) simulated draft-depth interaction for clayloam and moist sand. The simulated and experimental values indicated a curvilinear relation for operation in moist sand and an almost linear relation for operation in clay loam. McKyes (1978)

compared the previously reported values by Dransfield *et al.* (1964) and Payne (1956) with simulated values. The predicted curvilinear draft-depth relation was observed to yield a good fit for the experimental values. Godwin *et al.* (1981) reported forces on mole plough as a function of depth of operation. The force-depth relations were linear in a soil with 34 per cent clay but was curvilinear in a soil with 46 per cent clay. Perumpral (1983) predicted a curvilinear draft-depth relation which closely fitted experimental values. The draft force was found to vary as the square of tool depth. McKyes and Desir (1984) reported an increase in specific draft with share aspect ratio. Upadhyaya (1984) fitted draft-depth relation into a linear equation of the form D=Bo(CIw)d for quasistatic operation implying that the draft was analogous to cone penetrometer resistance. Garner *et al.* (1987) fitted draft-depth relation for five types of soil into linear equations. The greatest slope of the draft-depth line was 9900 kg/m, observed in an sandy loam soil. Owen (1989) measured the force-depth relation for a pedogenetically compacted clay loam soil. The draft was found to increase as the square of operating depth. Dechao and Yusu (1992) used dynamic model to simulate draft-depth relation and obtained linear draft, vertical force - depth relations.

b. Speed of Operation

Rowe and Barnes (1961) investigated the mechanics behind the draft increase with increase in speed. The analysis of the draft-speed relation indicated that the draft increase resulting from increasing the speed of tillage tool was primarily caused by increase in shear strength of soil due to the high rate of shear. The draft increase was not as large for soils low in clay as it was for those having considerable proportion of clay. The draft component due to acceleration was estimated to be small compared to total increase in draft. Siemens *et al.* (1965) observed that the draft of inclined tools were related both to the first and second powers of speed. Luth and Wismer (1971) investigated the influence of speed on soil reaction. Soil reaction was found to be a non-linear function of speed. However the dimensionless draft force term and inertia force term V^2/gl were found to be linearly related. The mechanics of deep tillage tool was investigated by

Collins and Lalor (1973). The investigations showed that in the speed range of 0.32 to 1.1 m/s, tool speed had no significant effect on draft. Hendrick and Gill (1973) observed that soil acceleration could account for only a fraction of the increased reaction but the increase was due mainly to change in soil strength with speed. Godwin *et al.* (1981) investigated the influence of speed on forces acting on subsoilers. The tool force was a linear function of speed in the range of 0.2 to 1.2 m/s. The relation between draft and speed was also found to be dependent on mode of failure, Stafford (1984). The draft speed relationship under brittle failure was a second order polynomial while that under flow failure was a decaying exponential, Stafford (1984). Upadhayaya *et al.* (1984) through field measurements observed that the draft of a subsoiler with inclined straight shank changed as the square of the travel speed. Studies by Summers *et al.* (1986) to investigate the effect of speed and depth on chisel ploughs showed that the draft was linearly related to depth and speed of operation. Owen (1988) measured the effect of tool speed on subsoiling forces in compacted soils. In the soils tested, the magnitude of vertical force on tine increased significantly with tool speed and the relation was observed to be linear. Horizontal and total forces varied significantly with square of tool speed. Smith and Williford (1988) evaluated the effect of subsoiler geometry and speeds on power requirement. Three designs of subsoilers viz., conventional, parabolic and triplex were operated in the speed range of 0.89 to 1.4 m/s. The draft was observed to decrease with increase in speed upto a speed of 1.16 m/s and later increase with speed. The vertical force for conventional and triplex subsoilers decreased with increase in speed while that for parabolic subsoilers increased with increase in speed. Glancy *et al.* (1991) found that the effect of speed on draft of a chisel plough was small, even when statistically significant when compared to depth effect. Speed squared was found to be statistically significant but was found to be a negligible factor. Dechao and Yusu (1992) developed a dynamic model incorporating the rate effect on shear and frictional properties of soil as proposed by Yao and Zeng (1990) and Zeng and Yao (1991). The predicted force-speed relation was linear for loamy soil and slightly curvilinear for clay soil.

2.3.3 Tool Geometry and Soil Reaction

The different configurations of deep tillage tools listed in Table 2.2 brings out two broad categories of deep tillage tools viz., chisels and subsoilers with and without wings. The tool geometry is described by the geometry of standard and share or wings.

a. Lift angle of Share

The lift angle or rake angle of share has a dominant influence on soil reaction. Gill and Vandenberg (1967) reported studies by Kawamura (1953) on soil reaction by inclined tools operating at shallow depths which indicated that the draft forces were minimum at 20° lift angle. Payne and Tanner (1959) did detailed investigations on influence of share lift angle on draft and vertical force. They observed that the rate of increase of draft with lift angle became greater for lift angles above 50°. They concluded that draft of tines raked at a little less than 20° represented a minimum value. They also observed that the vertical reaction was downwards for rake angles up to 45°. Osman (1964) investigated behaviour of wide cutting blades and observed that the draft was minimum at a lift angle of 20°. O'Callaghan and McCullen (1965) observed that the transition from shallow to deep mechanism of soil cleavage occurred at a greater depth for raked shares than for vertical shares. The shares of lower lift angles were also observed to be more efficient in soil loosening. Siemens *et al* (1965) developed equations to predict forces on an inclined tool and compared them with experimental results. The resultant forces were observed to be minimum at a tool lift angle of around 25°. Godwin and Spoor (1977) observed through prediction models and experimental measurements in sandy loam soil that the draft force decreased with share lift angle. The vertical force changed direction at a lift angle of 67.5°. McKyes and Ali (1977) observed draft to decrease with lift angle. The efficiency was observed to be maximum at the lowest lift angle. McKyes *et al* (1977) investigated forces on slurry injection tines and observed that the draft force was minimum at a lift angle of 20° McKyes (1978) predicted forces on shares at three different soil conditions and compared them with reported experimental results. This showed that the draft requirement was minimum at a lift angle of 20° for clay, sandy loam and sand. Wildman

(1978) investigated performance of slip ploughs and found that the optimum lift angle for clay loams to be 30° and that for sandy loam to be 25°. Perumpral (1983) also predicted a share lift angle of 20° for minimum draft. McKyes and Desir (1984) recommended a lift angle of 20-25° based on predicted and measured values of draft requirement. Filke and Riley (1991) applied the universal earth moving equation to chisel plough wings. The study showed that the draft would be minimum at a wing lift angle of 20° over the range of speeds investigated. Decahao and Yusu (1992) used a dynamic model and predicted that the draft would be minimum at a lift angle of 20°. For the given conditions used for simulation, the vertical force changed direction at about 75°

b. Share Width

Payne and Tanner (1959) observed that the draft varied linearly with width at all rake angles and soil conditions. O'Callaghan and Farrelly (1964) observed that the transition from shallow to deep mode of failure for vertical tines occurred at a greater depth for wider tines and hence narrower tines would experience more pressure than wide tines operating at shallow depth. The same theory was also used by O'Callaghan and McCullen (1965) for angled blades. Investigations by Siemens *et al* (1965) showed that the draft and vertical force varied linearly with width of tool at different rake angles. Luth and Wismer (1971) observed that the non dimensional draft force term varied as the logritham of depth/width ratio. Godwin and Spoor (1977) predicted a slightly curvilinear draft-width and vertical force-width relationships. McKyes and Ali (1977) investigated the influence of share width through simulation studies and experimental measurements They observed that over a width to depth ratio of 0.2 - 0.5 range, the efficiency of a deep tillage tool remained constant.They reported that there exists a lower limit to share width with limiting values of depth/width ratios in the range of 6-15 for different soils and rake angles. McKyes (1978) predicted a linear draft-width relationship and observed that they yielded a good fit with the experimental values reported by Balaton (1971). Spoor and Godwin (1978) reported effect of wing width on draft and vertical force which was observed to be linear, Wildman *et al* (1978) observed that the draft of slip ploughs varied

linearly with width. Perumpral (1983) predicted a linear width-draft relationship and confirmed the same by experimental results. Owen (1989) measured the depth and vertical reaction on shares of 40-260 mm width. The variations in soil reaction due to width was minimum as compared to depth effect. Filke and Riley (1991) applied universal earth moving equation to chisel plough wings. A linear depth-width relation and vertical force-width relation were observed.

C. Length of Share

The length of share determines the relative location of share's cutting edge from standard. Nichols and Reaves (1955) attributed the reduced draft of subsoilers with curved shanks as compared to straight-shank subsoilers to the distance between the chisel point and the standard. Further soil bin studies by Nichols and Reaves (1958) showed that the lower value of draft for subsoilers with curved standard was due to lesser buckling pressure on the soil cone formed at the tip of the share. Luth and Wismer (1971) investigated shares of different lengths on dry sandy soil and analysed the effect of share length by considering the amount of lift ($l \sin\alpha$) as the parameter influencing soil reaction. The dimensionless draft and vertical reaction terms were found to vary almost linearly with depth to lift ratio. The influence of depth to lift ratio was observed to the minimum at lower rake angles. Wildman *et al.* (1978) investigated soil reaction on slip ploughs by varying the location of cutting edge from the standard at a constant lift angle. The draft was greatest when the cutting edge was close to the standard and decreased as the distance was increased. The vertical force increased only slightly when the cutting edge was shifted forward from the standard. At a constant lift angle, the change in length altered the lift height. Spoor and Godwin (1978) investigated the effect of lift height of wings and found that wing lift height in the range of 60-100 mm to be acceptable over a wide range of soil conditions for deep loosening. Harrison (1982) observed that for a wide blade operating in sand, the draft and vertical forces increased with increase in blade length.

2.4 Factors Influencing Furrow Geometry

The influence of tool and operational parameters on geometry of furrow loosened by passage of a deep tillage tool had been investigated by various researchers. Payne and Tanner (1959) reported work by Payne (1956) which suggested that furrow width was independent of width of tine provided that the tine was wide enough to bring the soil into plastic equilibrium, this for vertical tines was found to be a width of 37 mm. Payne and Tanner (1959) measured the geometry of failure crescent. They observed a good correlation between the length of crescent and draft. The width of furrow was plotted against tine aspect ratio. It was observed that the curve had a tendency to flatten out above an aspect ratio of 0.3. O'Callaghan and Farrelly (1964) measured the geometry of furrow formed by vertical blades; careful excavation of the furrow showed that in addition to the soil around the path of tine which underwent fragmentation, there was a region within boundary slipline in which slight movement had taken place. The furrow aspect ratio - share aspect ratio relationship obtained confirmed earlier results by Payne (1956) that the furrow width reaches a constant value after particular depth. Willat and Willis (1965) observed that the furrow width varied linearly with depth and that the area of furrow varied as square of depth. It was also observed that the area of furrow increased slightly with increase in speed.

McKyes and Ali (1977) predicted that the overall disturbance efficiency in terms of area per unit force to be maximum at lowest rake angles. Over the width to depth ratio range of 0.2 - 5, the efficiency of soil disturbance per unit force was relatively insensitive to blade width. The area disturbed per unit force decreased with increase in depth of operation. Spoor and Godwin (1978) investigated deep loosening of soil by rigid tines. They concluded that there existed a critical working depth for all deep working tools below which compaction would occur instead of soil loosening. This critical depth was found to be dependent upon the width, inclination and lift height of tine foot and moisture and density status of soil. The soil disturbance pattern of mole ploughs was investigated by Godwin *et al.* (1981). The depth of work was observed to have an

important effect on type of soil disturbance; wide and low rake angle tines were more likely to cause brittle crescent failure than the narrow vertical standard of a mole plough. Ahmed and Godwin (1983) observed that there was difference in furrow geometry due to position of wing in a subsoiler. Spoor and Fry (1983) investigated soil disturbance by deep working low rake angle narrow tines. Shallow tines operating above critical depth caused minimal soil disturbance beyond the major failure plane. The transition from predominantly brittle failure above critical depth to predominantly shear flow failure below critical depth was observed to be gradual. Field experiments were conducted by McKyes and Desir (1984) in clay and sandy loam soil to measure soil disturbance by deep tillage tools. The data revealed trend towards higher degree of soil loosening for blades with low d/w ratio. Higher rake angles also had an discernible effect in increasing soil loosening. Plasse *et al.* (1985) predicted the variations in furrow geometry due to changes in shear and frictional properties of soil. They observed that in addition to blade aspect ratio and lift angle the internal angle of friction of soil also influenced soil disturbance. Owen (1987) investigated soil disturbance associated with deep subsoiling in compact soils. Experiments were conducted with and without wings at depths of 0.37, 0.52 and 0.72 m. The type of soil had a significant effect on width of disturbance. The wing width was observed to have a significant effect on width of disturbance. However the major advantage observed for winged subsoilers was the increase of critical depth with wing width. The results showed that 26 cm wide wing had no advantage over 7.5 cm share in terms of area of soil disturbed when operating above critical depth.

2.5 Models for prediction of soil reaction on deep tillage tools

Soil cutting by a deep tillage tool is usually a three dimensional problem. Several models have been proposed to evaluate the force required for soil failure.

Payne (1956) developed the first three dimensional soil failure model. The soil was assumed to fail in a crescent shape which was further divided into a triangular centre crescent and two side blocks. O'Callaghan and Farrelly (1964) model assumed an

upward failure zone above critical depth and an lateral failure below critical depth. This model was used to predict forces on a vertical blade. Hettiaratchi and Reece (1967) developed a three dimensional failure model. In this model the soil failure configuration was divided into forward failure ahead of soil tool interface and transverse failure below critical depth. They modeled the transverse failure by using the two dimensional failure equation similar to that developed by O'Callaghan and Farrelly (1964).

Godwin and Spoor (1977) proposed a model based on the assumption of a three dimensional crescent failure above critical depth and two dimensional lateral failure below critical depth. The crescent failure was modeled by assuming a parallel central wedge flanked by two curved side crescents. The lateral flow failure was similar to that proposed by O'Callaghan and Farrelly (1964) and Hattiaratchi and Reece (1967).

McKyes and Ali (1977) developed a model which assumed a crescent failure ahead of the tine. This model assumed the bottom surface of the central wedge to be flat and the flanks of the side crescent were assumed to be a straight line. This model was easier to use since it required no prior knowledge about failure geometry.

Perumpral *et al* (1983) developed a model for three dimensional failure by replacing side crescent by two sets of forces acting on the sides of the central wedge. Swick and Perumpral (1988) proposed a dynamic soil cutting model which included the effect of travel speed. The failure zone was modeled similar to McKyes and Ali model. This model used empirical relation for the angle of the side crescent. Dechaoand Yusu (1992) developed a dynamic soil cutting model which included the acceleration and damping effect. They used the strain rate dependent soil strength parameters developed by Zeng and Yao (1991) and Yao and Zeng (1990) to model the performance of cutting blades. Detailed description of the models developed by Godwin and Spoor (1977), McKyes and Ali (1977) Perumpral *et al* (1983) and Swick and Perumpral (1988) are given in Sec.3.6.

Plasse *et al.* (1985) used models by Hattiaratchi and Reece (1967), Godwin and Spoor (1977), McKyes and Ali (1977) and Grisso *et al.* (1980) to simulate performance of deep tillage tools under different soil conditions. The comparisons showed that the Hettiaratchi and Reece (1967) model gave a better prediction for the area of soil disturbance but over-predicted draft values. All other three models were found to yield a reasonable estimate of draft force. Grisso and Perumpral (1985) compared the performance of deep tillage tools as predicted by the simulation models by Hettiaratchi and Reece (1967), Godwin and Spoor (1977), McKyes and Ali (1977) and Perumpral *et al* (1983) for different combinations of tool depth, width and lift angle. The comparisons showed that all models were useful in predicting rupture distance. All models except Hettiaratchi and Reece (1967) model gave reasonable prediction of draft. The vertical force was predicted reasonably by all models except McKyes and Ali (1977) model. An exhaustive review of the analytical and numerical models for predicting soil forces on deep tillage tools was presently by Kushwaha *et al.* (1993).

Albuquerque and Hettiaratchi (1980) developed mechanics of a subsurface cutting blade. The model considered the blade as being operated in an embedded condition. The failure zone was accordingly modeled. This model was realistic in that it did not assume that the blade extends up to the ground level. The problem was solved using numerical procedure developed by Sokolovski (1965). Tables were prepared to directly predict the forces on deep tillage tools of different geometries. However the major drawback of this model was the assumption of a plane failure condition.

Numerical prediction models using finite element analysis have been developed by Chi and Kushwaha (1989, 1990, 1991) and Young and Hanna (1977). These models do not require prior knowledge about the failure geometry. However they require accurate soil constitutive models for predicting tool performance.

2.6 Design of Deep Tillage Tool

Wolf and Luth (1979) observed that to popularise and broaden the use of subsoilers for clod forming soils the implement should have the following characteristics.

1. Decreased draft
2. More aggressive action to expose clods
3. Increased strength of standard and decreased wear.

Brown *et al.* (1989) analysed the stresses on a chisel plough frame using finite element analysis technique. The dimensions of the cultivator frame were obtained and the stresses on the members were simulated by using ANSYS finite element computer package.

The following were the steps adopted in applying finite element method

1. Establishment of suitable coordinate system
2. Defining nodes
3. Defining elements
4. Listing geometric constraints
5. Establishing displacement constraints and
6. Determination of applied force and moments.

Utilizing the predicted stress values the Shear Energy Theory or Von Mises - Hencky Theory was used to predict whether an element was over stressed or under stressed.

Palmer and Glasbey (1990) measured the load cycles generated by fixed tines working in soil. They developed a specially designed dynamometer to measure the cyclic variations in forces. They used the measured load histories to predict the life time of the tillage tool. Harral (1990) measured the structural loading on a rigid cultivator frame. A simple structural analysis of the frame was carried out using the computer programme SPACEF to identify the most highly stressed areas. Stresses at critical areas were measured by positioning strain gauges at locations optimised through lacquer technique.

2.7 Evaluation of Performance

Wolf *et al.* (1981) evaluated the performance of tractor - implement system by developing suitable instruments that measured draft and speed. The system performance was predicted by calculating the tractive efficiency and traction ratio. Dynamometer systems used for evaluating draft energy requirement under field conditions have already been described in Sec.2.2.2. The procedures for testing tillage tools have been proposed by IS 9253 (1979) and RNAM (1983). These include details regarding description of experimental conditions and standard techniques for measuring various parameters of performance.

METHODS AND MATERIALS

CHAPTER III
METHODS AND MATERIALS

In this chapter, the instruments specially developed for determining the soil strength, soil reaction forces and degree of soil manipulation are explained. The methodology adopted to determine the effect of soil, tool and operating parameters on soil reaction and manipulation are presented. The procedure followed for adoption of selected soil dynamics models to simulate the performance are presented. The sequence followed to develop the deep tillage implement and the procedure adopted for evaluating its performance are also presented.

3.1. Development of Instruments

To investigate the soil-tool interaction of deep tillage tools, three instruments were specially developed. They are,

1.	Cone penetrometer	-	To characterise soil strength
2.	Tillage dynamometer	-	To measure soil reaction to tillage tool
3.	Furrow profilemeter	-	To measure the furrow geometry

3.1.1. Cone penetrometer

Cone penetrometers are extensively used in tillage and traction studies. The commercially available penetrometers are mostly hand-held and cannot be used when penetration resistance exceeds the weight of the operator. It can be used only upto a depth of 10-18 cm in hard soil. Moreover, it is difficult to maintain a constant rate of penetration. Hence, a tractor mounted cone penetrometer was designed, developed and tested for field performance.

a. Salient features:

The cone penetrometer designed and developed had the following features:

1. Capacity to measure penetration force within a range of 0-250 kg
2. Maximum depth of operation of 60 cm.
3. Capacity to maintain constant penetration speed of 3mm/s
4. Accurate measurement of force and depth
5. Simple in design and easy to operate
6. Provision for multiple measurement in a given location with minimum disturbance of the soil.

b. Construction:

The cone penetrometer (Plate 3.1) was fabricated with the following sub-assemblies.

1. Mounting frame
2. Penetrometer column
3. Drive mechanism
4. System for measurement of load
5. System for measurement of depth

The mounting of the penetrometer to the tractor is shown in Fig 3.1. The mounting frame consisted of a 2.5 m long channel section of size 75 x 40 mm. It was provided with a standard three point hitch bracket. Provision was made to hitch the frame to category I or category II hitch system of tractors. Adjustable check chains were provided to restrain the upward motion of the tractor lower links during operation of penetrometer.

The penetrometer assembly is shown in Fig.3.2. The column was made of hollow steel tube of size 50 x 3 mm. The mounting clamps were welded to the column. The column supported the bearing housing, bottom guide bush and motor mounting flange.

PLATE 3.1. GENERAL VIEW OF CONE PENETROMETER

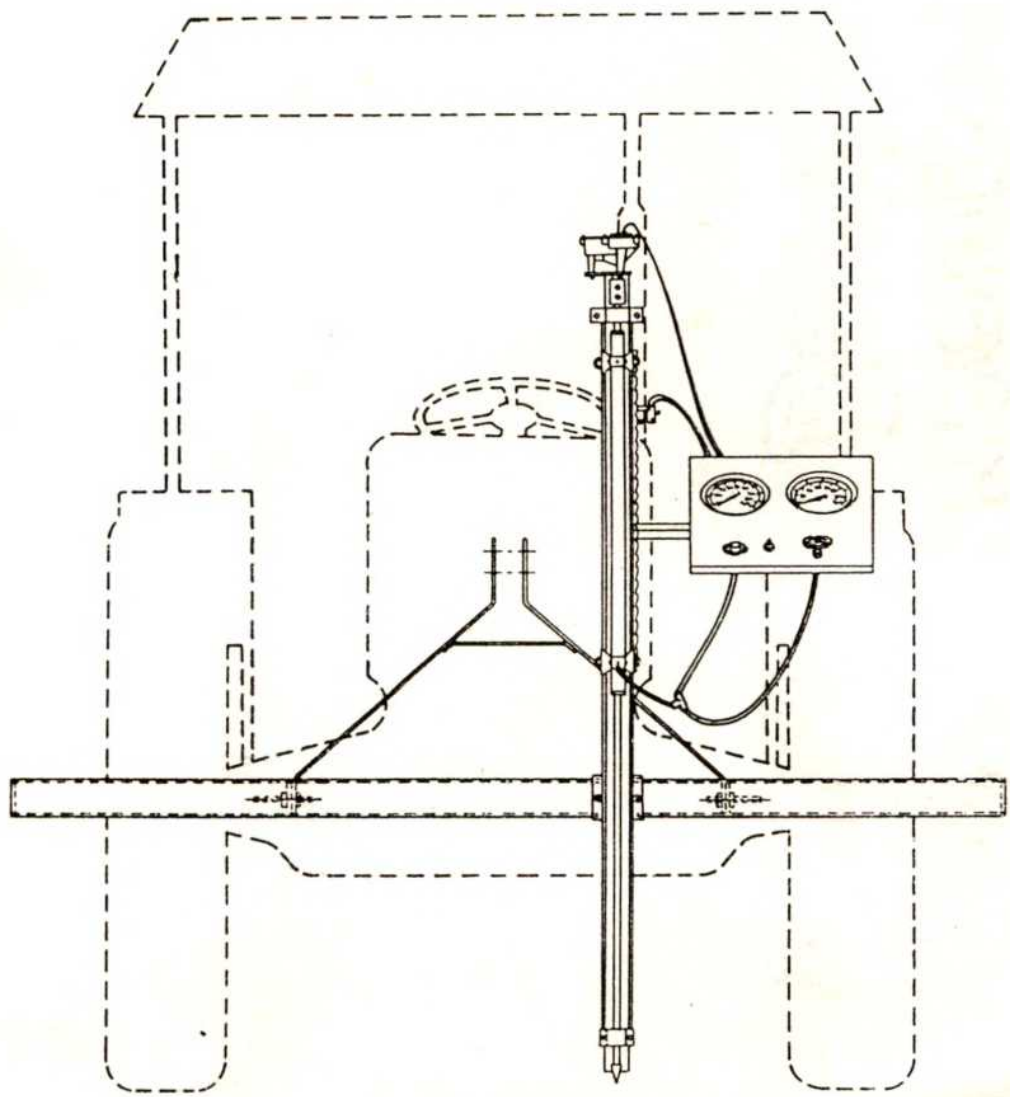

Fig.3.1. CONE PENETROMETER MOUNTED TO TRACTOR

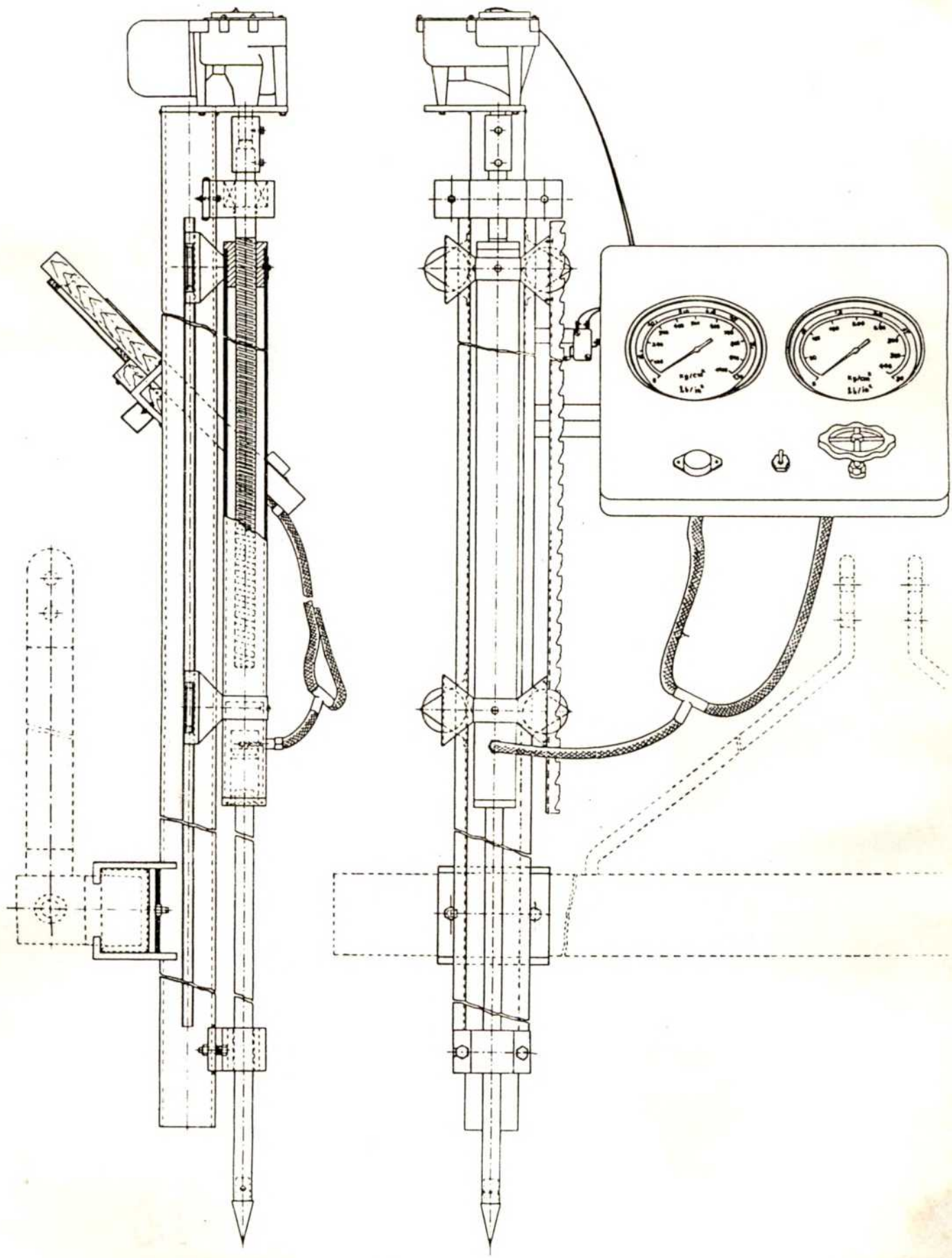

Fig. 3.2. ASSEMBLED VIEW OF CONE PENETROMETER

Both sides of the column were provided with channels of size 12 x 12 mm for guiding the penetrometer.

The penetrometer was actuated by a screw and nut mechanism powered by a 17 watts wiper motor. The motor was driven by a 12 volts D.C. supply from the tractor battery. The speed of the output shaft of the drive unit was in the range of 45-54 rev/ min depending on the applied load. The nut was fixed to one end of an aluminium tube of size 40 x 3 mm , the other end of the tube was fitted with dynamometer. The screw rod was mounted on bearing at its upper end. The lower end carried a nylon bush to ensure the alignment of the screw rod with the tube. The tube was guided by the channels.

The penetrometer was fitted with a standard cone confirming to ASAE specifications S313.1. The cone had a base area of 320 mm^2 and an apex angle of 30°. The cone was machined out of stainless steel and polished. It was mounted to a solid stem of diameter 16 mm. The stem was guided by a nylon bush. The upper end of the stem was fitted with a piston.

The penetration force was sensed by a hydraulic dynamometer, Fig.3.3. The fluid was sealed by a hydraulic seal. The piston was guided by the dynamometer. During retraction, the piston was retained by a circlip. The dynamometer was connected to two pressure gauges mounted on the panel to indicate pressures in the ranges of 0-28 and 0-70 kg/cm^2. The low pressure gauge was fitted with a shut off valve to disconnect the gauge when the pressure exceeds its range of measurement. This arrangement helped to read the values accurately at low levels of penetrometer resistance.

In order to ensure convenient and instantaneous measurement of load for every 2 cm of depth, a audio depth indicator was provided(Fig.3.4). A microswitch was triggered by rack mounted to the tube. the microswitch switched on a 12 v piezo buzzer at a depth of every 2 cm to produce an audio signal.

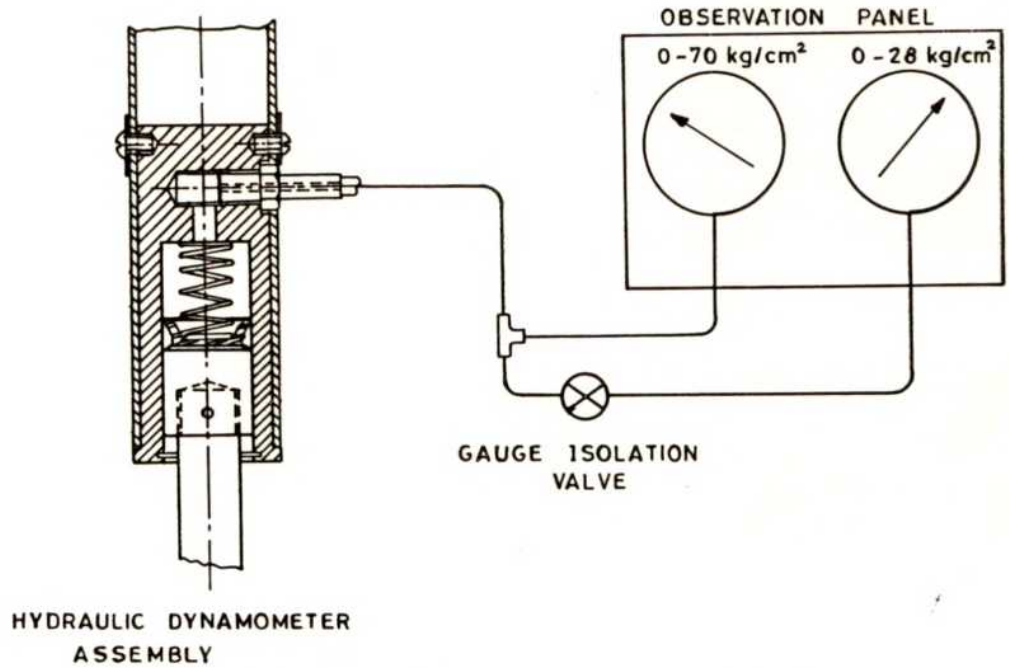

Fig. 3.3. CONE PENETROMETER - FORCE MEASUREMENT SYSTEM

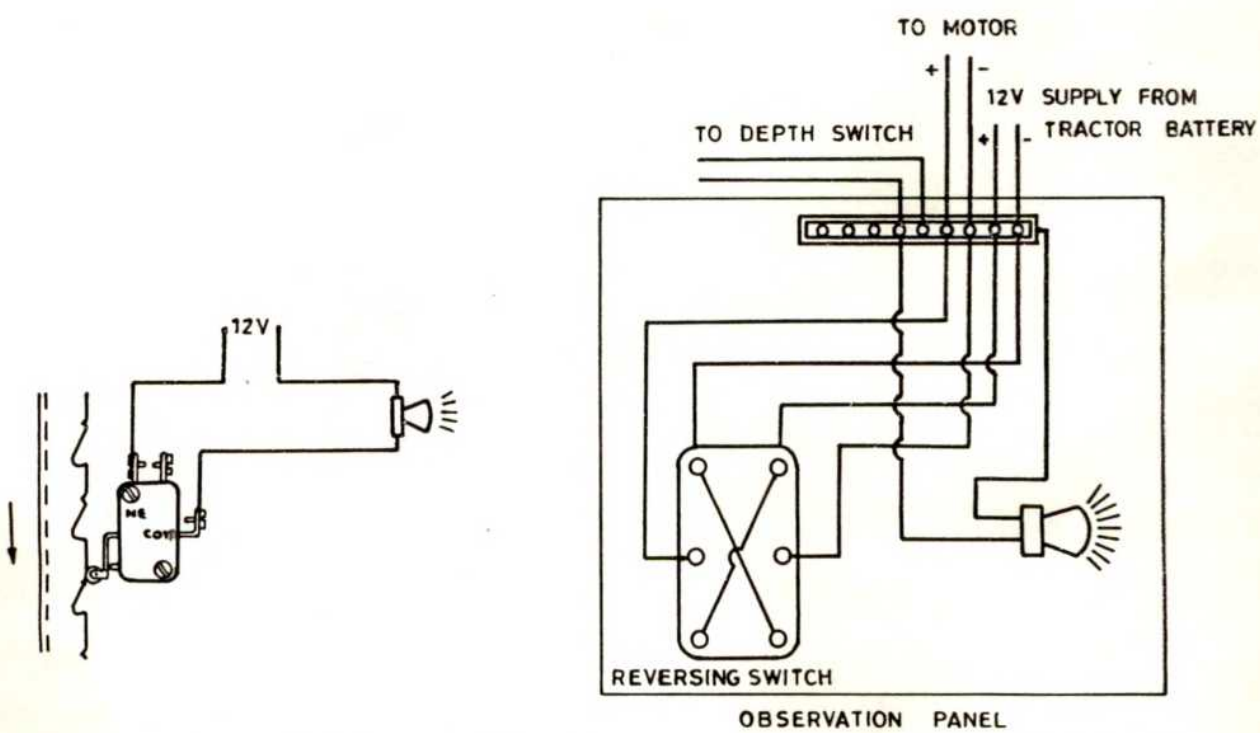

Fig. 3.4. CONE PENETROMETER - DEPTH MEASUREMENT SYSTEM AND MOTOR CONTROL CIRCUIT

c. Calibration and operation:

The dynamometer system was filled with brake fluid. Air was completely removed from the system. It was fitted with piston and a 200 kg compression type proving ring was mounted between the dynamometer's piston and the guide bush(Plate 3.2). Force was applied by rotating the screw rod. The deflection of the proving ring and the indicated pressure were recorded and the calibration curve was plotted.

The penetrometer was mounted to the mounting frame and transported to the field. the lower links were arrested using the check chain. The penetrometer was positioned over the location and clamped. The unit was switched on and the observations were made from the pressure gauges whenever the audiosignal was received. The cone was retracted by reversing the drive motor. The penetrometer was used throughout the study by repeating the same procedure to measure CI values in the field.

3.1.2. Tillage Dynamometer

The soil reaction force exerted on a tillage tool was measured by tillage tool dynamometer. A tractor mounted tillage tool dynamometer was developed to measure soil reaction on deep tillage tools when tilling dry clay soils. The principle of operation of the dynamometer was similar to that of the tillage meter developed by Clyde(1936) and subsequently modified(Clyde, 1939). the working principle of tillage meter is illustrated in Fig.3.5. The tool was mounted on a subframe and was held in equilibrium by the reactions provided by a system of six dynamometers. Three forces are sufficient for symmetrical tools having forces in a single plane. The tillage dynamometer previously developed by the author was modified and used in the present study.

a. Salient features:

The tillage dynamometer developed is shown in Plate 3.3. It had the following features.

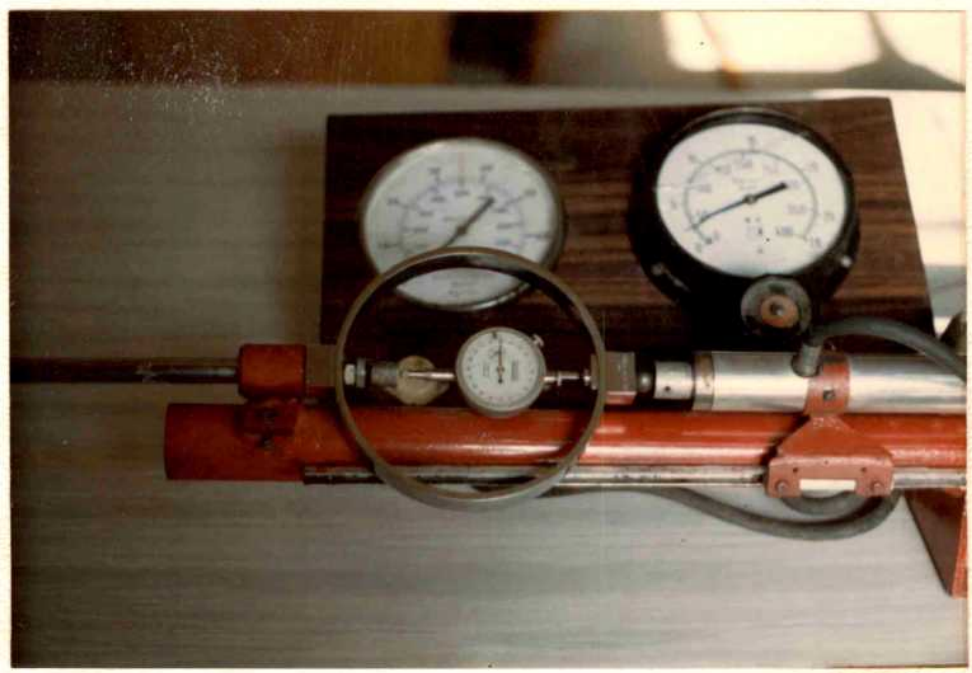

PLATE 3.2. CALIBRATION OF CONE PENETROMETER

PLATE 3.3. GENERAL VIEW OF TILLAGE DYNAMOMETER

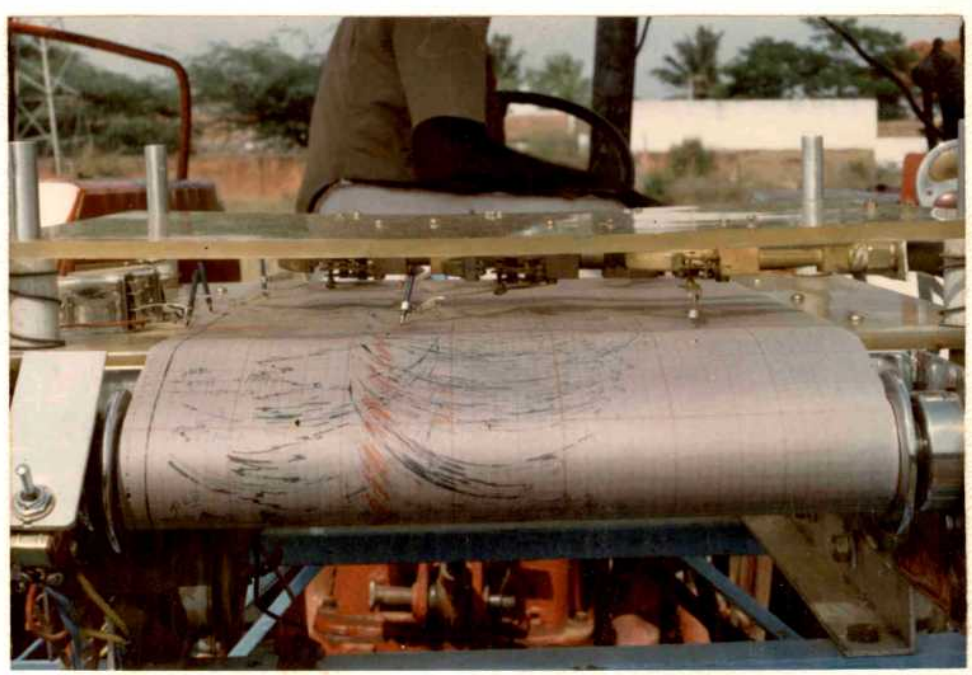

PLATE 3.4. TILLAGE DYNAMOMETER IN OPERATION

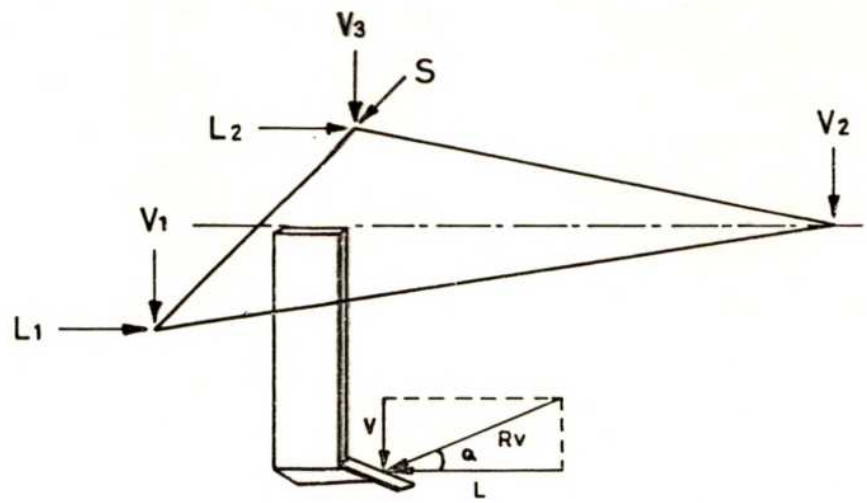

Fig.3.5. TILLAGE DYNOMOMETER - ARRANGEMENT OF LOAD CELLS RELATIVE TO TOOL

1. Suitability to measure soil reaction under field condition.
2. It can be mounted to the tractor through standard three point hitch.
3. Capable of complete measurement of generalised force system with six dynamometers.
4. Force sensing, using reliable and accurate hydraulic dynamometers.
5. Recording pressure gauges mounted on electrically driven six channel strip chart recorder for simultaneous and accurate recording of forces.
6. Provision for continuous recording of velocity.
7. Accurate adjustment of depth.
8. Large diameter trailing pneumatic ground wheel for minimum sinkage and slip.
9. Single integrated unit to obtain direct recording of tool forces.
10. Simple in design and easy to operate.
11. Low cost design with high reliability.

b. Construction

The tillage dynamometer(Fig. 3.6) was fabricated with the following sub assemblies.

1. Main frame
2. Sub frame
3. Recording dynamometer
4. Strip chart drive
5. Speed recording arrangement

The main frame was rectangular in shape and it was made of channel sections. The mast and lower hitch pins were provided for mounting the frame to the tractor. The adjustable ground wheel assembly was mounted at the rear side of the frame on a swiveling

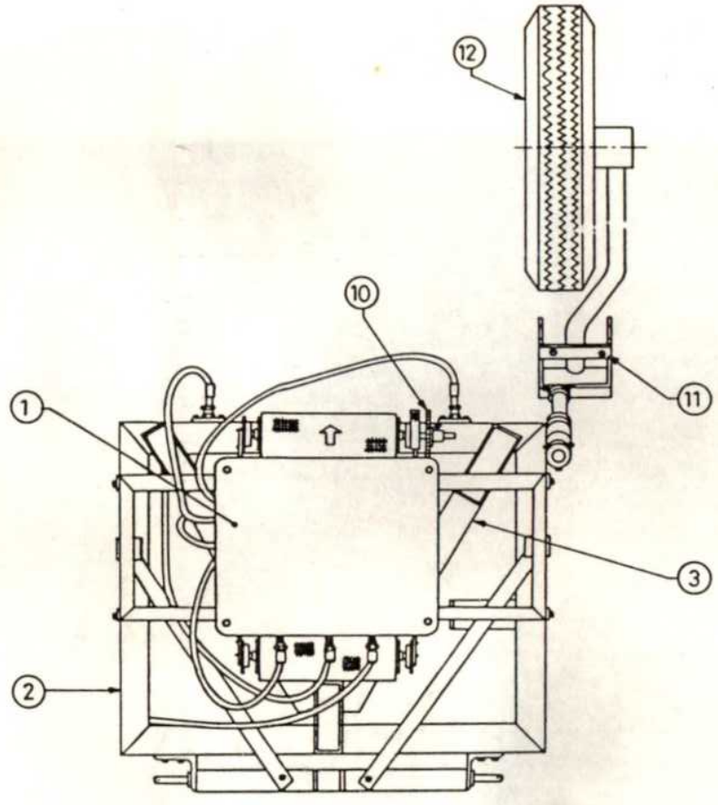

1	Recording Dynamometer
2	Main Frame
3	Sub-Frame
4	Corner braces
5	Standard
6	Hitch assembly
7	Recorder mounting plates
8	Share
9	Foot
10	Strip chart drive
11	Depth adjustment screw
12	Ground Wheel

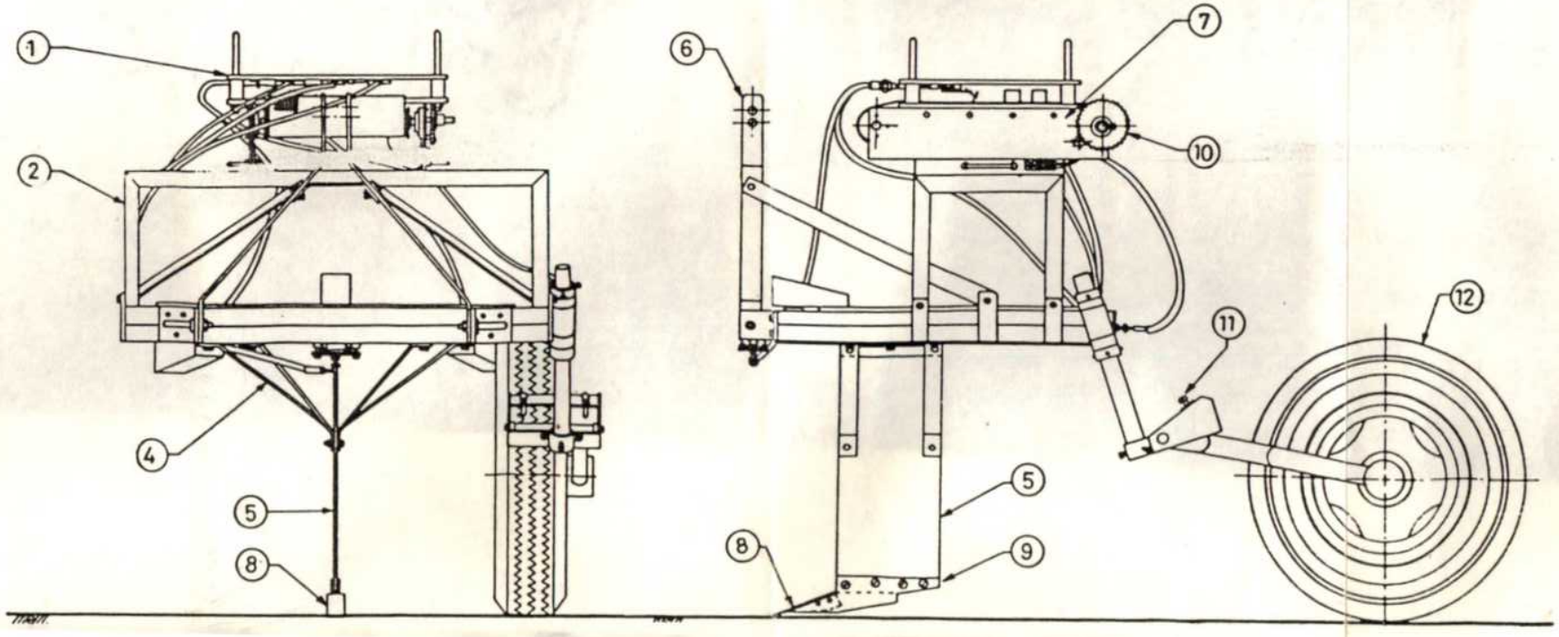

kingpin. A pneumatic implement tire was used as the ground wheel. The main frame was provided with six bored holes to mount the dynamometer.

The sub frame was a triangular frame. Three support brackets were provided at each corner to receive vertical support from the dynamometer V_1, V_2 and V_3(Fig. 3.5). In order to mount shares of different geometry, a standard and foot were fabricated and fitted to the sub frame. The standard had a section of 200 x 6 mm and was provided with corner braces to arrest lateral deflection. The thin standard was used to minimise the effect of standard on soil reaction. The sub frame was provided with adjustable stops to restrain free movement of subframe during transport.

To measure and record the pressures, hydraulic pressure recording dynamometers were used (Fig. 3.7). The sensing element consisted of a cylinder fitted with piston and sealing element. The dynamometer had an inner diameter of 45 mm, giving a sensing area of 15.9 cm^2. Dynamometers were machined out of mild steel and the inner surfaces were bored and honed. Flanges were provided for clamping the dynamometer to the main frame. A lipped rubber seal was mounted with a light spring behind it to seal the hydraulic fluid. Load was applied to the dynamometer by means of an aluminium piston fitted with a hardened steel ball, revolving freely in its seat. This facilitated application of point load with minimum cross sensitivity. The dynamometers were connected with pressure gauges by flexible hoses confirming to SAE100R_1-1/4" having working pressure of 650 ksc. The Bourden tube assembly from pressure gauge was carefully removed and mounted on the movable plate of the recorder, facing downwards as shown in Fig. 3.8. Recording was done by small pens mounted on pen arms which replaced the pressure gauge needles. The pens were made by mounting microtip pen point to a tube of 1 mm diameter and 25 mm length. The pen was hinged to the end of the writing arm(Fig. 3.7). the pen assembly was made light and rigid to have minimum inertia. The hinged pen ensured uniform, light contact pressure. The strip chart pressure recorder had a square frame fitted between mounting plates. A 10 mm thick acrylic sheet was mounted above the frame to provide

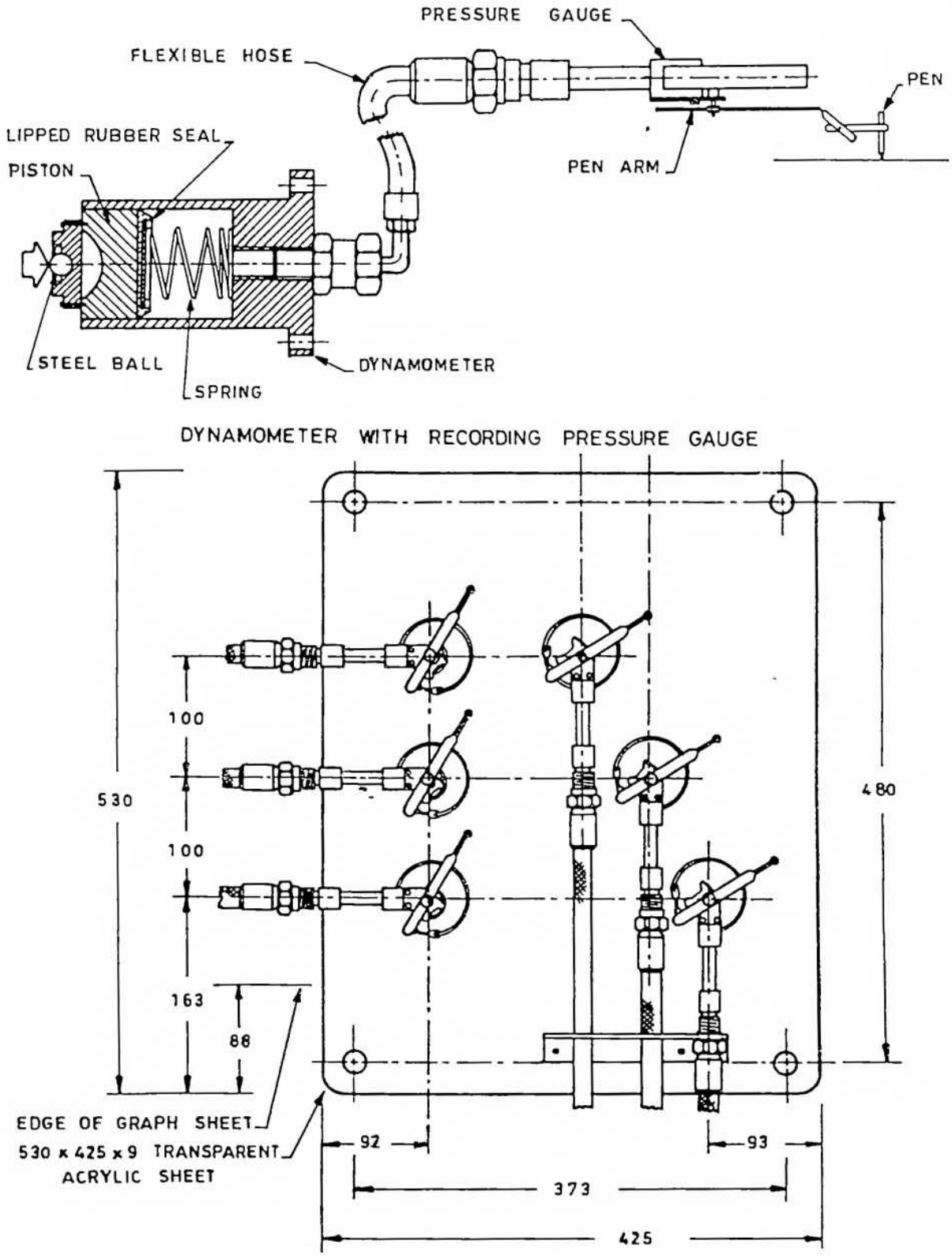

Fig. 3.7. DYNOMOMETER WITH RECORDING PRESSURE GAUGE

the recording surface. The recording pressure gauges were mounted on a movable plate guided by guide pins at each corner. The movable plate was mounted parallel to the recording surface by collars provided on the guide pins. The chart feed arrangement consisted of a form payoff drum at one end and take up drum at the other end. The chart paper was fed by the traction from the take up drum. The diameter of payoff and take up drums was 51 mm and the drums were mounted on bearings. The take up drum was driven through a commercial wiper motor through a reduction gearing of 1:5.5. The motor was driven at a speed of 4.3 rpm by a 2.0 volt supply from the tractor battery. This arrangement gave a chart speed of 2.08mm/sec when the take off drum was bare. The motor was controlled through a reversible switch (Plate 3.4)

The forward speed was recorded by recording continuous timebase marks at intervals of 10 sec and event markings once every revolution of ground wheel, Fig.3.9. The recordings were done by solenoid operated pens. The time base signal was generated by an electronic timer circuit. A microswitch activated by a small projection on the ground wheel hub was used to trigger the event marker.

The recorder was mounted over the mainframe so that it can be monitored and operated from the rear. An electric horn was fitted at the rear to signal the tractor operator.

C. Calibration

The investigation of soil reaction on symmetrical tools require measurement of three forces as $L_1=L_2$, $V_1=V_3$ and S=0, Fig.3.5. However, all the six dynamometers were assembled and calibrated. The V_1 and V_3 dynamometers were fitted with pressure gauges of different capacity so that any one channel can be used as per requirements. The L_1 and L_2 channels were retained so that any one channel can be used in case of failure of the other. Thus additional flexibility and reliability were provided. The specification of pressure gauge used for each channel are given in Table 3.1.

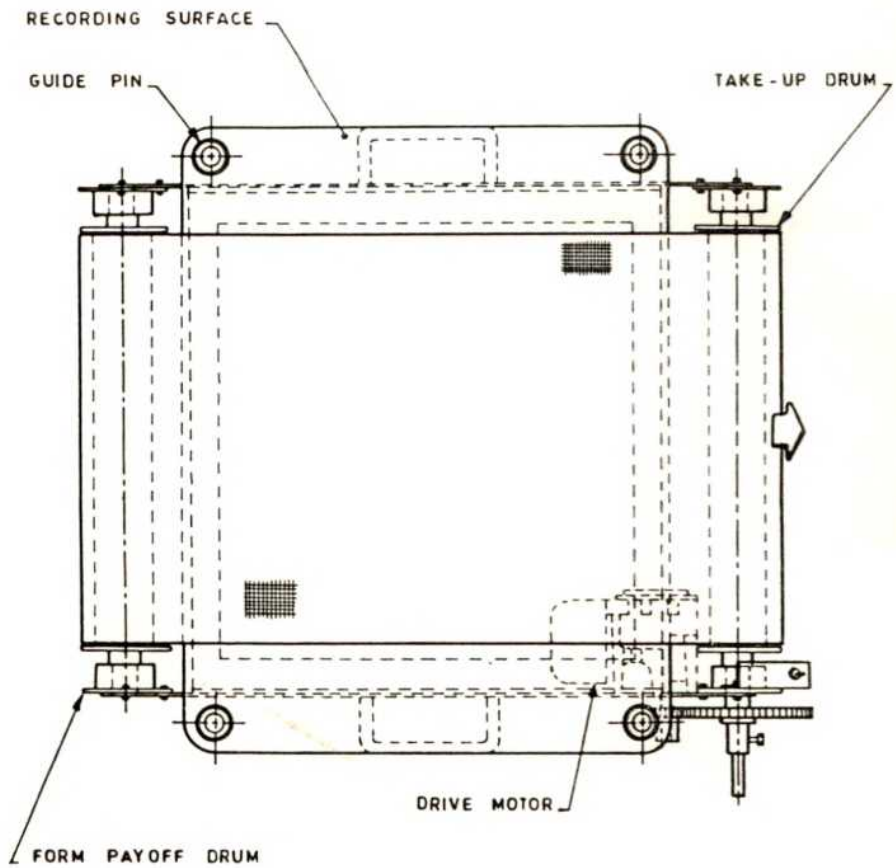

Fig.3.8. STRIP CHART DRIVE UNIT

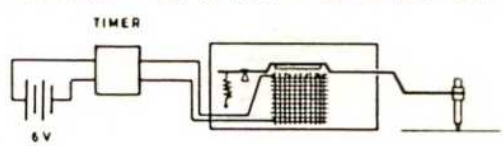

a)TIME BASE MARKER

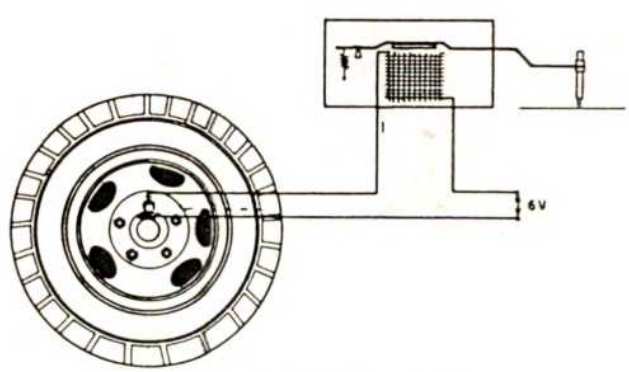

b) EVENT MARKER

Fig.3.9. SPEED RECORDING ARRANGEMENT

The dynamometers were filled with brake fluid and air was removed from the system. Each dynamometer was checked for leakage under load. The dynamometers were mounted to an arbor press and the response was checked by applying sudden loads. The sluggishness, if any, was eliminated by removing the entrapped air.

Different types of pen arrangement were investigated to arrive at a configuration that ensured maximum linearity of calibration curve. Calibration was done with the chart

Table 3.1 Specification of pressure gauges

Channel No.	1	2	3	4	5	6
Dynamometer	L_1	L_2	S	V_1	V_2	V_3
Pressure gauge (Max.Pr in Kg/cm^2)	28	28	10	70	140	105

drive on. The dynamometers were calibrated against a 200 kg. proving ring in a hydraulic press. The proving ring was mounted with ball supports, Plate 3.5. The dynamometer was loaded in a series of steps and each load was held for a short time interval so that a clear parallel line was drawn. The proving ring deflection was noted at each load and converted to load values. The recordings obtained were converted into angular deflection of pen-arm from the null reading. The calibration curve was drawn between the applied load and corresponding angular deflection. The calibration procedure was repeated and a straight line was fitted using least square method.

The timer circuit was adjusted to switch off once in 10 sec. The forward distance traveled per revolution of ground wheel was measured to be 2.23 m. The timer circuit was provided with separate 6 V battery to avoid interference due to switching of event marker.

PLATE 3.5. CALIBRATION OF DYNAMOMETER USED IN TILLAGE DYNAMOMETER

d. Operation

The dynamometer was hitched to the tractor and transported with the ground wheel raised and pens disengaged. The unit was brought to operating position, electrical connections given and all pens were filled with ink. The share to be tested was mounted and operated at the desired depths and speed. The implement was controlled using the position control system of the tractor. Reference marks were made on the chart to identify the recordings. The recorder was switched on to obtain recordings of dynamometer loads and speed of operation. The procedure was repeated for different tests.

To obtain corresponding pen positions at any instant, a transparent template was used, Plate 3.6. The pen position read from the graph were converted into dynamometer loads by using a ready reckoner table which took into account, the calibration constant, pen's initial position, location of pen arm center, pen arm radius and corrections for deadweight on dynamometer. The dynamometer loads were later combined to obtain the soil reaction on the tillage tool. The forward speed was measured by counting the event markings in a given span of time.

3.1.3. Furrow Profile Meter

The geometry of soil failure caused by the passage of deep tillage tool was measured by using a specially designed furrow profile meter. The device was similar to the roughnessmeter developed by Tessier et al (1989). It was modified by providing plotting board and provisions for mounting continuous stationary.

a. Salient features

1. Can measure furrows upto 70 cm width.
2. Wide range of depth measurements from 10 cm above to 50 cm below ground level.
3. Close measurement interval of 1 cm between pins.

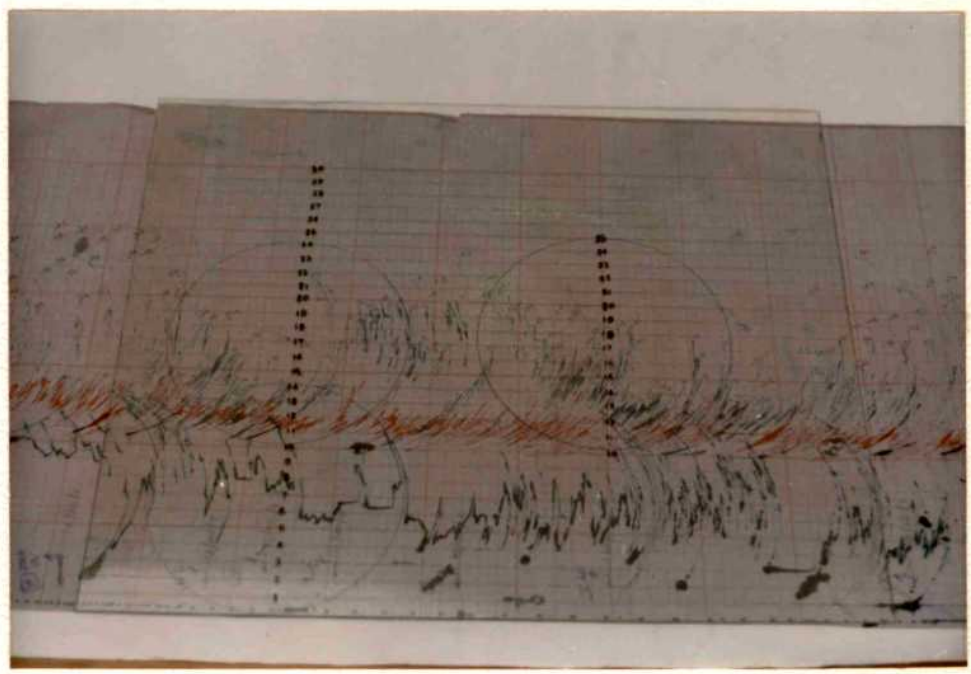

PLATE 3.6. TEMPLATE FOR READING CHART RECORDINGS MADE BY TILLAGE DYNAMOMETER

4. Facility to make direct plotting of furrow profile
5. Light in weight (8.5 kg) and compact (77 cm x 87 cm)
6. Convenient pin holding and relaxing mechanism for ease of operation.
7. Rugged construction for extensive field use.

b. Construction

The furrow profile meter (Fig.3.10) had the following major components.

1. Frame and plotting board
2. Measuring pins
3. Pin holding and release mechanism
4. Paper feeding arrangement

The frame was fabricated from aluminium sections. The two upright members of size 40 mm x 40 x 3 mm were riveted to cross members. The two cross members at the bottom had guide holes drilled in them to receive the measuring pins. The upper cross member provided at the back facilitated easy handling of the profile meter. A 3 mm thick Hylam sheet riveted to the frame formed the plotting board. Aluminium tubes of 9.5 mm outer diameter and 76 cm length, each weighing 46 g were used as measuring pins. The ends of the pins were plugged with plastic caps. The pins were mounted to slide freely in the guide holes drilled at 1 cm interval. The pins were held in place by a clamping arrangement, Fig.3.11. The clamping was effected by pressing a rubber lined aluminium section against the measuring pins by a set of leaf springs. The pins were released by a release lever mechanism, Fig.3.11. The graph sheet for recording the furrow profile was fed from a roller mounted behind the plotting board and taken up by another roller at the upper rear side (Fig.3.12). This arrangement eliminated the necessity to mount paper and a series of plots could be made by incremental feeding of graph sheet.

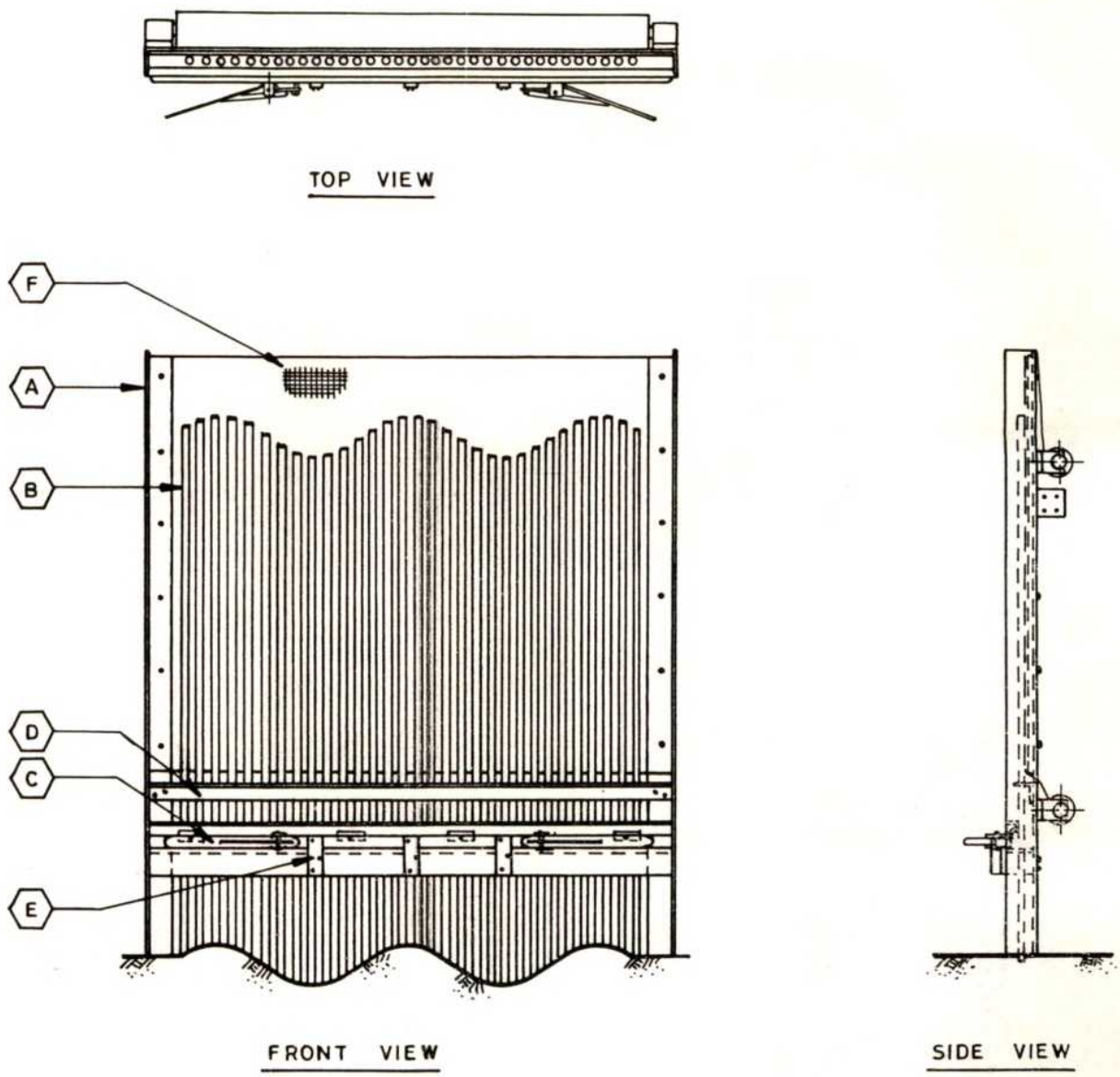

Fig. 3.10. FURROW PROFILE METER ASSEMBLY

A - Aluminium Frame

B - Pins

C - Pin Release Lever

D - Pin Guide Bar

E - Press Bar Brace

F - Profile Marking Sheet

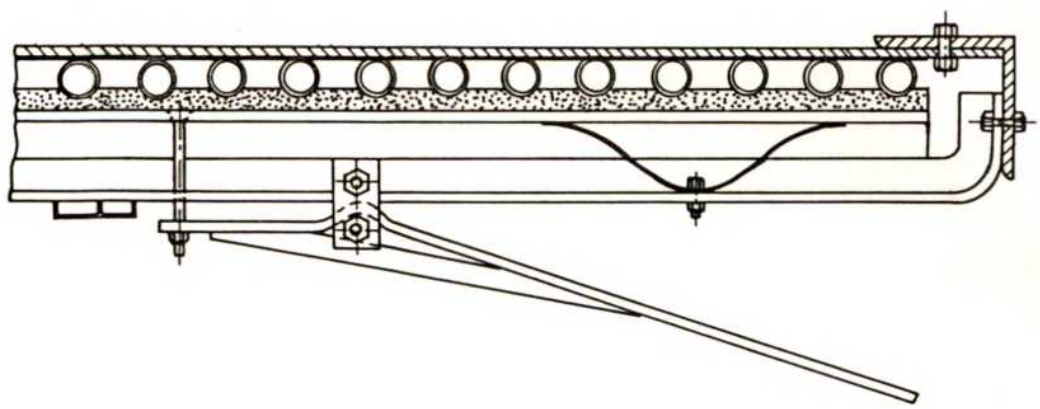

FURROW PROFILE METER

Fig. 3.11. PIN PRESS AND RELEASE ARRANGEMENT

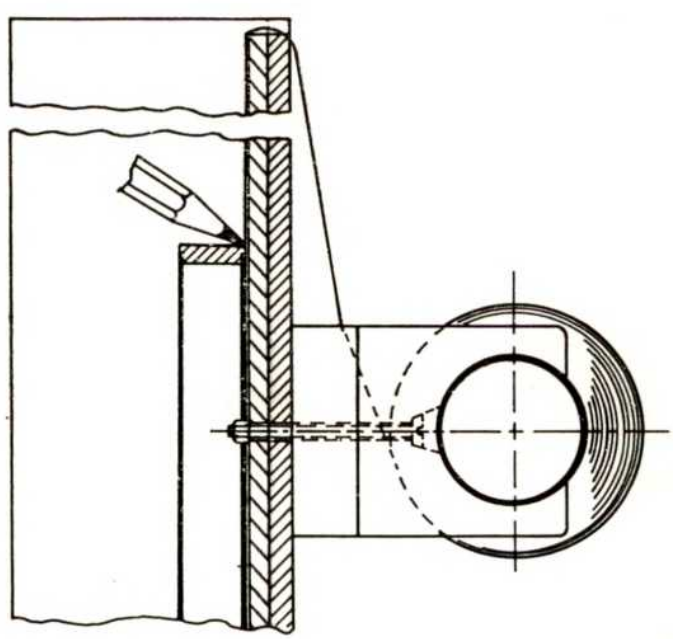

FURROW PROFILE METER

Fig. 3.12. PAPER FEED AND MARKING ARRANGEMENT

C. Operation

The furrow to be measured was carefully excavated by hand without disturbing the surrounding soil. The furrow profile meter was placed across the furrow and the measuring pins were released by operating the release lever. The furrow profile was recorded on the graph sheet by drawing a line through the tips of all the measuring pins, Plate 3.7. The profile meter was lifted out and the measuring pins brought to original position by pressing the frame against firm soil while depressing the release lever. The depth and width of furrow can be measured from the graph directly. The area of furrow was measured using a planimeter as shown in Plate 3.8. The furrow profile meter developed was used throughout the study to make measurements of furrow geometry.

3.2 Effect of Tool Geometry On Soil Reaction

Tool Geometry is the principal design factor under the control of the tool designer. Hence selection of proper tool geometry is of utmost importance in design of a tillage tool. Studies by Payne and Tanner (1959), Siemens et al (1965), Luth and Wismer (1971) McKyes and Ali (1977) Godwin and Spoor (1977) Wildman et al (1978) and Perumpral et al (1983) indicate that the draft of a chisel type tillage tool is influenced by the share lift angle α, width of share w, and length of share, l. The lift angle of share predominantly influences the soil reaction share lift angle is the angle formed between the face of share and the horizontal.

The investigations by Osman (1949) Payne and Tanner (1959), Siemens et al (1965), Mc Kyes and Ali (1977) Perumpral et al (1983), Plasse et al (1985) and Dechao and Yusu (1992) clearly indicate that a share lift angle of 20° encounters minimum draft forces and also that the draft per unit area of soil disturbed was minimum at 20° share lift angle. Hence the lift angle of share was kept constant at 20° throughout the present investigation and the width and length of share were varied.

PLATE 3.7. FURROW PROFILEMETER IN OPERATION

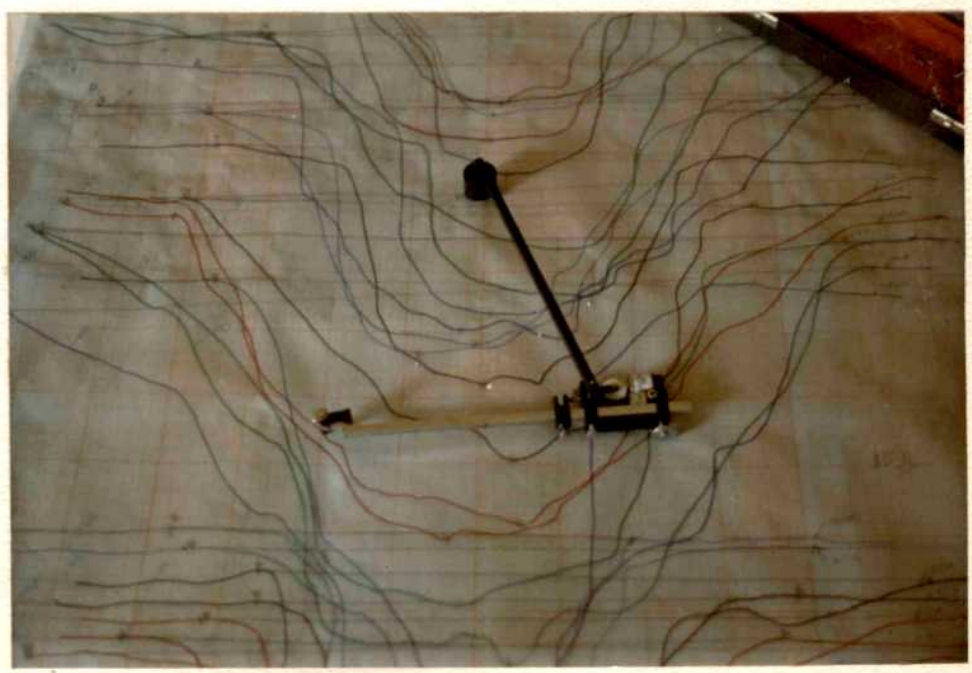

PLATE 3.8. MEASUREMENT OF FURROW CROSS SECTIONAL AREA BY PLANIMETER

The range of share width investigated was two to five centimeter so that the minimum share width was greater than the width of standard and the maximum width of share was within the draft capacity of the primemover (35 HP tractor). The length of share, l, should be sufficient to cause enough vertical displacement of soil to ensure soil failure. Reducing the length of share will reduce the influence of share on total soil reaction and the soil reaction will be predominantly influenced by the standard. Increasing the length of share will increase soil tool interface area and associated adhesive forces; also the work done on vertical displacement of soil mass will be increased.

Based on the above factors, the share geometry taken for the study was as follows:

Share Lift angle :	20°				
Share Width w, mm	20	25	30	40	50
Share length l, mm	100	150	200		

Fifteen shares with the above dimensionswere fabricated out of mild steel, Plate 3.9. All the shares were plane shares with a flat face. The shares were fabricated with a 'T' cross section for mounting to the foot provided in the tillage tool dynamometer. To reduce the rubbing of the sides of share with the furrow, the sides were machined with a 45° inward chamfer. The front cutting edge was machined to give a clearance of 5° between the bottom of tool and furrow bottom. The tool provided in the dynamometer was designed to ensure a lift angle of 20° when shares were fitted to the dynamometer. The details of a typical share are shown in Fig.3.13. Soil reaction on the different shares were measured under field conditions in the experimental plot, using the tillage tool dynamometer and the performance was investigated.

3.3 Effect of Operational Parameters on Soil Reaction

Depth and speed of operation are the two principal parameters which are under the control of the operator. These operational parameters are varied by the operator to

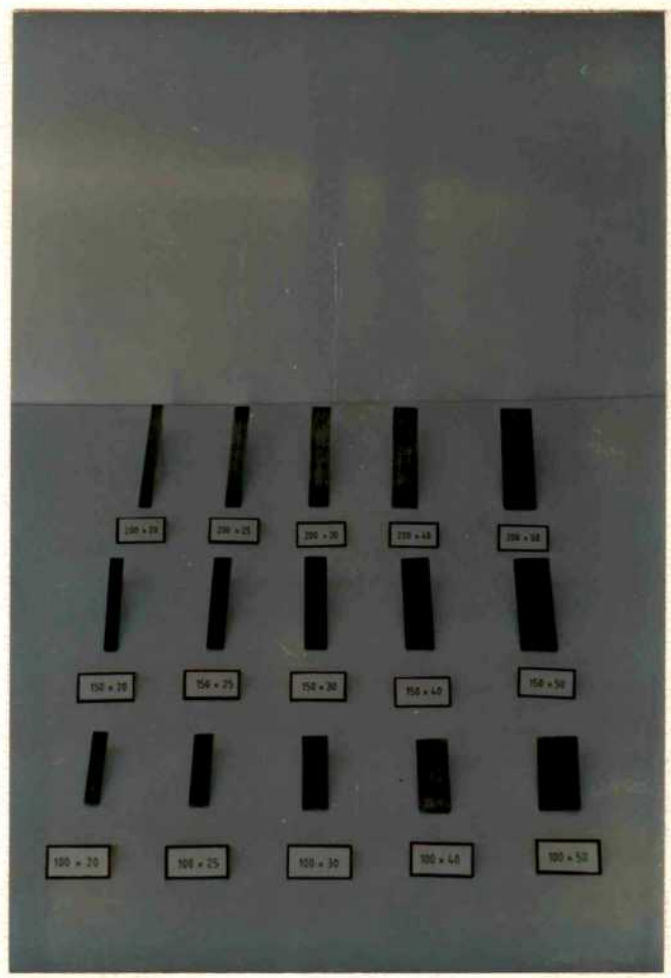

PLATE 3.9. SHARES USED IN THE EXPERIMENT

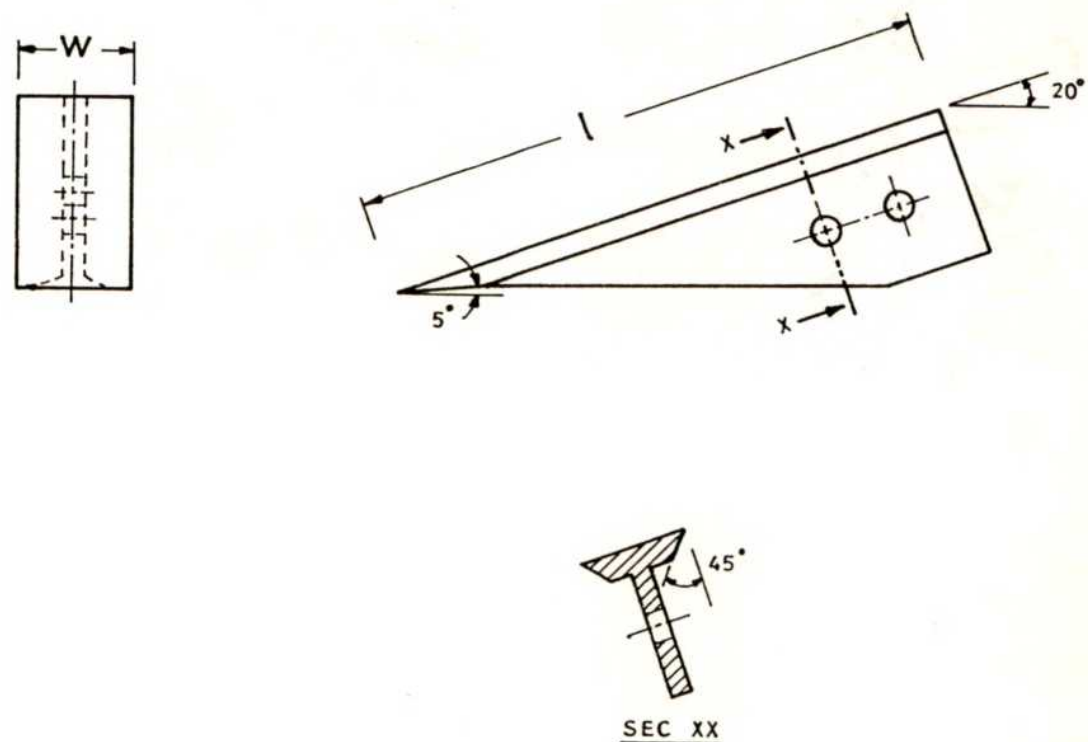

Fig.3.13. SHARE GEOMETRY OF TYPICAL EXPERIMENTAL SHARE

obtain the desired soil manipulation with minimum use of energy and in the shortest possible time.

3.3.1 Depth of operation

Depth of tillage is a significant factor in the soil plant relationship and the soil-machine relationship. The main objective of the present investigation is to develop a deep tillage tool to operate at depths more than the conventional ploughing depth of 15 to 20 cm. It was proposed to investigate performance of tools upto a maximum depth of 40 cm. To obtain the relation between depth of tillage and soil reaction, tools were tested at five target depths of 10, 20, 30, and 40 cm. The depth of tillage was varied by using the ground wheel of the dynamometer and tractor hydraulics. The ground wheel was adjusted by the depth adjusting screw and the position of the lower links were controlled through the position control system. The level of the dynamometer at each operating depth was corrected using the top link and checked by a spirit level to ensure correct tool lift angle. The implement was set to operate at different operating depths and the actual depth of operation was found by measuring the depth of furrow.

3.3.2 Speed of operation

To measure the soil reaction as a function of speed of operation, the tools were evaluated at five speeds. The speed was varied by using four transmission ratios in the lower range and one in the upper range in the tractor transmission. The speed of operation varied according to the throttle position and drawbar pull hence it was impractical to hold the speed at constant level. The actual speed of travel was obtained from the ground speed recording arrangement provided in the tillage tool dynamometer. It ranged from 0.25 to 1.25 m/s.

3.4 Effect of tool geometry and operational parameters on soil Manipulation

The typical behaviour of a narrow deep tillage tool is the three dimensional soil failure pattern. The mechanics of failure and geometry of failure depend on tool geometry and operational parameters. To investigate these interactions, the soil failure pattern created by the tools were observed by measuring the shape of furrow created by different tools at different depths of operation. As significant variation of furrow shape with change in speed of operation could not be observed, the data on furrow geometry was investigated with respect to the operating depth by pooling the data observed over different speeds. The furrow profile created by each share under varying depths of operation was measured at a minimum of fifteen locations. The furrow shapes were recorded by using a furrow profilemeter by following procedure outlined in sec. 3.1.3.

3.5 Experimental Design and Procedure

The experimental work was conducted at the College of Agricultural Engineering, Tamil Nadu Agricultural University, Coimbatore. The experiment was laid out in field No.75 of the Eastern Block. The field was fallow for a period of eight months after the previous crop of fodder sorghum. The physical characteristics of the soil in this field are tabulated in Table 4.2. The layout of the field is illustrated in Fig.3.14. The field was divided into fifteen blocks. The shares were assigned to each block randomly. Within each block the shares were operated in five depths and five speeds so as to obtain 25 treatments in each block. The pattern of variation of depth and speed within each block are shown in Fig.3.15.

3.5.1 Characterization of experimental field

The physical nature of each block was characterized by making measurements of cone index and moisture content. The moisture content was measured by gravimetric method. The soil samples for determination of moisture content were obtained by sampling through the soil profile immediately after the experiment. The cone index measurements

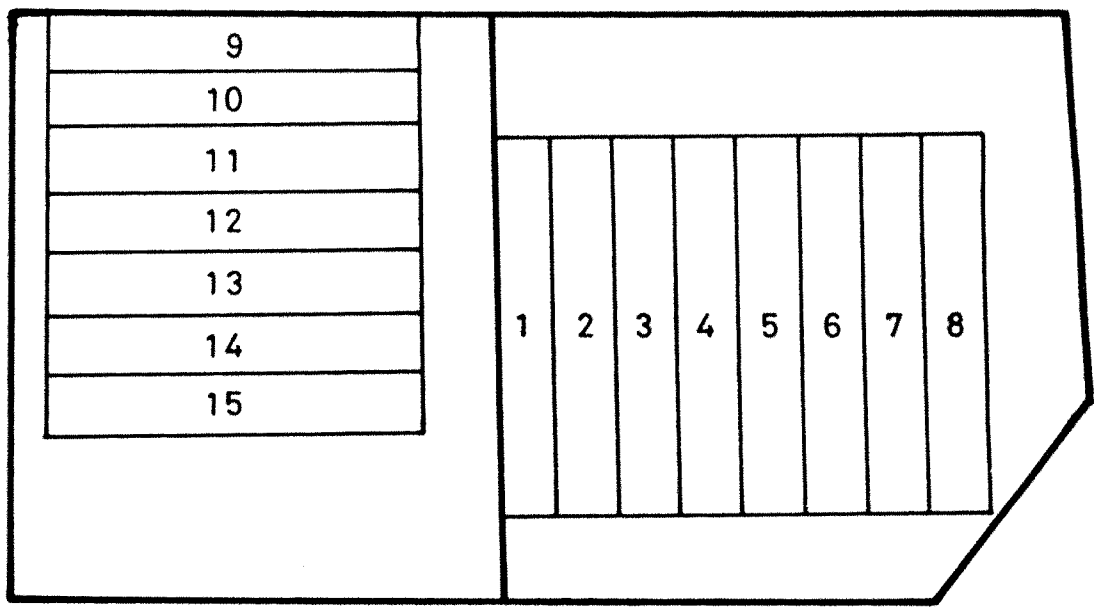

Fig.3.14. LAYOUT OF BLOCKS IN FIELD No. 75 OF EASTERN BLOCK

$D_1 S_1$	$D_1 S_2$	$D_1 S_3$	$D_1 S_4$	$D_1 S_5$
$D_2 S_1$	$D_2 S_2$	$D_2 S_3$	$D_2 S_4$	$D_2 S_5$
$D_3 S_1$	$D_3 S_2$	$D_3 S_3$	$D_3 S_4$	$D_3 S_5$
$D_4 S_1$	$D_4 S_2$	$D_4 S_3$	$D_4 S_4$	$D_4 S_5$
$D_5 S_1$	$D_5 S_2$	$D_5 S_3$	$D_5 S_4$	$D_5 S_5$

Fig.3.15. LAYOUT OF TREATMENTS IN EACH BLOCK

TABLE.3.2. RANDOMIZED ALLOTMENT OF SHARES

WIDTH mm / LENGTH mm	20	25	30	40	50
100	2	7	13	8	15
150	12	1	4	10	11
200	9	14	5	3	6

were made using the cone penetrometer as detailed in sec. 3.11. The cone index measurements were made before the commencement of the experiment. The cone penetrometer measurements were taken up to a depth of 40 cm.

3.6 Simulation Models for Deep Tillage Tool

To understand the behaviour of deep tillage tools when tilling compacted dry clay soils, the behaviour of the tool was simulated by using mathematical models. The following three dimensional soil failure model were used.

1. Godwin and Spoor 1977
2. McKyes and Ali 1977
3. Perumpral et al. 1983
4. Swick and Perumpral 1988

3.6.1 Measurement of soil parameters

Three soil values were used in simulating the performance of tillage tools. They are the bulk density, soil-metal friction and shear strength parameters.

a. Measurement of bulk density

To measure the bulk density of soil in situ, a technique similar to that adopted by Hakansson (1990) was used. A cylindrical steel tube of 102 mm inner diameter, 2 mm thickness and 250 mm length provided with a beveled cutting edge was driven into the soil. A tray was lowered around the tube and the level of soil inside the tube was noted. Then, a uniform layer of soil was excavated and weighed. The volume of soil was determined by the difference in level measurements. The procedure was repeated to get successive measurements. The moisture content of each sample was also measured. The experiment was replicated thrice in the experimental field. The bulk density and moisture content were used to obtain the dry bulk density or density at any specified moisture level using the formulae by Bernier et al. (1989) as

$BD_d = BD_w/(1+MC/100)$ 3.1

Where

BD_d = Dry bulk density

BD_w = Wet bulk density and

MC = Moisture content

b. Measurement of soil-metal friction

A rectangular mild steel slider (100 x 200 mm) was used to evaluate the soil metal friction. The slider was applied normal loads by deadweights and the frictional resistance was measured by spring balance.

c. Measurement of shear strength parameter

A torsional shear apparatus was fabricated and used to measure the shear strength of soil. The apparatus consisted of an annular shear ring with 50 mm inner diameter and 135 mm outer diameter. The annular ring was provided with eight grousers of 25 mm height. The shear ring was attached to a 1500 mm long, 50 mm diameter tube with a hexagonal head. The normal load was applied by placing dead weights above the shear box and the torque required to shear the soil was applied through a torque wrench. The torque setting of the wrench was gradually increased until the soil failed by shear, plate 3.10. From a plot of the shear stress - normal stress curve, the values of cohesion and angle of internal friction were determined.

3.6.2 Godwin and Spoor (1977)

a. Principle:

Godwin and Spoor model is based on the principle that the soil ahead of a narrow tillage tool failed in two modes (Fig.3.16a).

i. An upper failure zone where the displaced soil has forward, sideways and upward components, termed crescent failure.

ii. A lower failure zone where the displaced soil has components both in the direction of travel and sideways, termed lateral failure.

PLATE 3.10. TORSIONAL SHEAR APPARATUS IN USE

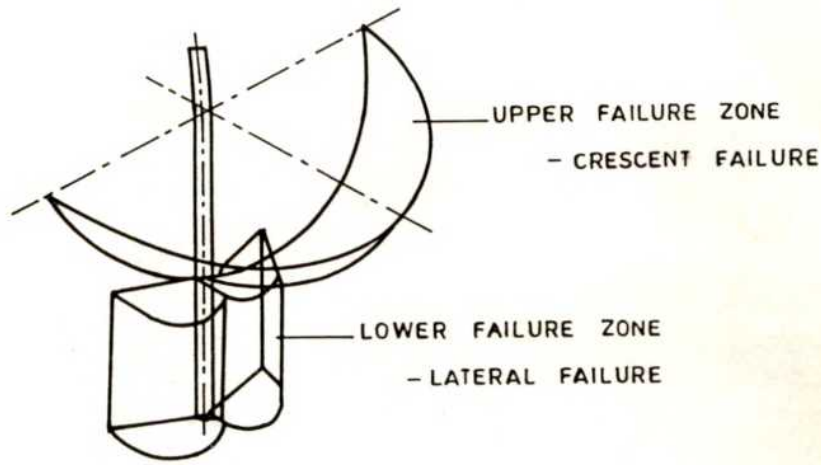

a) SOIL FAILURE MECHANISM

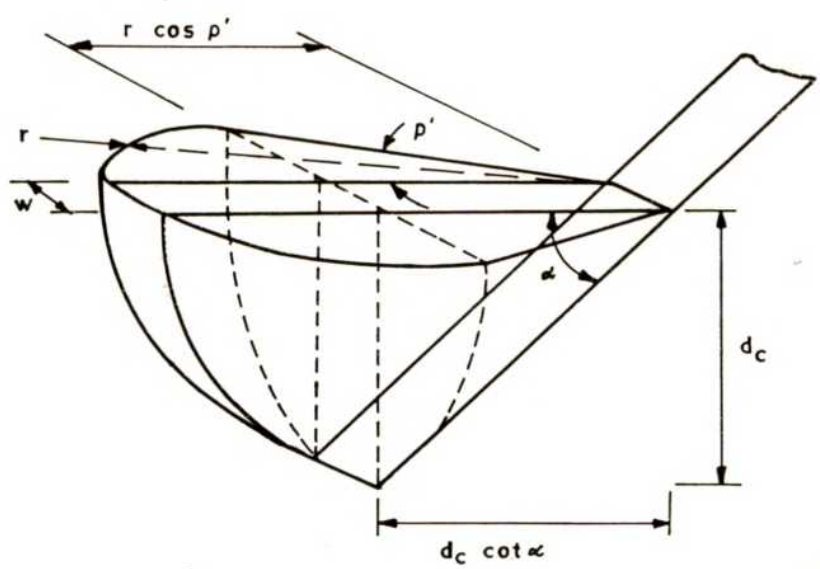

b) CRESCENT GEOMETRY

Fig.3.16. GODWIN AND SPOOR MODEL (1977)

The critical depth at which the transition occurs is a function of working depth/ width ratio. This model estimates the forces on tool and the position of critical depth for a wide range of tine aspect ratios.

b. Prediction Equations

Simple passive failure is considered to occur in the upper failure zone and was estimated by using the prediction equation given by Hettiaratchi et al (1966) as

$$P = \gamma Z^2 N_\gamma + CZN_c + C_aZN_a + qZN_q \quad \ldots. \quad 3.2$$

where

P = Passive force on crescent element

γ = soil bulk density

Z = depth

N_γ, N_c, N_a and N_q are Dimensionless numbers for gravitational, cohesive, adhesive and surcharge components respectively

C = Cohesion

C_a = Soil-metal adhesion

q = surcharge pressure

α = rake angle or lift angle

δ = angle of soil-metal friction and

ϕ = angle of shearing resistance

The N factors were given as a family of curves for different values of α, ϕ, $\delta = 0$ and $\delta = \phi$. The three dimensional failure crescent is modeled with a central linear section flanked by two curved sections of constant radius. The forces due to side crescents were arrived at by integrating the force on an elemental section. The total horizontal force component for the linear and two curved sections is given by

$$H_T = [\gamma d_c^2 N_\gamma + Cd_cN_c + qd_cN_q]\ [w + md_c \sin(\cos^{-1}(\cot\alpha/m))]$$
$$\sin(\alpha+\delta) + C_awd_c(N_a \sin(\alpha+\delta) + \cos\alpha) \quad \ldots. \quad 3.3$$

where

m = rupture distance ratio

d_c = critical depth

and the total vertical force component for crescent failure, V_T is given by

$$V_T = -[\gamma d_c^2 N_\gamma + C d_c N_c + q d_c N_q][w+m d_c \cos^{-1}[\cot\alpha/m) \quad \ldots. 3.4$$

$$\cos(\alpha+\delta) - Cawdc[Na\cos(\alpha+\delta) - \sin\alpha]$$

where

$m = r/d_c$ and

.... 3.5

$$\rho' = \cos^{-1}(\cot\alpha/m) \quad \ldots. 3.6$$

where

ρ' = maximum angular limit of crescent element

The failure below the critical depth is analysed similar to the case of a deep narrow footing using technique developed by Meyerhof(1951). The total horizontal force on tine face below critical depth is expressed as

$$Q = WCN_c'(d-d_c) + 0.5\ K_0 \gamma w N_q'\ (d^2-dc^2) \quad \ldots\ldots 3.7$$

Where

$K_0 = (1-\sin\phi)$

Q = force on tine face at depths greater than critical depth

N_c' = Dimensionless number - cohesive

N_q' = Dimensionless number - gravitational

Godwin and Spoor gave the values of N_c' and N_q' as a function of shearing resistance.

The critical depth at which the transition from crescent failure takes place can be experimentally or analytically found out.Differentiating the total tool force with respect to critical depth and equating to zero, Godwin and Spoor gave the following equation to evaluate critical depth.

$$d_c = [-b\pm(b^2-4ac')^{0.5}]/2a \quad \ldots. 3.8$$

Where

$$a = 3\gamma N_\gamma \sin(\alpha + \delta)\ m \sin(\cos^{-1}(\cot\alpha/m)) \quad \ldots. 3.9$$

$$b = 2(CN_c + qN_q)m \sin(\cos^{-1}(\cot\alpha/m))\ \sin(\alpha + \delta) + 2\gamma N_\gamma \sin(\alpha + \delta)w$$

$$- (1 - \sin\phi)\gamma w N_q' \quad \text{.... 3.10}$$

$$C' = (CN_c + C_a NA + qN_q)\mathrm{Sin}(\alpha + \delta)w + C_a w\cos\alpha - w_c N_c' \quad \text{....3.11}$$

c. Simulation procedure

The values of m, N_γ, N_c, N_a, N_c' and N_q' were obtained from curves given by Godwin and Spoor (1977) and Hettiaratchi et al (1966) for different values of tool lift angle. A computer program was written in FORTRAN 77 to calculate the tool forces and critical depth. The soil parameters measured were used to predict performance of tools of different geometry. The programme listing is given in Appendix A. The values of N factors used are tabulated in Appendix A.

3.6.3 McKyes and Ali (1977)

a. Principle

The three dimensional soil failure model for narrow blades developed by McKyes and Ali breaks the complex crescent shape of failure boundary into simple geometries by suitable approximations. This model predicts the size of failure crescent and tool forces. The logspiral failure surface is replaced by a straight plane making an angle β with the horizontal. The central section of failure zone is modeled by a simple wedge for lift angle α less than $90°-\phi$ and by two simple wedges for α greater than $90°-\phi$. The side crescents were assumed to be circular. The geometry of failure boundary is illustrated in Fig.3.17a. From the geometry of failure,

$$r = d(\cot\alpha + \cot\beta) \text{ and} \quad \text{.... 3.12}$$

$$\mathrm{Cos}\ \rho' = (d/r)\cot\alpha \quad \text{.... 3.13}$$

Where

r = = Radius of crescent and

β = Angle made by rupture envelop with horizontal .

b. Prediction Equation

The forces acting on the central section and side crescents are illustrated in

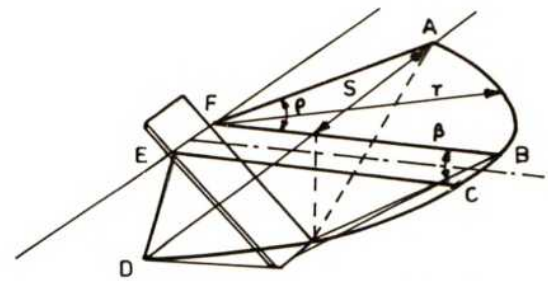

a) SOIL FAILURE MODEL

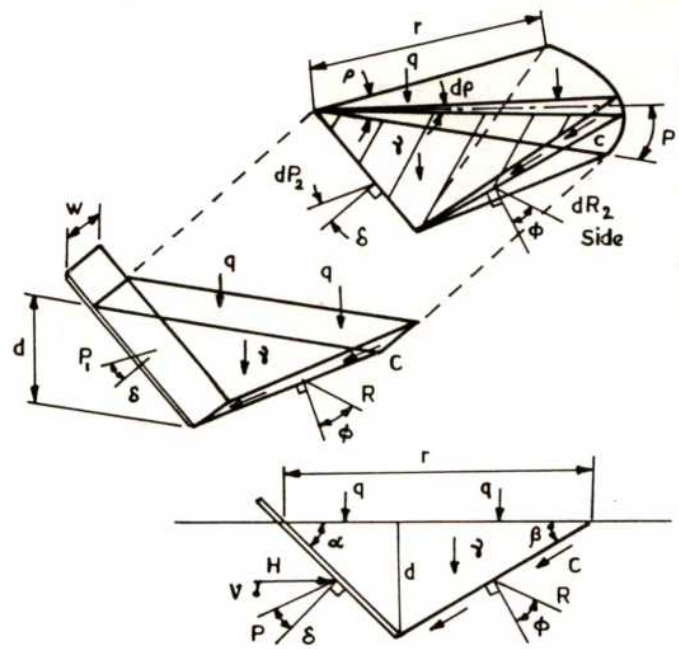

b) FORCES ACTING ON SOIL SEGMENTS

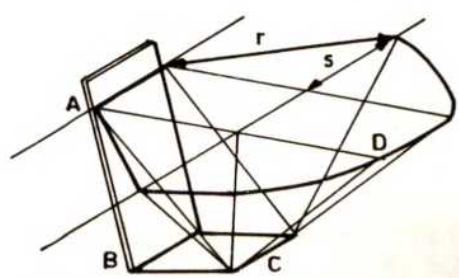

c) MODEL FOR BLADES OF HIGH RAKE ANGLE

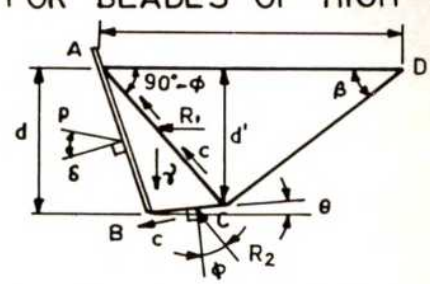

d) FORCES ACTING ON WEDGE ABC

Fig. 3.17. MEKEYES AND ALI MODEL (1977)

Fig.3.17b. Resolving the forces on the central section and writing the equations for equilibrium, we obtain the horizontal component.

$$H_1 = \{(\gamma d^2 r/2d) + Cd(1+\cot\beta\,Cot(\beta+\phi) + (qdr/d)\}w/(Cot(\alpha+\delta) + Cot(\beta+\phi) \quad \ldots. 3.14$$

Considering the equilibrium of an elemental segment of the crescent and integrating the forces, the horizontal forward force on each side crescent, H_2 were arrived as

$$H_2 = \{(1/6)\gamma dr^2 + (1/2)Cdr(1+Cot\beta\ Cot(\beta+\phi)) + (1/2)qr^2\}sin\rho' /(cot(\alpha+\delta) + Cot(\beta+\phi) \quad \ldots. 3.15$$

The total horizontal soil reaction on tool can be written in the form

$$H = (\gamma d^2 N_{\gamma H} + CdN_{cH} + qdN_{qH})w \quad \ldots. 3.16$$

where

$$N_{\gamma H} = (r/2d)(1+(2rd\ Sin\rho'/3dw))/(Cot(\alpha+\delta) + Cot(\beta+\phi)) \quad \ldots. 3.17$$

$$N_{CH} = (1+Cot\beta Cot(\beta+\phi))(1+(rdSin\rho'/dw))/(Cot(\alpha+\delta) + Cot(\beta+\phi)) \quad \ldots. 3.18$$

$$N_{qH} = (r/d)(1+(rdSin\rho'/dw))/(Cot(\alpha+\delta) + Cot(\beta+\phi)) \quad \ldots. 3.19$$

and the vertical force on tool can be found as

$$V = H\ Cot(\alpha+\delta) \quad \ldots. 3.20$$

The value of rupture angle β is chosen as the value at which $N_{\gamma H}$ is minimum.

When the tool lift angle α is greater than $90-\phi$, the two wedge model (Fig.3.17c) is used to predict the tool forces. By geometry of failure, for the case When $\delta = \phi$,

$$d' = (dCos\phi/Sin\alpha)(Sin(\alpha+\phi) + Cos(\alpha+\phi)tan(135 - (5\phi/2)-\alpha) \quad \ldots. 3.21$$

The forces on the wedge are resolved (Fig.3.17d) to obtain the force factors when $\delta = \phi$

$$H_1 = \{\gamma d'^2 N_{\gamma H}' + Cd'N_{cH}' + qd'N_{qH}'\}w \quad \ldots. 3.22$$

where

$$N_{\gamma H}' = (d'/2d)(\tan\phi - \cot\alpha + (2d'/d)N_{\gamma H}^{*}\cot(\theta+\phi)/(\cot(\alpha+\delta) + \mathrm{Cot}(\theta+\phi)) \quad \ldots. 3.23$$

$$N_{CH}' = \{1-(2d'/d) - ((2d'/d)\tan\phi - \cot\alpha)\mathrm{Cot}(\theta+\phi) + d'/dN_{cH}^{*}\cot(\theta+\phi)\}/(\cot(\alpha+\delta) + \cot(\theta+\phi)) \quad \ldots.3.24$$

$$N_{qH}' = (d'/d)N_{qH}^{*}\cot(\theta+\phi)/(\cot(\alpha+\delta) + \cot(\theta+\phi)) \quad \ldots.3.25$$

where

$\theta = 135 - (3\phi/2) - \alpha$ and

N^{*} are values obtained for simple wedge for a blade rake angle of $90 - \phi$. The N values for intermediate values of δ were arrived through an interpolation formula

$$N_\delta = N_{\delta=0}(N_{\delta=\phi}/N_{\delta=0})^{\delta/\phi} \quad \ldots. 3.26$$

The extent of the crescent at each sides is given by

$$S = r\ \mathrm{Sin}\rho' \quad \ldots. 3.27$$

$$= d(\mathrm{Cot}\alpha + \mathrm{Cot}\beta)\ \mathrm{Sin}\rho' \ ;\ \alpha < 90 - \phi \quad \ldots. 3.28$$

$$= d'(\tan\phi + \mathrm{Cot}\beta) \qquad \alpha > 90 - \phi \quad \ldots. 3.29$$

The area of furrow can be approximated as

$$A = (w+S)d \quad \ldots. 3.30$$

c. Simulation procedure

A computer programme was written in FORTRAN 77 to calculate the tool forces and furrow geometry for tools of different geometry and aspect ratios. The soil parameters measured in situ were utilized. The programme was designed to arrive at the rupture angle β by repeated iterations in small increments so that $N_{\gamma H}$ was minimized. The programme is listed in Appendix A.

3.6.4. Perumpral Grisso and Desai (1983)

a. Principle

This model is based on limit equilibrium analysis. The model incorporates the three-dimensional aspect of the problem by considering the total crescent formation in front of tool. For simplicity the side crescents were replaced with a set of forces on either side of central wedge. Also, the curved surfaces are assumed to be straight. The dimensions of the idealized wedge are shown in Fig.3.18 a.

b. Prediction Equations

The force vectors acting on the idealized wedge are shown in Fig.3.18b. The effect of the side crescent are represented by the force vectors R,SF_2 and CF_2 on the faces abc and def

$$R = \gamma K_o Z A \quad \text{.... 3.31}$$

where

R = Normal force on abc and def

$$K_o = (1 - \sin\phi) \text{ and} \quad \text{.... 3.32}$$

$$Z = (1/3)(d+H) \quad \text{.... 3.33}$$

The area of surface abc & def are given by

$$A = 0.5d^2(1+H/d)[(1+H/d)(\cot\alpha + \cot\beta)] \quad \text{.... 3.34}$$

where

d = tool depth

H = Height of soil heave in front of tool at failure

$$SF_2 = R\tan\phi \quad \text{.... 3.35}$$

$$CF_2 = CA \quad \text{.... 3.36}$$

where

SF_2 = Frictional force on abc and def

CF_2 = Cohesional force on abc and def

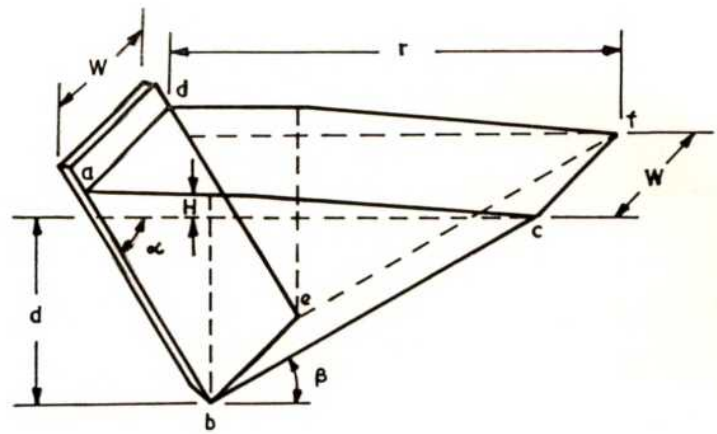

a) GEOMETRIC BOUNDARIES OF AN IDEALIZED FAILURE WEDGE

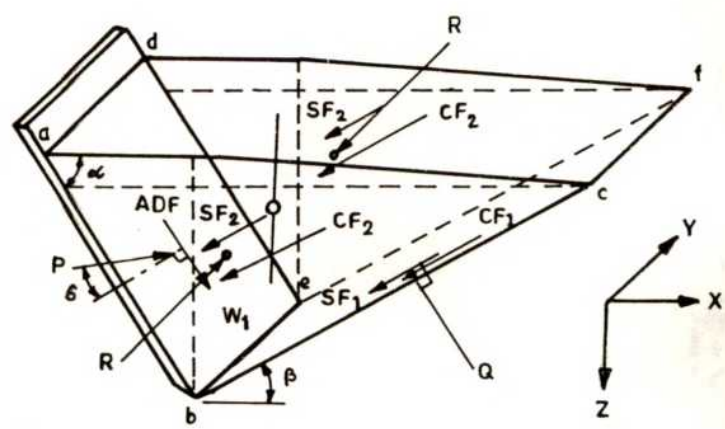

b) AN IDEALIZED FAILURE WEDGE AND THE FORCES ACTING AT FAILURE

Fig.3.18. PERUMPRAL MODEL (1983)

The forces on the rupture plane bcfe are

$$CF_1 = CwD/\sin\beta \quad \ldots. 3.37$$

$$SF_1 = Q \tan\phi \quad \ldots. 3.38$$

The adhesional force in the soil tool interface is given by

$$ADF = A_d Bd(1+H/d) \sin\alpha \text{ and} \quad \ldots. 3.39$$

$$W = \gamma wA \quad \ldots. 3.40$$

Considering the equilibrium of wedge in two directions and eliminating Q we get

$$P = [1/\sin(\alpha+\phi+\beta+\delta)] [-ADF\cos(\alpha+\phi+\beta) + 2SF_2\cos\phi + W\sin(\phi+\beta) + 2CF_2\cos\phi+CF_1\cos\phi] \quad \ldots. 3.41$$

Considering that the value of H is negligible it was omitted. Since the tool movement causes a passive failure, the passive earth pressure theory (Terzaghi 1959) was used. Accordingly the rupture angle β was that angle at which P is minimum.

C. Simulation procedure

A computer programme was written in FORTRAN 77 to consider different rupture angles in small increments and evaluate the value of β at which P is minimum. The programme listing is available in Appendix A. The programme was run using soil properties measured in the experimental field for different geometrical configurations of tool.

3.6.5. Swick and Perumpral (1988)

a. Principle

This model is based on earlier model developed by Perumpral et al (1983). The salient feature of this model is the inclusion of the effect of tool speed. It was concluded experimentally that soil shear strength and soil-metal friction are independent of shear rate . Hence only the effect of acceleration of soil mass due to tool speed was included. A three dimensional soil failure model with explicit consideration of side crescent was used

b. Prediction Equations

The central wedge and forces on it are represented in Fig.3.19a. The acceleration force acts parallel to the rupture surface and is given by

$$F_{a1} = (\gamma/g)wd\gamma v^2 \sin\alpha/\sin(\alpha+\beta) \quad \ldots. 3.42$$

The force due to surcharge pressure q is

$$F_{q1} = qwr \quad \ldots. 3.43$$

The rupture distance r is given by

$$r = d(\cot\alpha + \cot\beta) \quad \ldots. 3.44$$

The cohesional and frictional forces on rupture surface are

$$CF_1 = Cwd/\sin\beta \quad \ldots. 3.45$$

$$SF_1 = Q_1 \tan\phi \quad \ldots. 3.46$$

The adhesional force ADF on soil-tool interface is

$$ADF = A_d wd/\sin\alpha \quad \ldots. 3.47$$

The weight of the central wedge is given by

$$W_1 = (1/2)\gamma wdr \quad \ldots. 3.48$$

The geometry of the side wedge is shown in Fig.3.19b. The maximum width of side wedge was obtained from experimental relation as

$$S = -6.03 + 0.460r + 0.0904\beta \quad \ldots. 3.49$$

where

S and r are in cm and β in degrees and

$$\rho' = \text{Arcsin}(S/r) \quad \ldots. 3.50$$

The tool force in the direction of movement due to the side wedge is evaluated by integrating the forces on an elemental wedge as illustrated in Fig.(3.19c). By

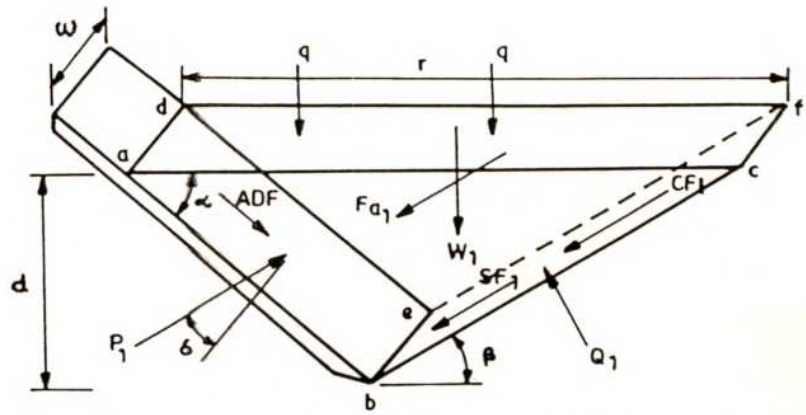

a) IDEALIZED FAILURE WEDGE AND FORCES AT FAILURE

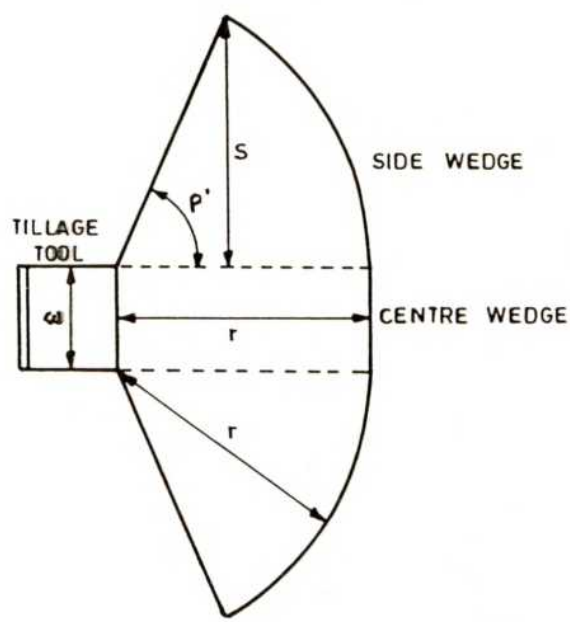

b) TOP VIEW OF SOIL FAILURE WEDGE

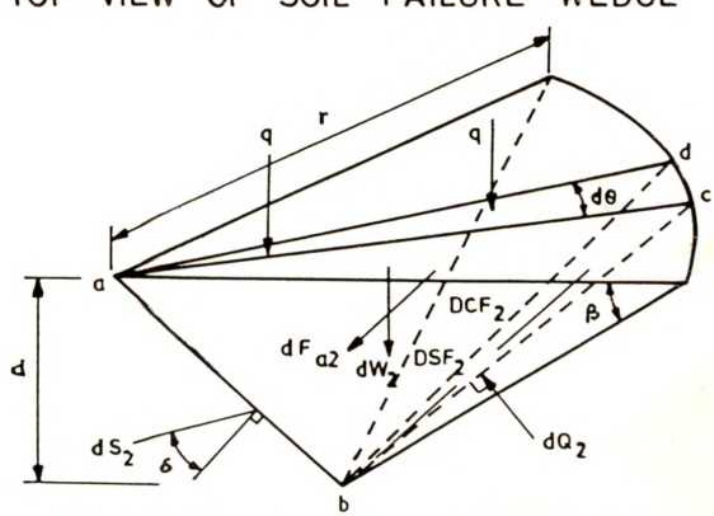

c) A SIDE PORTION OF THE IDEALIZED FAILURE WEDGE

Fig. 3.19. SWICK AND PERUMPRAL MODEL (1988)

considering the equilibrium of the central and side wedges, the total tool force can be obtained as

$$P = P_1 + 2P_2 \quad \ldots. 3.51$$

where

$$P_1 = [-ADF\ \cos(\alpha+\phi+\beta) + (W_1 + F_{q1})\sin(\phi + \beta) + (CF_1 + F_{a1})\cos(\phi)] / [\sin(\alpha + \phi + \beta + \delta)] \quad \ldots. 3.52$$

and

$$P_2 = [(W_2+F_{q2})\ \sin(\phi+\beta)\ \sin\rho'+f_{a2}\ Cos\phi(\rho'/2+(\sin 2\theta)/4) + Cf_2\cos\phi\sin\rho'\theta)/[\sin(\alpha+\phi+\beta+\delta)] \quad \ldots. 3.53$$

where

$$f_{a2} = (1/2)(\gamma/g0drV^2\sin\alpha/\sin(\alpha+\beta) \quad \ldots. 3.54$$

$$f_{q2} = (1/2)^{qr}2$$

$$Cf_2 = (1/2)Cdr/\sin\beta \quad \ldots. 3.55$$

$$W_2 = (1/6)\gamma dr^2 \quad \ldots. 3.56$$

Since the tool movement in soil creates a passive condition. The failure takes place when the resistance by the soil wedge is minimum, the value of β for which P is minimum gives the values of β and P.

C. Simulation Procedure

The tool forces encountered by tools of different geometries when operated at varying depth and speed of operation were simulated using the above model. The soil properties measured in the experimental field were used. A computer programme was written in FORTRAN 77. The programme was designed to calculate the value of P in small increments of β to arrive at the minimum value. The program is listed in Appendix A.

3.7 Optimisation of Parameters

Optimum tillage should compromise between two main factors (Wolf et al 1981)

i. Soil conditions that optimise crop development for maximum yield with available nutrient resources.

ii. Minimum operational cost especially in tillage energy.

The optimal combination of tool geometry and operational parameters was arrived by evaluating different combinations with respect to the second criteria. The performance of tools with different geometrical configurations when operated at different operational conditions was obtained from the results of the field test. The results were processed to obtain the soil reaction on the tool. The soil reaction on each tool was fitted into a regression equation of the form.

$$F = C_0 + C_1 d + C_2 S + C_3 d^2 + C_4 S^2 \quad \ldots\ 3.57$$

From the above equation, the soil reaction on different tool geometries under any given combination of depth and speed of operation were compared. Similarly the performance of the tool was analysed on the basis of the furrow geometry created. The depth-furrow cross sectional area relationship was used to compare the soil loosening by different tool geometries.

3.8 Development of an Implement for Deep Tillage

A chisel plough incorporating the following design features was developed.

1. Share geometry - optimized through experimental investigations and simulation studies.
2. Straight vertical standard with optimaly designed section
3. Frame - Light weight trihedral framed structure with tubular construction.
4. Compatibility with catagory I and II hitch systems as per IS 4468-1977.
5. Overload protection with shear pin.

3.8.1 Design parameters

The mechanical design of the chisel plough was based on the following design parameters

a. Frame geometry

i. Maximum depth of operation - 40 cm

ii. Minimum ground clearance with implement in transport position - 20 cm

iii. Hitch geometry as per IS 4468 - 1977

b. Share geometry

i. Width of share 2.5 cm

ii. Length of share 15.0 cm

iii. Share lift angle 20°

c. Design forces

i. Longitudinal soil reaction,L = 1000 kg

ii. Vertical soil reaction, V = 500 kg

iii. Location of resultant - at tip of share.

3.8.2 Mechanical design of critical components

The structural members of the implement like frame, standard and foot were designed to withstand the design loads. The frame and standard were designed out of mild steel the foot was designed with high tensile steel.

The share was designed with tempered spring steel. The structural analysis and design of the frame and standard were based on the properties of structural steel (standard Quality) -St 42-S as per IS: 226-1976. The important properties are

1. Tensile strength - 42-54 kg/mm^2
2. Yield point - 23-26 kg/mm^2
3. Modulus of elasticity - 2×10^6 kg/cm^2
4. Poisson's ratio - 0.3

The concept of load factor design (Robert et al, 1979) was adopted to estimate the desired margin of safety The ultimate load factor was based on the following ranking.

a. Material workmanship, inspection and maintanance - good
b. Accuracy of loading, control of usage of structure - poor
c. Accuracy of analysis - very good
d. Damage to life and property due to collapse - not serious

For the above ranking, the ultimate load factor was arrived from tabulated values as 2.05.

3.8.3 Design of Implement Frame

The implement frame was designed to provide a stable structure for mounting the standard with suitable overload protection. The geometry of the structure was designed to ensure proper hitch geometry.

A three-dimensional rigid framed structure was designed for the frame. The entire structure was designed with rectangular tubular members of size 80 x 40 x 3 mm. This tubular construction was to ensure a light weight structure with maximum rigidity. The three dimensional structure was the combination of two triangular framed structures in the horizontal and vertical planes. The mounting for the standard was provided between two horizontal members. The standard was pivoted between the members and retained in the vertical position by a shear pin.

The idealized structure of the frame is shown in Fig.3.20a. The orientation of the members was based on structural effectiveness and ease of fabrication. The sectional

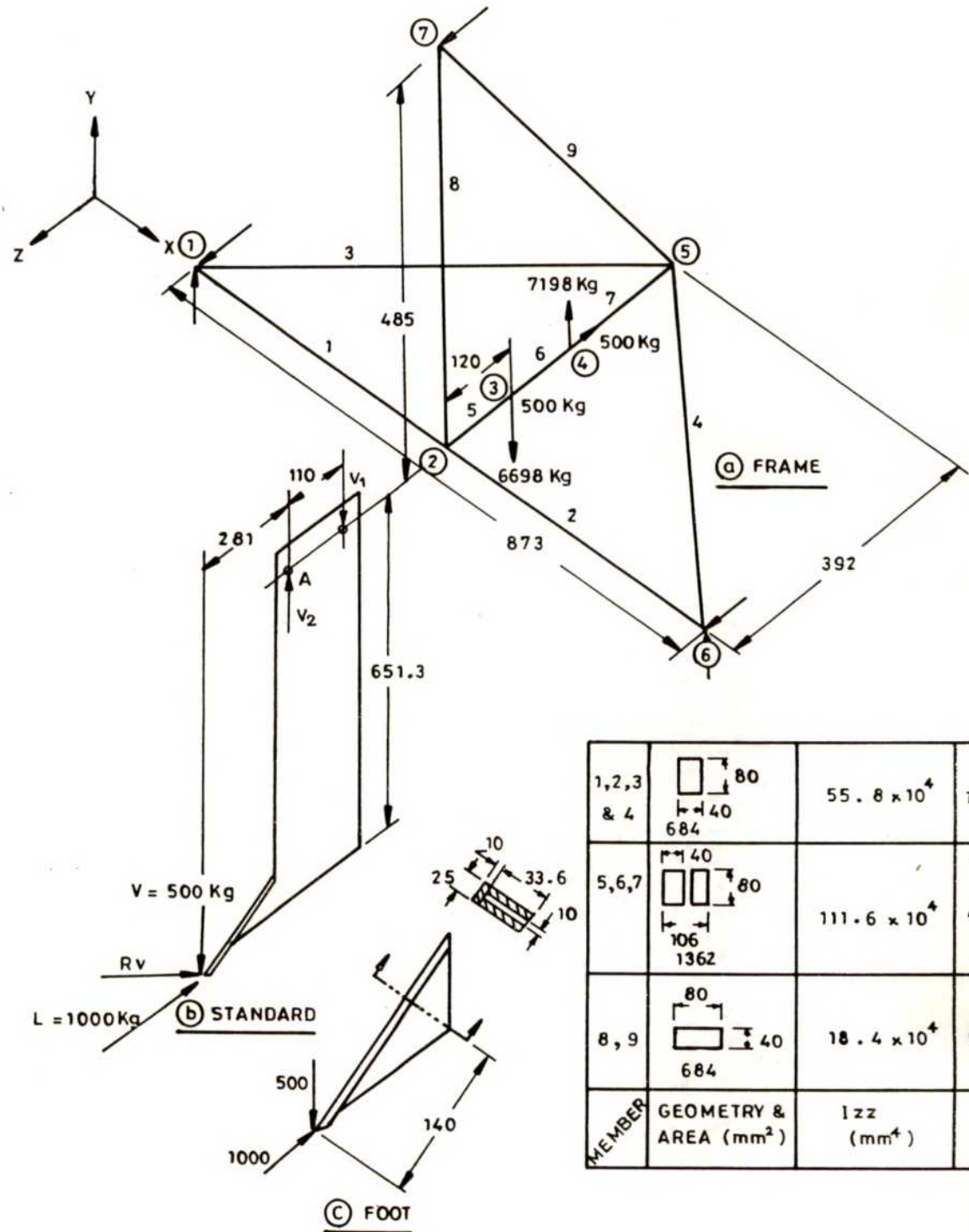

MEMBER	GEOMETRY & AREA (mm^2)	Izz (mm^4)	Iyy (mm^4)
1,2,3 & 4	80 × 40, 684	55.8×10^4	18.4×10^4
5,6,7	40 × 80, 106, 1362	111.6×10^4	401.8×10^4
8,9	80 × 40, 684	18.4×10^4	55.8×10^4

Fig.3.20. FORCES ON STRUCTURAL COMPONENTS OF CHISEL PLOUGH

properties of the member are given along with Fig.3.20a. The loading exerted on the frame when design loads were applied at the share was calculated by equating moments about A (Fig.3.20b).

$$1000 \times 651.3 + 500 \times 281 - V_2 \times 110 = 0 \quad \ldots\ldots 3.58$$

Hence $V_2 = 7198$ kg, $V_1 = -6698$ kg

and $H_1 = H_2 = 500$

The three dimensional rigid framed structure was analysed by ANSYS 4.4 structural analysis software. Each member was modeled as a three dimensional beam element. The structure had nine beam elements connecting seven nodal points. The geometry of the structure and the properties of the section were used as input data. The structure was assumed to be suported at the three hitch points and loaded as illustrated in Fig.3.20 a. The lower link hitch points were modeled to take longitudinal and vertical reactions alone. The top link hitch point was assumed to support horizontal force only. Due to the hitch point design with ball joints, the reaction moments at supports were set to zero. The analysis yielded the following results.

1. Estimated mass of structure
2. Location of centeroid of structure and moment of inertia of structure
3. Displacement solution
4. Member stresses
5. Member forces and moments in local and global co-ordinates.
6. Support reactions in local and global co-ordinates.

The results of the structural analysis are presented in sec.4.13. The analysis proved that the structure was stressed within limits when design loads were encountered.

3.8.4 Design of standard and foot

The standard was designed to ensure adequate mechanical strength at the same

time the thickness was held to a minimum. The standard was designed out of 12 mm thick mild steel plate. Its loading was similar to a cantilevered beam (Fig.3.20b).

Bending moment = 1000 x 65.13 = 65130 kg cm

Permissible tensile stress = 1122 kg/cm^2

By applying flexural equation the width of standard was calculated to be 17.03 cm.

The maximum sideways force that can be with stood by the standard having the above section was calculated to be 70 kg.

The standard was provided with a foot for mounting the share at 20°. the foot was designed out of a high-tensile steel bar (St5B-HT) with a vetical cross section of 25 x 35 mm. The overhanging section of the foot was considered as a cantilever beam and was analysed for conditions of plastic failure. The section along the upper bolt hole was considered for the design. The moment about the plane was calculated. Referring Fig.3.20c.

M = 14(500 cos 20 + 1000 sin 20) kgcm

= 11354 kg cm 3.59

Elastic modulus of section = 1.5 x 3.36^2/6

Shape factor = 2.05

For ultimate tensile strength = 500 kg/cm^2

and load factor = 2.05,

maximum permissible moment = 2.82 x 1.5 x 5500/2.05

= 11348 kg cm

Hence the foot would be safe even when the design loads were considered to be concentrated at the tip of the share.

3.8.5 Design of welded connections

The entire frame work was joined by welded joints. the optimum size of fillet weld according to IS816(1969) is 3 mm for plates with minimum thickness of 3 mm. To

ensure that each joint was atleast as strong as the parent metal, The joints were initially butt welded and then strengthened by fillet welds. The welding was done all around. The hitch forces on the lower link was distributed between two hitch plates, fillet welded to the crossbeam. The load carrying capacity of the hitch plate was calculated:

Size of fillet weld	= 3 mm
Throat area	= 24 x 0.3 x 0.7
	= 5.04 cm^2
Permissible shear stress	= 1025 kg/cm^2
Hence the load carrying capacity	= 5166 kg

However, the maximum design load on the hitch plate is only 600 kg.

3.8.6 Design of shear pin

The chisel plough was protected from damage due to overload by a shear pin. The standard was pivoted about a hinge pin and its rotation was restrained by the shear pin. Refering Fig.3.20b. the maximum resultant shear load on pin is 6717 kg. Since the design of the shear pin will allow it to fail by double shear, the diameter of the shear pin was calculated by assuming that the shear stress at failure for the high tensile steel bolt is 3000 kg/cm^2

Hence $\pi \times d^2 \times 3000/4 = 6716/2$ 3.60

or d = 11.938 mm.

To ensure that the shear bolt will fail at loads less than design load, a 9.5 mm diameter high tensile steel bolt was used.

3.8.7 Constructional Features

The chisel plough (Plate 3.11) was fabricated in the workshop of the department of farm machinery. The specifications of the first prototype are given in Fig.3.21

The frame members were cut and welded together taking adequate precaution to

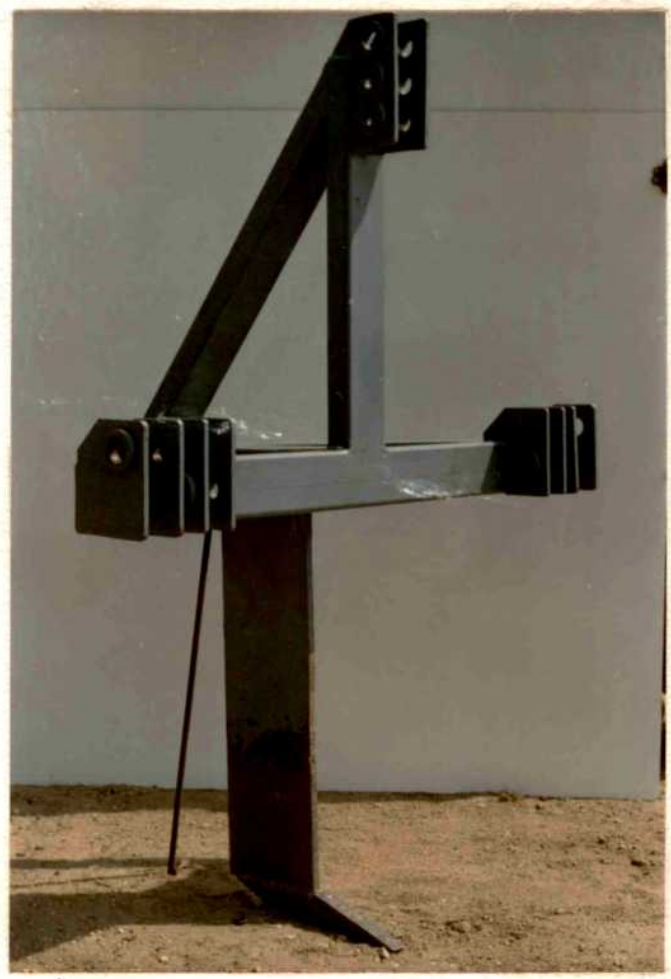

PLATE 3.11. PROTOTYPE CHISEL PLOUGH

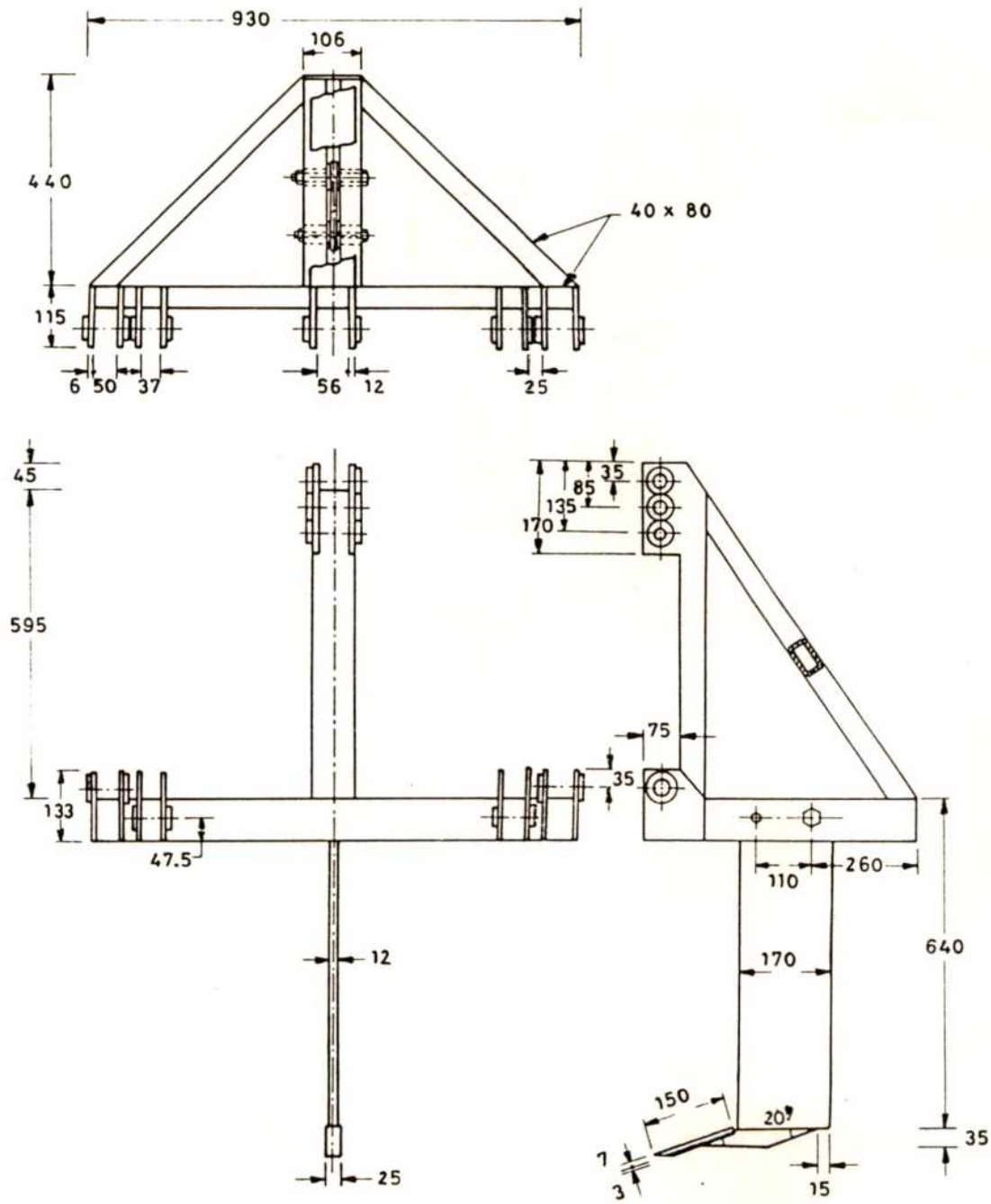

Fig. 3.21. PROTOTYPE CHISEL PLOUGH

avoid distorsion. The hitch plates were cut out of 6 mm thick mild steel plate and finished by machining the edges. The hitch plates were welded with suitable inserts to ensure adequate thickness of bars at hitch point as per standards. The hitch plates were aligned and welded to the frame. The points of attachment of the standard to the frame were reinforced by welding bushes in the members. these bushes ensured safe transfer of load to the frame and avoided local failure. The standard was cut out of 12 mm thick mild steel plate and the foot was welded at its base. The foot was machined with a 12 x 3 mm slot to retain the share latrally. The share was fastened to the foot by three bolts that passed through the foot. The share was fabricated out of 10 mm thick spring steel strip. The share was cut annealed, drilled with bolt holes and then square countersunk holes were forged. The mounting tonque and relief angle at front cutting edge were machined. The share was tempered and mounted.

3.9 Evaluation of performance

The chisel plough developed was tested to evaluate its draft, energy requirement and field performance.

3.9.1. Measurement of soil reaction

The soil reaction on the chisel plough was evaluated by measuring the draft, vertical lift force on lower link, and compression on the top link by using hydraulic dynamometers, Plate 3.12.

The draft was measured by using a hydraulic dynamometer of 1000 kg capacity, mounted between the test tractor hitched with the implement and the hauling tractor (Narayanarao and Verma 1982, RNAM 1983, Sherwddin Bukhari et al 1992). The test tractor was run with transmission in neutral and the hydraulic system fully operational. The dynamometer was hitched to ensure a horizontal pull. The rolling resistance of the test tractor under each test condition was measured by towing the tractor, with the implement in the raised position. The draft requirement was evaluated by substracting the

PLATE 3.12. MEASUREMENT OF FORCES ON IMPLEMENT THROUGH THREE DYNAMOMETER SYSTEM USING TWO TRACTORS

rolling resistance from the gross pull required. The measurement of draft is shown in Plate 3.13.

The vertical soil reaction was evaluated by measuring the lift forces exerted by the lower links. The lift force was measured by the pressure of hydraulic fluid inside the lift cylinder. The pressure gauge was mounted at the external hydraulic outlet. The ram cylinder pressure was calibrated against vertical load on lower link with the lower links in horizontal position. When the implement was operated under automatic position control mode, the lift cylinder pressure had sharp spike due to dynamic lifting action by automatic position control system. Hence the lift cylinder pressure was recorded only during stedy state condition.

The compressive force on the top link was measured by a instrumented top link, previously developed. The construction of the top link is given in Fig.3.22. The orientation of the top link at each depth of operation was also measured. The measurement of lower link lift force and top link compression is shown in plate 3.14.

The dynamometer readings were converted to corresponding values of loads. The centre of gravity was located by method of suspension (Steinbruegge 1969). The weight of the implement was also measured.

Fig.3.21b illustrates the free body diagram of the implement. From conditions of equlibrium,

Draft, P_x	=	1	
V	=	$V_L + L_C \sin\alpha - W$	.... 3.61
R	=	$\sqrt{L^2 + V^2}$	.... 3.62
θ	=	$\tan^{-1}(V/L)$ and	.... 3.63
R'L	=	$(T_c \cos\alpha xh + Wa)/L$	.... 3.64

The magnitude, location and orientation of the soil reaction on the implement was evaluated with the implement operating at different depths and speeds.

PLATE 3.13. HITCHING OF DYNAMOMETER BETWEEN TRACTORS TO MEASURE DRAFT

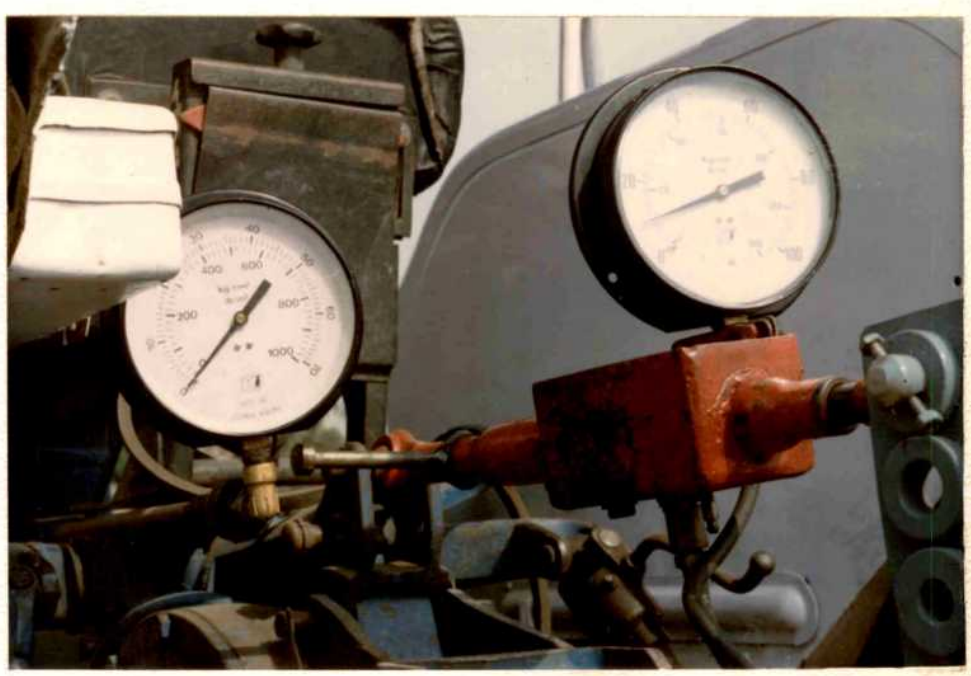

PLATE 3.14. ARRANGEMENT OF DYNAMOMETER TO MEASURE LIFT FORCE AND TOP LINK COMPRESSION

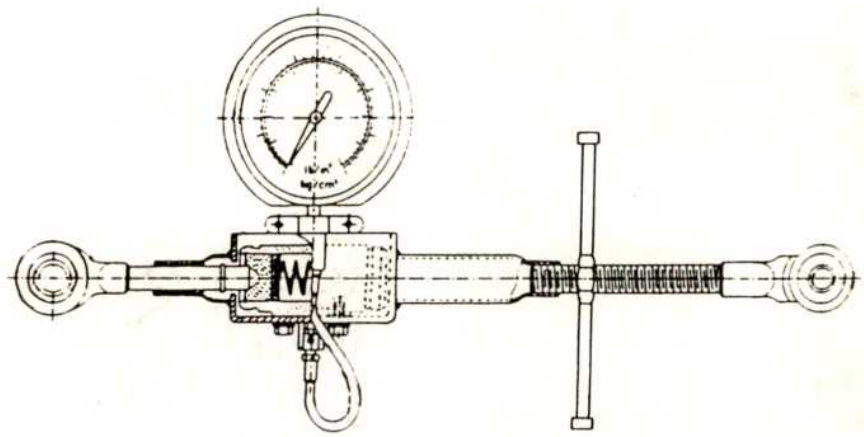

Fig.3.22. TOP LINK COMPRESSION MEASUREMENT DEVICE

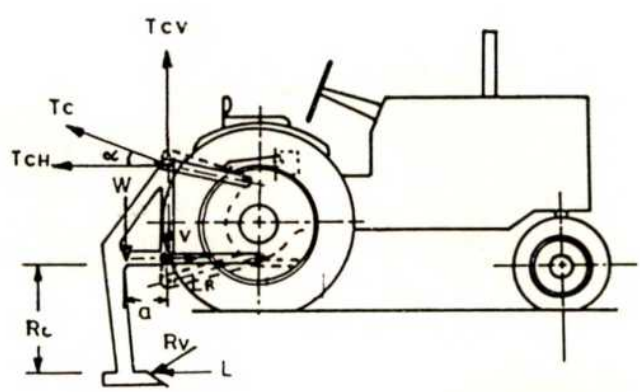

Fig.3.23. SYSTEM OF FORCES ON IMPLEMENT AND HITCH LINKS

3.9.2 Performance of tractor implement system

To evaluate the performance of the tractor implement system, the following measurements were made.

i. Top link compression and lower link lift force to evaluate draft

ii. Wheel slip

iii. Fuel consumption

The test tractor was instrumented as described earlier to measure compression in top link and lower link lift force, plate 3.15. The implement was operated by the test tractor at different depths of operation and forward speeds. The wheel slip was measured by counting the number of revolutions of the rear wheel under load and no load conditions. A counter fitted with a friction wheel was used to measure the revolution of the rear wheel as shown in plate 3.16. The fuel consumption was measured by an arrangement similar to that used by Reid (1979). The tractor was fitted with a polypropelene measuring cylinder of 1.0 litre capacity. the measuring cylinder was connected to the fuel supply system at the inlet of the fuel filter and the overflow from all points were collected and returned to the measuring cylinder plate 3.17. the fuel consumed for each test run was recorded.

From the measured values of top link compression force, lower link lifting force and previously determined values of the location of the soil reaction, the draft force was evaluated. From these informations the energy requirement and energy utilization efficiency for the tractor implement system under different operating conditions was evaluated.

3.9.3 Experimental Procedure

The evaluation of the chisel plough for its draft energy requirement and field performance was conducted under two soil conditions viz., black clay loam soil and red gravely soil. The black clay loam soil had previously tilled soil overlying compact soil and the red gravely soil was undisturbed. Cone index of the soil was measured before

PLATE 3.15. PERFORMANCE TESTING OF PROTOTYPE IMPLEMENT

PLATE 3.16. ARRANGEMENT FOR MEASURING REAR WHEEL REVOLUTIONS

PLATE 3.17. ARRANGEMENT FOR MEASURING FUEL CONSUMPTION

the experiment. The field performance trials were conducted following procedures outlined earlier. The fuel consumption measurements under red soil were not taken due to damage to the equipment during transport. To ensure correct depth of operation, the implement standard was marked with depth graduations. The implement was operated in the position control mode and minor corrections in depth of operation were signaled to the operator. The speed of operation was varied by selecting different transmission ratios. The actual forward speed was arrived by timing the test runs over fixed distance. The observation of the field trials were recorded and analysed following standard procedures.

RESULTS AND DISCUSSION

CHAPTER IV
RESULTS AND DISCUSSION

The results of the study undertaken to develop a deep tillage tool for rainfed agriculture are presented and discussed in this chapter under the following main headings.

1. Performance of instruments developed for deep tillage studies.
2. Effect of operational parameters on soil reaction
3. Effect of tool geometry on soil reaction
4. Effect of tool geometry and operational parameters on furrow geometry
5. Development of deep tillage tool
6. Performance of prototype deep tillage tool

4.1 Performance of Instruments Developed for Deep Tillage Studies

A tractor mounted cone penetrometer, recording tillage dynamometer and furrow profile meter were specially designed for investigating the performance of deep tillage tools. The performance and application of these instruments are discussed.

4.1.1. Cone Penetrometer

A tractor mounted cone penetrometer was specially designed for deep tillage studies. The salient features, construction and operation of the penetrometer are presented in Sec. 3.1.1.

The specifications of the cone confirmed to the standard cone described by Garner *et al.* (1987) and specifications confirming to ASAE standard S 313.1 (Morrison and Bartak 1987). However the power of the drive motor was insufficient to drive the cone at the ASAE standard speed of 3.1 cm/s. Hence the cone index values were standardised using the formulae developed by Perumpral (1987).

$$(C_x/C_s) = [(V_x/D_x/(V_s/D_s)]^N \quad \text{.... 4.1}$$

Where

C = penetration resistance

D = base diameter (D_s = 2.03 cm)

V = penetration rate (V_s = 182.9 cm/min).

The performance of the load measuring system was evaluated by calibrating the hydraulic dynamometer against a standard proving ring. The calibration curve is shown in Fig.4.1. The dynamometer system indicated good linearity with $R^2 = 0.9943$. The two stage indicating system offered adequate resolution necessary to map the soil strength variations in surface soil layer. Theoretically, the 17 W motor could drive the penetrometer at a speed of 0.2 cm/s with a thrust of 850 kg. Due to the resistance encountered in the slides, drive screw and bottom guide bush, the maximum thrust exerted at the penetrometer tip was 250 kg. Above this value the motor stalled due to load. Hence the penetrometer could be made to measure CI values of up to 7.8 MPa. The CI values were expressed in MPa as per standard procedure. The penetrometer was used extensively throughout the study. The guide rollers were replaced with sliding guides to ensure sturdiness.

4.1.2 Tillage Dynamometer

A tillage dynamometer was developed to measure the soil reaction forces on deep tillage tools under field conditions. The unit was configured with main emphasis on reliability and simplicity. The frame and dynamometer assemblies were sufficiently strong to withstand the enormous forces encountered by deep tillage tools. The main advantage of the system was the ready availability of force recordings for easy monitoring of tool performance.

The dynamometers were calibrated against standard proving ring as described in Sec.3.1.2. The load cells were calibrated individually. However, it was assumed that the sliding action of the hardened steel rolling ball rests would keep the cross sensitivity to

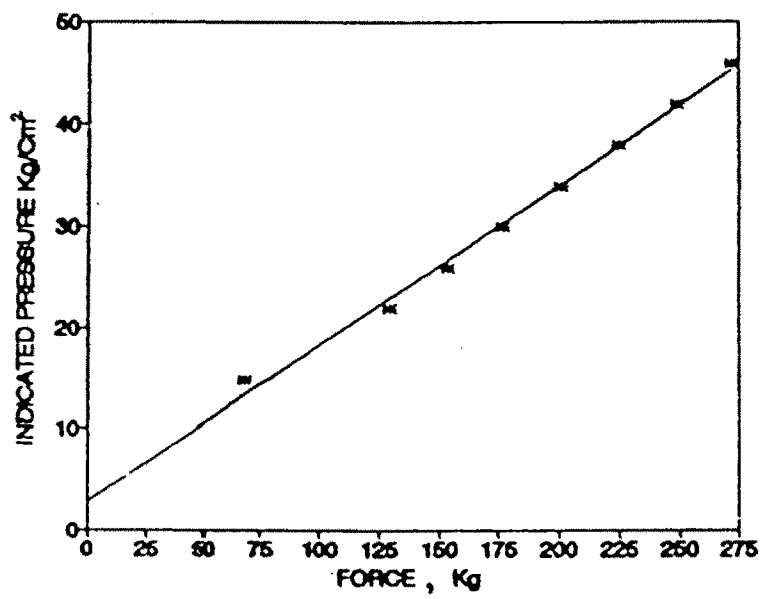

Fig 4.1 Calibration curve for hydraulic dynamometer used in cone penetrometer

a minimum. The recordings of the calibration test are presented in Appendix B. The pen positions, as recorded were used to calculate the angular deflection of the pen arm. The calibration curve was plotted with the angular deflection of pen in the Y axis and dynamometer load in the X axis. The calibration curves are shown in Fig.4.2 to Fig.4.7. Table 4.1 summarises the dynamometer details and their regression coefficients.

The calibration curves indicated a linear relation between recorded angular deflection and applied load. Except the V_2 dynamometer, which had a R^2 value of 0.952, all other dynamometers exhibited a very high degree of linearity with R^2 varying from 0.982 to 0.997. The regression equations yielded a small negative intercept for most dynamometers due to slackness in the linkages of the pressure sensing elements. The performance characteristics of tillage dynamometers developed by various researchers are presented in Sec. 2.2.2. It was observed that the accuracy of the sensing unit in most of the state of art dynamometer systems exceeded 99.9 per cent. This was achieved

Table 4.1. Calibration constants for dynamometers

Sl. No.	Location	Pr. range (Kg/cm^2)	No. of obser.	Calibration equation C_0	C_1	R^2
1	L_1	0-28	28	-7.20	0.375	0.982
2	L_2	0-28	24	-4.40	0.370	0.986
3	S	0-10	25	-6.90	1.436	0.987
4	V_1	0-70	30	1.86	0.240	0.993
5	V_2	0-105	30	-3.39	0.130	0.952
6	V_3	0-140	14	-0.86	0.129	0.997

Angular deflection,° = C_0 + C_1 x Applied load, Kg

through the use of strain gauge sensing elements. Though the accuracy of the hydraulic dynamometer system developed was slightly less than that of strain gauge based systems, the hydraulic dynamometer system proved to be highly reliable and inexpensive. It had

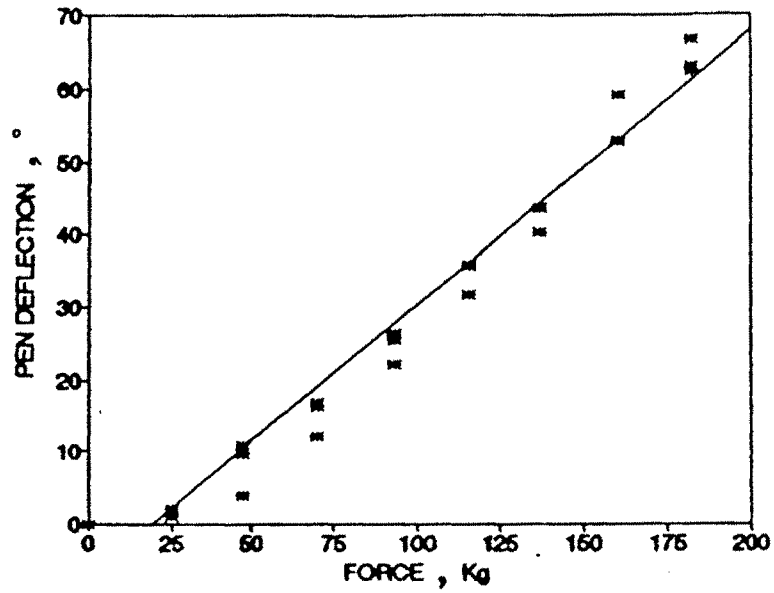

Fig 4.2 Calibration curve for hydraulic dynamometer-L_1, used in tillage dynamometer

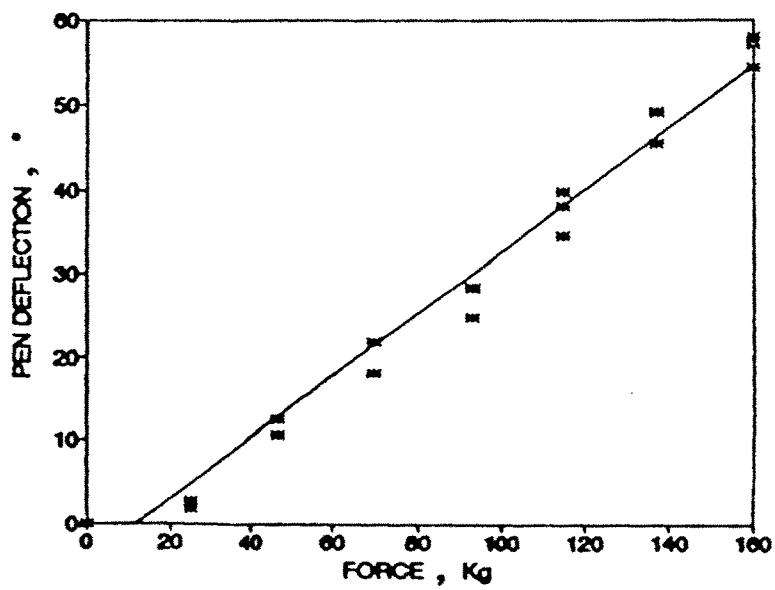

Fig 4.3 Calibration curve for hydraulic dynamometer-L_2, used in tillage dynamometer

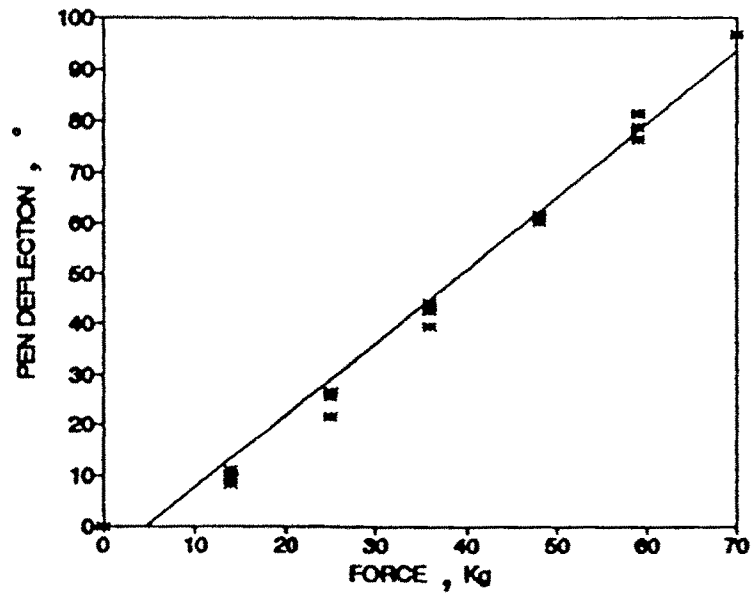

Fig 4.4 Calibration curve for hydraulic dynamometer-S, used in tillage dynamometer

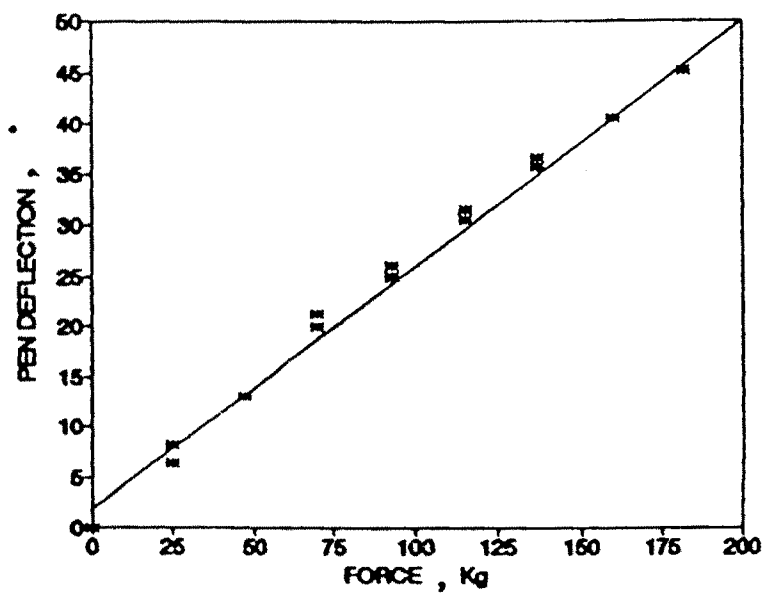

Fig 4.5 Calibration curve for hydraulic dynamometer-V_1, used in tillage dynamometer

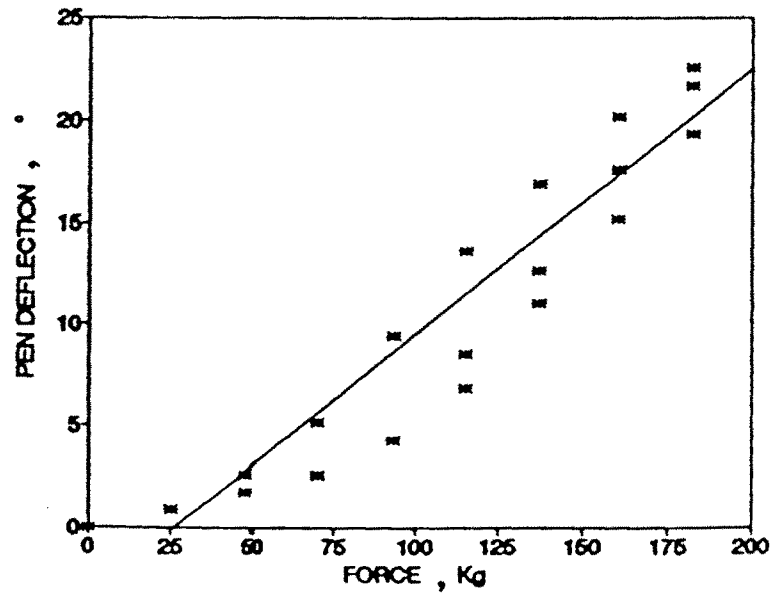

Fig 4.6 Calibration curve for hydraulic dynamometer-V_2, used in tillage dynamometer

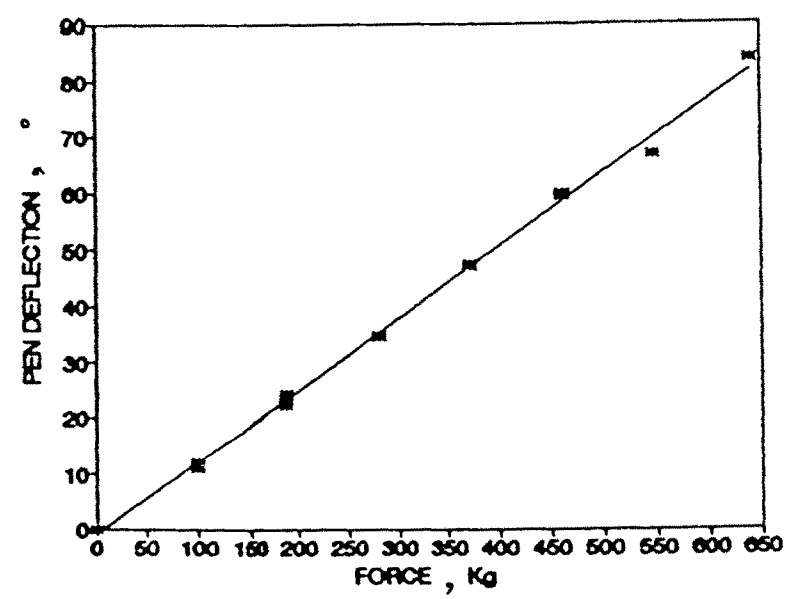

Fig 4.7 Calibration curve for hydraulic dynamometer-V_3, used in tillage dynamometer

the added advantage of producing a hard copy of recordings which had practical utility under field conditions as had been expressed by Harrison (1975). Considering the fact that the variations in soil reaction due to non homogeneous field conditions were expected to be greater than the variability in the instrumentation system, (Garner *et al.* 1988), the dynamometer system was considered suitable for tillage studies.

The soil reaction on the tool was calculated by considering the equilibrium of the sub frame as was done by Clyde (1936). Due to the symmetry of tool, only three force parameters were required for arriving the tool forces (Clyde 1961). From Fig.3.5

$$L = 2L_1 \quad \text{.... 4.2}$$

$$V = V_2 - 2V_1 \quad \text{.... 4.3}$$

$$R_v = (L^2 + V^2)^{1/2} \quad \text{.... 4.4}$$

$$\theta = \tan^{-1}(V/L) \quad \text{.... 4.5}$$

$$x = 2V1x75/L \text{ (75 = distance from } V_1 - V_3 \text{ line to } V_2) \quad \text{.... 4.6}$$

where

L = longitudinal reaction, Kg

V = Vertical reaction, Kg

θ = Angle of resultant reaction, radians

R_v = Resultant soil reaction, Kg.

X = Location of R_v, measured directly below V_2, cm

The calculation procedure is illustrated through sample calculations in Appendix C.

The tillage dynamometer gave a satisfactory performance throughout the study. The major drawback of the system was the difficulty in manual digitalization of the recorded analog signal. The operation of the recorder also required constant attention by the recorder operator walking behind the unit.

4.1.3. Furrow Profile Meter

A profilemeter was developed to make measurements of furrows created by passage of deep tillage tools. The furrow profile meter proved to be a very useful tool

for convenient and accurate measurement of furrow profiles. More than 180 furrow profiles were recorded using this instrument, throughout the study. From the furrow geometries recorded, the depth, width, area and shape of furrow were evaluated. The furrow profile meter was used to measure furrow widths of up to 65 cm and furrow depths up to 40 cm without any difficulty.

4.2 Soil characteristics of Experimental Field

The performance of chisels of different geometry, under varying operational conditions was tested in a clay loam soil. The characteristics of the field were representative of the soil conditions at the regions under rainfed agriculture in Tamil Nadu and in similar semi arid tropics.

4.2.1 Nature of soil and textural composition

The soil was fine, mixed, isohyperthermic and belonged to the sub group typic Ustopept with a 0-19 cm depth of Ap horizon and 19-42 cm depth of B21 horizon. The field was fallow for over eight months succeeding the previous maize crop. The soil was dry with wide surface cracks and a blocky structure. The soil had a compact subsoil below the normal tilling depth of about 20 cm. The above conditions were typical of conditions existing during summer fallow tillage in semi arid tropics (Wolf and Luth 1979).

The results of the mechanical analysis of the soil are presented below

Table 4.2 Soil Textural composition

Sl. No.	Fraction	Size mm	Sample 1 %	Sample 2 %	Average %
1	Course sand	> 0.50	5.24	7.46	6.35
2	Medium sand	0.50 - 0.25	11.75	11.85	11.80
3	Fine sand	0.25 - 0.10	17.84	15.93	16.89
4	Very fine sand	0.10 - 0.05	12.50	07.87	10.18
5	Silt	0.05 - 0.002	22.76	23.80	23.28
6	Clay	< 0.002	29.91	33.09	31.50

From the mechanical analysis, it was inferred that the soil was a clay loam. This had made the soil inherently susceptible to compaction. The low proportion of soil organic matter increased the tendency towards compaction (Gaultney 1982).

4.2.2 Soil moisture content

The experiments were conducted over a period of one month. the soil moisture content was measured during each run. The randomized order of evaluation of different tool shapes and average moisture content during each run are tabulated in Table 4.3. It

Table 4.3 Moisture content of soil in experimental blocks

Block No.	Sharesize mm x mm	SoilMoisture % db
1	25x150	3.23
2	20x100	2.87
3	40x200	3.87
4	30x150	4.82
5	30x200	4.81
6	50x200	4.01
7	25x100	4.15
8	40x100	3.01
9	20x200	6.03
10	40x150	7.35
11	50x150	6.92
12	20x150	6.95
13	30x100	7.72
14	25x200	8.10
15	50x100	8.47

was observed that the moisture content varied between 2.87 to 8.47 percentage(db). The variation in moisture content was due to rains during the later part of the experiment. The variations could not be avoided with the existing experimental set up.

4.2.3. Cone Index

Penetration resistance served as an index of uniformity of the field and quantify the variation in soil strength and associated variations in the experiment The penetration resistance was also used to characterize the soil structure an subsoil compaction.

The tractor mounted cone penetrometer was used to obtain penetration profiles to a depth of 40 cm below the nominal soil surface elevation. Five per probes were performed in each block. The soil strength profiles of the fifteen l illustrated in Fig.4.8.

The pooled data of average resistance for all penetrations gave a mea MPa with a standard deviation of 0.47. Analysis of variance of the cone-Ind averaged over 40 cm depth showed that the within block variance was large variance among blocks. This indicated that the within block variance was to mask any significant variation among blocks.

Though uniform soil condition is desirable in tillage studies, varia unavoidable. The data on soil strength distribution was used in analysing the ex data. The variation among blocks was taken care of, by assigning the sha evaluated, to the blocks in a random order.

The average cone index profile for each block (Fig.4.8) was compared of the average cone index over 40 cm depth (CI_{avg}), Maximum penetration (CI_{max}) and penetration resistance at 20 cm (CI_{20}). The above values for eac tabulated in Table 4.4.

From this data, the CI_{avg} for the blocks was expressed within confiden at 10 per cent level as 1.872 ± 0.106 MPa. Oskavi and Witney (1982) obs the soil cone indices at half the maximum depth of ploughing were more reli to soil strength than the value averaged over the whole profile. From the tabula CI_{20} for the blocks was expressed within confidence interval at 10 per cent leve ± 0.125. This indicated that either CI_{avg} or CI_{20} could be used as an index of soi

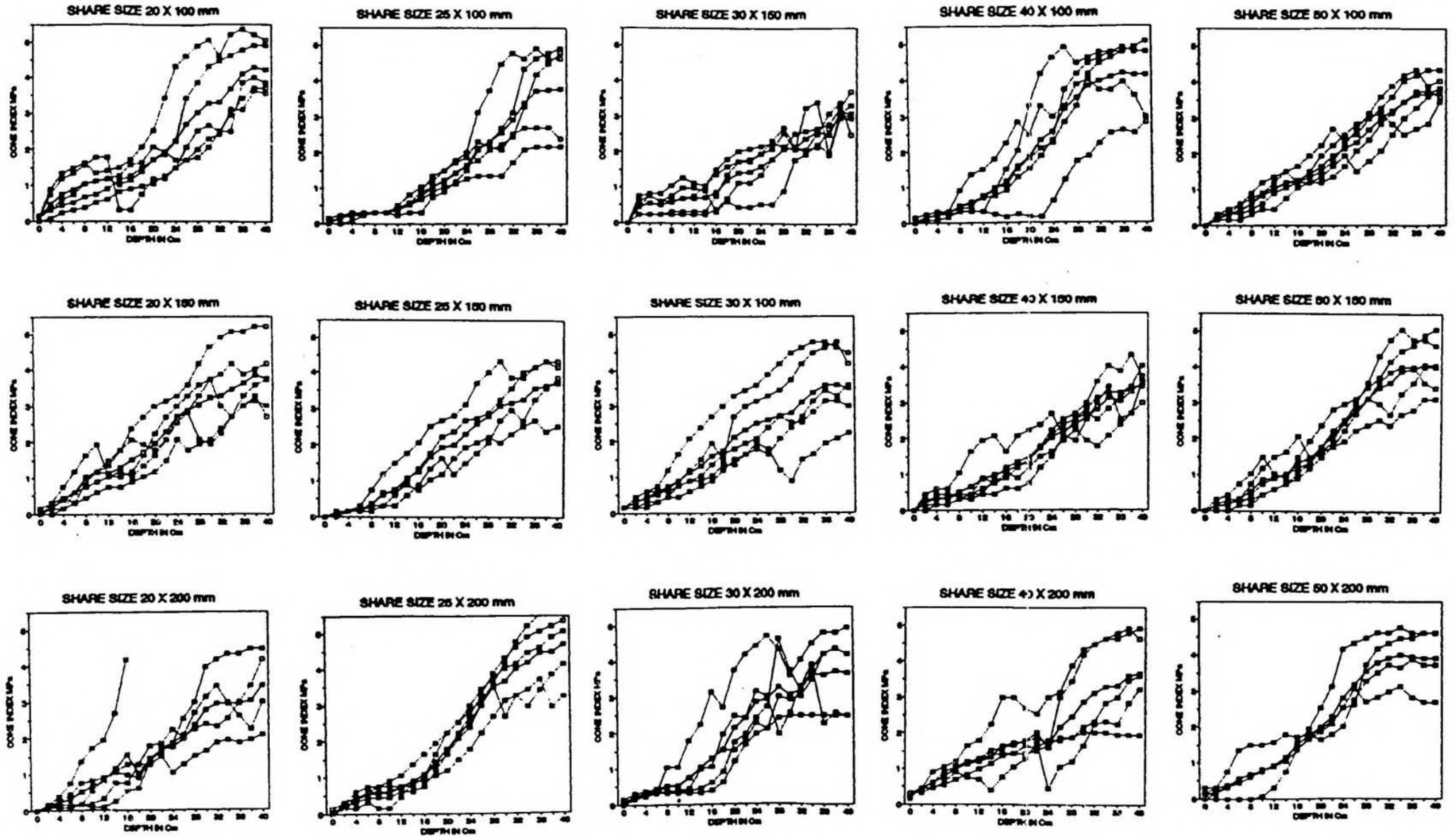

Fig 4.8 Soil strength profiles for experimental blocks.

Table 4.4. Cone penetration resistance for experimental blocks

Block No.	CI_{avg} MPa	CI_{Max} MPa	CI_{20} MPa
1	1.827	3.72	1.935
2	2.077	4.30	1.712
3	1.881	3.64	1.757
4	1.446	3.17	1.400
5	1.946	3.17	2.114
6	2.154	4.00	1.991
7	1.566	3.76	1.220
8	2.083	4.19	1.831
9	1.501	3.42	1.433
10	1.633	3.54	1.480
11	2.000	4.07	1.780
12	2.047	3.63	1.965
13	1.944	3.57	2.114
14	2.138	4.70	1.786
15	1.836	3.81	1.637

The cone index profiles showed three soil strength regimes. The 0-12 cm depth exhibited low soil strength. The soil strength increased from 12 cm to about 26-36 cm. Then the soil strength remained constant. This indicated the presence of a compacted subsoil below the arable layer. The progressive increase of penetration resistance indicated the presence of continuous compacted subsoil. This may be due to the calcarious layer below 60 cm depth and other pedogenettic characteristics of the soil. The degree of subsoil compaction as measured by the penetration resistance indicated that the penetration resistance exceeded 2 MPa at a depth of 22 to 26 cm. Camp and Lund (1968), Taylor and Gardner (1963) Threadgill (1977) and Canarache (1990) have reported that the root growth is restricted when the penetration resistance exceeded a value of about 2 MPa. Hence it was concluded that the root zone depth even for deep rooted plants would be restricted to 22-26 cm. This confirmed that the experimental field exhibited severe subsoil compaction.

4.3 Soil Reaction on Deep Tillage Tools

The soil reaction forces on shares of different geometry under various oper conditions were measured as explained in Sec.3.5. Fifteen share geometries with levels of width and three levels of length (Table 3.2) were tested under five oper depths and five speeds. The average values of soil reaction for each experimental ru tabulated in Appendix D. The depth of operation and speed could not be pre controlled under the experimental conditions. Hence the speed and depth were rec for each experimental run. To compare the performance of shares under diff operational conditions, the soil reaction on each share was combined into a regre equation of the form.

$$F = C_0 + C_1 d + C_2 s + C_3 d^2 + C_4 s^2 \qquad \ldots. 4.7$$

The suitability of multiple regression equations of similar form for fitting reaction forces had been reported by Summers *et al.* (1986), Owen (1988), Oni e (1992) and Gebresenbet and Jonsson (1992). The regression equation for longitu reaction, vertical reaction and resultant reaction were tabulated. The patterns of vari of the reaction forces with change in depth and speed were also illustrated graphi

4.4. Influence of depth of operation on soil reaction

The force-depth relationship illustrated in Fig.4.9 to Fig.4.11. indicate the s influence of depth of operation on the longitudinal, vertical and resultant reactions

4.4.1. Influence of Depth on Longitudinal Soil Reaction

The longitudinal soil reaction (L) is of primary importance in tillage studies. the parasitic forces of a mounted symmetrical tool equals zero, the longitudinal soil rea equals the draft requirement for the tool. The regression equations for longitudinal rea (Table 4.5) gave a value of R^2= 0.86 to 0.98 indicating the goodness of fit offered b multiple regression model. The regression equations had a small negative intercept at depth, except for the two shares which exhibited a positive intercept. The draft inter

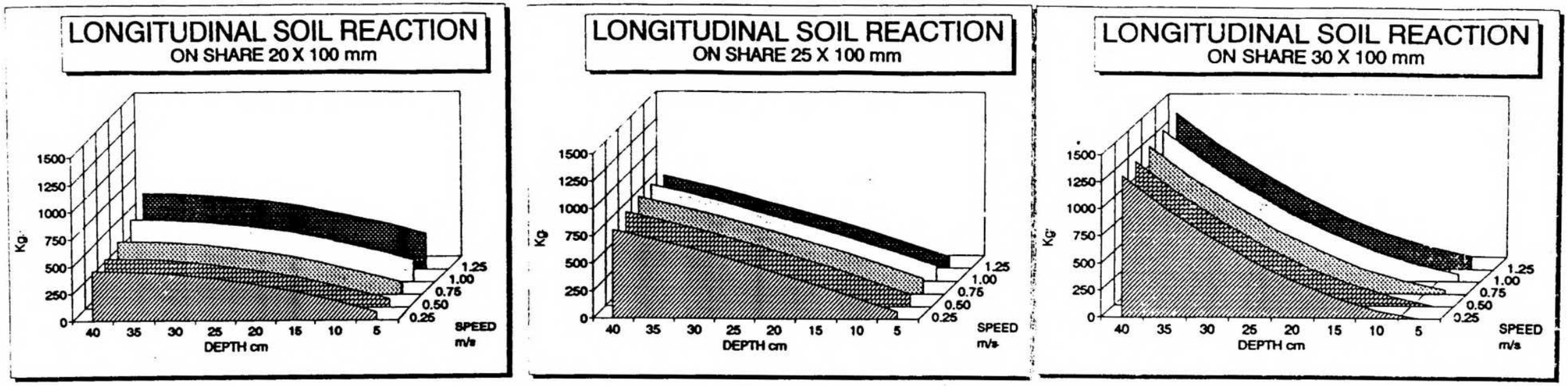

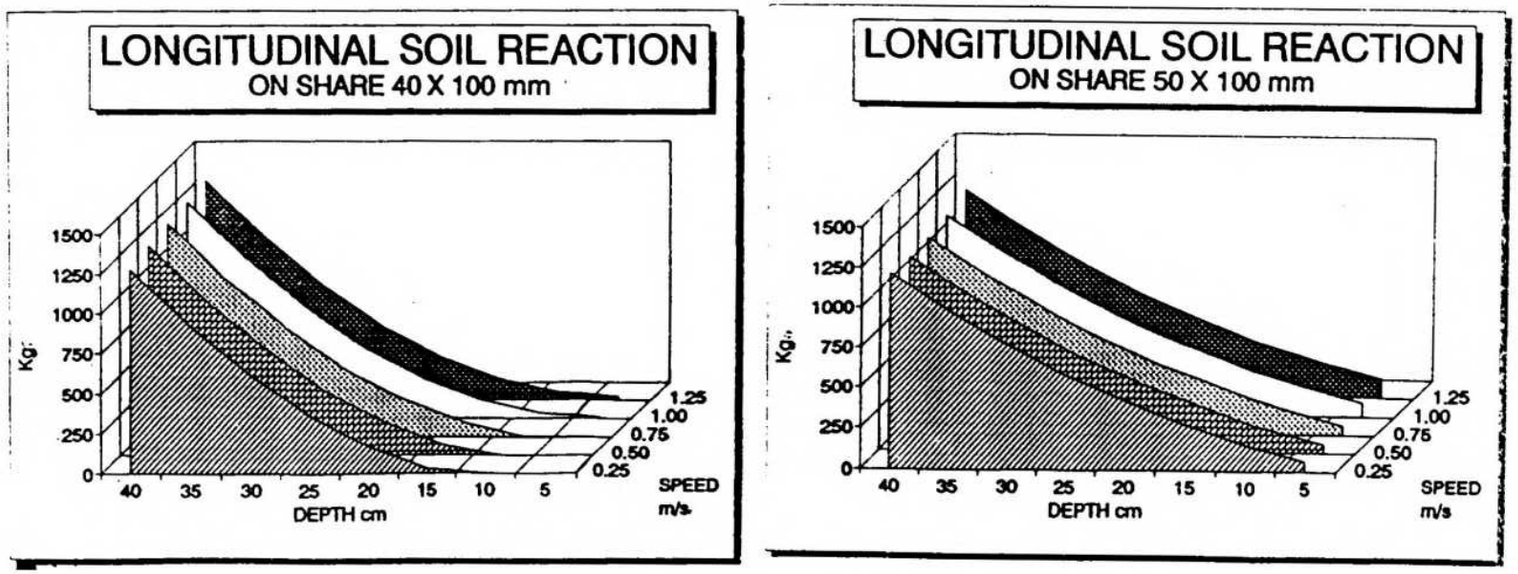

Fig 4.9 Longitudinal soil reaction as a function of depth and speed of operation-regressed relation for measured values

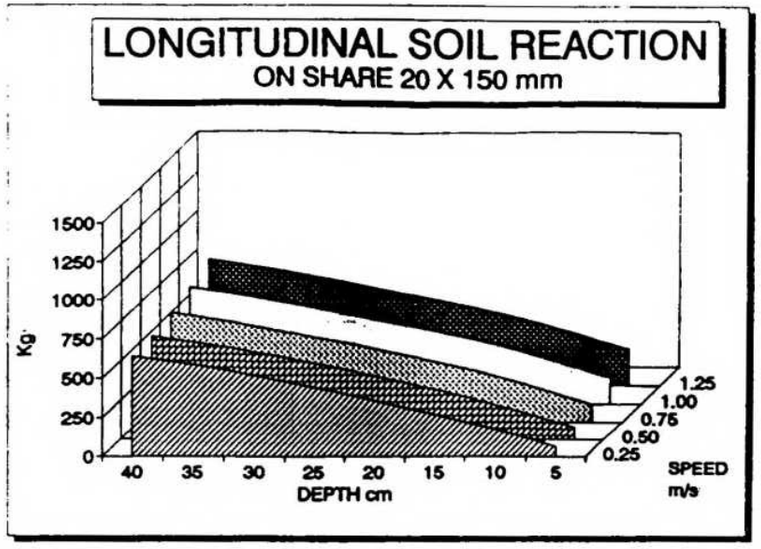

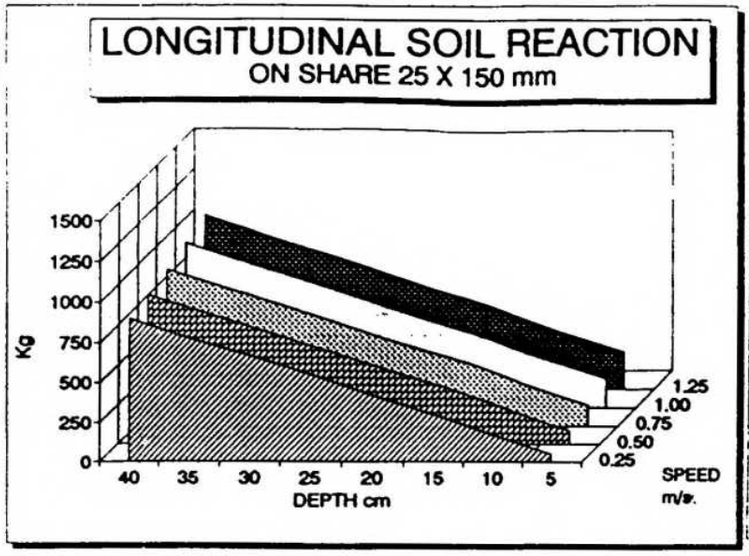

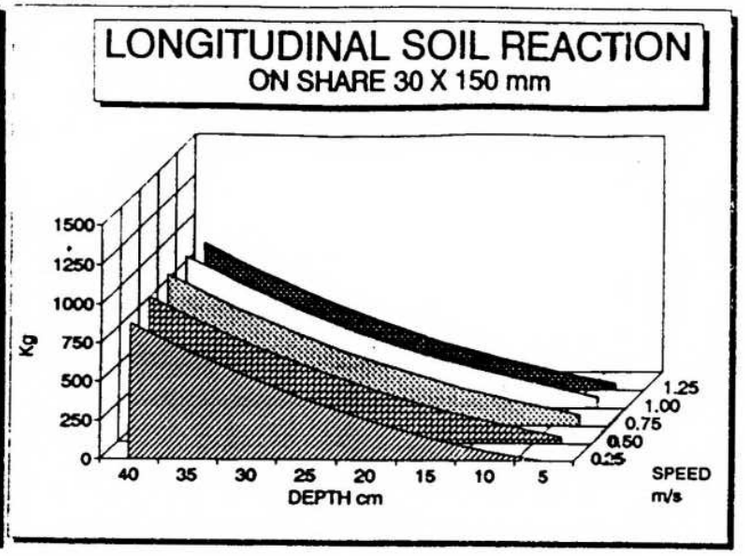

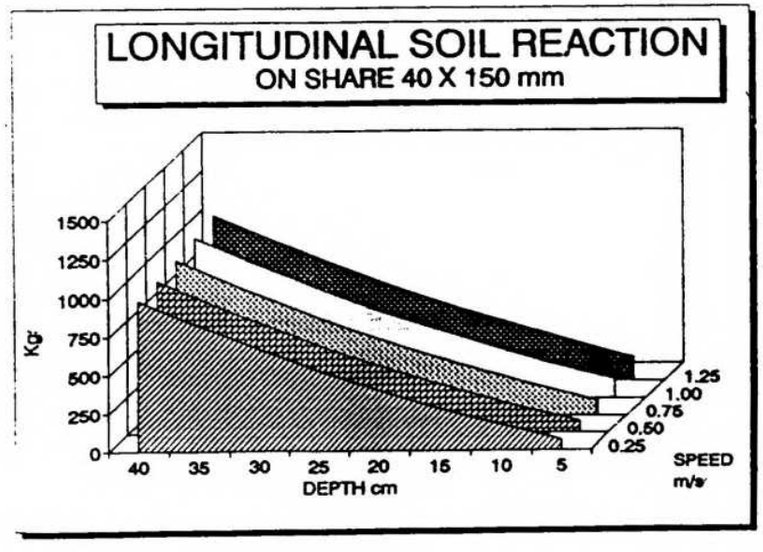

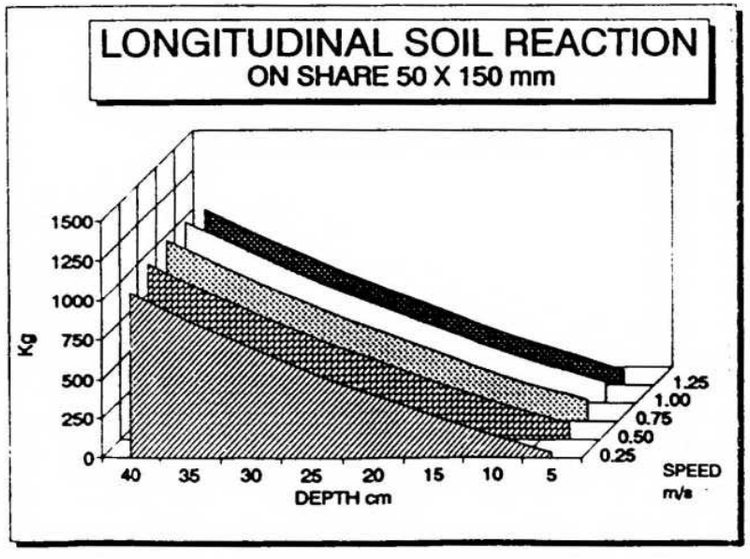

Fig 4.9 Longitudinal soil reaction as a function of depth and speed of operation-regressed relation for measured values

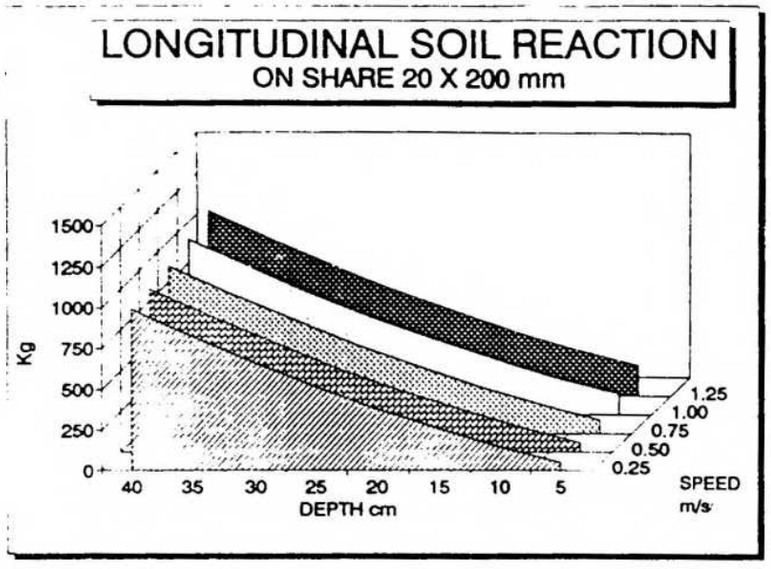

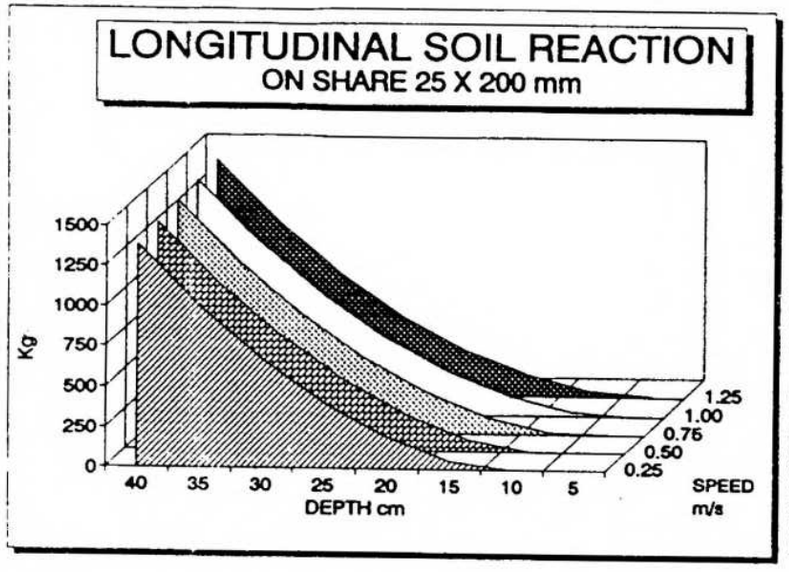

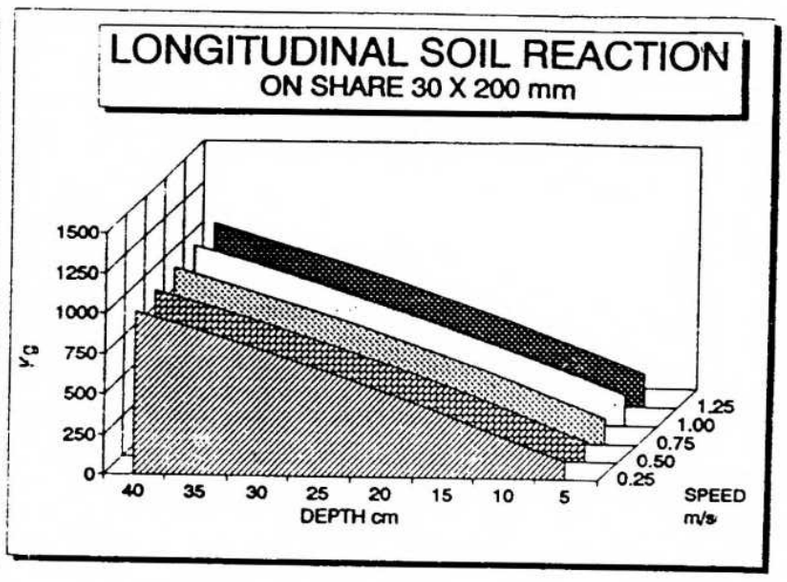

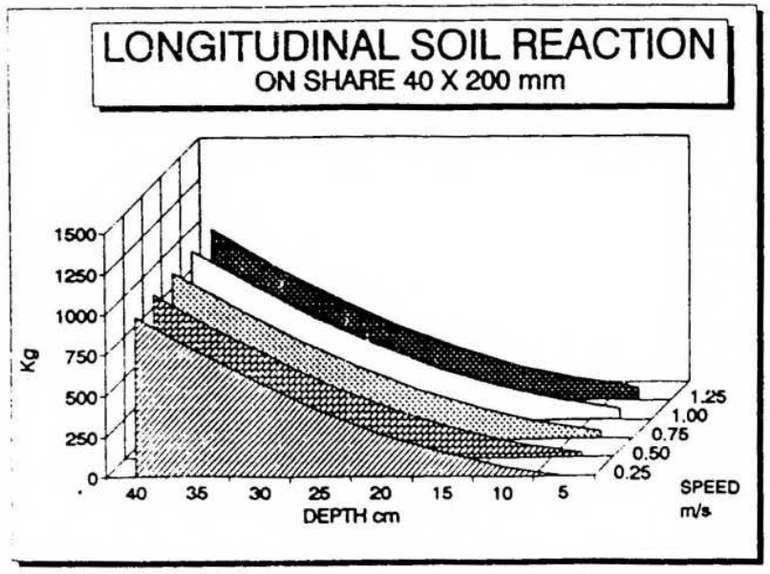

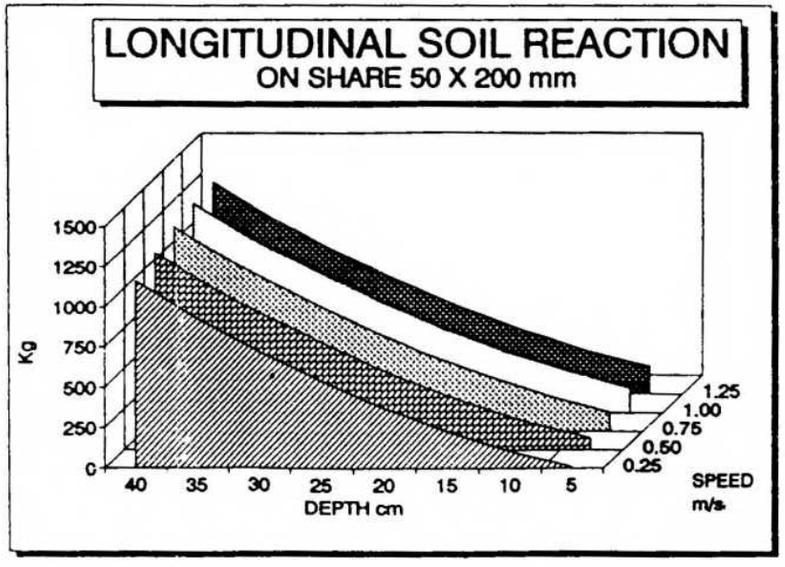

Fig 4.9 Longitudinal soil reaction as a function of depth and speed of operation-regressed relation for measured values

C_0, varied between 17.96 kg and -146.4 kg. This was due to the extrapolation of the results observed in the compacted subsoil. The coefficients of the first and second order depth terms C_1 and C_3 were highly significant. The depth coefficient C_1 varied from -11.02 to 31.53 while depth squared coefficient, C_3 varied from -0.309 to 1.108. A positive value of C_1 was observed for all but two shares. The negative value of C_1 observed for 40 x 100 mm and 25 x 200 mm shares was due to the high value of C_3. The quadratic relationship yielded a convex or concave relationship depending on the sign of C_3 term. Though the depth-force relation was quadratic, if a shorter interval of 20 to 35 cm depth was considered, the force-depth relationship could be approximated by a straight line without much loss of fit.

Table 4.5 Results of non-linear least square regression between depth and speed of operation on longitudinal reaction for different share geometries

$$L = C_0 + C_1 d + C_2 S + C_3 d^2 + C_4 S^2$$

S.No.	Share size	C_0	C_1	C_2	C_3	C_4	R^2
1.	25 x 150	-102.307	25.187	98.133	-0.021	55.098	0.962
2.	20 x 100	6.984	24.754	-270.046	-0.309	347.054	0.889
3.	40 x 200	-54.789	4.095	98.091	0.532	-14.447	0.959
4.	30 x 150	-146.416	8.842	390.204	0.368	-225.187	0.970
5.	30 x 200	-64.048	31.528	80.704	-0.128	9.940	0.984
6.	50 x 200	-143.986	13.289	338.209	0.433	-120.216	0.970
7.	25 x 100	-138.701	26.750	352.048	-0.125	-208.844	0.866
8.	40 x 100	-87.136	-11.206	156.996	1.108	-35.769	0.956
9.	20 x 200	-30.345	16.055	-70.093	0.243	140.524	0.967
10.	40 x 150	-26.998	17.239	-4.476	0.199	61.280	0.984
11.	50 x 150	-162.701	18.199	458.218	0.239	-262.459	0.953
12.	20 x 150	-41.051	23.976	-57.106	-0.171	146.112	0.918
13.	30 x 100	-73.413	5.953	30.250	0.708	67.007	0.887
14.	25 x 200	-77.767	-11.024	136.942	1.168	-38.033	0.973
15.	50 x 100	17.963	12.667	-148.118	0.448	136.691	0.898

The pattern of depth force relation was partly explained by the depth-cross sectional area relation which showed considerable similarity with the dept relation. The longitudinal reaction, at a reference speed of 1 m/s and a depth of op of 35 cm, for all shares except the smaller shares of size 20 mm x 100 mm, 25 100 mm and 20 mm x 150 mm was found to vary between 778 kg and 1065 k the average value being 890 kg. For the same share geometries and operational con the average increase in draft per unit increase in depth of operation was 21.96 kg the depth range of 10-15 cm and the same was 44.92 kg/cm in the depth range 40 cm. This implied a 100 per cent increase in slope of longitudinal force-depth r when the depth was increased from 12.5 cm to 37.5 cm. The longitudinal reac an increasing rate was visualised as being due to the increased volume of soil di as depth was increased. The decreasing rate of increase of longitudinal reaction ex by some shares may be due to the insufficient spread of the depth variable duri experimental runs. The quadratic depth longitudinal reaction relationship was in agr with the results by Luth and Wismer (1971), McKyes (1977), Johnson (1980), (1984), Owen (1989) though the above observations were made in soils diffe properties from the soils under investigation. The force depth relation was also infl by variations in soil strength. The plot of the mean cone index profiles is illustr Fig.4.8. The increased soil reaction at greater depths was also due to the con subsoil.

The quadratic nature of the depth-longitudinal reaction curve implies tl increase of draft is at an increased rate at greater depths. Hence even slight va in depth of operation will result in considerable variations in draft. This would the depth of operation to be precisely controlled during deep tillage so as to ensu the draft is within limits of the tractive capacity of prime mover.

4.4.2 Influence of depth on vertical soil reaction

The vertical reaction force on all shares were observed to be generally dow (Fig. 4.10) except for shallow depths of operation (Appendix D). This was due low lift angle of the shares (20°). Payne and Tanner (1959) also observed similar bel

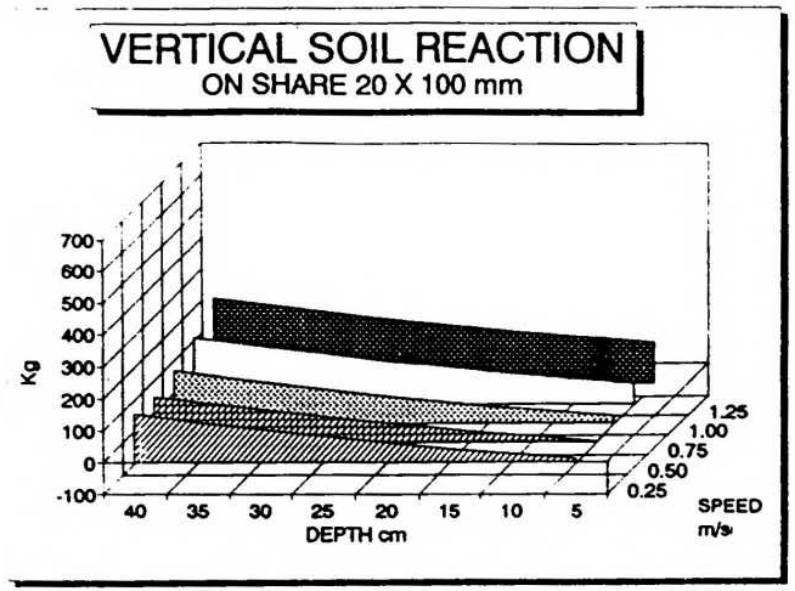

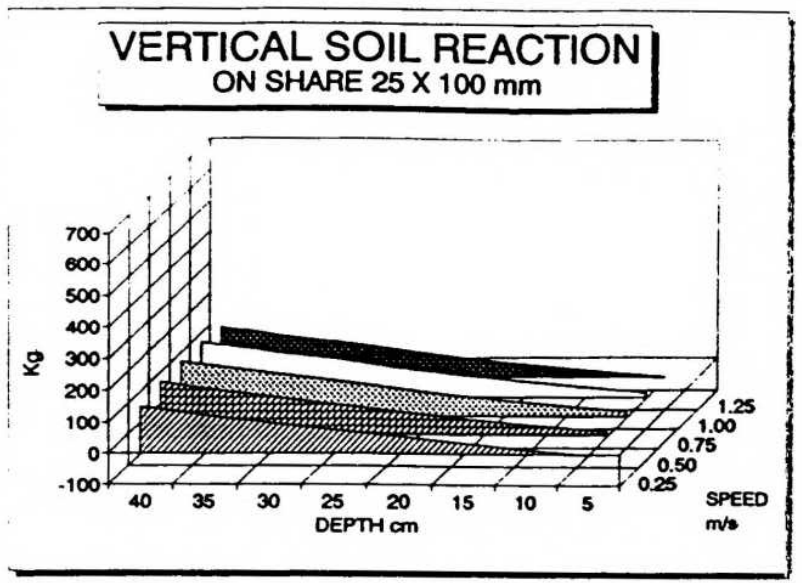

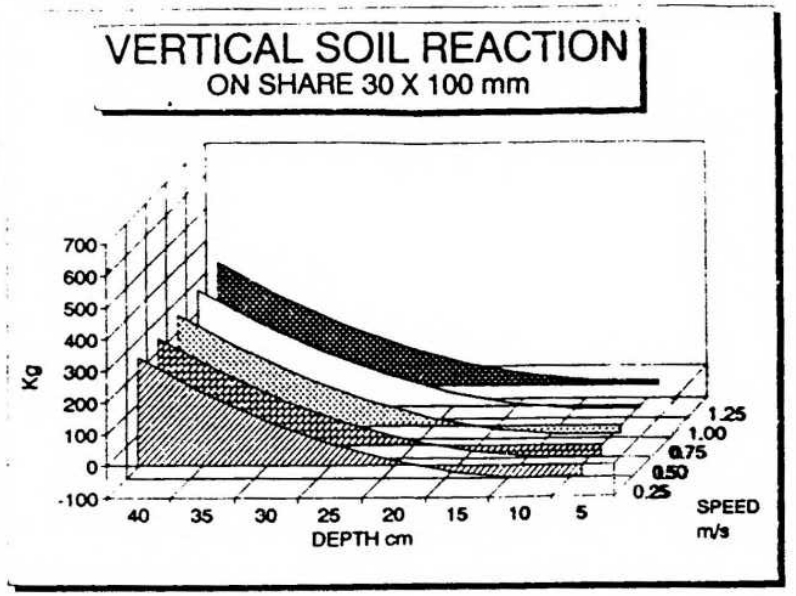

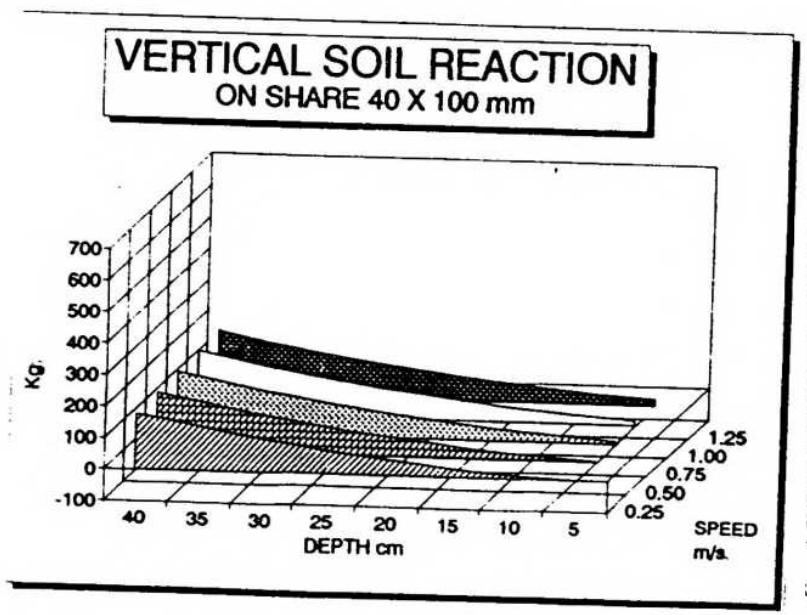

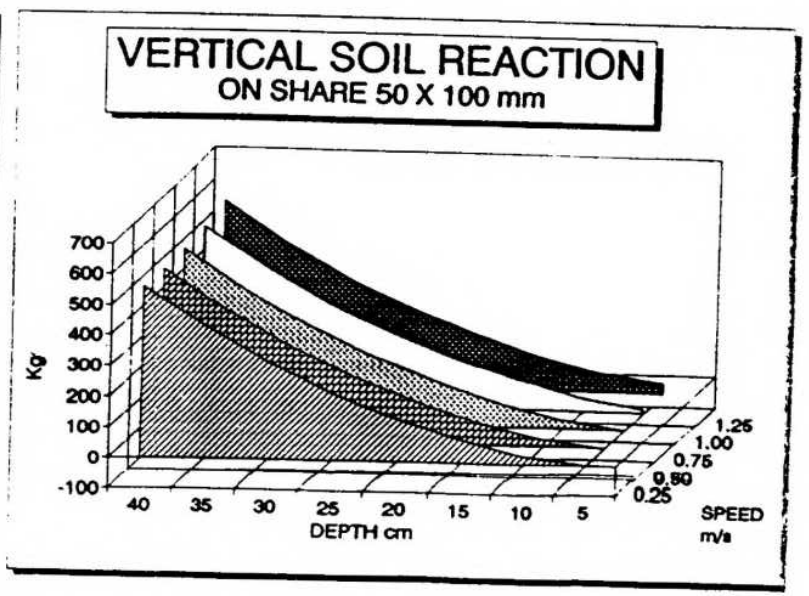

Fig 4.10 Vertical soil reaction as a function of depth and speed of operation-regressed relation for measured values

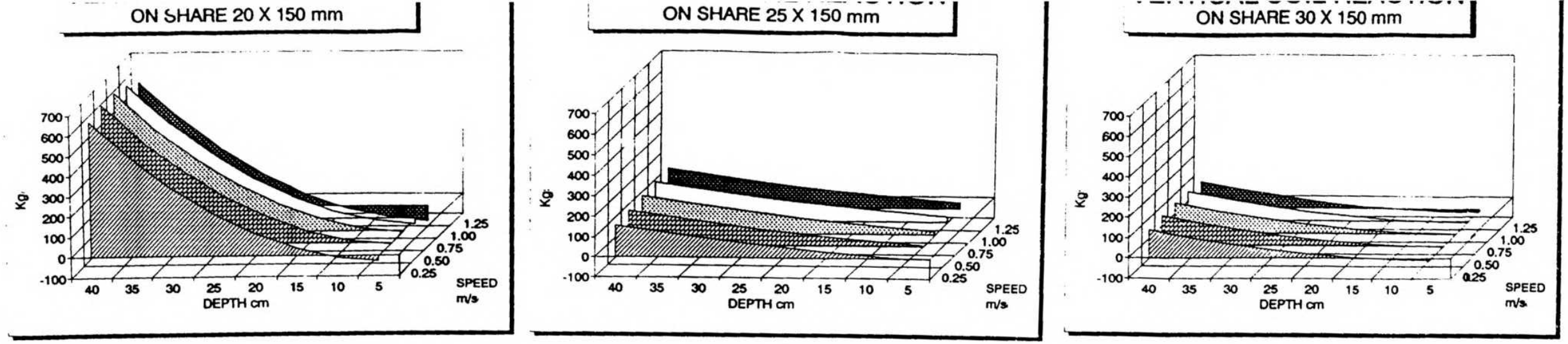

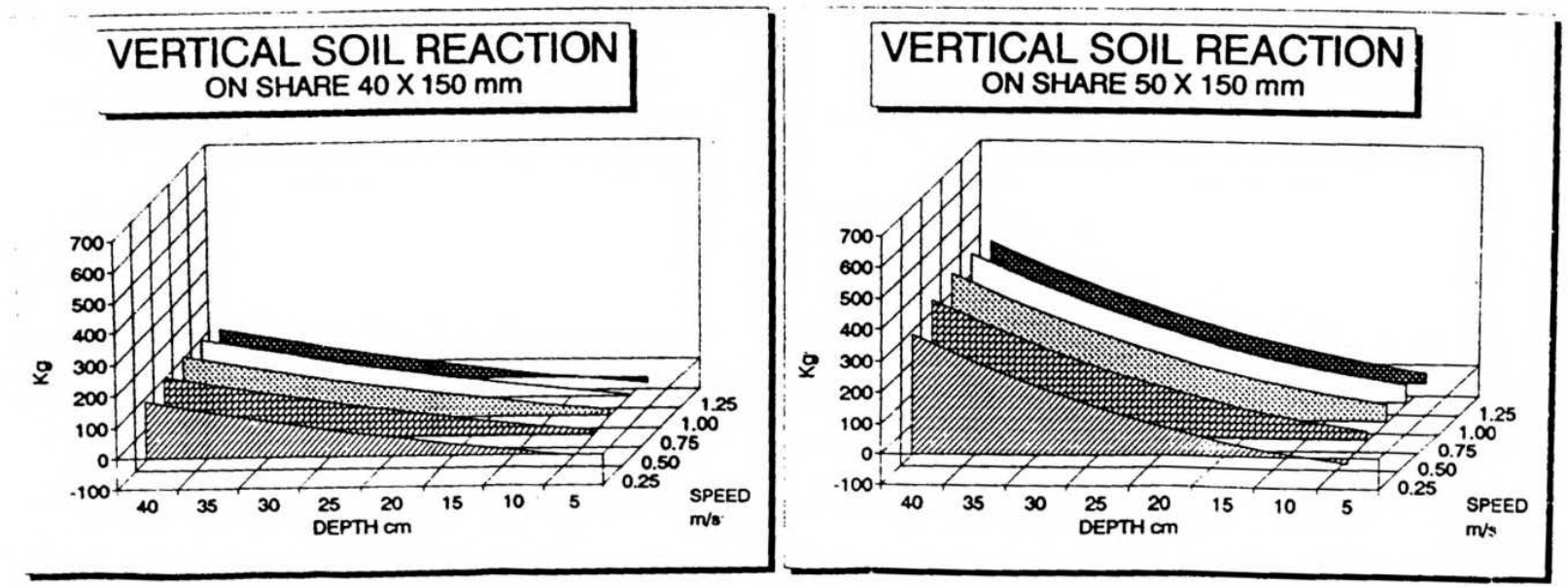

Fig 4.10 Vertical soil reaction as a function of depth and speed of operation-regressed relation for measured values

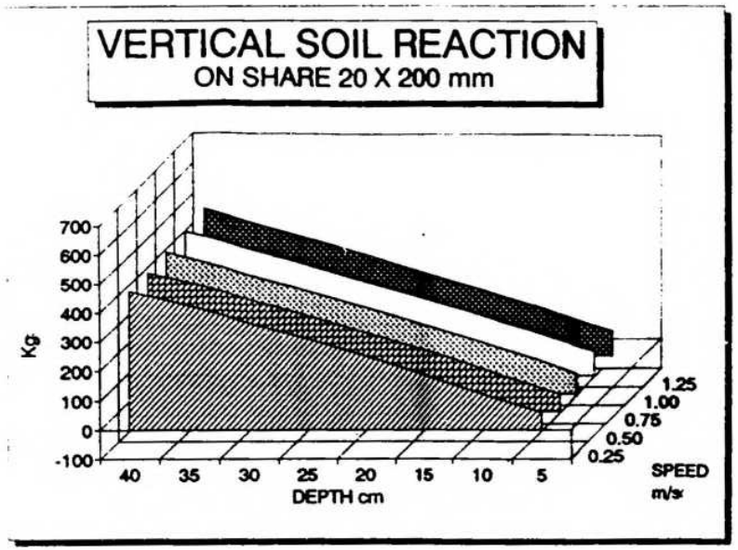

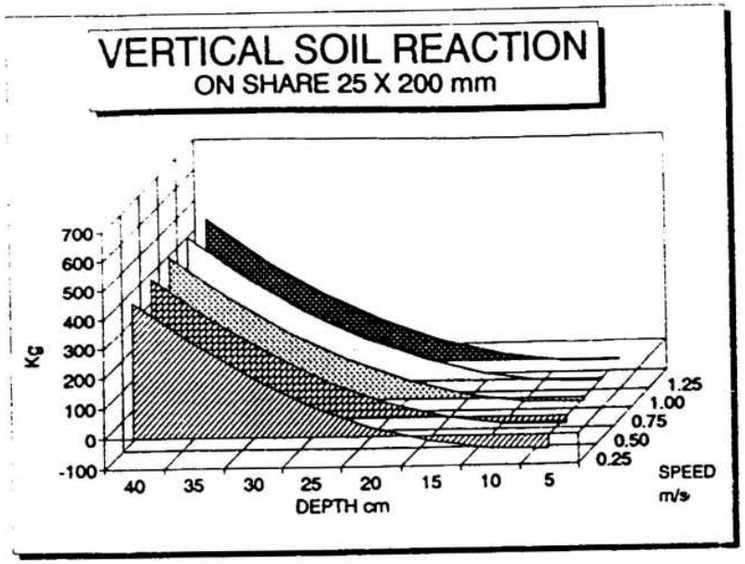

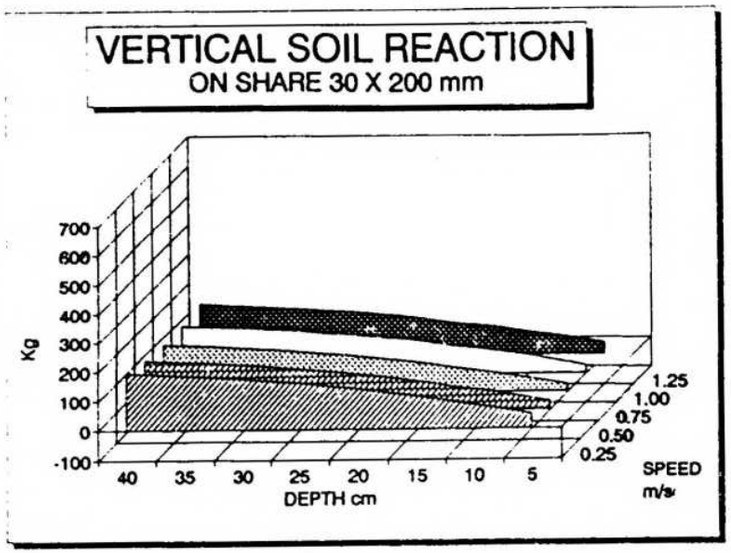

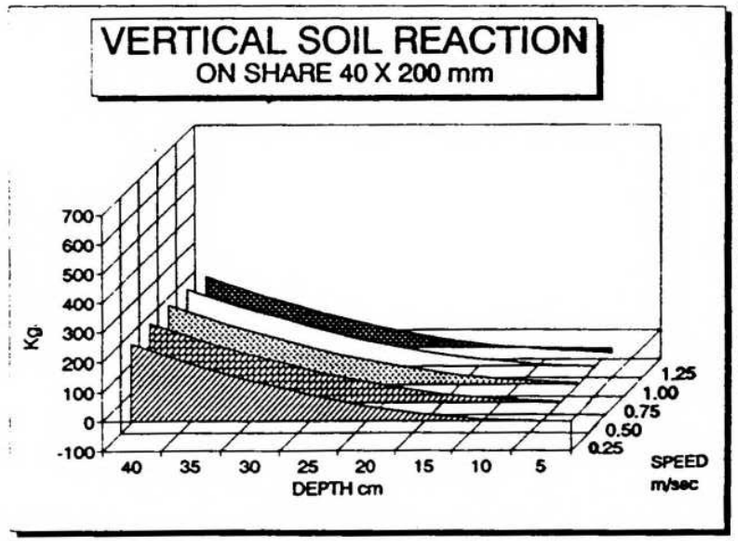

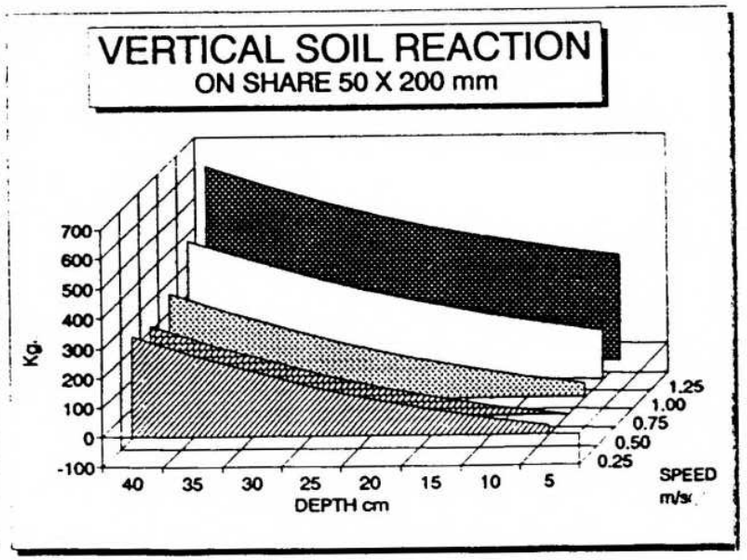

Fig 4.10 Vertical soil reaction as a function of depth and speed of operation-regressed relation for measured values

when lift angle was less than 45°. The regression equation for vertical force (Table 4.6) also indicated an upward vertical reaction at shallow depths of operation. Similar observations were reported by Gebresenbet and Jonsson (1992) and Payne and Tanner (1989); both studies attributed this upward thrust to the expansion of soil below the shear failure plane. When the depth was increased above 20 cm, the vertical reaction was directed downwards. This indicated that the tools tested had a better penetrating ability at increased depth of operation. In the regression equations the coefficient of the depth term, C_1 was positive or negative depending on the coefficient of the depth squared term, C_3. The depth coefficient C_1 was found to vary between -6.23 and 7.82 and the coefficient of depth squared term varied between -0.041 and 0.529. The net effect of increase in depth was an increase in vertical reaction. Comparing the vertical reaction among shares

Table 4.6 Results of non-linear least square regression between depth and speed of operation on vertical soil reaction for different share geometries

$V = C_0 + C_1 d + C_2 S + C_3 d^2 + C_4 S^2$

S.No.	Share size	C_0	C_1	C_2	C_3	C_4	R^2
1.	25 x 150	-26.140	2.525	44.965	0.046	-7.112	0.495
2.	20 x 100	27.145	2.459	-161.562	0.035	186.440	0.873
3.	40 x 200	-14.494	-1.357	78.408	0.197	-62.875	0.888
4.	30 x 150	-21.807	-1.037	72.099	0.118	-53.116	0.859
5.	30 x 200	43.288	7.824	-146.729	-0.082	94.618	0.719
6.	50 x 200	109.589	3.126	-543.253	0.129	578.178	0.819
7.	25 x 100	-38.614	2.733	108.519	0.036	-69.687	0.677
8.	40 x 100	-13.800	1.462	15.449	0.081	6.199	0.729
9.	20 x 200	-8.486	13.823	-13.456	-0.041	30.578	0.902
10.	40 x 150	-48.912	2.769	159.160	0.055	-117.706	0.740
11.	50 x 150	-112.209	2.991	336.255	0.191	-186.242	0.824
12.	20 x 150	-64.384	-3.994	222.333	0.529	-181.865	0.719
13.	30 x 100	-9.583	-5.695	-49.974	0.366	70.254	0.710
14.	25 x 200	-52.421	-6.230	110.103	0.459	-45.251	0.902
15.	50 x 100	3.711	0.684	-75.257	0.341	73.145	0.876

of different geometry, it was observed that the vertical force on shares were significantly lesser than the horizontal force. The vertical reaction at a speed of 1 m/s and at a depth of operation of 40 cm, for all shares tested at lower moisture levels (<5%), excepting the 50 mm x 200 mm share varied between 144 kg and 261 kg with average value being 189.8 kg. The vertical reaction under the above operational conditions for all shares tested at higher moisture levels (> 5%), excepting 40 mm x 150 mm share varied between 368 kg and 663 kg with the average value being 510 kg. This indicated that the shares tested at higher levels of soil moisture exhibited significantly higher vertical reaction. This might be due to the increase in frictional forces at the soil-metal interface. For shares tested at lower moisture levels (<5%) and at a speed of 1 m/s, the average slope of vertical force-depth relationship was 3.55 kg/cm at 10-15 cm range of depths, and the same for 35-40 cm range was found to be 6.6 kg/cm. The corresponding values at higher moisture levels (> 5%) was 7.9 kg/cm at 10-15 cm range and 23.36 kg/cm at 35-40 cm range. The average variation in the slope of the vertical force-depth relation at a speed of 1 m/s for all shares tested varied from 8 kg/cm at 15-25 cm range of depths to 12.96 kg/cm at 30-40 cm range. The above observations clearly showed that though a good fit for the experimental values were obtained by using a quadratic force-depth relationship, except at higher moisture conditions, the vertical force-depth relationship was linear especially if a shorter range of depths between 20-35 cm was considered. This is in conformity with the results reported by Luth and Wismer (1971) and Owen (1989). The predominantly linear vertical force relationship as against a quadratic longitudinal force relationship implied that the angle of resultant soil reaction decreased with depth. Similar behaviour was observed by Owen (1989). This could have been due to the super imposition of the effect of vertical standard, whose resultant reaction in the upward direction would increase with increased depth. The vertical reaction was due to the upward shearing force exerted by the tine. Hence the vertical force was influenced by the soil strength variations represented by the penetration resistance profiles. The increased vertical force due to increase in depth indicated the ability of shares to penetrate the

compacted subsoil. The increased vertical force would also aid weight transfer and he improve traction. Thus the shares of low lift angle would improve performance of tra - implement system.

4.4.3. Influence of Depth on Resultant Reaction

The regression equations for the resultant reaction on different shares are tabul in Table 4.7. The variation of resultant reaction with depth and speed of operation presented in Fig.4.11. The resultant reaction was predominantly influenced by longitudinal reaction which was significantly higher than the vertical reaction. intercept term C_0 varied from - 31 kg to -303 kg. The regression equations indic a linear to strongly quadratic relation. The coefficient of the depth term C_1 varied f -11.95 to 33.23 with only two shares exhibiting negative C_1 term. the coefficient of

Table 4.7 Results of non-linear least sqyare regression between depth and speed operation on resultant soil reaction for different share geometries

$$R_v = C_0 + C_1 d + C_2 S + C_3 d^2 + C_4 S^2$$

S.No.	Share size	C_0	C_1	C_2	C_3	C_4	R^2
1.	25 x 150	-136.8770	22.9590	184.608	0.1189	8.6980	0.975
2.	20 x 100	-211.4020	18.9850	503.544	-0.0340	-271.2910	0.934
3.	40 x 200	-54.4450	4.2740	95.220	0.5424	-10.3830	0.959
4.	30 x 150	-303.7860	17.4360	918.665	0.2765	-567.5300	0.887
5.	30 x 220	-44.2098	33.2260	21.953	-0.1540	43.1590	0.981
6.	50 x 200	-132.6680	14.0250	284.348	0.4380	-60.5790	0.971
7.	25 x 100	-142.9350	27.1295	362.691	-0.1240	-214.7680	0.868
8.	40 x 100	-91.8340	-10.1640	171.644	1.0850	-45.9300	0.957
9.	20 x 200	-31.4240	21.2250	-70.546	0.1750	143.5210	0.971
10.	40 x 150	-127.6720	12.8270	330.921	0.4470	-176.7030	0.932
11.	50 x 150	-159.2790	17.4470	435.377	0.3399	-231.0096	0.962
12.	20 x 150	-100.7660	10.9740	96.403	0.4298	-168.7580	0.915
13.	30 x 100	-72.9740	6.0093	18.856	0.7222	78.9250	0.886
14.	25 x 200	-85.0450	-11.9470	146.535	1.2400	-37.9870	0.972
15.	50 x 100	-57.8270	9.2630	91.900	0.7210	-14.1670	0.989

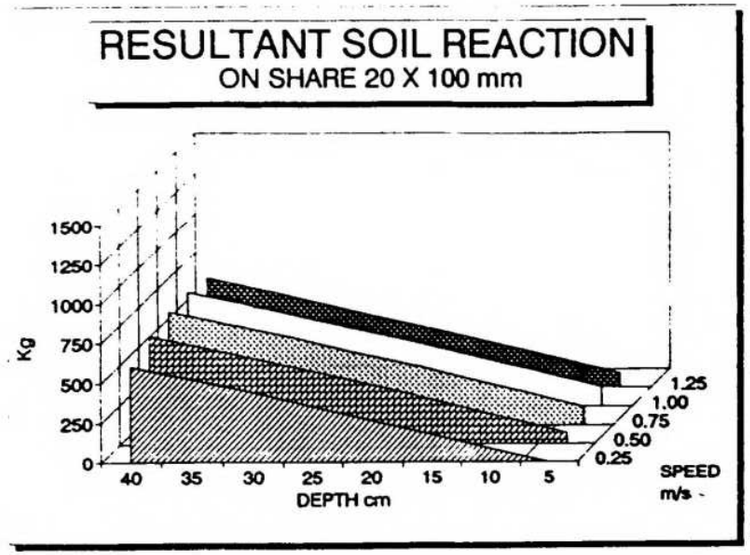

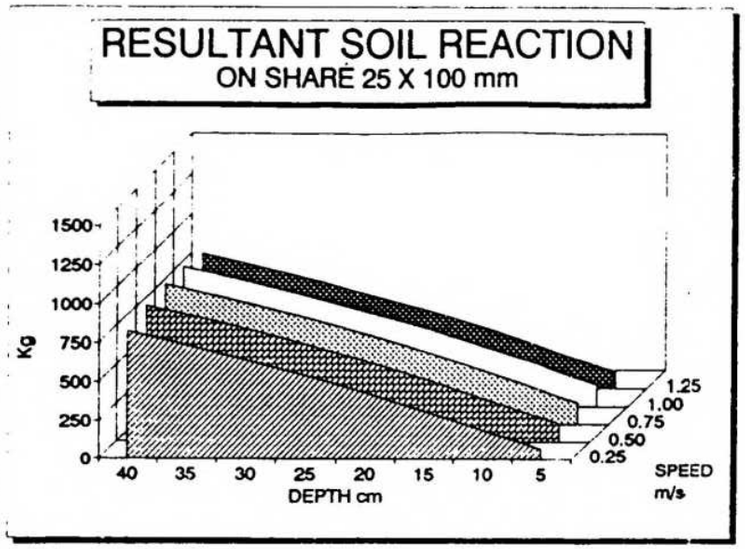

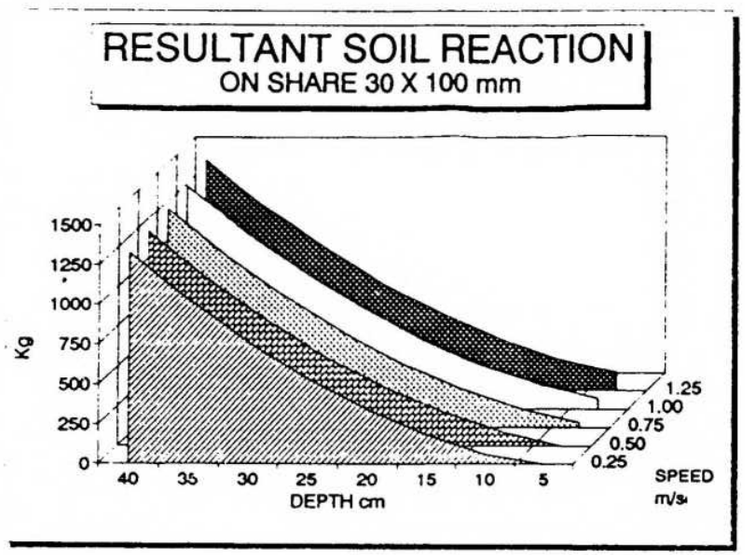

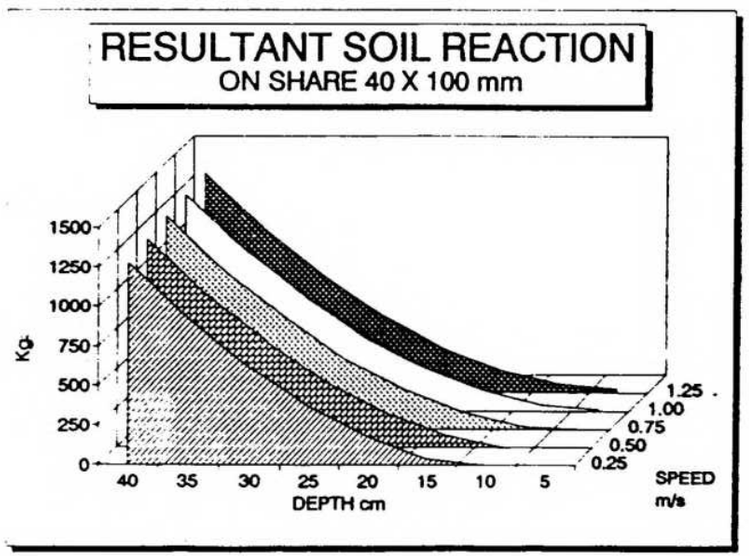

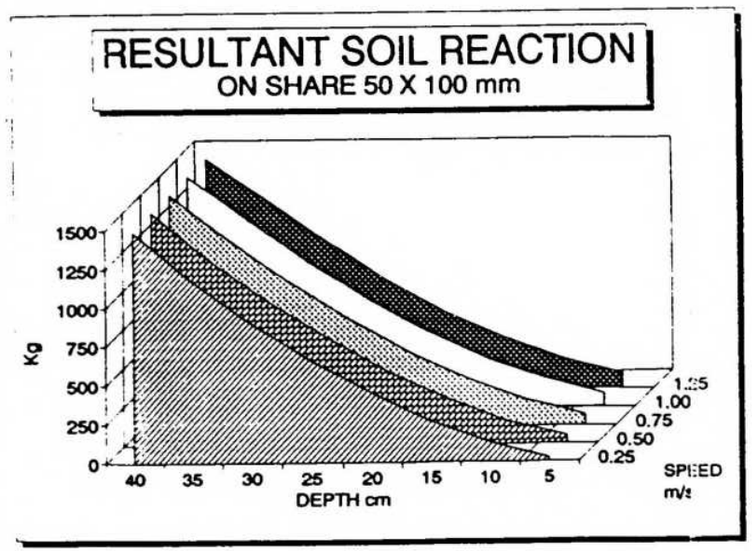

Fig 4.11 Resultant soil reaction as a function of depth and speed of operation-regressed relation for measured values

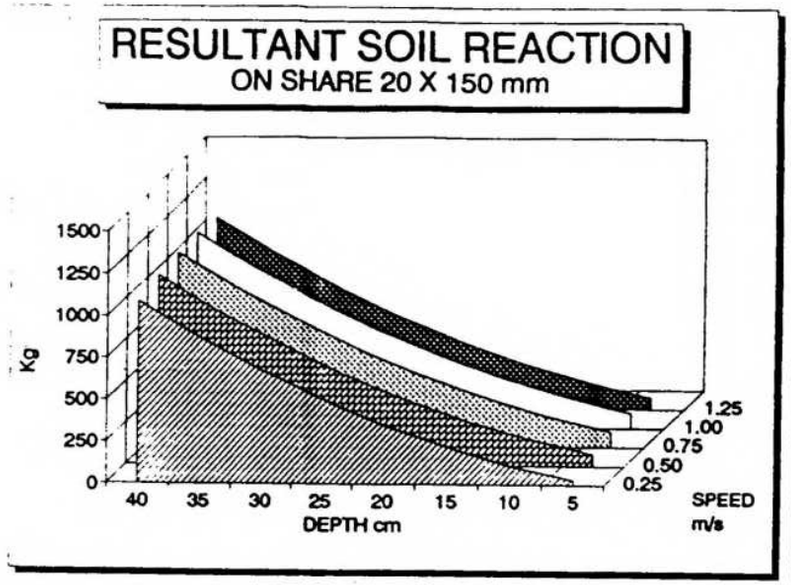

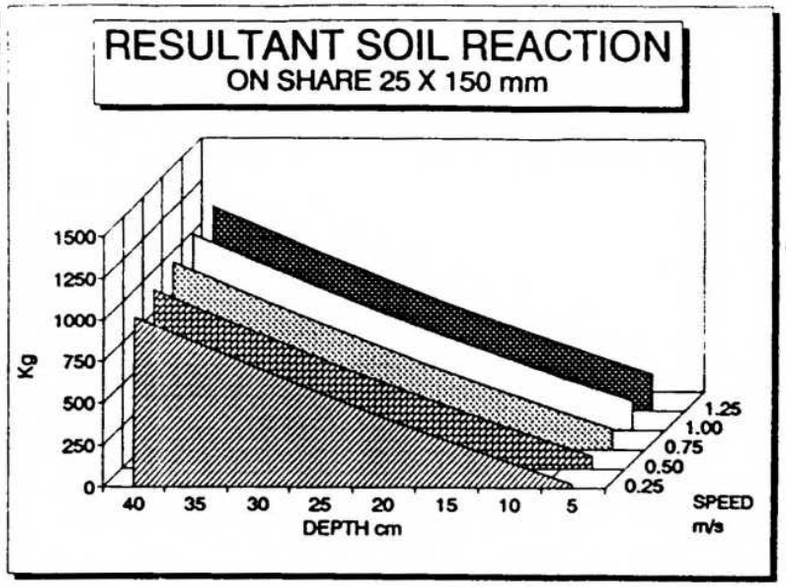

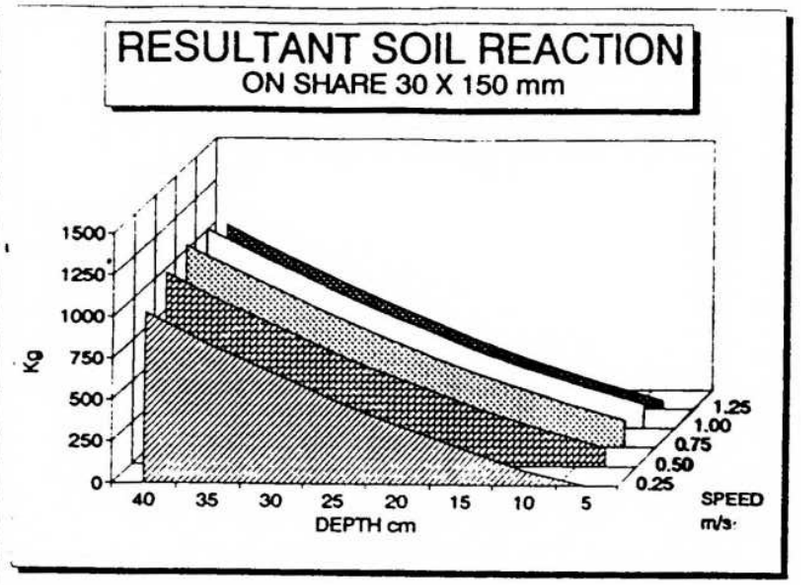

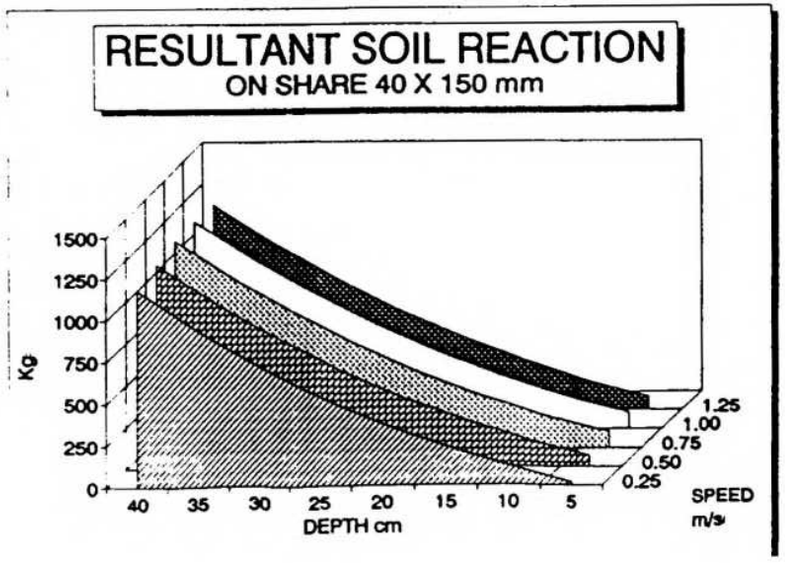

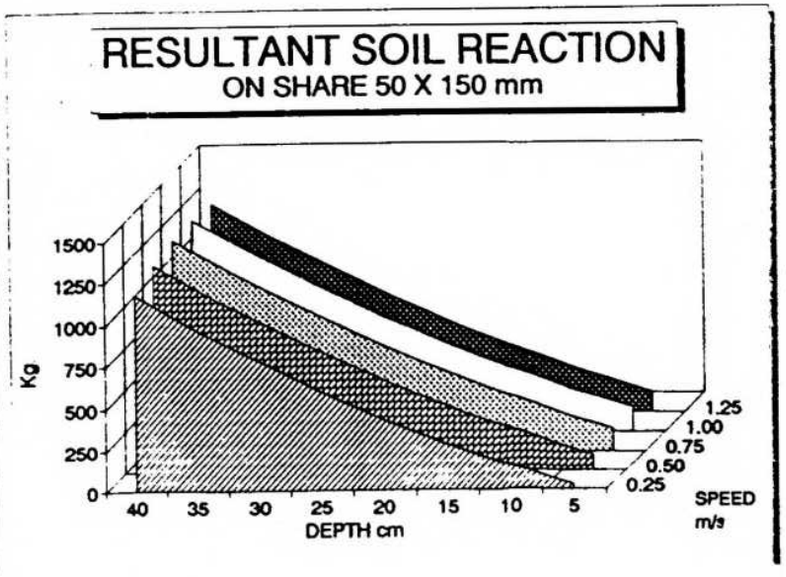

Fig 4.11 Resultant soil reaction as a function of depth and speed of operation-regressed relation for measured values

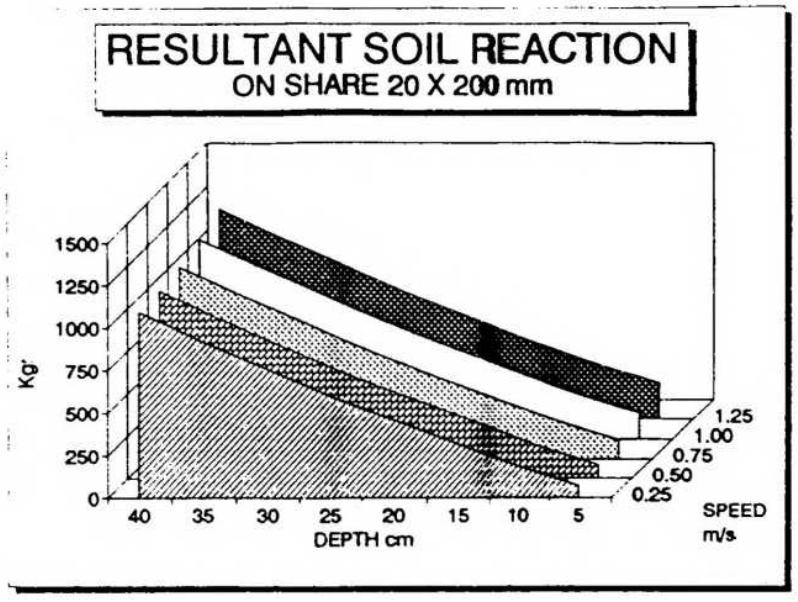

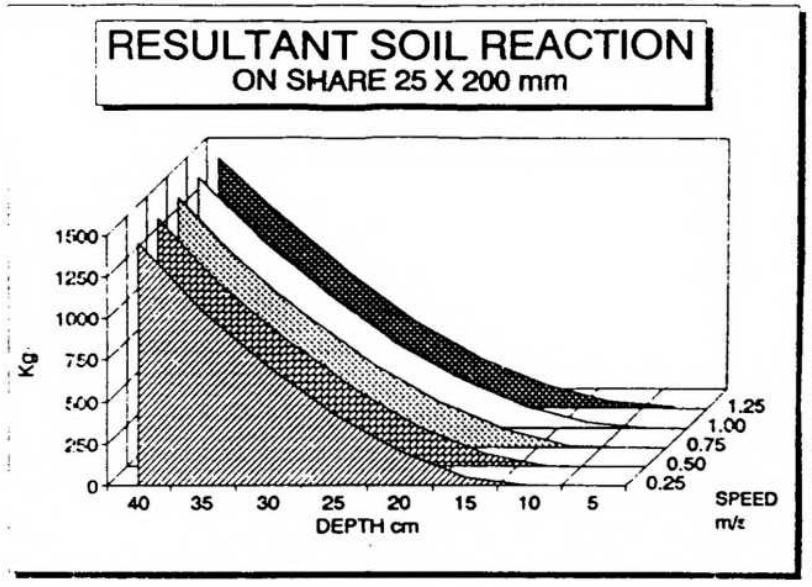

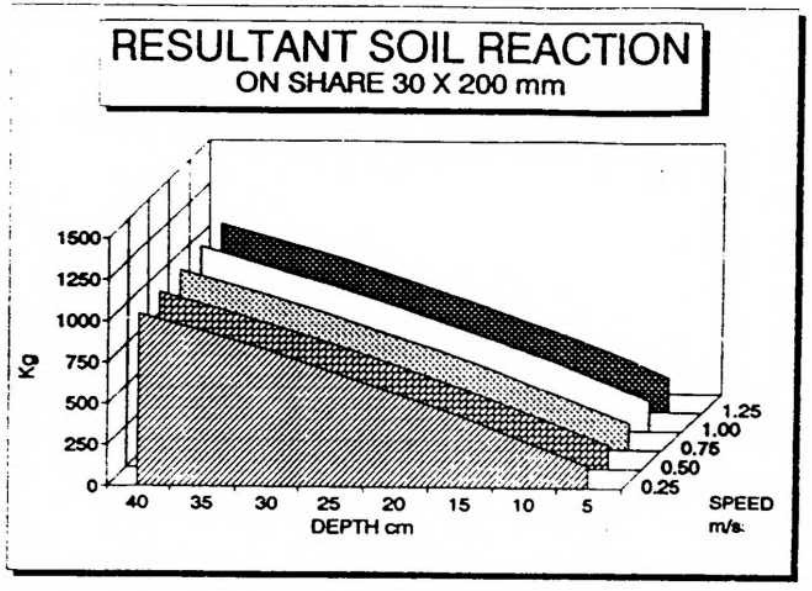

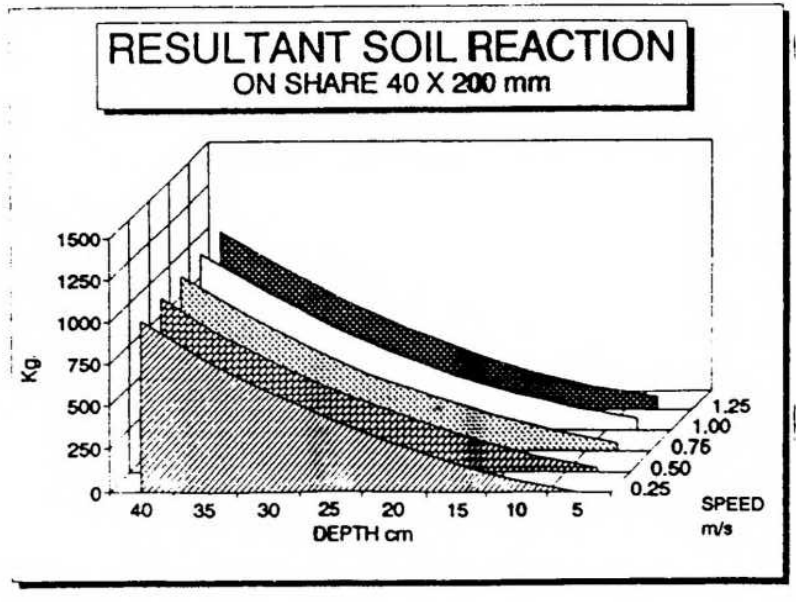

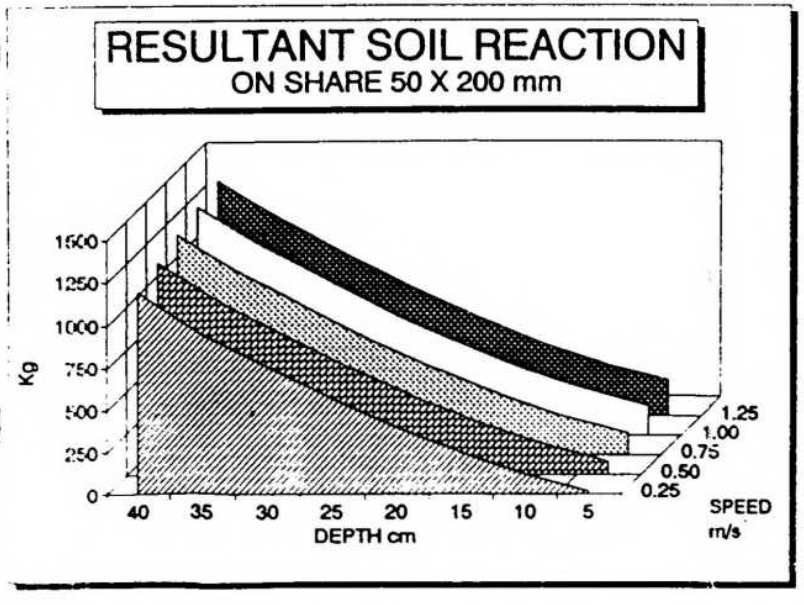

Fig 4.11 Resultant soil reaction as a function of depth and speed of operation-regressed relation for measured values

depth squared term, C_3, varied between -0.124 and 1.24 with the higher values of C_3 being associated with negative values of C_1 term. It was observed that the regression equation gave a better fit for the resultant reaction than the horizontal or vertical reaction. With R^2 values ranging from 0.86 to 0.989. These observations concurred with observations by Owen (1989) in pedogenetically compacted clay soil. The resultant soil reaction is a single force parameter and could be resolved into component reactions by assuming that the resultant reaction is inclined at an angle of soil-metal friction to the normal to the tool interface.

4.5 Effect of Speed of Operation on Soil Reaction

The effect of operational speed on soil reaction is illustrated in Fig.4.9 to Fig. 4.11. The curves represent the regression equation in the speed range of 0.25 to 1.25 m/s. or 0.9 to 4.5 km/hr. This corresponds to the normal speed range of operation of tractors with heavy duty implements.

4.5.1. Effect of speed on Longitudinal Reaction

The multiple regression equation for shares of different geometry with speed coefficient C_2 and speed squared coefficient C_4 are presented in Table 4.5. The curves illustrated in Fig.4.9 clearly showed that the influence of speed in the range of 0.25 to 1.25 m/s was negligible when compared to the influence of depth in the range of 0 to 40 cm. The coefficients C_2 and C_4 showed considerable variation in magnitude and sign thus resulting in different forms of speed-force interactions. The coefficient of speed term C_2 varied between -270 and 458 and the coefficients of speed squared term C_4 varied between -262 and 347. The average slope of the longitudinal reaction - speed relation for all shares tested varied from 115 kg/m/s in the speed range of 0.25 - 0.5 m/s to 118 kg/m/s in the speed range of 1.0 to 1.25 m/s. Hence the longitudinal force-speed relation was considered to be linear. Collins and Lalor (1973) investigated deep working tillage tools in clay soils through soil bin studies and found that the effect of speed was insignificant in the speed range of 0.3 to 1.13 m/s. These observations closely resemble

the observations made in the present study. Similar results were also reported by Rowe and Barnes (1961), Summers *et al.* (1986), Owen (1988) and Boccafogli *et al.* (1992). However a quadratic or exponential speed-draft relation had been reported by Luth and Wismer (1971), Siemens *et al.* (1965) and Wadhwa (1980). Kepner *et al.* (1972) reported studies by McKibben and Reed (1952) which yielded a second order speed-draft relation for chisel type tools. The contrasting results of the above studies could be attributed to the mode of failure, effect of inertia of soil failure wedge and strain rate effect on shear and frictional properties. A quadratic speed force relationship was visualised as being due to inertial effects (Luth and Wismer 1971, Perumpral 1988). Investigations by Kliopa (1958), Lucins 1971, Sprinkle *et al.* (1970) and Wismer and Luth (1974) have demonstrated that soil acceleration could account for only a fraction of the increased reaction and the major effect was due to the change in the soil strength. Rowe and Barnes (1961) found that the shear strength increased with the rate of shear especially for soils of higher clay content. Since the soil in the experimental field had a high clay content, the effect of speed could have been due to strain rate effect on shear strength. The pattern of draft-speed relationship obtained could have been due to the effect of the combination of the above effects.

4.5.2. Effect of speed on vertical reaction

The regression equation for vertical force-speed relation for shares of different geometries are given in Table 4.6 and the same is graphically represented in *Fig.4.10.* The curves representing the regression equations clearly illustrated that the vertical force was influenced to a lesser extent by variations in speed of operation in the range of 0.25 - 1.25 m/s than by variations in depth of operation in the range of 5 - 40 cm. All shares exhibited only minor variations in vertical force due to change in speed. The variation in vertical reaction at an operational depth of 40 cm for all share geometries was -50 kg to 57 kg in the speed range of 0.25 to 1.25 m/s except for the largest share of size 50 x 200 mm. The regression equations with both first and second power of speeds gave a good fit for the vertical reaction with R^2 values mostly within the range of 0.7 to 0.9

except for the 25 mm x 150 mm share. This was in conformity with observations by Gebresenbet and Jonsson (1992). The pattern of variation was from slightly concave to slightly convex. The coefficient of speed term C_2 varied between -543 and 336 and the coefficient of the speed squared term C_4 varied between -117 and 578. Since the equations with negative values of C_4 were associated with positive values of C_2. The net effect is a constantly increasing value of vertical force with increase in speed for most shares tested. This indicates that the penetration ability of tools increase with increase in speed. This is in agreement with the results by Siemens *et al.* (1981) and Gebresenbet and Jonsson (1992). However Smith and Williford (1988) found the vertical force to decrease with speed due to the effect of standard. A linear speed-vertical force relationship was also reported by Owen (1988). The effect of speed on vertical force was due to the acceleration of soil mass and change in soil strength parameters as discussed in the previous section. The vertical reaction was also influenced by the angle of soil-metal friction which in turn was related to the velocity of tool (Stafford 1983). Stafford and Tanner (1983) found that the angle of soil metal friction varied with speed in an logarithmic pattern and most variations were noticed in the speeds up to 0.5 to 1 m/s. The angle of soil metal friction for sandy loam soil at 5 per cent moisture content was calculated to vary from 27.16° at 0.25 m/s to 30.21° at 1.25 m/s. Hence the observed increase in vertical force could be attributed to the above strain rate effects.

4.5.3. Effect of speed on resultant reaction

The effect of speed on resultant reaction is shown graphically in Fig.4.11. The resultant reaction was predominantly influenced by the longitudinal reaction due to the low angle of resultant reaction. Hence the pattern of variation of resultant force was much similar to the variations in longitudinal reaction. It was observed that the regression equation for the resultant reaction yielded a good fit with R^2 values ranging from 0.86 to 0.989. This was in accordance with the observation, by Owen (1988), who observed a linear relation between resultant reaction and speed. The regression equations are presented in Table 4.7. The 20 x 200 mm share tested exhibited a large C_4 coefficient

associated with a negative C_2 coefficient. All other shares exhibited a positive C_2 coefficient ranging from 18.85 to 503.54. The C_4 Coefficient was positive for four shares tested and negative for all other shares thus indicating a convex shaped speed-resultant reaction characteristic. The slope of the resultant reaction-speed relation at a depth of operation of 40 cm was 176.5 kg/m/s in the speed range of 0.25 to 0.5 m/s and was 24 kg/m/s in the speed range of 1.0 to 1.25 m/s. This implied that within the range of speeds tested, the resultant reaction tends to level off at high speeds.

4.6 Effect of tool geometry on soil reaction

The geometry of a chisel type deep tillage tool could be described by the geometry of share and standard (Kepner *et al.* 1972). The influence of the standard on soil reaction had been investigated by Nichols and Reaves(1955, 1958)Godwin *et al.* (1981) and Smith and Williford (1988). These studies indicated a better performance by subsoilers with raked and curved standards. The effect of standard was not included in the present study. Since all the tests were done above critical depth and at low moisture content, the forces on the standard were expected to be minimum (Godwin *et al.* 1981). In the present study the effect of share geometry alone was studied. The reasons for selecting length and width of share as the geometrical parameters to be investigated had already been presented in Sec. 3.2.

From the regression equations for share forces (Table 4.5-4.7), the forces on shares at different combinations of depth and speed of operation were obtained and compared.

4.6.1. Effect of width of share on soil reaction

The horizontal reaction on shares of different widths at various depths of operation at a reference speed of 1 m/s were compared (Fig.4.12). It was observed that there was a considerable scatter indicating a poor fit. The increase in horizontal reaction with increase in share width was attributed to the larger area of soil disturbed. However for

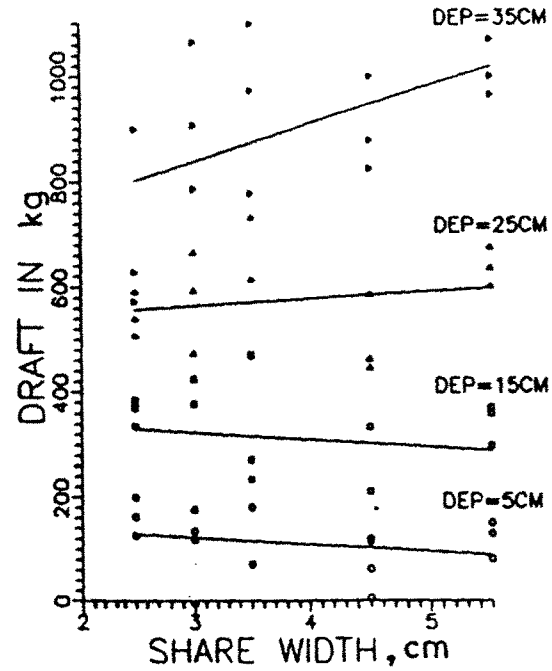

Fig 4.12 Effect of share width on longitudinal force at a speed of 1.0m/s at different depths of operation

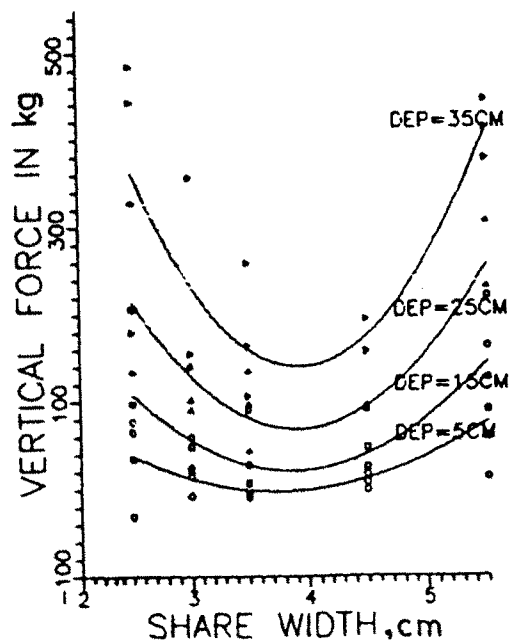

Fig 4.13 Effect of share width on vertical force at a speed of 1.0m/s at different depths of operation

narrow tillage tools which exhibit a three dimensional failure boundry, the width of tool would have lesser effect on tool forces compared to wide blades. The draft-width relationship (Fig.4.12) clearly showed that even when the share width reduces to zero there would be a draft requirement 155 kg at a depth of operation of 5 cm and 658 kg. at a depth of operation of 35 cm. Investigations by Payne and Tanner (1959), Balaton (1971), Godwin and Spoor (1977), McKyes and Ali (1977), Spoor and Godwin (1978), Perumpral *et al.* (1983), Owen (1989), Rajaram (1990) and Fielke and Riley (1991) reported results that concur with the experimental results of the present study eventhough some studies relate to plane narrow chisels and others relate to chisel with wings. It was observed that at shallow depths of operation, increase in width of share had negligible effect on horizontal soil reaction. However at 35 cm depth, a significant increase in soil reaction was observed with increase in width. The slope of the horizontal reaction - share width relation was almost constant at - 13.31 kg/cm to 13.77 kg./cm when the depth was varied from 5 cm to 25 cm. When the depth of operation was increased to 35 cm, the regressed slope increased to 71.9 kg/cm. Similar observations were also reported by Godwin and Spoor (1977) and Balaton (1971). Studies by Payne and Tanner (1959) on draft width relationship for tines of different lift angles showed that the effect of width on draft was minimal at low lift angles. Since all tines tested had a lift angle of 20°, it could be inferred that the slow rate of increase of draft with width was due to low lift angles of the shares. The above results indicated that for minimising draft requirement, the width of share should be minimum. However when the width approaches zero, the mechanism would be similar to that for extreme angles of sharpening in vertical tines where the raise in area of soil metal interface would more than offset the drop in normal pressure (Payne 1956). It was also recogonised (McKyes and Ali 1977) that there existed a lower limit of the width of a tool operating at a specified depth in order that it will still disturb the soil to the sides and lift it. The limiting ratio of depth to width was found to range from 6 to 15 for different soils and lift angles (Payne 1956). The minimum width of share was also constrained by the width of the standard and foot. The share

should be of sufficient width to facilitate mounting using standard fasteners. Since it was proposed to provide a 12 mm thick standard and a 25 mm wide foot, the width of share for the deep tillage tool to be developed was taken as 25 mm.

4.6.2 Effect of share width on vertical soil reaction

The vertical soil reaction on shares of different widths at varying depths at a reference speed of 1 m/sec were compared by pooling the results of shares of all lengths together (Fig.4.13). It was observed that the width - vertical force relationship was markedly curvilinear with the minimum vertical force occuring at a share width between 3 and 4 cm. The increasing trend of later part of curve confirmed previous experimental results by Godwin and Spoor (1977), Spoor and Godwin (1978), Grisso and Perumpral (1985), Owen (1989) and Fielke and Riley (1991). The reason for the increased vertical force for narrower shares was not clear. However, it could be attributed to other uncontrolled variables like share edge shape (Nichols *et al.* 1958 and Harrison 1982) and soil strength variations. Observations by Godwin and Spoor (1977) and Spoor and Godwin (1978) indicated a curvilinear relation between width of share and vertical reaction. However Grisso and Perumpral (1985) and Fielke and Riley (1991) indicated a linear relationship. Hence it was concluded that the increased share width will aid better penetration. However due to the low rake angle, all shares tested exhibited a downwards reaction indicating the ability of all shares to ensure penetration.

4.6.3. Effect of length of share on horizontal reaction

The horizontal soil reaction for shares of different lengths at a reference speed of 1 m/sec is presented in Fig.4.14. It was observed that the length of share had negligible influence on draft. The share length-horizontal reaction relationship was slightly convex at shallow depths and as depth increased, it transformed into a concave shape with the minimum horizontal force occurring at a length of 150 mm. Investigations by Wildman (1978) on slip plough shares showed that the horizontal reaction decreases with increase in length between share edge and standard. Nichols and Reaves (1955) also reported that

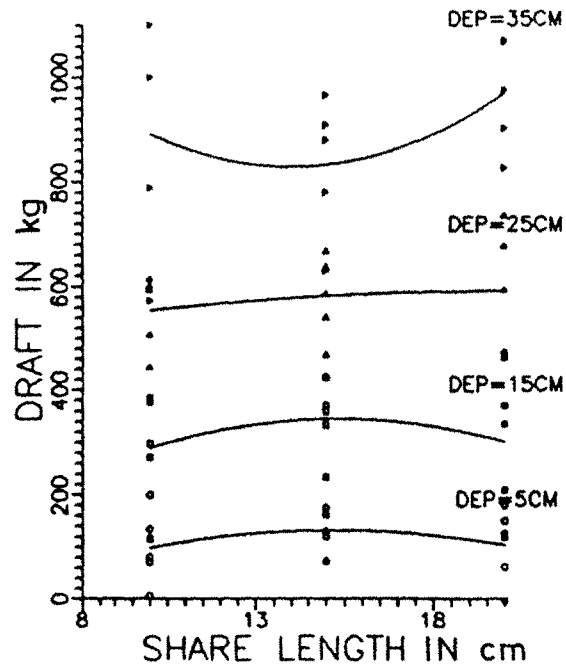

Fig 4.14 Effect of share length on longitudinal force at a speed of 1.0m/s at different depths of operation

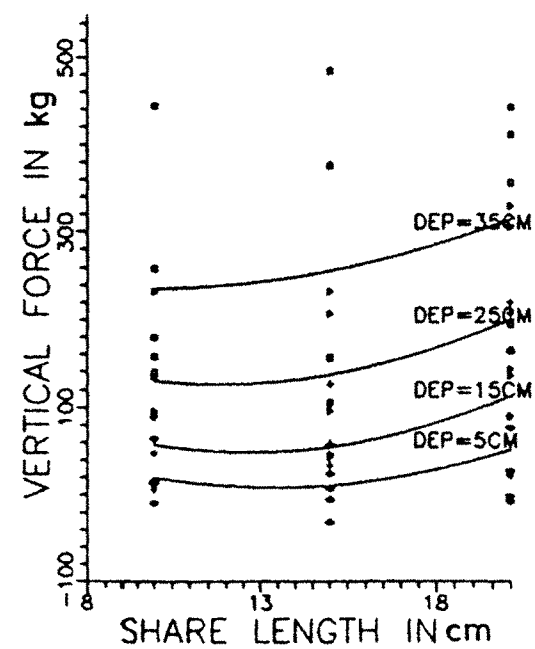

Fig 4.15 Effect of share length on vertical force at a speed of 1.0m/s at different depths of operation

a subsoiler with curved standard experienced reduced soil reaction due to the location of standard, farther away from the cutting edge. These factors could have resulted in the downward trend of the curve. When the length of the share was increased, the total height of upward deformation or lift height was increased, thus resulting in increased horizontal reaction. This behaviour had been observed by Luth and Wismer (1971) for narrow blades in sand and by Harrison (1982) for wide blades. The longer length of soil-metal interface associated with longer shares also resulted in the increased draft. It was concluded that the optimum share length would be 150 mm to ensure minimum draft requirement. An excessively longer share would result in greater bending moments at the foot and would require stronger sections for the foot, at the same time, it would be difficult to ensure adequate clearance between the furrow bottom and the foot, if the share was shorter. A share length of 150 mm offered a good balance between the above mentioned conflicting requirements. Hence the length of share was fixed as 150 mm.

4.6.4 Effect of share length on vertical soil reaction

The influence of share length on vertical soil reaction is represented for different depths at a reference speed of 1 m/s in Fig 4.15. It was observed that the vertical soil reaction increased with an increase in length of share. This behaviour was similar to that reported by Luth and Wismer (1971) Wildman (1978) and Harrison (1982). This increase was due to the increase in vertical deformation or lift height of share. Hence under circumstances requiring more vertical force, the length of the share could be increased. However since all the shares tested, exhibited a downward vertical force, the necessity to increase share length did not arise as it will increase the draft requirement.

4.7 Orientation and Location of Resultant Reaction

The magnitude (Rv), and Orientation (θ) of the resultant reaction were obtained from the regression equation for the forces on each share geometry. The location of the resultant reaction (x) was expressed as the distance between the point of intersection of the line of action of the resultant force and the vertical passing through the location of

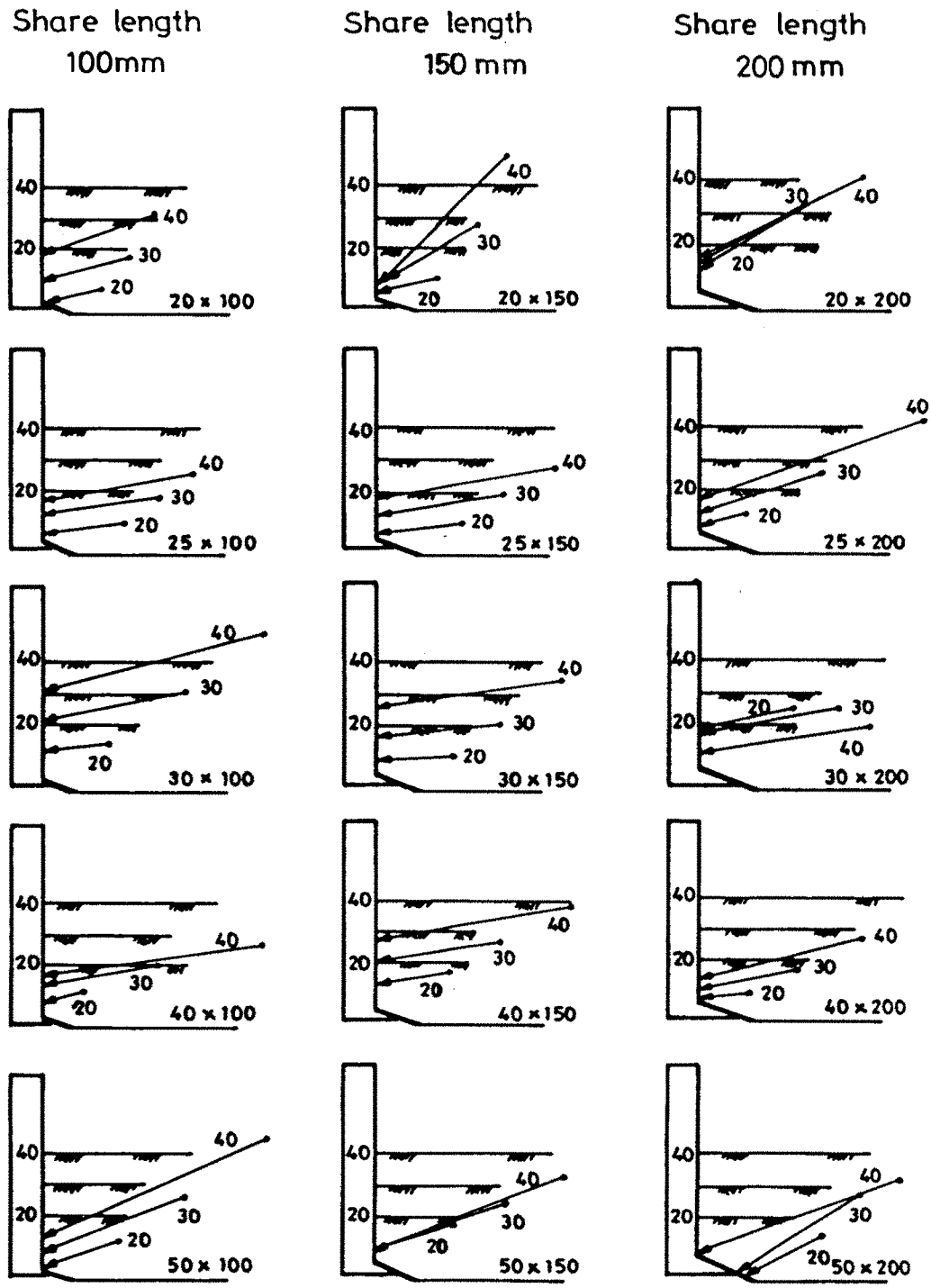

Fig 4.16 Magnitude, location and orientation of resultant soil reaction on shares of different geometry at 20,30 and 40cm depths of operation at a speed of 1m/s

V_2. It was observed that the location of the resultant varied with the depth of operation. The location of the resultant reaction was regressed with depth of operation as the independent parameter by pooling the values of x obtained at different speeds.

The magnitude, orientation and location of the resultant reaction for all share geometries tested are presented for a speed of 1 m/s and at depths of 20, 30 and 40 cm in Fig.4.16. It was observed that except for few exceptions, most shares encountered resultant reaction at almost identical orientation. The measured values of θ under field conditions are presented in Appendix D. The average orientation of the resultant reaction was found to be 11.6° since the variation in θ was very low, it was infered that the orientation of the resultat reaction was not much influenced by the operational parameters and share geometry. Since the lift angle of all the shares tested were same, the orientation of the resultant reaction was governed mainly by angle of soil-metal friction. This observation concurred with those by Payne andTanner (1959) and Siemens *et al.* (1965). The observed variations in θ were thought to be due to changes in angle of soil-metal friction brought about mainly by variations in soil moisture content.

The location of Rv determines the moment tending to rotate the tool about the horizontal transverse axis, which inturn determines the compressive force sensed by the top link of the three point hitch system, Fig.4.16. illustrates the location of the resultant force in relation to share geometry and operating depth. These plots of the resultant force indicated the combined effect of the share and standard. Under most situations, the resultant reaction passed through a point slightly above the rear edge of the share. It was observed that the resultant reaction of 200 mm long shares were more closer to the share than 100 mm and 150 mm long shares. Increase of width of share tend to lower the lcoation of the resultant reaction. This clearly indicated that longer and wider shares tend to minimise the influence of standard. The location of the resultant force was very much similar to those reported by Godwin *et al.* (1981). It was observed from the location of the resultant that the standard also contributed to considerable portion of the draft of

a deep tillage tool. This was in confirmity with the studies by Nichols and Reaves 1958 and Godwin *et al.* (1981).

4.8 Combined influence of depth and width of tool on soil reaction

In order to gain an understanding of the nature, magnitude and effect of physical parameters and to predict the prototype performance, the principles of similitude could be used (Freitag *et al.* 1970). In the present investigation, shares of different geometry were operated under varying depths and speeds of operation and their influence on soil reaction were enumerated. The possibility of arriving at a simplified model to fit the observed behaviour based on principles of similitude was investigated. Upadhayaya *et al.* (1984), observed that for tools moving at slow speeds,

$$(H/CI\ w^2) = B_0(d/w) \qquad \ldots. 4.8$$

Where H = Draft

CI = Cone Index

and B_0 = Constant

In the range of speeds tested, the effect of speed on horizontal reaction was minimum. Hence the horizontal reaction at a reference speed of 1 m/sec was analysed using the quasistatic model by Upadhayaya *et al.* (1984). The plot of $(H/CI\ w^2)$ against (d/w) is shown in fig.4.17. It was observed that the draft for all share geometries tested exhibited identical pattern of variation with respect to the dimensionless depth term. Attempts to incorporate the scale effect due to the non homogeneous strength profile (Verma and Schafer 1971) failed to enhance the fit of the experimental data to the regression equation. The highly significant regression coefficient ($R^2 = 0.83$) for the curve (Fig.4.17) implied that the regression equation (4.9) could be used to predict the tool forces as

$$(H/CIw^2) = -0.28 + 0.3468(d/w) + .0160\ (d/w)^2 \qquad \ldots..4.9$$

From the above equation, the draft at any share depth and width could be predicted if the soil strength is known.

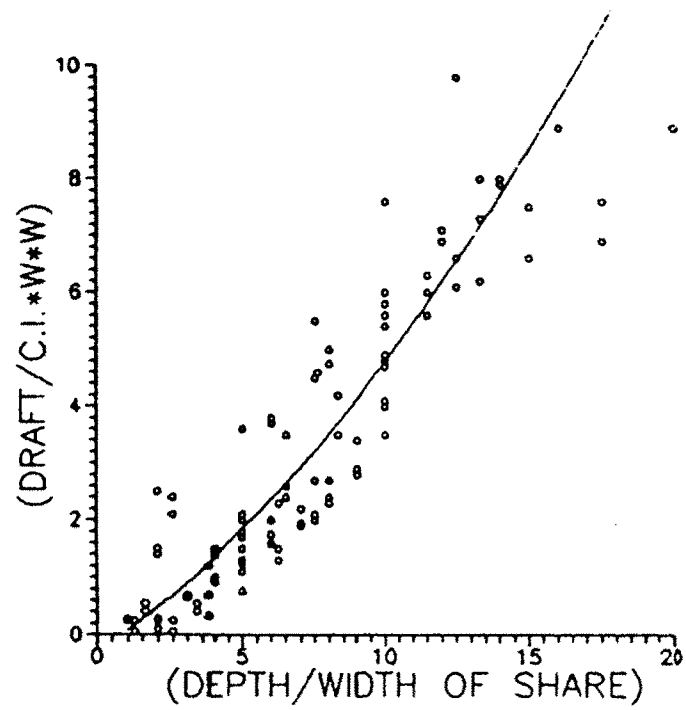

Fig 4.17 Relation between dimensionless draft term, (H/CI w^2) and share aspect ratio (d/w) at a speed of 1.0m/s

4.9 Effect of operational parameters and tool geometry on soil disturbance

The soil disturbance created by tools of different geometry under varying operational conditions were observed. Since the compaction and fragmentation effects created by the passage of tool were of lesser importance than the rupture geometry, the quality of work under different treatments was evaluated in terms of the soil disturbance pattern. The geometry of the furrows loosened by the shares were measured as explained in Sec.3.1.3. The disturbance pattern for different shares are illustrated in Fig.4.18. The measured depth, width and area of furrow are tabulated in Appendix E. The observed data exhibited a high degree of scatter due to the loose top soil, blocky sub soil and chance variations in soil condition. Similar variations in furrow geometry measurements under field conditions had been observed by Willatt and Willis (1965), Spoor and Godwin (1978) and Owen (1987). This confirmed the validity of the experimental results. It was observed by Willatt and Willis (1965) that speed of operation had negligible effect on furrow geometry. Since the experimental scatter would mask any minor difference in furrow geometry due to variations in speed, the furrow geometry was recorded only with respect to depth of operation. The width and area of furrow as function of furrow depth was plotted for each share geometry (Fig.4.19, 4.21). It was observed that the furrow width varied linearly with depth and the area of furrow had a curvilinear relation to depth. Regression equations for area and width of furrow were obtained and are presented in Tables 4.8 and 4.9.

4.9.1. Effect of depth of operation on furrow width

The experimentaly observed values of furrow width for different depths of operation for the fifteen shares tested are shown in Fig.4.19. The linear regression equation for furrow width-depth relation (Table 4.8) yielded R^2 values in the range of 0.63 to 0.90. This indicated that the depth-furrow width relationship was linear for all the shares tested. This was due to the triangular shape of the furrow section. Similar linear depth-furrow width relationship was also observed by Willatt and Willis (1965), and Owen (1987).

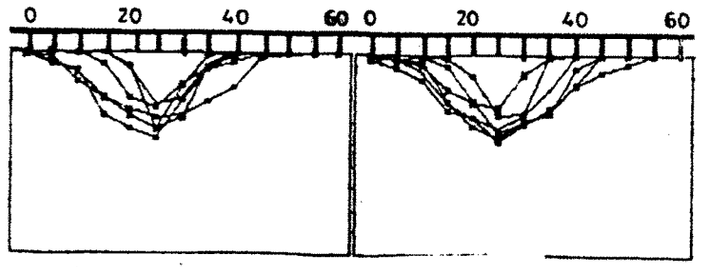

SHARE SIZE 20 x 100 mm

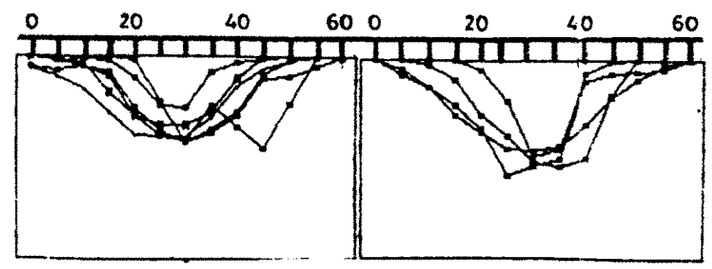

SHARE SIZE 20 x 150 mm

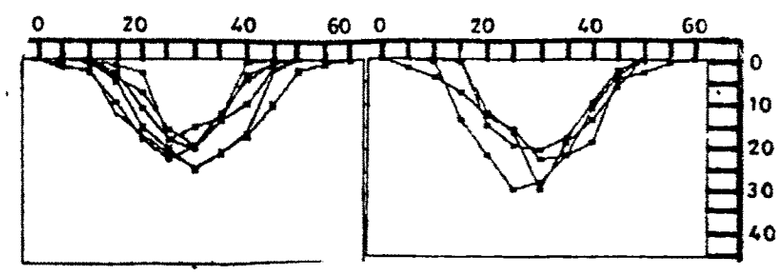

SHARE SIZE 20 x 200 mm

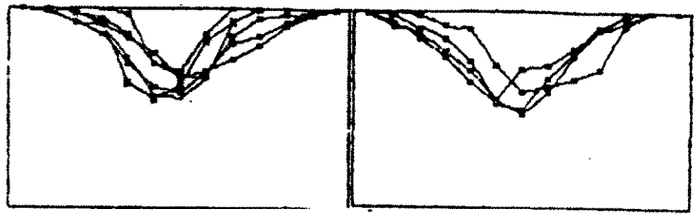

SHARE SIZE 25 x 100 mm

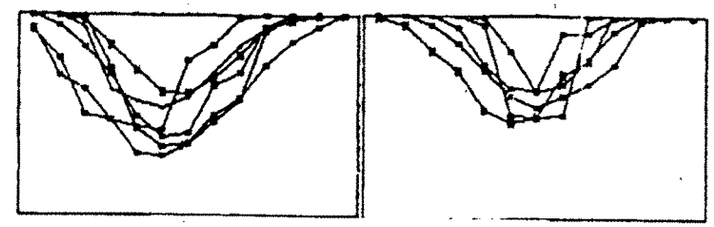

SHARE SIZE 25 x 150 mm

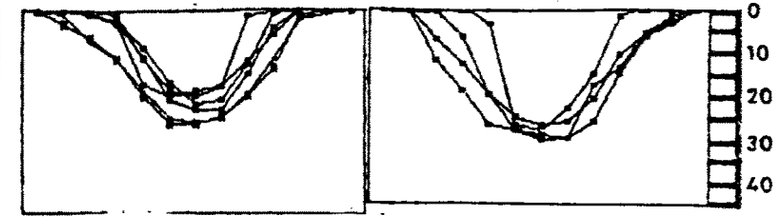

SHARE SIZE 25 x 200 mm

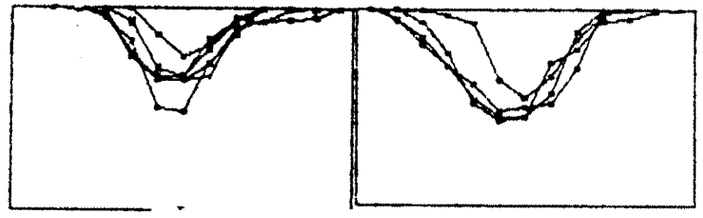

SHARE SIZE 30 x 100 mm

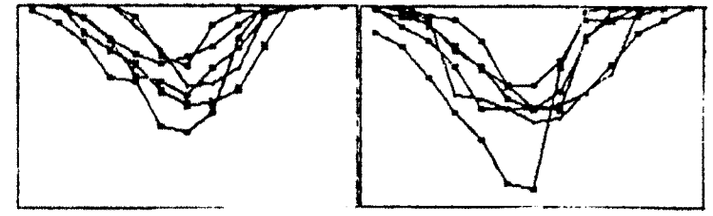

SHARE SIZE 30 x 150 mm

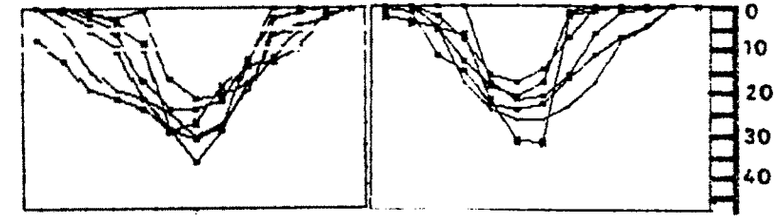

SHARE SIZE 30 x 200 mm

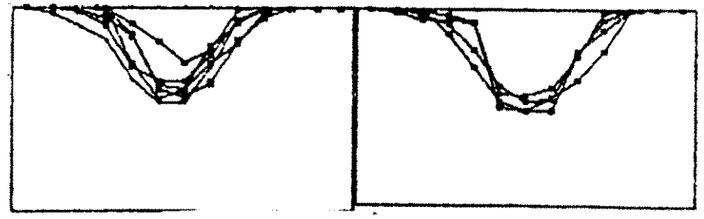

SHARE SIZE 40 x 100 mm

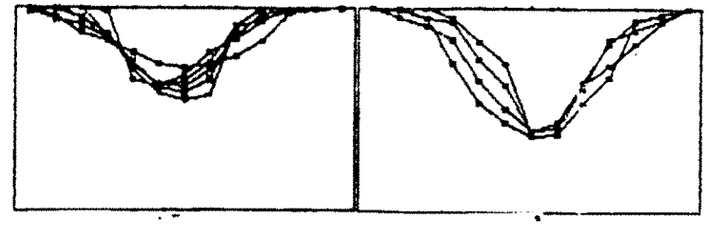

SHARE SIZE 40 x 150 mm

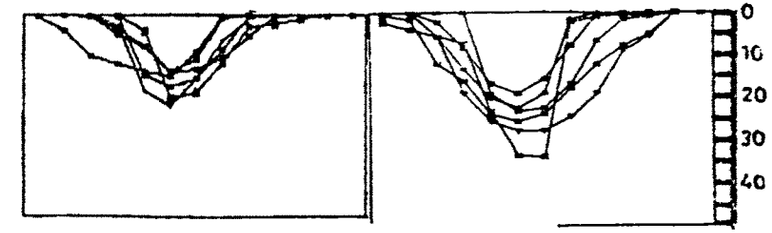

SHARE SIZE 40 x 200 mm

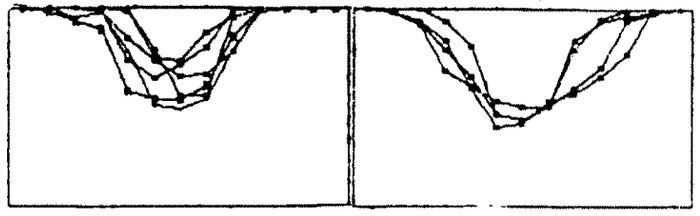

SHARE SIZE 50 x 100 mm

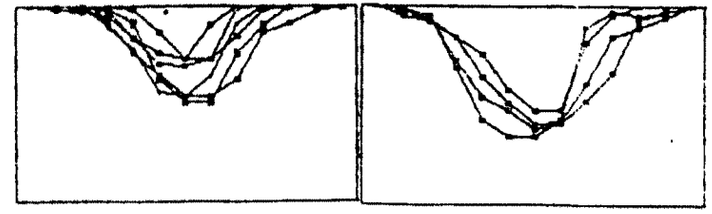

SHARE SIZE 50 x 150 mm

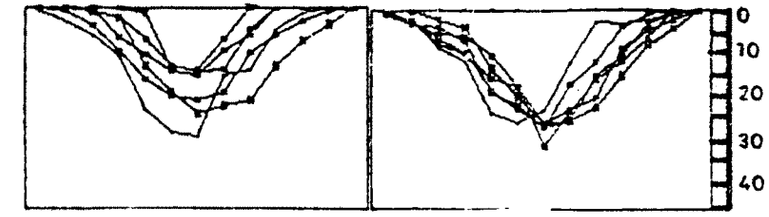

SHARE SIZE 50 x 200 mm

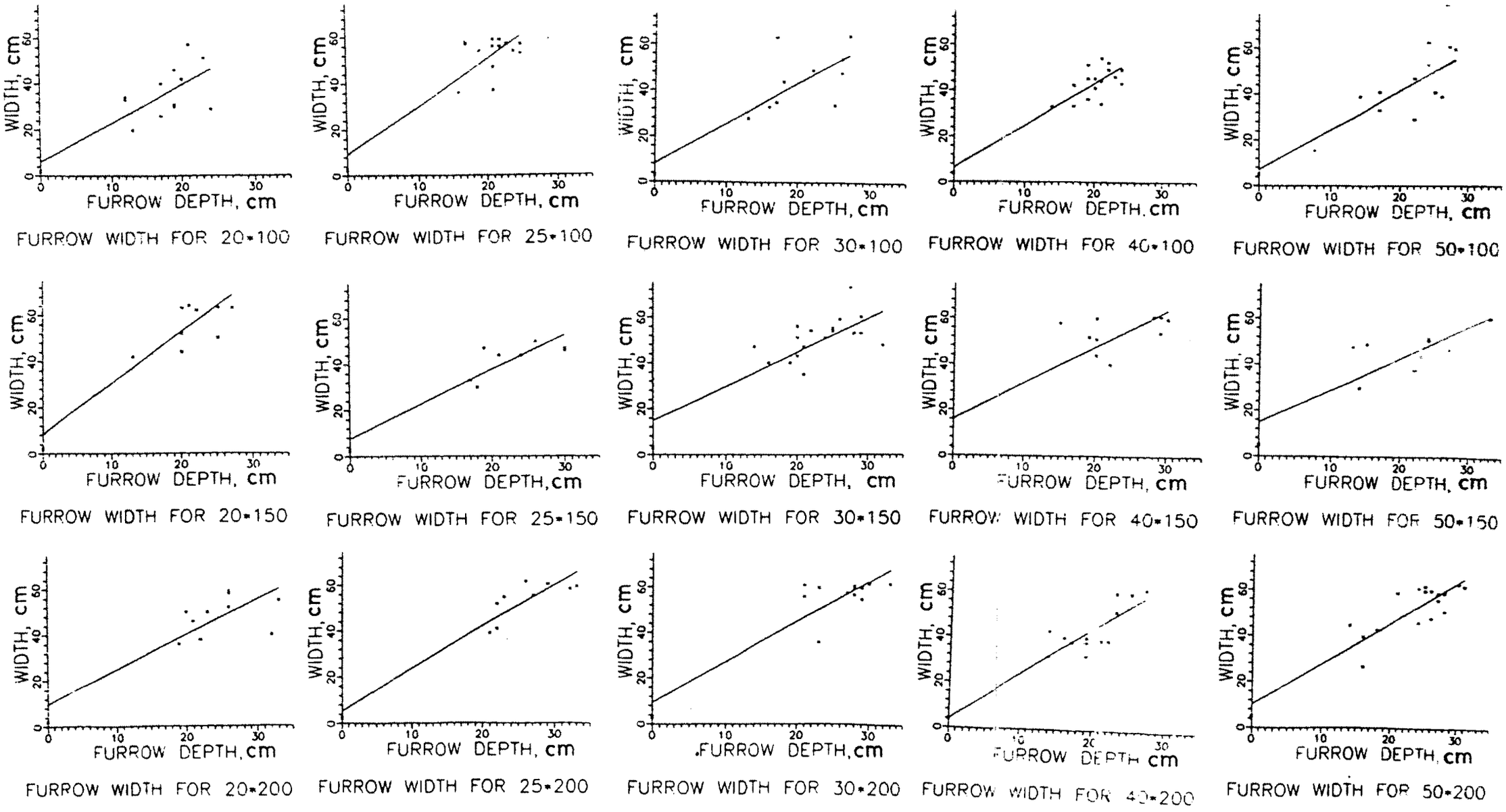

Fig 4.19 Relation between width of furrow and its depth for shares of different geometries

This confirmed the validity of the depth-furrow width relationship. The regression equations for furrow width exhibited an intercept of 4 to 16 cm at zero depth except for 20x100 mm share. Logicaly the width of furrow should be equal to the share width at zero depth. The difference between the observed and theoretical behaviour was due to the transition from a shallow tine behaviour to deep tine behaviour as depth was increased as was observed by O'Callaghan and Farrelly (1964). The depth coefficient showed considerable variation between 1.41 and 2.24. These variations were random and were

Table 4.8 Regression equations for the furrow width-depth relationship for shares of different geometry

$W = C_0 + C_1 d$ W,cm; d,cm

S.No.	Share size, mm	C_0	C_1	R^2
1	25x150	7.57	1.57	0.84
2	20x100	-42.90	20.68	0.81
3	40x200	4.01	2.01	0.81
4	30x150	14.84	1.48	0.68
5	30x200	9.44	1.78	0.79
6	50x200	10.17	1.78	0.80
7	25x100	9.13	2.06	0.71
8	40x100	6.24	1.84	0.77
9	20x200	9.74	1.53	0.70
10	40x150	15.86	1.59	0.68
11	50x150	14.82	1.41	0.71
12	20x150	8.12	2.24	0.81
13	30x100	8.19	1.76	0.63
14	25x200	5.21	1.85	0.90
15	50x100	7.11	1.73	0.68

due to the inherent scatter of the experimental values. However superimposition of the regression lines showed that the behaviour of all shares were similar with all regression lines lying inside a band of ±7.5 cm. This indicated that the share geometry had minimum effect on furrow width. Payne (1956) suggested that the furrow width of vertical tines was independent of width of share provided that the tyne was wide enough to bring soil into plastic equilibrium. The present study also confirmed the observations by Payne (1956) and Payne and Tanner (1959).

In order to bring the depth-furrow width relation into a relation between dimensionless parameters, the ratio of furrow width to share width was plotted against the depth to width ratio of shares (Fig.4.20). It was observed that the experimental data on furrow width for all the shares tested could be fitted into a single regression equation as

$$W/w = 2.28 + 1.859\ (d/w) \qquad \ldots 4.10$$

Where

W = width of furrow in cm.

The regression equation yielded a good fit with $R^2 = 0.7$. The regression equation indicated that the furrow aspect ratio varied linearly with share aspect ratio. This concurred with the findings by Payne and Tanner (1959) in clay loam soil.

4.9.2. Effect of Depth of operation on area of furrow

The experimentaly observed values of furrow area for different depths of operation for the fifteen shares tested are given in Fig.4.21. Since the furrow width was a linear function of depth, the area of furrow was fitted to a quadratic equation in depth. The regression equations for area of furrow are presented in Table 4.9. It was observed that the regression equation showed a good fit with the experimental data with R^2 values ranging from 0.75 to 0.96. This furrow area depth relationship was similar to that observed by Willatt and Willis (1965), McKyes and Ali (1977) and Owen (1987).

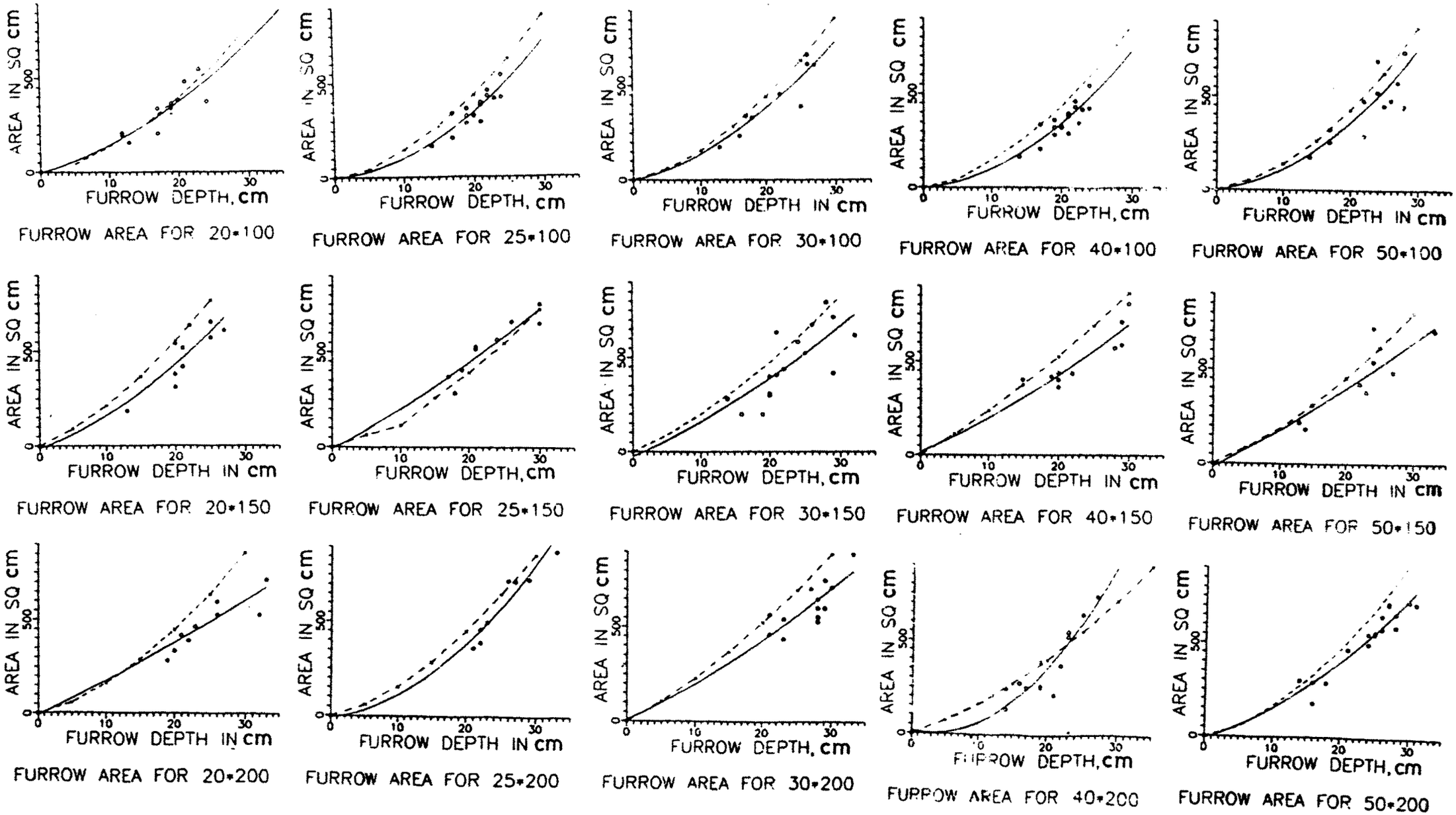

Fig 4.21 Relation between furrow cross sectional area and furrow depth for shares of different geometries

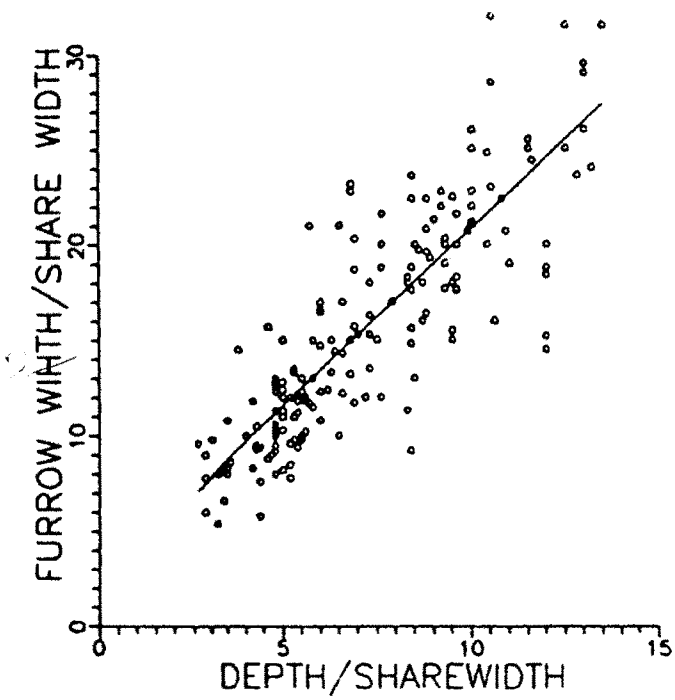

Fig 4.20 Relation between furrow aspect ratio (W/w) and share aspect ratio(d/w)

The furrow cross sectional area was taken as an indicator of furrow shape. The area of furrow was calculated for each share from the furrow width-depth relation by assuming a triangular furrow shape and was plotted along with the observed furrow area curve. It was observed that the calculated area of furrow mostly overpredicted the furrow area. This indicated a convex shaped furrow flank. Similar convex furrow flanks

Table 4.9 Regression equations for the furrow area-depth relationship for shares of different geometry

$A=C_0 + C_1 d + C_2 d^2$, A, cm^2; d,cm.

S.No.	Share size, mm	C_0	C_1	C_2	R^2
1	25x150	-8.50	19.05	0.19	0.94
2	20x100	-1.55	8.91	0.48	0.87
3	40x200	8.63	-6.9	1.22	0.89
4	30x150	-12.63	14.98	0.26	0.76
5	30x200	9.27	16.58	0.23	0.87
6	50x200	-10.10	11.57	0.45	0.93
7	25x100	-3.11	9.85	0.51	0.84
8	40x100	-0.28	2.95	0.71	0.87
9	20x200	-11.46	17.06	0.11	0.89
10	40x150	15.88	15.82	0.23	0.91
11	50x150	-19.26	18.21	0.13	0.84
12	20x150	-11.39	12.10	0.50	0.85
13	30x100	-2.03	8.83	0.52	0.91
14	25x200	-7.00	4.15	7.66	0.96
15	50x100	-8.00	3.99	0.69	0.83

were observed by O'Callaghan and Farrelly (1964) Willatt and Willis (1965) and McKyes and Desir (1984). However, detailed investigations made by Spoor and Fry (1983) indicated a convex failure profile only for tines operating below critical depth. The

difference between observed and theoretical failure profile was attributed to the soil structural rearrangement taking place outside major failure plane (McKYes and Desir 1984). Spoor and Fry (1983) observed only minimal disturbance outside major failure planes when tines operated above critical depth. In the present study, the soil had a cemented structure (Kepner *et al.* 1972) hence considerable deformation was observed beyond the failure planes. This could have been one of the reasons for obtaining a convex shaped furrow flank. Another probable reason for the convex furrow flank shape was the weak top soil. The furrow profile geometry illustrated in Fig.4.18 also substantiates the above reason.

Since the furrow aspect ratio was observed to be a linear function of share aspect ratio, the furrow area divided by the product of share depth and width (A/wd) was expected to be a linear function of share aspect ratio. The plot of A/wd) against d/w is shown in Fig.4.22. It was observed that the furrow area created by all the shares could be fitted into a linear regression equation as

$$(A/wd) = 0.9066 + 0.7787\ (d/w) \qquad \ldots 4.11$$

Where

A = Area of furrow

The regression equation yielded a significant fit with $R^2 = 0.73$. this indicated that the furrow geometry created by all shares could be predicted by the above equation.

4.9.3 Effect of critical depth on furrow geometry

The tines investigated were 2 to 5 cm wide and working depth was 20-40 cm. This meant a share aspect ratio of 4 to 20. The mechanics of soil failure had been observed to be dependent on the tine aspect ratio. The tine aspect ratio was related to the critical depth at which the transition occured from vertical plane strain or upheavel to horizontal plane strain or soil being pushed aside (Collins and Lalor 1973). For vertical tines Kostritsyn (1956) and O'Callaghan and Farrelly (1964) calculated that the transition occured at a tine aspect ratio of 0.6. O'Callaghan and Farrelly (1964) observed the furrow aspect ratio curve to level off at the transition aspect ratio of 3.0.

O'Callaghan and McCullen (1965) gave the tine aspect ratio at critical depth as a function of tine rake angle. This exponential relation when extrapolated yielded an aspect ratio of 5.2 for a 20° raked tine. The critical depth for 20°share operating under conditions of the experimental field was calculated by using method outlined by Godwin and Spoor (1977). The share aspect ratio at critical depth was found to vary from 81.0 cm to 95.4 cm for shares of 2 to 5 cm width. The very high value of critical depth was due to high values of shear strength exhibited by the soil. This was in confirmity with observations by Spoor and Godwin (1978). This clearly indicated that in the present study, the shares were operated at depths less than critical depth. Hence all experimental results were considered as being due to cresent failure only. The furrow aspect ratio curve (Fig.4.22)also clearly indicated that the soil failed by cresent failure within the range of depths considered. However when shares were operated below critical depth, the width of furrow would reduce with increased depth of operation as was observed by Owen (1987).

4.10 Efficiency of tillage using Chisel type tools

According to Gill and Vanden Berg (1967). The efficiency of performance could be measured as the energy required to obtain the required soil condition. In deep tillage where loosening of the compacted subsoil is done, the width of furrow, area of soil loosened, degree of soil loosening (density reduction) and fragmentation obtained are the indicators of performance. In deep summer fallow ploughing, the first two parameters are of maximum importance. The furrow should have the maximum width to aid infiltration (Payne and Tanner 1959) and maximum area should be loosened to ensure adequate root development. The draft per unit width of furrow and unit area of furrow were obtained from generalized equations for draft, width of furrow and area of furrow.

4.10.1. Draft requirement for unit width of furrow

The draft per unit width of furrow was obtained by dividing Equation 4.9. by Equation 4.10 and rearranging the terms we get

$$(H/W) = CIw(0.176 + 8.61 \times 10^{-3}(d/w) \quad \ldots 4.12$$

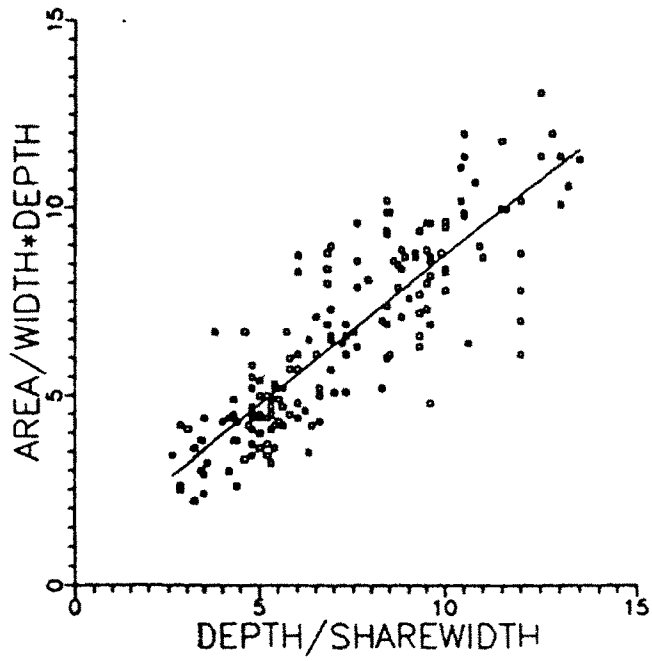

Fig 4.22 Relation between dimensionless furrow area term, (A/dw) and share aspect ratio(d/w)

This implied that for a given soil, (H/w) was the sum of the depth related factor and width related factor. The effect of width and depth are clearly brought out in Table 4.10 which represents (H/w) at two share width, and different operating depths at a CI value of 18.72 kg/cm^2, which corresponds to the average soil strength of the experimental field.

It was clear from Table 4.10 that at any depth, narrower shares were preferable to obtain maximum surface disturbance with minimum draft force. Though Payne and Tanner (1959) did not notice any appreciable effect of width of share on (H/W), the present study indicated that the width of share has a significant effect on (H/W). This might be due to the nature of soil. It was predicted that the draft per unit furrow width would be 13 kg/cm when using a 2 cm wide share and the same would be 22.9 kg/cm when using a 5 cm wide share.

Table 4.10 Draft per unit width and unit area of furrow

(CI = 18.72 kg/cm^2)

Sl.No.	Depth cm	Share width cm	H/W Kg/cm	H/A Kg/cm^2
1	10	2	8.2	1.14
2	20	2	9.8	1.03
3	30	2	11.4	0.84
4	40	2	13.0	0.74
5	10	5	18.1	1.81
6	20	5	19.7	1.59
7	30	5	21.3	1.33
8	40	5	22.9	1.15

4.10.2 Unit Draft

The draft per unit cross sectional area of furrow was obtained by dividing equation 4.9 by equation 4.11. For accuracy of analysis the equations were retained in their generalised form as

$$H/A = (CI/(d/w)(0.016(d/w)^2 + 0.3468(d/w)-0.28)/(0.7787(d/w)+ 0.9066) \quad \ldots 4.13$$

The values of (H/A) for different depths of operation and for two share widths are tabulated, Table 4.10. The unit draft for a 2 cm wide blade operating at a depth of 40 cm was predicted to be 0.74 kg/cm^2 and the same for a 5 cm wide blade was predicted to be 1.15 kg/cm^2. The unit draft for a 2 cm wide share was predicted to decrease from 1.14 kg/cm^2 at an operational depth of 10 cm to 0.74 kg/cm^2 at a depth of 40 cm. The reduction of unit draft with increased depth of operation implied that the rate of increase in area with depth was more than rate of increase in draft force with depth. This behaviour contradicted the behaviour derived by MckYes and Ali (1977). This was due to the difference in soil conditions. The high values of unit draft indicated the extraordinary field conditions with very high values of soil strength. The values are however comparable to those obtained by McKyes and Desir (1984) in clay soil. The reduction of unit draft with decrease in width of share clearly indicated that the share width should be minimum to increase efficiency. This further justified the decision to use a narrow share for the prototype implement.

4.11 Simulated performance of deep Tillage Tools

An attempt was made to use the existing soil mechanics models to predict the performance of narrow, deep, tillage tools operating in dry compacted clay soils. The results of the prediction study were applied to valididate the experimental findings, evaluate the suitability of models to predict performance under the given soil conditions to obtain better understanding of the soil tool interaction and to aid in the design and development of the deep tillage tool. The following four models were used due to their unique features.

1. Godwin and Spoor (1977)
2. McKyes and Ali (1977)
3. Perumpral *et al.* (1983)
4. Swick and Perumpral (1988)

All models were simulated for identical input parameters. The effect of speed was predicted by Swick and Perumpral model alone. Table 4.11 tabulates the input parameters used for simulation.

4.11.1 Soil properties used for simulation studies

The techniques adopted for measurement of soil properties used in the simulation are presented in Sec. 3.6.1. The average bulk density of the experimental field was measured to be 1.37 g/cm^3 at a moisture content of 5 per cent. The shear strength of the field soil was measured using an annular shear apparatus. The shear envelop is plotted in Fig.4.23. The regression equation yielded the following constants

Cohesion, C = 110 g /cm^2

Angle of internal friction of soil = 44.5°

The above values of cohesion and internal friction reflected the very high shear strength of the soil. The soil-metal friction(δ) was measured using a mild steel slider. The plot of frictional load against normal load for the 200 cm^2 slider is given in Fig.4.24. The following frictional parameters were obtained from this relation

Soil-metal adhesion = 8.6 g/cm^2

Angle of soil-metal friction, = 33.8°

The Perumpral model and Swick and Perumpral model used values of angle of soil-metal friction, expressed as a function of share lift angle, α and the adhesional factor was taken as 0.5C To suit the form of equation developed by Grisso (1980), as proposed by O'Callaghan and McCullen (1965), a linear relation was assumed between δ and α

The transition in δ was assumed to occur at a critical angle of rupture surface, β cr. βcr was arrived from McKyes and Ali model as (90-ϕ). Similar procedure was also used by Boccafogli *et al.* (1992). The equation for soil-metal friction was arrived as

$$\delta = 0.94 - 0.45\alpha \text{ rad } (\alpha > 0.794) \quad \ldots. 4.14$$

$$\delta = 0.59 \text{ rad } (\alpha > 0.794) \quad \ldots. 4.15$$

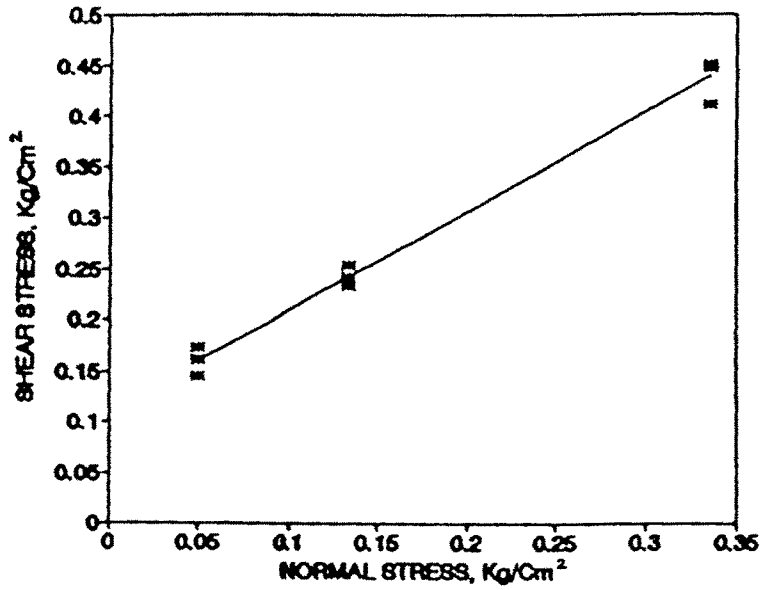

Fig 4.23 Shear stress as a function of normal stres for experimental field conditions

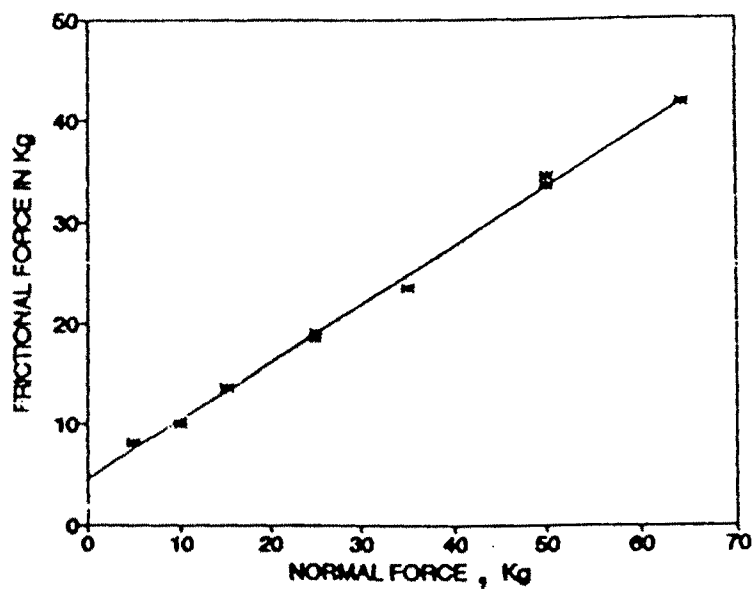

Fig 4.24 Frictional force-normal force relation for experimental soil condition

4.11.2 Results of model simulation

The longitudinal reaction, vertical reaction, width of furrow and area of furrow were the four output parameters of the models considered. However, the Perumpral model predicted only the tool forces. The independent parameters and the range of values used are given in Table 4.11. The results of the simulation were plotted as graphs for selected combination of parameters.

4.11.3 Effect of depth of operation on horizontal soil reaction

The horizontal reaction is presented as a function of depth, for different lift angles for the four models simulated, Fig.4.25. It was clearly observed that the horizontal reaction-depth relation was parabolic. The horizontal reaction-depth relation reflected the depth-furrow geometry relation. To ensure uniformity among modes,the Swick and Perumpral model was modified by replacing the emphirical equation for the sector width, S with McKyes and Ali's analytical relation. However the Godwin and Spoor model used the empherical values of rupture distance ratio. It was observed that all models predicted closely similar force-depth relationship. The horizontal force-depth relation was similar to those reported by McKyes and Ali (1977). McKyes *et al.* (1977), McKyes (1978) and Grisso and Perumpral (1985) from simulation studies. The parabolic force-depth relationship was similar to the two dimensional soil cutting models by Osman (1964), Reece (1965) and Hettiaratchi *et al.* (1966). This was later used by Godwin and Spoor (1977) for the three-dimensional force prediction model. Due to the parabolic relationship, the difference in the values predicted by the models increased with increase in depth. The curves (Fig.4.25) also indicated that shares of higher lift angles experienced greater draft than shares of lower lift angles.

4.11.4 Effect of depth of operation on vertical soil reaction

The vertical soil reaction - depth relationship for shares of different lift angles is presented in Fig.4.26. The vertical force also was found to increase with depth of

Table 4.11 Values of variables used for numerical prediction

Variable	Value when used as Variable	Value when used as constant
Tool parameters		
Tool width w, cm	2,2.5,3,3.5,4,4.5,5	2
Tool depth d, cm	5,10,15,20,25,30,35,40	35
Tool lift angle α, rad	0.15,0.35,0.55,0.75,	
	0.95,1.15,1.35 and 1.55	0.35
Tool velocity v, m/s	0.25, 0.5, 0.75,1.00 and	
(Swick and Perumpral)	1.25	0.25
Soil parameters		
Cohesion C, g/cm^2	110	
Internal soil friction angle ϕ, rad	44.5°	
Bulk density γ, g/cm^3	1.37	
Soil-tool interface parameters		
For Godwin and Spoor and		
McKyes and Ali models		
Angle of soil metal friction	33.8°	
Adhesion, g/cm^2	8.6	
For Perumpral and Swick and		
Perumpral models		
Angle of soil-metal friction δ	0.94 - 0.45α (α > 0.794)	
	δ 0.59 ($\alpha \leq$ 0.794)	
Adhesion factor, g/cm^2	55	

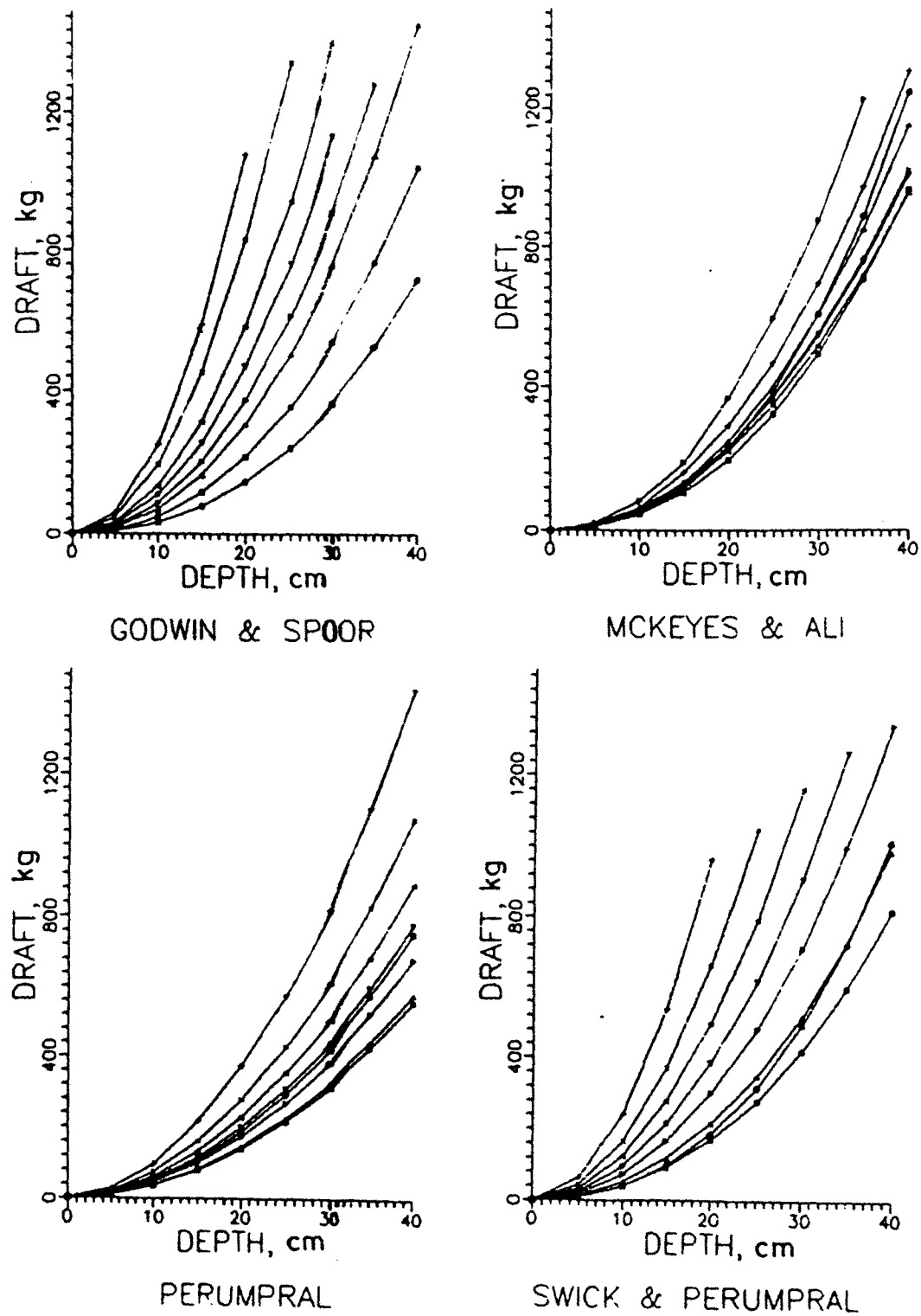

Fig 4.25 Predicted draft-depth relation at different share lift angles using different prediction models at a share width of 2cm.
0-8.6°, □ -20°, Δ -31.5°, ▷ -43°, ▽ -54.4°, ◁ -65.9°, X-77.3°, +-88.8°.

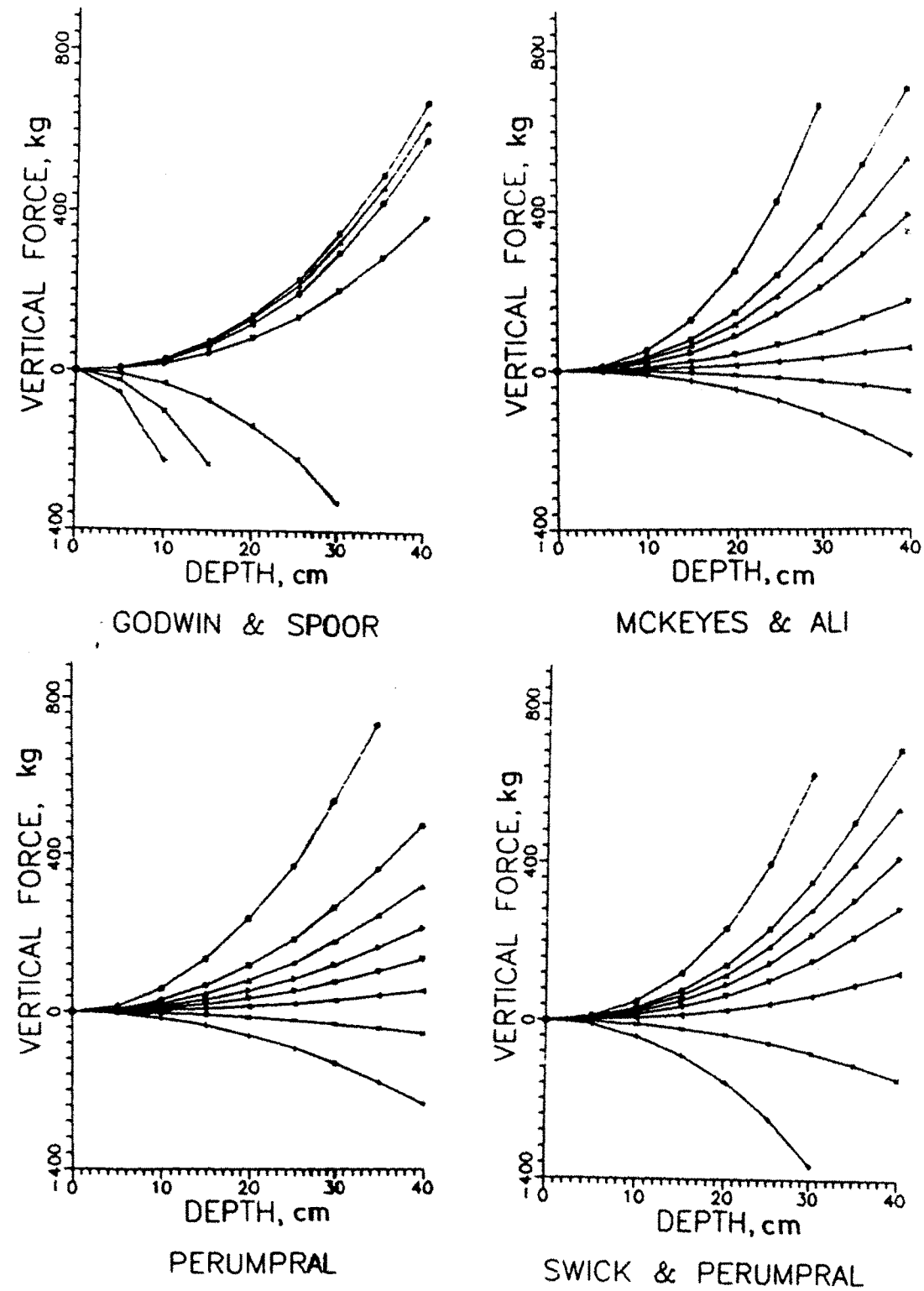

Fig 4.26 Predicted vertical force-depth relation at different share lift angles using different prediction models at a share width of 2cm. 0-8.6°, □ -20°, △ -31.5°, ▷ -43°, ▽ -54.4°, ◁ -65.9°, X-77.3°, +-88.8°.

operation in a parabolic manner. This concurred with the observations by Grisso and Perumpral (1985) from similar model studies. Though the vertical force-depth relation was parabolic, at lift angles in the range of 20 to 42°, the vertical force predicted by all models except Godwin and Spoor model was found to be almost linear. It was observed that the vertical force decreased with increase in lift angle and at higher lift angles, the vertical force was negative. Except Godwin and Spoor model, all other models exhibited similar vertical force-depth relation.

4.11.5 Effect of speed of operation on horizontal reaction

The effect of speed of operation was simulated by Swick and Perumpral model (1988). The effect due to accleration of cresent shaped failure wedge was simulated through this model. The model assumed that the rupture geometry was independent of the speed of operation. The effect of speed for a 2 cm wide, 20°lift angle share as a function of depth are presented in Fig.4.27. It was observed from Fig.4.27, that speed of operation had only a marginal effect on the longitudinal reaction in the range of speeds simulated. The effect of speed was increased at greater depths of operation due to the increase in volume of soil disturbed. The horizontal reaction-speed relation was almost linear due to the lesser interval of speed range simulated. The vertical force-depth relationship was similar to the horizontal force-depth relation. However the effect was correspondingly lesser.

4.11.6 Effect of lift angle on longitudinal soil reaction

The effect of lift angle on longitudinal reaction for a 2 cm wide share at different depths of operation is presented in Fig.4.28. The longitudinal force calculated by all the models was found to be minimum at a rake angle of 20°. Though the Godwin and Spoor model predicted a monotonicaly increasing longitudinal reaction-lift angle relation, the other three models indicated a reduction in longitudinal reaction when the lift angle was increased from 8 to 20°. Though effect of lift angle was minimum at a shallow depth of operation, as the depth was increased, shares with greater lift angles exhibited very high values of

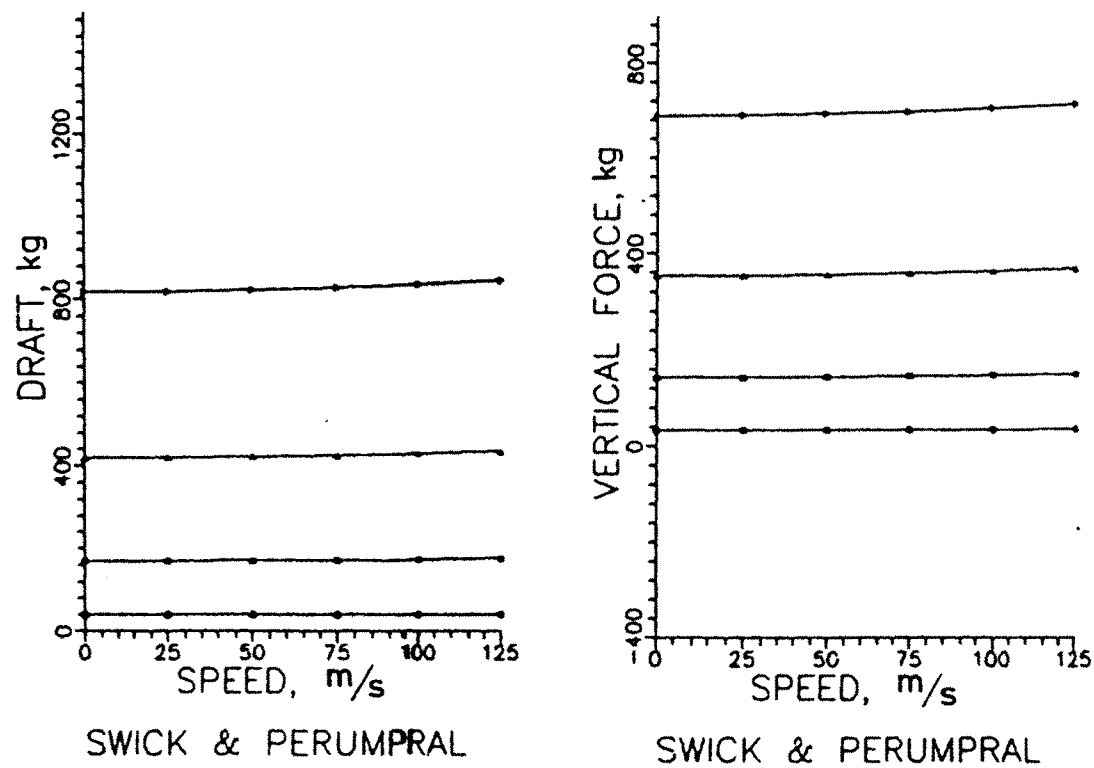

Fig 4.27 Predicted effect of speed on draft and vertical force on a 2cm wide share using Swick and Perumpral (1988) model at different depths of operation.
0-10cm, ▫ -20cm, △ -30cm, ▷ -40cm

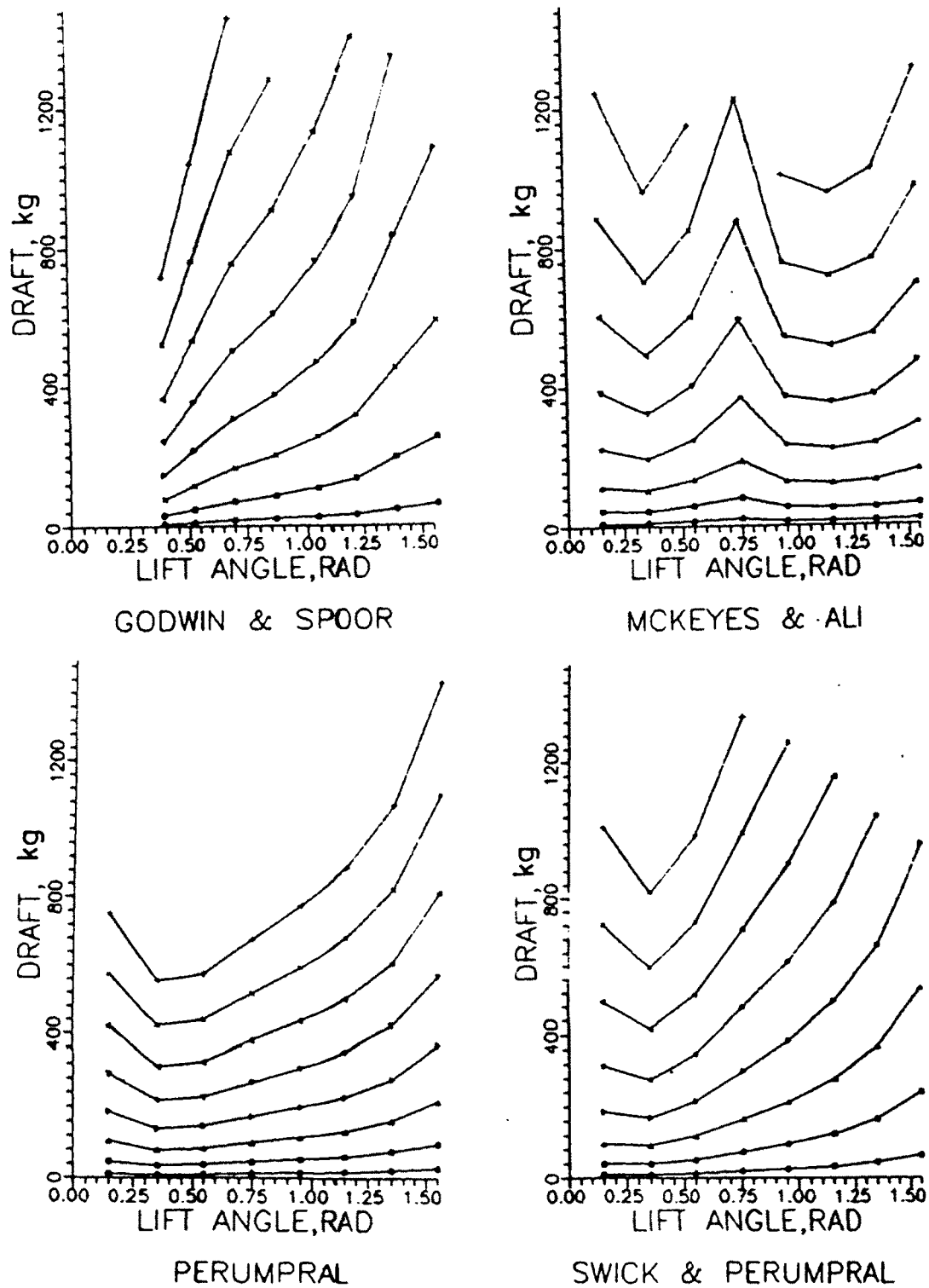

Fig 4.28 Predicted draft-lift angle relation at different depths of operation using different prediction models at a share width of 2cm. 0-5cm, ▫ -10cm, △ -15cm, ▷ -20cm, ▽ -25cm, ◁ -30cm, X-35cm, + -40cm.

draft forces. Similar results obtained by McKyes and Ali (1977), McKyes *et al.* (1977) McKyes (1978) and Grisso and Perumpral (1985) indicated the validity of the results obtained by the experimental investigation. The pattern of longitudinal force-lift angle relation indicated significant difference between models. A definite discontinuity was exhibited at an angle of 42° by the McKyes and Ali model. This was due to the difference in the mechanics of failure which changed from a single wedge model to a two wedged model as the lift angle was increased. It was clearly observed that using the single wedge model over the entire range of lift angle would have resulted in considerable over prediction. The Perumpral model and the Swick and Perumpral model approximated the behaviour of the McKyes and Ali model by changing the angle of soil-metal friction with increase in lift angle. The closely similar behaviour of the two modes of calculation clearly indicated their validity. However the Perumpral and Swick and Perumpral models yielded a smoother transition at βcr. The Godwin and Spoor model yielded values broadly similar to other three models.

4.11.7 Effect of lift angle on vertical Reaction

The effect of lift angle on vertical reaction on a 2 cm wide share at different depths of operation is presented in Fig.4.29. It was observed that the vertical force changed from a downward to upward direction at a particular lift angle for each model depending on the value of soil-metal friction. The transition occured at a share lift angle of $(90-\delta)$. This was due to the angle between the normal to the tool surface and the resultant reaction being taken as δ for all the models simulated. The Godwin and Spoor model alone exhibited a slight increase in vertical reaction as the lift angle was increased from 8° to 20°. The general vertical reaction-lift angle relation was similar to that observed by Grisso and Perumpral (1985).

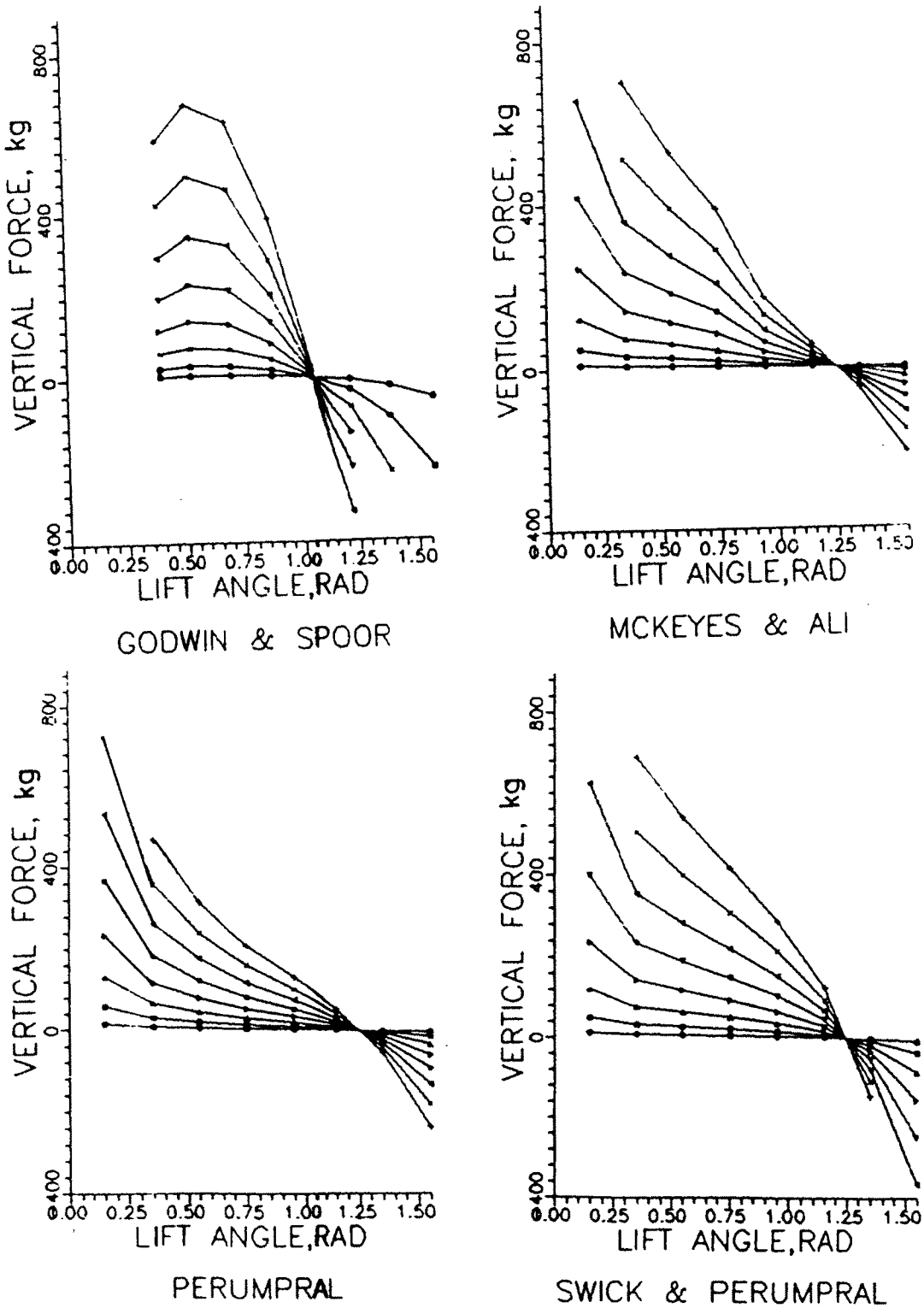

Fig 4.29 Predicted vertical force-lift angle relation at different depths of operation using different prediction models at a share width of 2cm. 0-5cm, □ -10cm, △ -15cm, ▷ -20cm, ▽ -25cm, ◁ -30cm, X-35cm, +-40cm.

4.11.8 Effect of share width on soil reaction

The effect of width of share on soil reaction is presented in Fig.4.30. All curves correspond to values obtained at a lift angle of 20° at four different depths. It was observed that the longitudinal and vertical reactions increased with width of share in a linear manner. The rate of increase was less at shallow depths of operation. The curves indicated the dominent effect of depth of share in determining soil reaction. The curves indicated that considerable soil force would exist even when the share width approaches zero. The vertical force also exhibited similar behaviour

4.11.9 Effect of operational parameters and share geometry on furrow geometry

The width of furrows created by shares operating at different depths, lift angle and share width are presented in Fig.4.31. The furrow geometry was simulated by three models only. The effect of speed on furrow geometry could not be simulated since the Swick and Perumpral model assumed the furrow geometry as being independent of the speed of operation Fig.4.31 shows the width of furrow as a function of depth and lift angle. All models predicted a linear increase in furrow width with depth. For the McKyes and Ali model and Swick and Perumpral model, the width of furrow at a constant depth of operation decreased with increase in lift angle in the range of 8° to 42° and later increased with further increase in lift angle. shares with lower lift angle exhibited greater value of rupture distance, r. However at low lift angles, the bottom edge of share would be ahead of its top edge thus reducing the angle substended by the side cresent, ρ'. As the lift angle was increased, the furrow rupture distance r decreased and at the same time the value of ρ was increased. This interaction between the forward rupture distance and angle substended by side cresent resulted in the furrow width-lift angle relation exhibited by the simulation models. However, for Godwin and Spoor model, the interaction between r and ρ resulted in a behaviour opposite to that predicted by McKyes and Ali model. This was due to the use of experimentaly observed values of rupture distance ratio by this model.

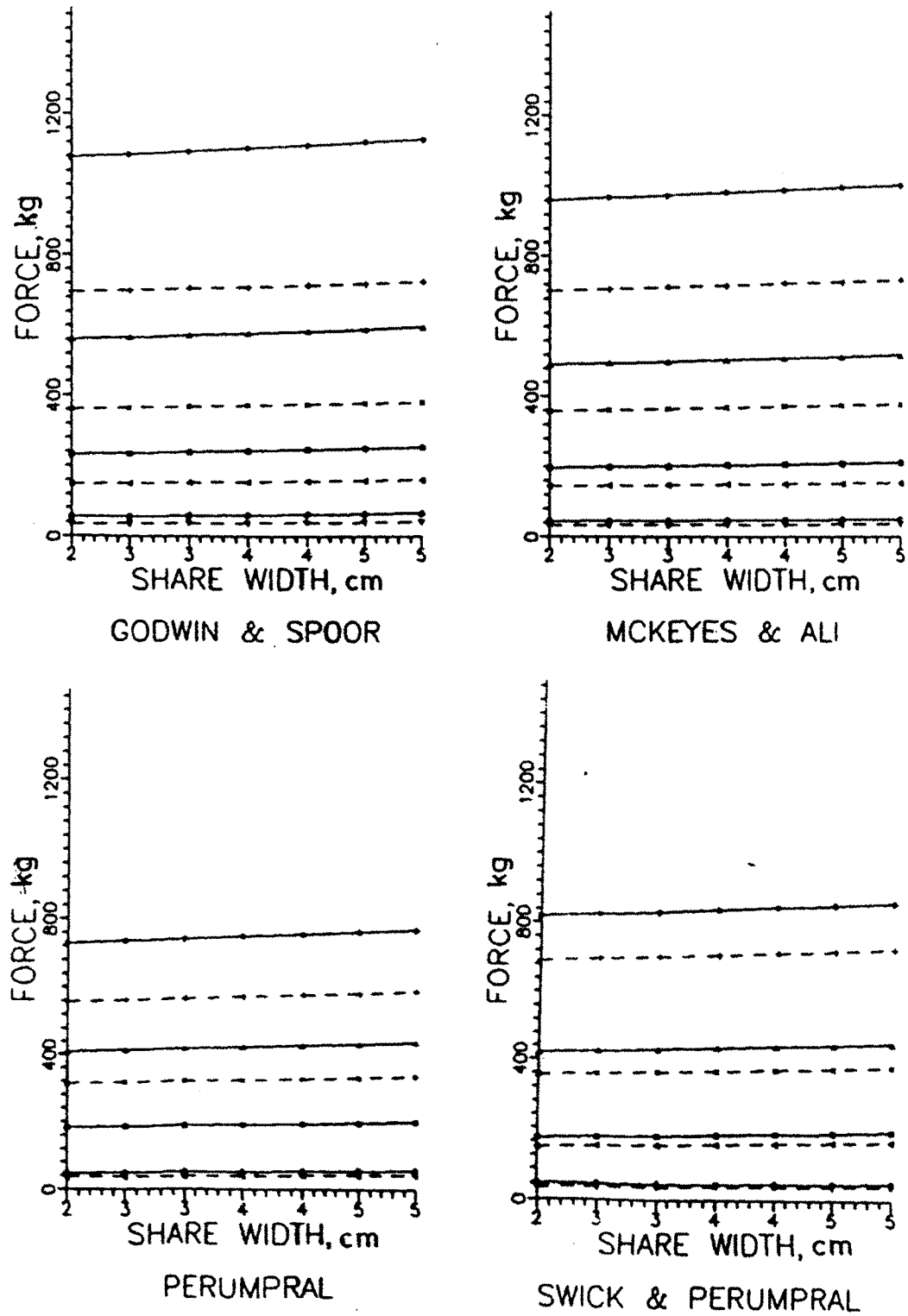

Fig 4.30 Predicted effect of width of share on draft and vertical reaction at a lift angle of 20° using different prediction models.
Draft; o -10cm, □ -20cm, Δ -30cm, ▷ -40cm,
Vertical force; ∇ -10cm, ◁ -20cm, X-30cm, +-40cm.

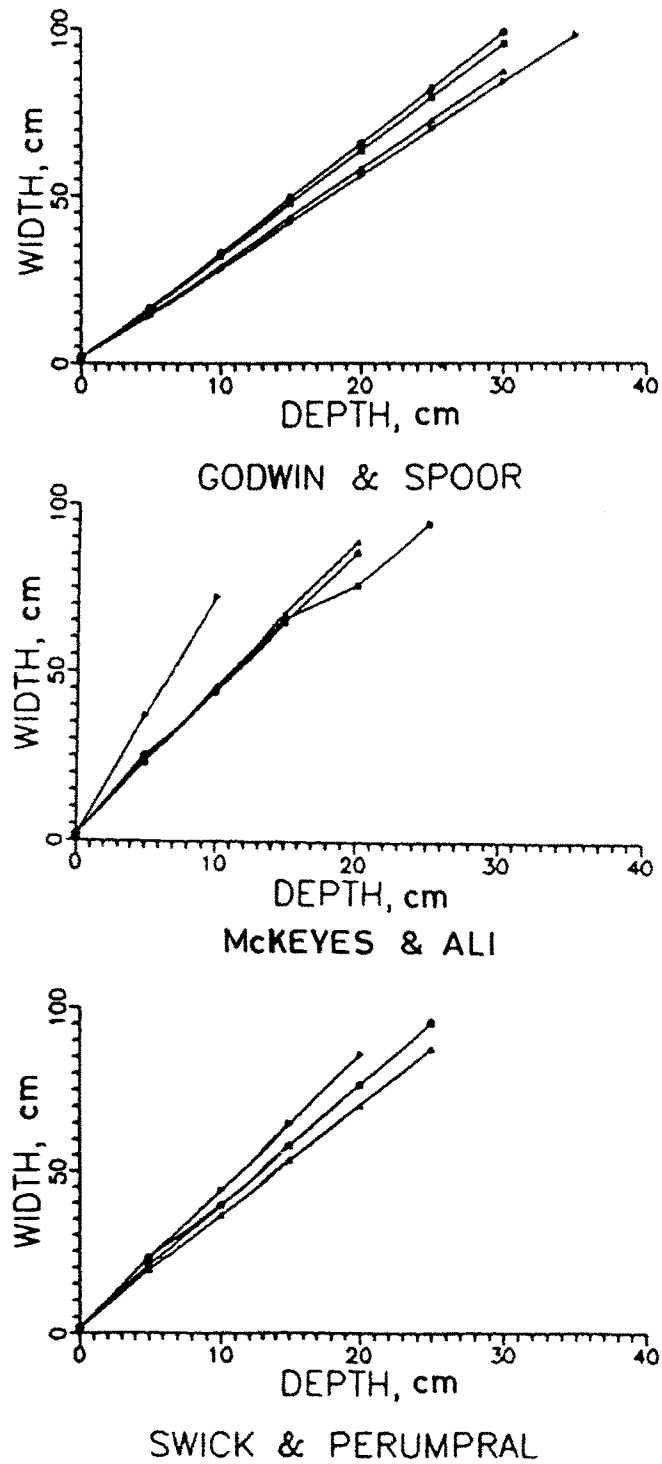

Fig 4.31 Predicted relation between furrow width and depth of operation for a 2cm wide share at different lift angles.
o -20cm, □ -43°, Δ -65.9°, ▷ -88.8°.

The area of furrow as a function of depth and lift angle is shown in Fig.4.32. It was observed that the depth-furrow area relation was quadratic. The depth of operation was observed to have a dominent influence on furrow area compared to share lift angle. The furrow area also reflected the effect of furrow width-lift angle relation exhibited by different models. It was observed that all the three models echibited identical values of furrow area.

Since the width of share had no influence on the forward rupture distance or angle of side cresent, the effect of width of share on furrow geometry was limited to the extent of variation in the geometry of the central wedge.

4.12.1 Comparison of simulated and experimental results

The performance of deep tillage tools as predicted by different models were compared with the experimentaly observed behaviour. Fig.4.33 shows the depth-horizontal reaction relationship as predicted by the simulation models and the experimentaly observed behaviour as obtained through equation 4.9., for a blade width of 2 cm and at average cone index of field (18.72 kg/cm^2). It was observed that all the models predicted similar depth-horizontal reaction interaction. The values of horizontal reaction predicted by the Perumpral model was observed to be considerably lesser than that predicted by the other three models. The lower value of horizontal reaction as predicted by Perumpral model was due to its failure to consider the side cresent in an explicit manner. The relative magnitude of simulated values were similar to those observed by Plasse *et al.* (1985) and Grisso and Perumpral (1985). Though the Godwin and Spoor model, McKyes and Ali model and Swick and Perumpral model used different approaches in modeling the mechanism of failure, the three models yielded values which were closely in agreement with each other and with the experimental values. This indicated that the above three models were well suited for simulating the performance of the tool. Even though the Perumpral model under predicted the tool forces, the simplicity of the model would make it suitable for approximate prediction of tool forces.

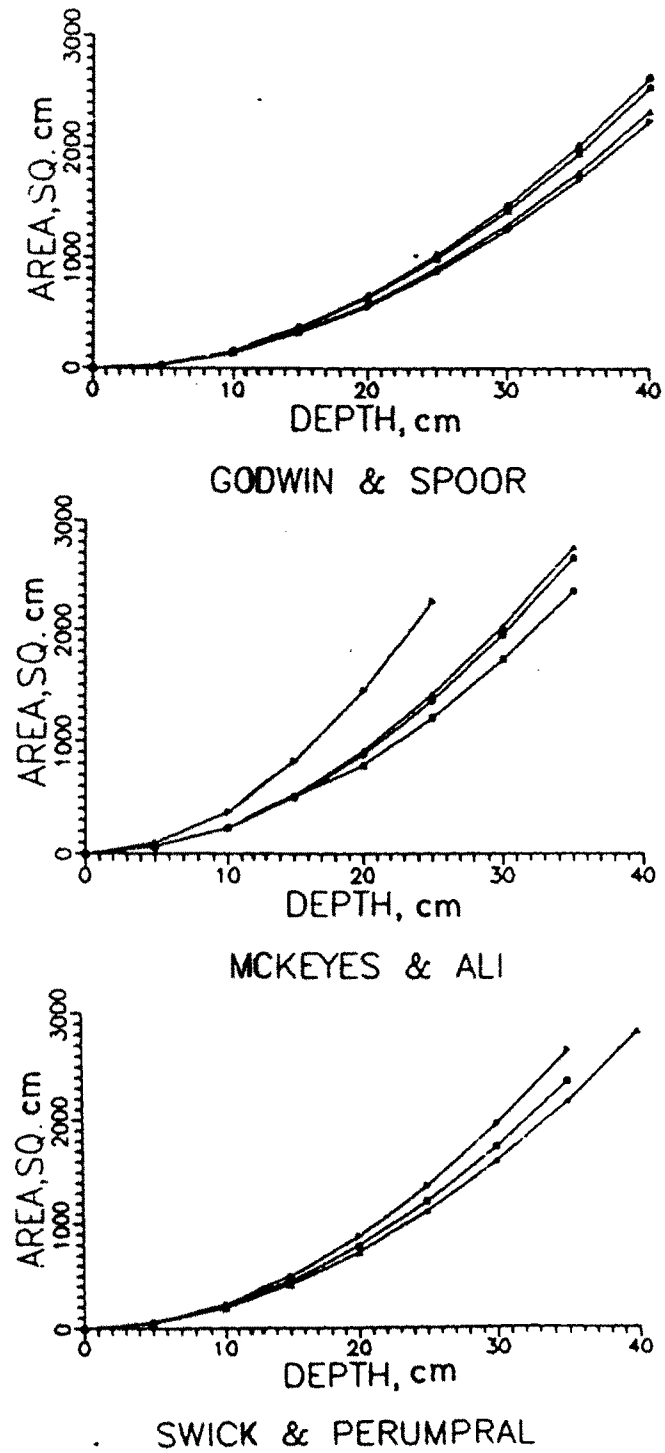

Fig 4.32 Predicted relation between furrow area and depth of operation for a 2cm wide share at different lift angles.
o -20°, □ -43°, Δ -65.9°, ▷ -88.8°

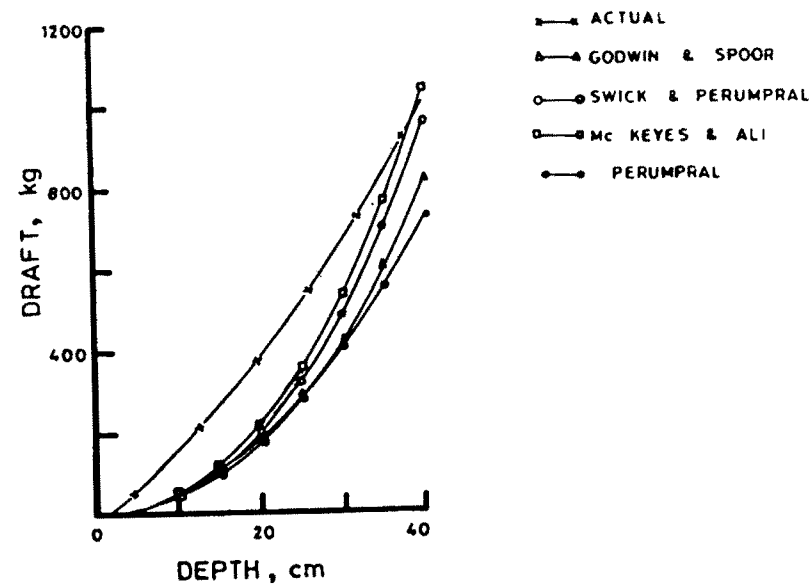

Fig 4.33 Comparison of draft -depth relation as predicted by different models and the experimentaly observed behaviour.

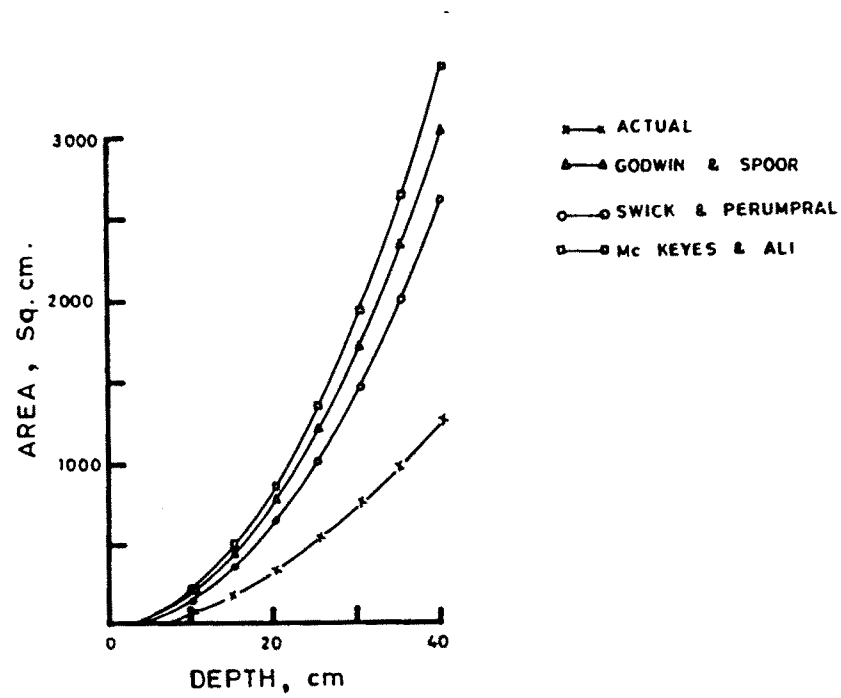

Fig 4.34 Comparison of furrow area-depth relation as predicted by different models and the experimentaly observed behaviour.

The rupture geometry as predicted by McKyes and Ali, Godwin and Spoor and Swick and Perumpral models were compared with the experimentally observed rupture geometry by plotting the furrow cross sectional area-depth relation (Fig.4.34). The experimentally observed values were those obtained from generalised equation, Eq.4.11. It was observed that the simulation models over predicted the furrow cross sectional area. This over prediction of furrow cross sectional area was partly due to the assumption of a straight furrow flank as against a convex furrow flank observed under experimental conditions. It was observed that the pattern of variation of furrow area with increase in depth closely resembled that obtained under experimental conditions.

4.13 Design of implement for Deep Tillage

The design of the implement for deep tillage was based on observed behaviour of tools of different geometry under typical conditions representing field conditions during summer fallow tillage, under semi arid climate. The behaviour of tool was also simulated through mathematical models.

4.13.1 Design Parameters

The influence of share lift angle on performance was simulated through mathematical models. The results of the simulation clearly revealed that the draft requirement would be minimum and the efficiency of the tool would be maximum when the share lift angle was close to 20°. Hence the implement was designed with a share lift angle of 20°.

The simulated results and the experimentally observed behaviour indicated that the draft requirement would be minimum for minimum width of share. Based on other design requirements, as explained in Sec.4.6.1., the share width was selected as 2.5 cm. The length of share was similarly optimised as 15 cm (Sec.4.6.3.).

The operational factors that could be varied by the operator are the depth and speed of operation. It was clearly brought out by the results of field experiment and simulation studies that the speed-draft interaction was negligible when compared to the depth-draft interaction. The maximum depth, the implement was designed to operate was matched with the predicted performance of the prime mover. The drawbar performance of selected models of tractors were predicted using the prediction equation by Zoz (1974) and specifications of tractors as published by CFMTTI (Table 4.12). From Table 4.12

Table 4.12 Specifications of selected models of tractors and their drawbar performanence predicted as outlined by Zoz (1974)

S.No.	Particulars	Ford 3000	MF 1035 DI	Mahendra B275	HMT 3511
1.	P.T.O. HP	41.4	31.6	30.5	31.3
2.	Axle HP	39.7	30.3	29.3	30.0
3.	Static rear				
	axle weight,Kg	1060*	880*	1090*	660*
		1970**	1610**	1795**	765**
	Perfromance at high soil strength 1.45 MPa (200 PSI)				
4.	Slip, %	14	14	14	14
5.	Tractive efficiency%	76	76	76	76
6.	DBHP	30.1	23	22.2	22.8
7.	Pull, Kg	883*	773*	908*	887*
		1641**	1341**	1495**	1429**
8.	Forward speed, m/s	2.55*	2.2*	1.8*	2.6*
		1.37**	1.28**	0.93**	1.19**
	Performance at low soil strength 0.36 MPa (50 PSI)				
9.	Slip, %	25	25	25	25
10.	Tractive effiicency,%	45	45	45	45
11.	DBHP	17.8	13.6	13.1	13.5
12.	Pull, Kg	301*	250*	309*	303*
		560**	457**	510**	487**
13.	Forward speed, m/s	4.4*	4.1*	3.2*	3.3*
		2.4**	2.2**	2.0**	2.1**

* - unballasted ** - ballasted

it was inferred that ballasting would not be necessary under favourable traction environment. The maximum drawbar pull under strong surface soil conditions without ballast was predicted to be around 900 kg. This meant that the tractors would be able to operate the implement up to a depth of 37 cm (Eq.4.9 β CI=18.72). The maximum depth of operation of a mounted implement was also limited by the lift height obtainable. According to IS 4468-1977 maximum list hight was 56 cm and 60 cm for category I and II hitch systems respectively. Hence to ensure a clearance of 20 cm between share and ground level during transport position, the maximum operating depth was limited to 40 cm. The maximum horizontal soil reaction was taken as 1000 kg. based on Eq.4.9 β CI = 18.72 Kg/cm^2 and depth of 40 cm. The results of the field experiment showed that the resultant force was at an angle of 11.6° to the horizontal. Hence the vertical soil reaction was taken as 500 kg. for design purpose.

4.13.2. Structural design of critical components

The critical components were designed to withstand the design load with suitable margin of safety and suitable materials and designs were selected. The salient feature of the prototype implement was the use of tubular rectangular members for the frame structure. This was done to ensure a light weight and rigid construction. The three dimensional frame structure adopted for the implement warranted a detailed structural analysis to ensure its safety. The structure was analysed using a finite element package (ANSYS 4.4).

The geometry of the frame is shown in Plate 4.1. The nodal forces and moments are given in Table 4.13. It was observed that the cross beam consisting of elements 1 and 2 served as struts with axial compressive force of 1323 kg. The ties 3 and 4 were subjected to a axial tension of 1780 kg. The mast, 8 was subjected to a tension of 1780 kg. The mast brace 9 was subjected to a maximum compressive force of 2253 kg. The mast brace was also the member with maximum length hence it was checked for failure by buckling and was found to be safe. The maximum bending moment as was expected occurred at the point of attachment of the standard to the frame.

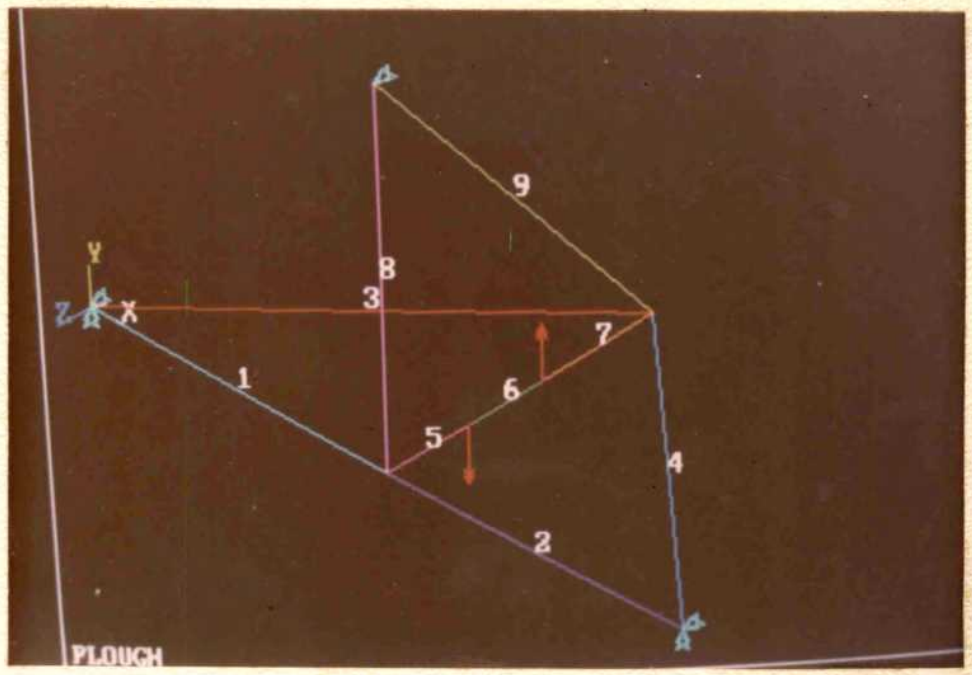

PLATE 4.1. GEOMETRY OF IMPLEMENT FRAME USED FOR STRUCTURAL ANALYSIS BY ANSYS

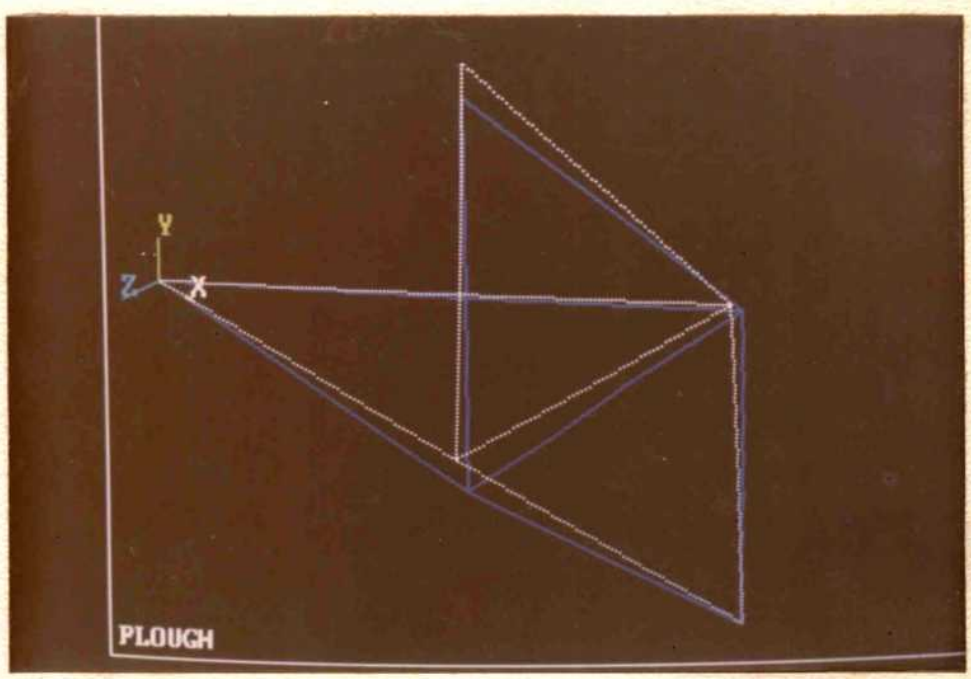

PLATE 4.2. GEOMETRY OF IMPLEMENT FRAME AFTER DEFORMATION AS PREDICTED BY ANSYS STRUCTURAL ANALYSIS PACKAGE

Table 4.13 Results of analysis of implement frame through ANSYS 4.4 - Member loads and moments about element coordinate axes

Member	Description	Node	Fx Kg	Fy Kg	Fz Kg	Mx Kg-m	My Kg-m	Mz Kg-m
1	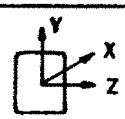	1	1323	257	32	2.2	-2.9	19.9
		2	-1323	-257	-32	-2.2	-11.3	92.3
2	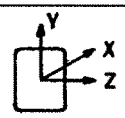	2	1323	-257	-32	-2.2	11.3	92.3
		6	-1323	257	32	2.2	2.9	19.9
3	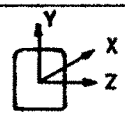	1	-1780	-2	1	11.6	2.9	16.3
		5	1780	2	-1	-11.6	-3.3	15.2
4	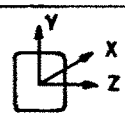	5	-1780	2	-1	-11.6	3.3	15.2
		6	1780	-2	1	11.6	-2.9	16.3
5	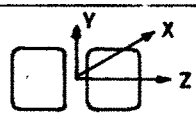	2	- 23	2294	0	0	0	5.3
		3	23	-2294	0	0	0	280.5
6	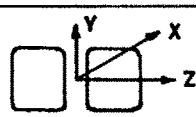	3	487	-5051	0	0	0	280.5
		4	-487	5051	0	0	0	275.1
7		4	997	1784	0	0	0	275.1
		5	-997	-1784	0	0	0	13.9
8	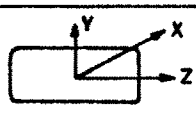	2	-1780	0	42	0	-9.7	0
		7	1780	0	-42	0	-10.4	0
9	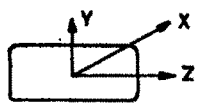	7	2253	0	44	0	-10.4	0
		5	-2253	0	-44	0	-16.9	0

Fx, Fy, Fz - Member forces along member coordinate axes

Mx, My, Mz - Moments on members about member coordinate axes

Table 4.14 Results of analysis of implement frame through ANSYS 4.4 - Axial stresses and bending stresses

Member	Description	Node	Axial streses	Bending stresses	
			SDIR, kg/cm²	SBZ, Kg/cm²	SBY Kg/cm²
1	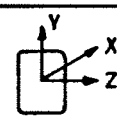	1	-193.5	31.5	-142.6
		2	-193.5	-122.2	661.1
2	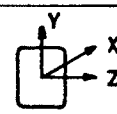	2	-193.5	-122.2	661.1
		6	-193.5	31.5	-142.6
3	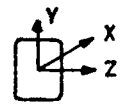	1	260.1	-31.5	116.85
		5	260.1	-35.8	108.9
4	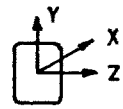	5	260.1	-35.8	108.9
		6	260.1	-31.5	116.8
5		2	1.7	0	18.7
		3	1.7	0	1005.2
6		3	-35.7	0	1005.2
		4	-35.7	0	-985.5
7	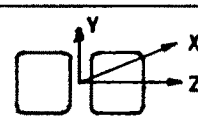	4	-73.1	0	-985.5
		5	-73.1	0	49.8
8	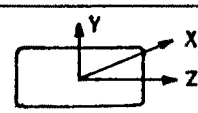	2	260.1	69.7	0
		7	260.1	-74.6	0
9	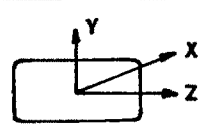	7	-329.3	74.6	0
		5	-329.3	-121.0	0

SDIR - Axial(Direct) stresses at end

SBZ - Bending stress on element +Z side of beam at end

SBY - Bending stress on element -Y side of beam at end

Table 4.15 Results of analysis of implement frame through ANSYS 4.4 - major and minor principal stresses σ_1, σ_3 and von Mises stresses, σ_{PRM}

Member	Node	σ1	σ3	σPRM
1	1	-19.2	-367.2	376.7
	2	589.9	-976.8	614.7
2	2	589.9	-367.2	614.7
	6	-19.2	-976.8	376.7
3	1	404.9	115.3	245.0
	5	408.0	111.8	241.0
4	5	408.0	111.8	241.0
	6	404.9	115.3	245.0
5	2	20.4	-17.1	7.4
	3	1006.7	-1003.4	58.0
6	3	969.0	-1040.4	272.5
	4	948.6	-1020.0	269.8
7	4	911.9	-1058.8	394.3
	5	-23.5	122.4	133.6
8	2	329.5	190.7	315.0
	7	334.6	184.6	309.6
9	7	-254.0	-403.9	515.5
	5	-208.0	-449.8	544.0

The member stresses at each end of the member are presented in Table 4.14. It was observed that the axial stress in the members were very low. The shear stresses created by the attachment of standard at nodes 3 and 4 were found to be appreciable reaching a magnitude up to 969 kg/cm^2. It was observed from Table 4.14 that the stresses created in the structure were within the permissible tensile stress of 2081 kg/cm^2 and permissible shear stress of 1045 kg/cm^2. This proved that the structure was safe against tension and shear failure. To predict whether an element was over-stressed or under-stressed, the Von Mises-Hencky Theory was employed. The values of major principal stress, σ_1 and minor principal stress, σ_3 were used to calculate the Von Mises stresses, σ_{PRM} (Table 4.15). It was observed that non of the element was stressed beyond the yield strength.

The deformation of the structure was also predicted and tabulated in Table 4.16. The geometry of the deformed structure is illustrated in Plate 4.2. The maximum displacement was predicted at node 2, which was displaced vertically downward by 0.44 mm. The angular rotation of the ends were predicted to be negligible. It was observed from plate 4.2 that the major deformation of the structure was due to the moment transferred by the standard to the frame. The provision of two parallel members to support the standard ensured that the members were safe against the transmitted moment. The point of mounting of the pivot pin and shear pin were further reinforced by collars welded through the box section.

The support reactions at the hitch points as predicted by the stress analysis are presented in Table 4.17. The predicted support reactions concurred with values calculated manually. All other critical components were also designed to withstand the design loads.

4.14. Field Performance of prototype chisel plough

The performance of the prototype chisel plough was evaluated as described in Sec.3.9.3. The magnitude, location and orientation of the resultant soil reaction was

measured as detailed in Sec.3.8.1. and are presented in Fig.4.35. It was observed that the resultant reaction was predominantly influenced by the depth of operation. Fig.4.35 clearly illustrated that the implement standard had a significant influence on soil reaction

Table 4.16 Results of analysis of implement frame through ANSYS 4.4 - Nodal deflections and rotations

Node	U_X	U_Y	U_Z	ROT_X	ROT_Y	ROT_Z
1	0.45E-01	0.00E+00	0.00E+00	0.56E-03	0.47E-03	-0.14E-02
2	0.49E-02	-0.4485	-0.162	0.40E-03	0.72E-20	-0.94E-20
3	0.49E-02	-0.371	-0.162	0.11E-02	-0.59E-20	-0.44E-20
4	0.49E-02	-0.222	-0.161	0.11E-02	-0.32E-19	0.29E-21
5	0.49E-02	-0.1375	-0.154	0.24E-03	-0.28E-19	0.71E-20
6	0.36E-02	-0.00E+00	-0.00E+00	0.56E-03	-0.47E-03	0.14E-02
7	0.49E-02	-0.388	-0.00E+00	0.41E-03	-0.19E-20	-0.98E-20

U_X, U_Y, U_Z - Nodal displacements in mm
ROT_X, ROT_Y, ROT_Z, - Nodal rotations in radians

Table 4.17 Results of analysis of implement frame through ANSYS 4.4 - Support reactions and moments on hitch points

Node	F_X	F_Y	F_Z	M_X	M_Y	M_Z
1.	0.00	250	1198	0.00	0.00	0.00
6.	0.00	250	1198	0.00	0.00	0.00
7.	0.00	0	-1395	0.00	0.00	0.00

F_X, F_Y, F_Z - Support reactions, Kg
M_X, M_Y, M_Z - Support moments, Kg

especially at greater depths of operation. The location of the resultant reaction as obtained by soil reaction measurements was used to calculate the draft requirement of the implement from measured values of top link compression force.

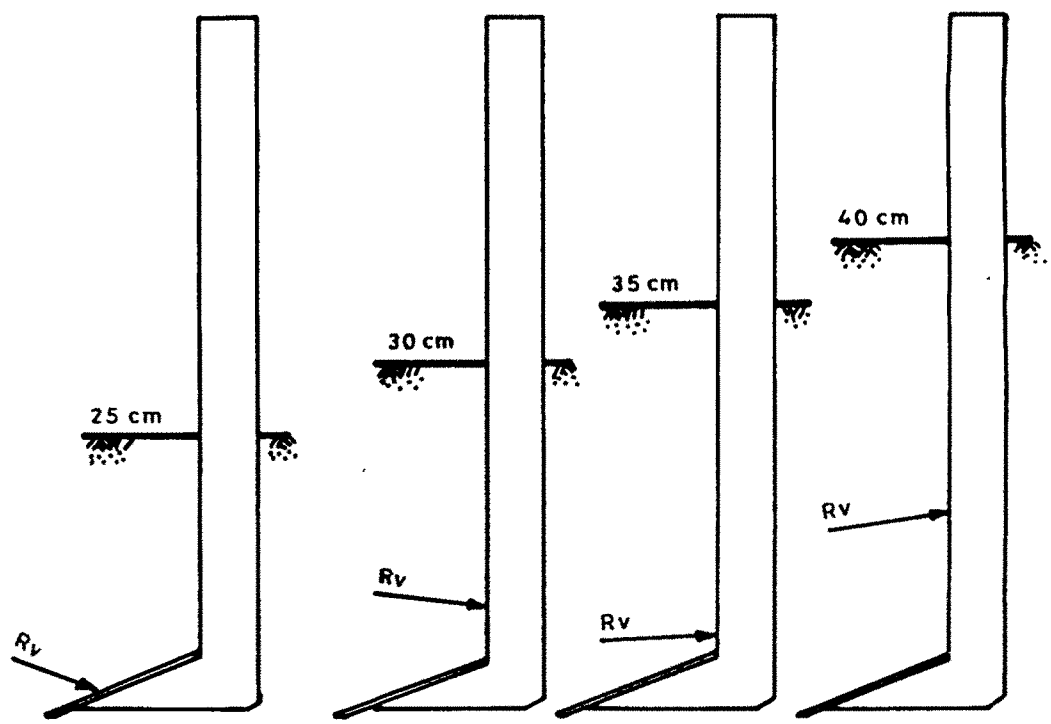

Fig 4.35 Location and orientation of resultant soil reaction acting on the implement at different operating depths.

The draft, slip, forward speed and fuel consumption were measured under two different soil conditions namely, site-I black clay loam soil (black soil) and site-II red gravelly loam soil (Red soil).

4.14.1. Effect of speed and depth on draft

The draft-depth relation at different speeds are presented in Fig.4.36. for black soil and red soil respectively. It was observed that the depth of operation predominantly influenced draft as compared to speed of operation under both soil conditions. This concurred with earlier results obtained with shares of different geometries. This clearly indicated that within the range of speeds investigated, the implement could be advantageously used at higher speeds without significant increase in draft requirement. The draft-depth relation exhibited significantly different pattern under different field conditions. The black soil field had a previously ploughed, top soil overlaying a heavy compacted soil. The red soil field had an undisturbed soil structure.

4.14.2 Effect of slip on draft and drawbar Power

The tractive performance of the tractor implement system was expressed as a function of the slip of the drive wheel. It had been frequently observed that deep tillage resulted in considerable slippage of the drive wheels. The drawbar pull obtained at different speeds and depth of operation were pooled to obtain the slip-drawbar pull relation presented in Fig.4.37. It was observed that at an optimum slip of 0.1 (Gee-Clough *et al.* 1982) the drawbar pull generated was 320 kg. under both field conditions. However when the permissible wheel slip was taken as 0.15 as recommended by IS 5994 (1979), the draw bar pull was found to be 400 kg. and 430 kg. in the black soil and red soil respectively. This clearly showed that though higher draw bar pull could be obtained at greater wheel slip, the drawbarpull under permissible level of slip was limited to 400 to 430 kg, under the given field conditions. It was observed that both the soils had poor soil strength at the surface layers indicated by the penetration resistance profiles (Fig.4.36).

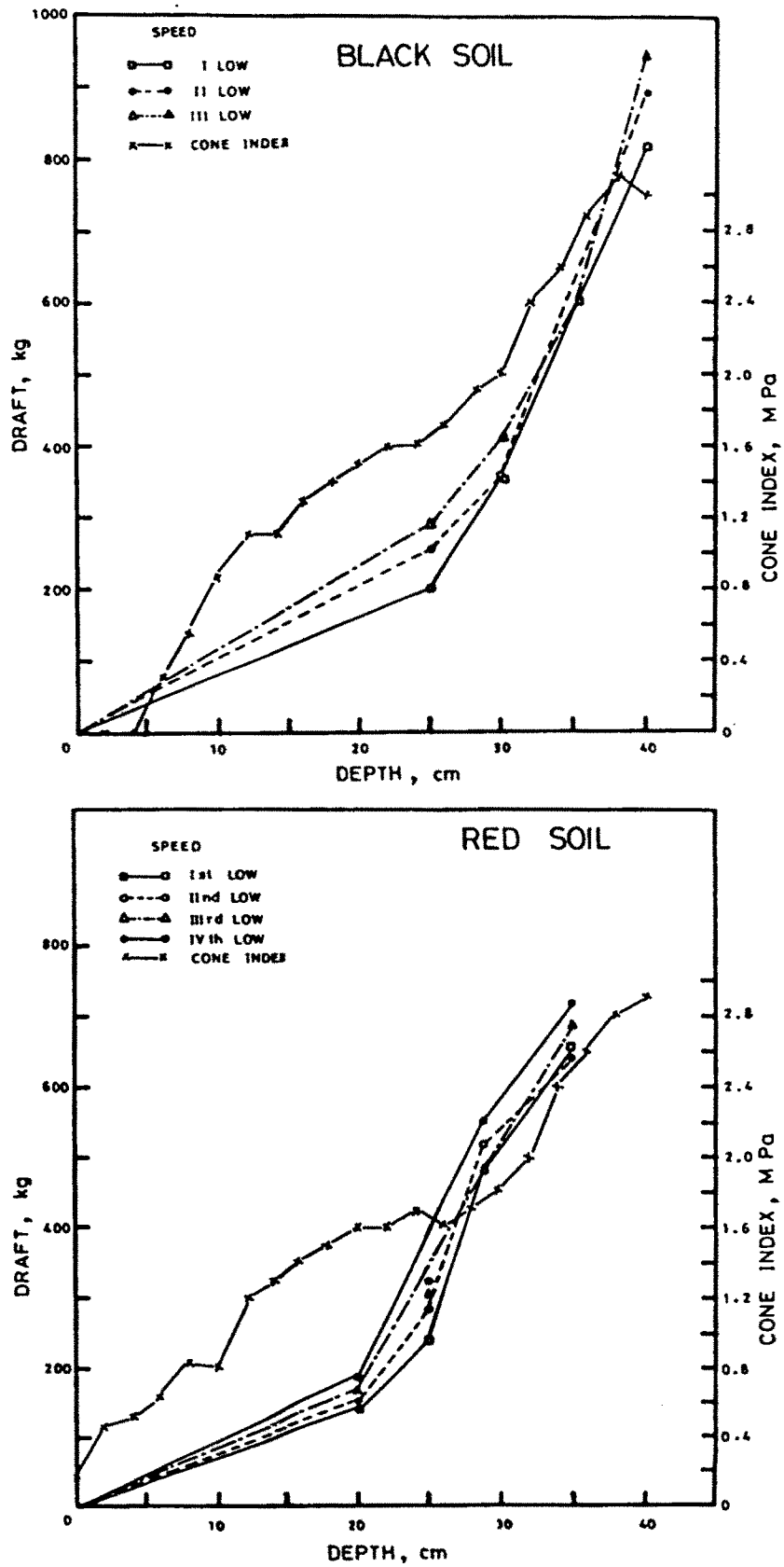

Fig 4.36 Relation between depth of operation and draft of the implement at different speeds under two soil conditions

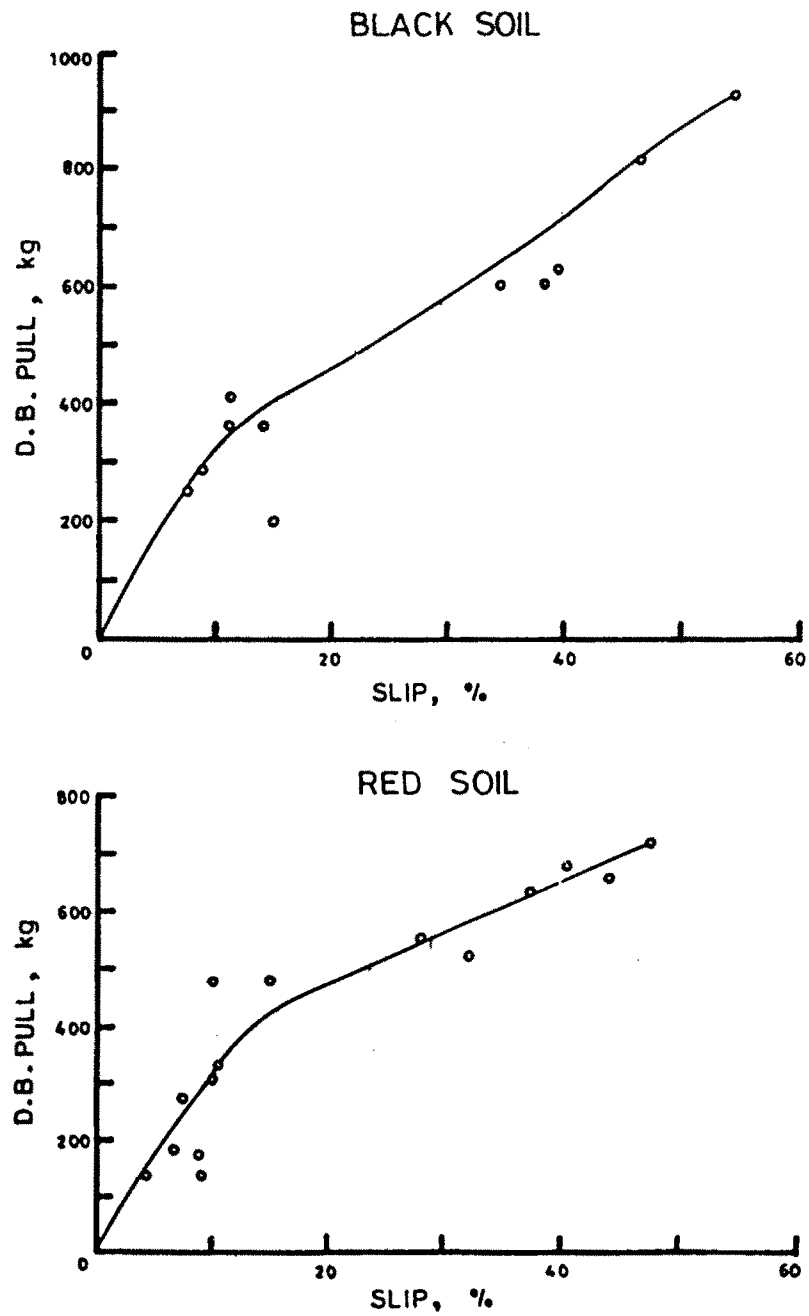

Fig 4.37 Relation between implement draft and slippage of drive wheel under two soil conditions

the drawbar pull values were comparable to those predicted for very low soil strength in Table 4.12. It was evident from Table 4.12 that the drawbar pull under such poor traction condition could be considerably increased by ballasting. From the experimental results it was evident that deep tillage of high resistance compacted hardpan required very high draft energy and when this was coupled with soft top soils with low traction ratios. It resulted in poor tractor- implement system performance. This concurred with the observations by Wolf *et al.* (1981).

The slip-drawbar power relation obtained in the blacksoil and red soil exhibited similar behaviour (Fig.4.38). The maximum drawbar power obtainable at I and II gear were around 3 HP and that at III gear was around 5 HP and that at IV gear was 9 HP. This indicated that since tractive performance was limited by poor soil strength, better performance could be obtained by increasing the forward speed. Under black soil conditions, the operation under III gear was possible up to a depth of 40 cm. In the red soil, speeds up to IV gear were used by limiting the depth to 35 cm. It was evident that when wheel slip was limited to 0.15, the maximum depth of operation under black and red soil would be limited to 26 cm and 29 cm respectively. It was inferred from Table 4.12 that when the same tractor (Ford 3600) were ballasted to the maximum limit and operated at the design slip of 0.25 (Zoz, 1974), the tractor would have developed around 560 kg. of pull and the implement could have been operated at a depth of 35 cm without excessive slippage.

4.14.3 Energy Requirement

Fuel consumption in the black soil field was measured under field conditions using procedure outlined in Sec.3.9.2. The fuel consumption per hectare is given as l/ha/DBHP - slip relation in Fig.4.39. From Fig.4.39 it was observed that the specific fuel consumption decreased with increase in speed. The specific fuel consumption reached a minimum value as the slip was increased to 0.10-0.15 and later gradualy increased. This indicated that at slip levels over 0.1 - 0.15, the energy was wasted in excessive soil deformation. This

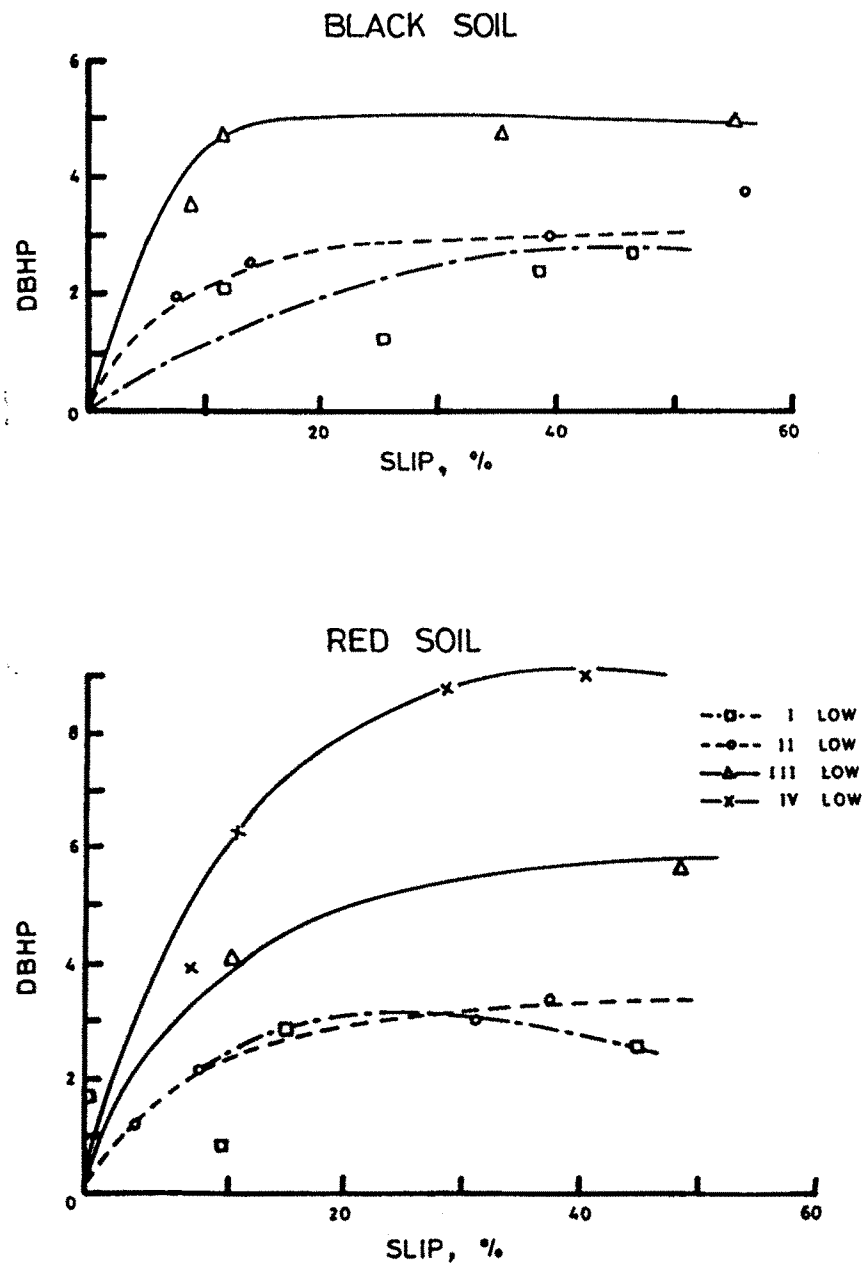

Fig 4.38 Relation between draw bar power and slip of drive wheels at different speeds of operation under two soil conditions

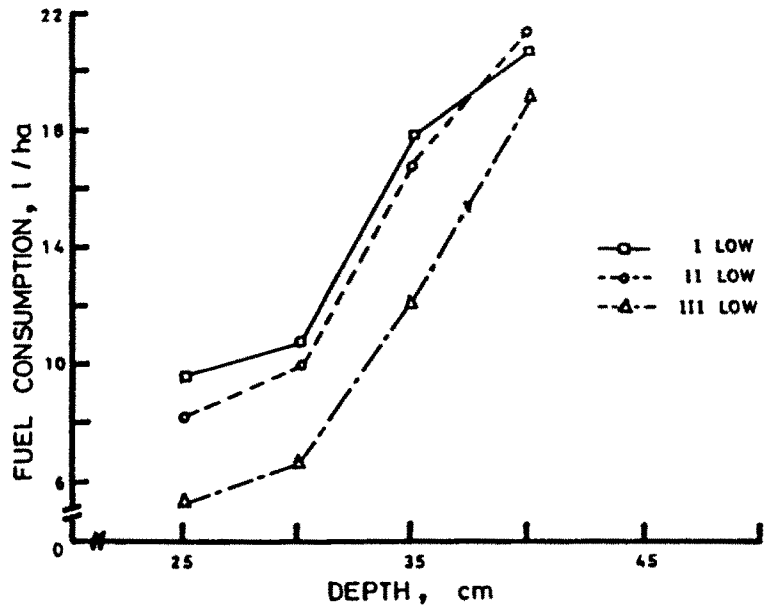

Fig 4.39 Relation between depth of operation and fuel consumption per hectare at different speeds under black soil conditions

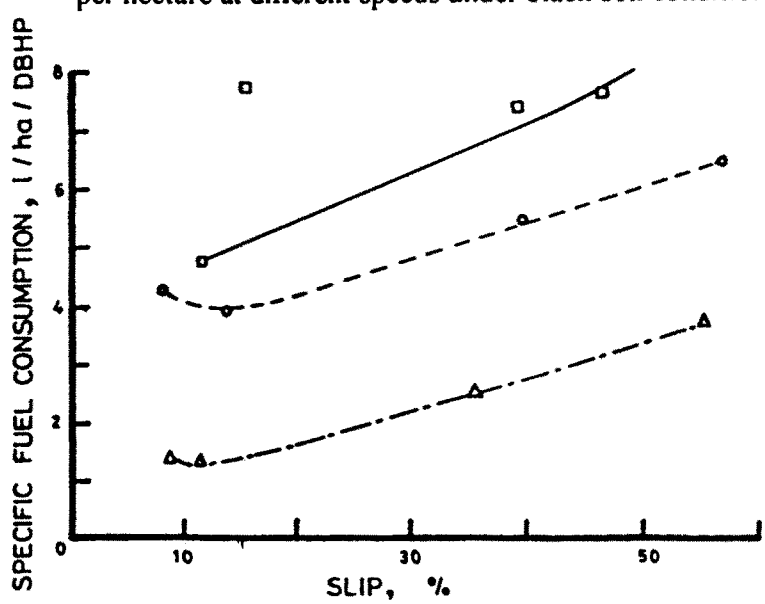

Fig 4.40 Relation between wheel slip and specific energy requirement under black soil conditions

was in accordance with optimum levels of slip proposed by Gee-Clough (1982). The depth of tillage - energy requirement relation for black soil is presented in Fig.4.40. It was observed that the fuel requirement is strongly influenced by the depth of tillage. The forward speed also influenced fuel requirement, but to a lesser extent. The values of fuel requirement for depths above 30 cm were very high due to greater draft energy requirement and decrease in tractive efficiency due to excessive slippage.

4.15 Cost of deep tillage

Based on the results of the field trial and cost of prototype, the cost of tilling using chisel plough was calculated. The cost of the chisel plough developed is Rs.5000. Cost of operation was worked out by assuming a fuel consumption rate of 3 l/h, and a spacing of 1.5 m between chiseled rows and field performance index of 0.8. The cost of operation was worked out to be Rs.265/ha at an average speed of operation of 3.5 Kmph. Details are shown in Appendix F. Using tractor test report by CFMTTI, the cost of disc ploughing using Ford 3600 tractor was worked out to be Rs.725/ha. Hence summer fallow tillage for better conservation of soil and water could be done with considerable cost advantage by using chisel plough in place of disc ploughs. Deep tillage using chisel ploughs also have considerable advantage from the agronomic stand point.

SUMMARY AND CONCLUSIONS

CHAPTER V

SUMMARY AND CONCLUSIONS

Summer fallow tillage is being practiced in many parts of Tamil Nadu where crops are grown under rainfed condition. Deep tillage using chisel ploughs could be a viable alternative to conventional practice of summer fallow ploughing using disc ploughs. Chisel ploughs shatter compacted subsoil and aid infiltration of rainwater. The root development of the crop is also increased, thus leading to better drought resistance and higher yields. Chiseling also ensures that the tilled soil is not washed away by summer shovers. These advantages of deep tillage using chisel type tools have been well recognised and chisel ploughing is practiced in many countries for summer fallow tillage. Deep tillage, as any other tillage practice should be based on crop requirements and soil conditions. Under typical conditions in Tamil Nadu where dry farming is practiced under red soil and black soil, the soil is susceptible to compaction. Hence deep tillage as a summer fallow tillage practice can improve the performance of most deep rooted crops like cotton, maize, sorghum etc.

The major bottle neck in adoption of deep tillage using chisel type tools during summer fallow ploughing in the limited availability of tractive power in the commonly used 35-45 HP range of tractors. To enable these tractors to operate chisel type deep tillage tools, the design of the tool should minimize draft requirement without reducing the effectiveness of disturbance. The soil conditions existing during summer fallow tillage could be described by the term 'clod forming soils'. These soils are characterised by high clay content and very low moisture content. Tilling these soils when they are dry will improve the shattering effect with minimum risk of compaction. The mechanics of failure and behaviour of tools while tilling soils under these conditions had not been investigated in detail until now.

This study was undertaken with a view to develop a deep tillage tool that would ensure minimum draft requirement and optimum soil disturbance when tilling dry compacted clay soils. Instrumentation were specially developed to investigate the behaviour of deep tillage tools. They included cone penetrometer, tillage dynamometer and furrow profile meter. The performance of shares of various geometry were investigated under different operational conditions. The validity of the existing prediction models for predicting the soil reaction under given soil condition was also investigated.

A prototype implement for deep tillage was designed and fabricated based on the results of the above investigations. The performance of the prototype deep tillage tool was evaluated under two soil conditions namely black soil and red soil.

The following conclusions were drawn from this study:

1. The penetration resistance of hard compacted clay soils up to a depth of 0.5 m could be easily measured by using a tractor mounted cone penetrometer developed for this study. The penetrometer had a standard cone geometry and was mounted to the rear of a tractor and was driven by electric motor. It was able to measure penetration resistance up to 7.8 MPa.

2. The tillage dynamometer developed for the above study had six hydraulic recording dynamometers. The dynamometers exhibited good linearity with R^2 values ranging between 0.952 and 0.997. The tillage dynamometer was used to measure the forces on tools of different geometry and was found to give consistently accurate measurements.

3. The furrow profile meter developed for measuring the geometry of furrow formed by deep tillage tools was used throughout the study. This instrument proved to be a convenient and accurate device for measurement of furrow profiles.

4. A field with clay loam soil and having a compacted subsoil was chosen for investigating the performance of shares. The field had 31.5 per cent clay, 23.3 percent silt and the rest were course sand and fine sand. The moisture content of the experimental blocks was found to vary between 2.87 and 8.47 percentage.

5. The penetration resistance profiles were measured to obtain the variations in soil strength among the blocks. This also served as an indicator of subsoil compaction. It was observed that the variations within blocks was too large to mask any significant variation in soil strength among the blocks.

6. The average penetration resistance over 0-40 cm depth was found to be 1.872 ± 0.106 MPa at 10 per cent level. For all the blocks the limiting value of about 2 MPa was reached at a depth of 22-26 cm. This clearly indicated the presence of a compacted restricting layer that would limit the root zone depth.

7. From the field measurement of forces on tillage tool, it was observed that the longitudinal soil reaction - depth relationship was quadratic in nature, thus resulting in a very high increase in longitudinal soil reaction for a small increase in depth of operation below 35 cm depth.

8. The vertical force on all the shares was observed to be generally downwards. The vertical force increased with depth of operation and the vertical force-depth relationship was observed to be linear under most conditions.

9. The influence of speed (0.25 - 1.25 m/s) on longitudinal reaction was observed to be significantly less than the influence of depth of operation (0 - 40 cm). Since the total change in longitudinal reaction with increase in speed was minimum, it could be represented by a linear relationship.

10. The vertical force increased with tool speed, indicating better penetration ability at higher speeds. The largest share tested, 50 x 200 mm, exhibited the maximum increase in vertical force with speed.

11. Within the range of speeds of 0.25 - 1.25 m/s, the resultant reaction tend to level off at higher speeds.

12. At shallow depths of operation, the width of tool was observed to have no significant effect on draft. At higher depths, the draft was found to increase with increase in width of share. The low rate of increase in horizontal soil reaction with increase in width was due to the low rake angle of the shares tested.

13. The vertical force-width relation was observed to be curvilinear with minimum vertical force occurring at a share width of 3 to4 cm.

14. The length of share was observed to have a negligible influence on draft. As the depth was increased, the draft-share length relation was slightly concave with minimum draft occurring at a share length of 150 mm.

15. The vertical soil reaction was observed to increase with increase in length of share. This was due to the greater amount of soil lift obtained with shares of greater length.

16. The location of the resultant soil reaction was observed to be almost identical for all shares. The resultant soil reaction was observed to be at an angle of 11.6° on an average for most shares tested. Since the angle of resultant reaction was mainly governed by soil metal friction and share lift angle, there was no appreciable difference in the orientation of resultant reaction between treatments.

17. The location of the resultant reaction indicated that at greater depths of operation, the standard contributes to a considerable extent to the total soil reaction. Longer shares had the location of soil reaction more close to the share thus indicating that longer shares tend to decrease the influence of standard.

18. The combined effect of depth and width of tool on draft was modeled using a curvilinear relation as

$$H/CIW^2 = -0.28 + 0.3468\ (d/w) + 0.0160\ (d/w)^2.$$

This equation gave a good fit for the experimental observations of all shares pooled together with R^2 value of 0.83. Hence this equation could be used to predict the draft requirement at any soil strength and share aspect ratio, (d/w) with reasonable accuracy.

19. The width of the furrow was found to vary linearly with depth of operation and the area of the furrow varied as the square of the depth.

20. Since the share width had no influence on the geometry of the side crescents, the share geometry had a minimum influence on furrow geometry. The dimensionless furrow width term and share aspect ratio were found to be related as $W/w = 2.28 + 1.859\ (d/w)$. This equation gave a good fit with $R^2 = 0.7$, implying a linear relation between furrow width and share width at any depth.

21. Comparison of area of furrow as calculated from the furrow width prediction equation and actual furrow area obtained through the regression equation indicated that most furrows had a convex flank.

22. The furrow area and the share aspect ratio were found to be related as, $A/wd = 0.9066 + 0.7787\ (d/w)$, with $R^2 = 0.73$.

23. Due to the high shear strength of soil and low rake angle of share, the critical depth for transition from upward crescent failure to lateral flow failure was estimated, using Godwin and Spoor (1977) model, to be 81 to 95 cm for 2 to 5 cm wide shares. The shape of the furrow area-depth relation also confirmed that the critical depth was not reached during the experiments.

24. From the generalised prediction equation for draft and furrow width, the draft requirement for unit width of furrow was obtained as :

$$H/w = CI\ w\ (0.176 + 8.61 \times 10^{-3}\ (d/w)].$$

This implied that for the experimental field conditions the draft requirement for unit furrow width would be 21.3 kg/cm and 23 kg/cm at 30 and 40 cm depths of operation respectively for a 5 cm wide share and the same would be 11.4 kg/cm and 13 kg/cm at 30 and 40 cm depths of operation for a 2 cm wide share.

25. The unit draft was also predicted using the generalised equations of draft and furrow area. For the experimental field conditions, the unit draft was 1.33 Kg/cm^2 and 1.15 Kg/cm} at 30 and 40 cm depths for a 5 cm wide share and the same was 0.84 Kg/cm^2 and 0.74 Kg/cm^2 at 30 and 40 cm depths for a 2 cm wide share.

26. The performance of shares of different geometry under varying operating condition was predicted by using four different models

a. Godwin and Spoor (1977)
b. McKyes and Ali (1977)
c. Perumpral *et al.* (1983) and
d. Swick and Perumpral (1988).

The soil strength parameters required by the prediction equations were measured by suitable techniques. The predicted performances showed close similarity.

27. The models predicted closely similar force-depth relationship. The draft-depth relation was parabolic. It was observed that shares of greater lift angles experienced higher soil reaction forces.

28. The vertical force-depth relation was observed to be parabolic at higher values of share lift angle and was almost linear for share lift angles of up to 42° for all models except Godwin and Spoor model.

29. In the range of speeds investigated through the Swick and Perumpral (1983) model, a slight increase in draft with speed was predicted. The draft speed relation and vertical force-speed relation were linear.

30. The draft lift angle relation predicted by all models except Godwin and Spoor (1977) model clearly showed that the draft was minimum at a share lift angle of 20°.

31. The vertical soil reaction changed direction from downwards to upwards at a share lift angle of (90-δ). The magnitude of vertical reaction decreased with lift angle for all models except Godwin and Spoor (1977) model which predicted a slight increase in vertical reaction for lift angles between 8° to 20°.

32. The draft-share width relation predicted by the models showed that the influence of width on draft requirement was marginal as compared to the effect of depth. The predicted pattern of variation indicated that considerable force would be required even when the share width approached zero.

33. Values of furrow geometry simulated through three simulation models indicated a linear relation between depth of operation and furrow width.

34. Predicted values of furrow width by McKyes and Ali model and Swick and Perumpral model showed that the width of furrow at a given depth of operation decreased with lift angle in the range of 8° and 42° and later increased.

35. The predicted relation between depth of operation and furrow area was quadratic. The depth of operation was found to have a more dominant influence than share lift angle.

36. The values of soil reaction predicted by the models were closely in agreement with each other. However the forces predicted by the Perumpral *et al.* (1983) model was slightly less than that predicted by the other three models.

37. The magnitude of draft predicted by all models were marginally less than that predicted by the generalized draft equation based on share aspect ratio.

38. It was observed that the simulation models considerably over predicted the area of furrow due to the assumption of straight furrow flank.

39. Based on the results of the field study and mathematical simulation, the geometry of the share was optimized as follows.

a. Share lift angle = 20°

b. Width of share = 25 mm

c. Length of share = 150 mm

The design loads were taken as 1000 kg of longitudinal force and 500 kg. of vertical force, with both being assumed to be located at the tip of share.

40. The chisel plough developed had a single tine mounted on a main frame. The main frame was designed to ensure conformity with standard category I and II hitch systems.

41. The main frame of the chisel plough was a three dimensional tubular structure. To ensure structural adequacy, the stresses on the structure were analysed through ANSYS, structural analysis computer software package. The structure was checked for its safety and was found to be sufficiently safe against all probable modes of failure.

42. A prototype chisel plough was fabricated as per the designed specifications.

43. The prototype chisel plough was tested under field conditions to evaluate optimum depth and speed of operation for the tractor-implement system.

44. The prototype chisel plough also exhibited similar draft-depth relationship as was predicted through generalized equation obtained through force measurement on shares using tillage dynamometer.

45. Under both black soil and red soil field conditions, the soft top soil resulted in excessive slip and hence the pull developed was in the range of 400 to 430 kg at 15 per cent slip. This clearly indicated drastic reduction in performance of tractor implement system when soft soils overlay heavy compacted soils. Since the drawbar pull was mainly limited by the traction requirement, increasing the forward speed resulted in increased utilization of drawbar energy. It was observed that the implement could be operated up to a depth of 40 cm under Low III gear and up to 35 cm depth under Low IV gear without stalling of engine or excessive wheel spin.

46. The specific fuel consumption - slip relation clearly indicated that for maximum efficiency the slip should be limited to 10 to 15 per cent.

47. The cost of the implement is Rs.5000/- and the cost of deep tillage using chisel plough works out to be Rs.265 per ha as against Rs.725 per ha for conventional practice of summer fallow tillage using disc ploughs.

Recommendations for future work

1. The cone penetrometer and tillage dynamometer may be provided with electronic load sensing and recording arrangement to further improve the accuracy and for easier recording of data.
2. Experiments may be carriedout with higher HP tractors (>50HP) to study the machanics of chisel type tool in larger depths and in higher speeds.
3. Field experiments may be conducted to investigate the effect of deep tillage on soil-water-plant relationship.
4. Chisel ploughing as an aternative to conventional summer fallow tillage practice may be investigated.

REFERENCES

REFERENCES

Adeoye, K.B., 1982. Effect of tillalge depth on physical properties of a tropical soil and yield of maize, sorghum and cotton. *Soil Tillage Research*, 2:225-231.

Ahmed, M.H. and R.J.Godwin, 1983. The influence of wing position on sub soiler penetration and soil disturbance. *J.agric. Engng Res.*, 28:489-492.

Albuquerque, J.C.D. and D.R.P.Hettiaratchi. 1980. Theoretical mechanics of sub-surface cutting blades and buried anchors. *J.agric. Engng Res.*, 25:121-144.

Anderson, G., J.D.Pidgeon, H.B.Spencer and R.Parks. 1980. A new hand-held recording penetrometer for soil studies. *Journal of Soil Science*, 31:279-296.

★ASAE. 1983. Soil cone penetrometer. ASAE standard S 313.1. Agricultural Engineers year book. p.283.

★ASAE. 1984. ASAE D230.4: Agricultural machinery management data. ASAE Standards, pp.156-162, ASAE St.Joseph, MI 49085-9659.

★Balaton, J, 1971. Study of the draft of subsoilers. *Per.Politechnica. Mech. Eng.* 15(4) 441-460 (USDA Translation) Reported by McKyes (1978).

Barber, R.G. and O.Diaz. 1992. Effects of deep tillage and fertilization on soya yields in a compacted Ustochrept during seven cropping seasons, Santa Cruz, Bolivia. *Soil Tillage Res.* 22:371-381.

Bernier, H., G. Bostock,G.S.V.Raghavan and R.S.Broughton. 1989. Subsoiling effects on moisture content and bulk density in the soil profile. *Transactions of the ASAE* 5(1):24-28.

Boccafogli,G., G.Busatti, F.Gherardi, F.Malaguti and R.Paoluzzi. 1992. Experimental evaluation of cutting dynamic models in soil bin facility. *Transactions of the ASAE* 29(1):95-105.

Bowers, C.G.J. 1985. Southeastern tillage data and recommended reporting. *Transactions of the ASAE.* 28(3):731-737.

Brown, N.H., M.A.Gerein and R.L.Kushwaha. 1989. Cultivator design modifications using finite element analysis. Applied Engineering in Agriculture, 5(2): 148-152.

Camp, Jr.C.R., and Z.F.Lund. 1968. Effect of mechanical impedance on cotton root growth. *Transactions of the ASAE* 11(2):188-190.

Carter, L.M. 1967. Portable Recording Penetrometer measures soil strength profiles. *Agricultural Engineering*, 47:348-349.

Carter,L.M. 1981. Instrumentation for measuring average draft. *Transactions of the ASAE,* 24(1):23-25

CFMTTI, 1991. Tractor performance results, central farm machinery testing and training institute. Published by Director CFMTTI, Budni - 466445.

Chaplin,J., C.Jenance and M.Lueders. 1988. Drawbar energy use for tillage operations on loamy sand. *Transactions of the ASAE,*31(6):1692-1694.

Chaudhary, M.R., P.R.Gajri, S.S.Prihar and Romesh Khera. 1985. Effect of deep tillage on soil physical properties and maize yields on coarse textured soils. *Soil Tillage Res.*, 6:31-44.

Chi,L. and R.L.Kushwaha. 1990. A non linear 3-D Finite element analysis of soil failure with tillage tools. *J.Terramechanics,* 27(4):343-366.

Chi,L. and R.L.Kushwaha, 1989. Finite element analysis of forces on a plane soil blade. *Can. Agric. Eng.*, 31(2):135-140.

Chi,L. and R.L.Kushwaha, 1989. Finite element analysis of forces on two shapes of tillage tools. *Can. Agric. Eng.*, 33(1):39-45.

Clyde, A.W. 1936. Measurement of forces on soil tillage tools. *Agricultural Engineering,* 17(1): 5-9.

Clyde, A.W. 1937. Load studies on tillage tools. *Agricultural Engineering,*, 18(3):117-121.

Clyde, A.W. 1939. Improvement of disk tools. *Agricultural Engineering,*, 20: 215-221.

Clyde, A.W. 1961. Force measurement applied to tillage tools. *Transactions of the ASAE,* 4(2):153-154,157.

Collins, E.R. and W.F.Lalor, 1973. Soil-bin investigation of a deep working tillage tool. *Transactions of the ASAE,*16(1):29-33.

Currence, H.D. and W.G.Lovely, 1970. The analysis of soil surface roughness. *Transactions of the ASAE* 13(6):710-713.

Curtis, R.W. and W.D.Cole, 1972. Micro-topographic profile gage. Agricultural Engineering, 53:17.

Dechao, Z. and Y.Yusu, 1992. A dynamic model for soil cutting by blade and tine. *J.Terramechanics* 29(3):317-327.

★ Dransfield, P. S.T.Willat and A.H.Willis, 1964. Soil to implement reaction experienced with simple tines with various angles of attack. *J.agric.Engg Res.*9(3): 220-224.

Doty, C.W. and D.C.Reicosky, 1978. Chiseling to minimize the effects of drought. *Transactions of the ASAE* 21(3):495-498.

Dowding, E., J.A.Ferguson and C.F.Becker, 1967. Comparison of four summer-fallow tillage methods based on seasonal tillage-energy requirement, moisture conservation and crop yield. *Transactions of the ASAE* 10:1-3,8.

Elijah, D.L. and J.A.Weber, 1971. Soil failure and pressure patterns for flat cutting blades., *Transactions of the ASAE* 14: 781-785.

Fielke, J.M. and T.W.Riley, 1991. The universal earthmoving equation applied to chisel plough wings. *J.Terramechanics* 28(1):11-19.

Fornstrom, K.J., and C.F.Becker, 1977. Comparison of energy requirements and machinery performance for four summer fallow methods. *Transactions of the ASAE*, 20:640-642.

Freitag, D.R. 1968. Penetration test for soil measurements. *Transactions of the ASAE*, 11(6) 750-753.

Freitag, D.R., R.L.Schafer and R.D.Wismer, 1970. Similitude studies in soil machine systems. *Transactions of the ASAE*, 13: 201-212.

Frisby, J.C. and J.D.Summers, 1979. Energy related data for selected implements. *Transactions of the ASAE*, 22: 1010-1011.

Garner, T.H., R.B.Dodd, D.Wolf and U.M.Peiper, 1988. Force analysis and application of a three-point hitch dynamometer. *Transactions of the ASAE*, 31(4):1047-1053.

Garner, T.H., W.R.Reynolds, H.L.Musen, G.E.Miles, J.W.Davis, D.Wolf and U.M.Peiper. 1987. Energy requirement for subsoiling coastel plain soils. *Transactions of the ASAE*, 30(2):343-349.

Gaultney, L., G.W.Krutz, G.C.Steinhardt and J.B.Liljedahl, 1982. Effects of subsoil compaction on corn yields. *Transactions of the ASAE*, 25(3): 563-569, 575.

Gebresebnbet, G. and H.Johnson, 1992. Performances of seed drill coulters in relation to speed depth and rake angles. *J.agric.Engg Res.*52:121-145.

Gebresenbet, and Girma, 1992. Dynamic effects of speed, depth and soil strength upon forces on plough components. *J.agric.Engg Res.* 51:47-66.

Gee-clough, D., G.Pearson and M.McAllister, 1982. Ballasting wheeled tractors to achieve maximum power output in fritctional- cohesive soils. *J.agric.Engg Res.*27:1-19.

Gill, W.R. and Vanden Berg, G.E., 1967. Soil dynamics in tillage and traction. USDA Agriculture hand book No.316. U.S.Government Printing office, Washington, Dc. 511 pp.

Glancy, J.L., S.K.Upadhyaya, W.J.Chancellor and J.W.Rumsey, 1991. Prediction of implement draft using an instrumented analog tillage tool. ASAE paper No.91-1065.

Godwin, R.J. and G.Spoor, 1977. Soil failure with narrow tines. *J.agric.Engg Res.* 22:213-228.

Godwin, R.J., G.Spoor and P.L. Harrison, 1981. An experimental investigation into the force mechanics and resulting soil disturbance of mole ploughs. *J.agric.Engg Res.*,26:477-497.

Godwin, R.J., G.Spoor and M.S.Soomro, 1984. The effect of tine arrangement on soil forces and disturbance. *J.agric.Engg Res.*,30:47-56.

Godwin, R.J., P.S.G.Magalhaes, S.M.Miller and R.K.Fry, 1987. Instrumentation to study the force system and vertical dynamic behaviour of soil-engaging implements. *J.agric.Engg Res.*, 30:301-310.

Godwin, R.J., A.J.Reynolds, M.J.O'Dogherty and A.A.Al-Ghazal, 1993. A triaxial dynamometer for force and moment measurement on tillage implements, *J.agric.Engg Res.*, 55: 189-205.

Grevis-James, I.W. and P.D.Bloome, 1982. A tractor power monitor. *Transactions of the ASAE*, 25(3):595-597.

★ Grisso, R.D., J.V.Perumpral and C.S.Desai, 1980. A soil tool interaction model for narrow tillage tools ASAE paper 80-1518 ASAE St.Joseph. MI 49085. Reporteod by Plasse et al (1985).

Grisso,R.D., and J.V.Perumpral, 1985. Review of models for predicting performance of narrow tillage tool. *Transactions of the ASAE*, 28(4):1062-1067.

Hakansson, I., 1990. A method for characterizing the state of compactness of the plough layer. *Soil Tillage Res.*, 16:105-120.

Harral, B.B., 1990. Structural loading on a rigid tine cultivator frame. *J.agric.Engg Res.*, 47:79-88.

Harrison, H.P., 1982. Soil reactions from laboratory studies with an inclined blade. *Transactions of the ASAE* 25(1): 7-12, 17.

Harrison, H.P., 1975. Instrumentation of a multicomponent sensor. *Transactions of the ASAE*, 18(4): 765-769.

Heitshu, D.C., 1952. The kinematics of tractor hitches. *Agricultural Engineering*, 33(6): 343-346, 356.

Hendrick, J.G. and W.R.Gill, 1973. Soil reaction to high speed cutting. *Transactions of the ASAE*, 16(3): 401-403.

Hendrick, J.G., 1969. Recording soil penetrometer. *J.agric.Engg Res.*, 14(2): 183-186.

Hettiaratchi, D.R.P., B.D.Witney and A.R.Reece, 1966. The calculation of passive pressure in Two-dimensional soil failure. *J.agric.Engg Res.* 11(2): 89-107.

★ Hettiaratchi, D.R.P., and A.R.Reece, 1967. Summetrical three-dimensional soil failure. *J.Terramechanics* 4(3): 45-67 Reported by Plasse et al (1985).

★ Hillel, D. et al, 1969. Soil-crop-tillage interaction in dryland and irrigated farming. Research report submitited to USDA. Reported by Wolf and Luth (1979).

Ide, G., Hofman, G., L.Ossemerct, M.Van Ruymbeke, 1984. Root growth response of winter barley to sub soiling. *Soil Tillage Res.* 4:419-431.

IS 4468, 1977 Dimensions for three-point linkage of Agricultural wheeled tractors, Indian Standards Institution, New Delhi.

IS 5994, (Part II), 1979 Test code for Agricultural tractors, Indian Standards Institution, New Delhi.

IS 9253, 1977 Guidelines for field performance evaluation of Agricultural wheeled tractors, Indian Standards Institution, New Delhi.

Jensen, J.K., 1954. Experimental stress analysis. *Agricultural Engineering,* 35(9):625-629,634.

★ Jensen, M.E. and W.H.Sletten, 1965. Effects of alfalfa, crop sequence, and tillage practice on intake rate of Pullman silty clay loam and grain yields. USDA conservation Res. Rpt.No.1. Quoted in *Transactions of the ASAE,* 18(2): 263.

Johnson, C.E. and W.B.Voorhees, 1979. A force dynamometer for three-point hitches. *Transactions of the ASAE,*22(2): 226-228, 232.

Jones, G.D, 1939. The method and effect of deep tillage. *Agricultural Engineering,* 20:61-63.

Jones, O.R., R.R.Allen and P.W.Unger, 1990. Tillage systems and equipment for dryland farming. *Advances in soil science,* 13:89-130.

Kanitkar, N.V., 1960. Dry farming in India. Indian Council of Agricultural Research, New Delhi.

Karlen, D.L., W.J.Busscher, S.A.Hale, R.B.Dodd, E.E.Strickland and T.H.Garner, 1991. Drought condition energy requirement and subsoiling effectiveness for selected deep tillage implements. *Transactions of the ASAE,*34(5): 1967-1972.

Kepner, R.A., Roy Bainer, E.L.Barger, 1972. Principles of farm machinery. Second edition. The AVI Publishing Co. Inc. Westport Cannecticut.

Ketter, R.L., G.C.Lee and S.P.Prawel, 1979. Structural analysis and design McGraw-Hill book Co. pp 40-42.

Khalilian, A., T.H.Garner, H.L.Musen, R.B.Dodd and S.A.Hale, 1988. Energy for conservation tillage in coastal plain soils. *Transactions of the ASAE,* 31(1): 1333-1337.

★ Kliopa, G.I., 1958. Influence of speed of cutting on soil resistance. *Stroilelnoei Dorozhnoe Mashinostroenie,* 8: 13-16.

Knight, S.J. and D.R.Freitag, 1962. Measurement of soil trafficability characteristics. *Transactions of the ASAE*, 5(2): 121-124.

★ Kostritsyn, A.K., 1956. Cutting of a cohesive medium with knives and cones, NIAE, Silsoe, Bedford translation 58, 1956, reported by Godwin and Spoor (1977).

Kuipers, H., 1980. Reflections on the 8th conference of ISTRO. *Soil Tillage Res.*, 1:7-10.

Kushwaha, R.L., L.Chi and J.Shen, 1993. Analytical and numerical models for predicting soil forces on narrow tillage tools-a review. *Can. Agric. Eng.* 35(3): 183-193.

★ Lucins, J, 1971. Study of the influence of speed of deformation on the strength of soil. *Deutsche Agrartechnik* 21(11): 526-528.

Luth, H.J. and R.D.Wismer, 1971. Performance of plane soil cutting blades in sand. *Transactions of the ASAE*, 14: 225-259, 262.

McClelland, J.H., 1956. Instrument for measuring soil condition. *Agricultural Engineering*, 37: 480-481.

★ Mckibben, E.G. and I.F.Reed, 1952. The influence of speed on the performance characteristics of implements. Paper presented at SAE National Tractor Meeting. Sept. 1952. Reported by Kepner et al 1972.

McKyes, E. and O.S.Ali, 1977. The cutting of soil by narrow blades. *J.Terramechanics*, 14(2): 43-58.

McKyes, E., S.Negi,R.J.Godwin, and J.R.Ogilvie, 1977. Design of a tool for injecting organic waste slurries in soil. *J.Terramechanics*, 14:127-136.

McKyes, E., 1978. The calculation of draft forces and soil failure boundaries of narrow cutting blades. *Transactions of the ASAE*, 21: 20-78.

McKyes, E., and F.L.Desir, 1984. Prediction and field measurements of tillage tool draft forces and efficiency in cohesive soils. *Soil Tillage Res.*, 4: 459-470.

★ Meyerhof, G.,C. 1951. The ultimate bearing capacity of foundations. *Geotechnique*, 2(4): 310-332. Reported by Godwin and Spoor(1977).

Mitchell, J.K. and B.A.Jones Jr, 1973. Profile measuring device. *Transactions of the ASAE*, 16(3): 546-547.

Morrison, E., and A.L.Bartek, 1987. Design and field evaluation of a hand-pushed digital soil penetrometer with two cone materials. *Transactions of the ASAE*, 30(3): 646-651.

Musick, J.T. and D.H.Dusek, 1975. Deep tillage of graded-furrow-irrigated Pullman clay loam. *Transactions of the ASAE*,18:263-269.

Narayanarao, P.V. and S.R.Verma, 1982. Performance of a tractor mounted oscilating soil working tool. *AMA*. 13(2): 11-13, 33.

Negi,S.C., E.McKyes, F.Taylor, E.Douglas and G.S.V.Raghavan, 1980. Crop performance as affected by traffic and tillage in a clay soil. *Transactions of the ASAE*, 23(6): 1364-1368.

Nichols, M.L. and C.A.Reaves, 1955. Soil structure and consistency in tillage implement design. *Agricultural Engineering*, 36(8): 517-520.

Nichols, M.L. and C.A.Reaves, 1955. Soil structure and consistency in tillage implement design. *Agricultural Engineering*,, 36(8): 517-520,522.

Nichols, M.L., and C.A.Reaves, 1958. Soil reaction to subsoiling equipment. *Agricultural Engineering*, 39: 340-343.

Nichols, M.L., I.F.Reed and C.A.Reaves, 1958. Soil reaction to plow share design. *Agricultural Engineering*, 39, 336-339.

O'Callaghan, J.R. and K.M.Farrelly, 1964. Cleavage of soil by tined implements. *J.agric.Engg Res.*,9(3): 259-270.

O'Callaghan, J.R. and P.J.McCullen, 1965. Cleavage of soil by inclined and wedge-shaped tines. *J.agric.Engg Res.*,10(3): 248-254.

Ohmiya, K., N.Noguchi and H.Terao, 1993. Cone resistance measuring system for generating cone resistance distribution map. *J.Terramechanics*, 30(3): 181-190.

Olsen, H.J., 1989. Technology showcase-electronic penetrometer for field tests. *J.Terramechanics*, 6(4): 287-293.

Oni, K.C., S.J.Clark and W.H.Johnson, 1992. The effects of design on the draught of under cutter-sweep tillage tools. *Soil Tillage Res.*, 22: 117-130.

Osburn, C.P., J.G.Hendrick and R.L.Schafer, 1970. An electronic hand-operated recording penetrometer. *Transactions of the ASAE*,13(1): 385-386.

Oskoui, E and B.D.Witney, 1982. The determination of plough draught-part-I, prediction from soil and meteorological data with cone index as the soil strength parameter. *J.Terramechanics*,19(2): 97-106.

Osman, M.S., 1964. The mechanics of soil cutting blades. *J.agric.Engg Res.*,9(4): 313-328.

Owen, G.T., 1987. Soil disturbance associated with deep sub soiling in compact soils. *Can. Agric. Eng.*, 30:33-37.

Owen, G.T., 1988. Sub soiling forces and tool speed in compact soils. *Can. Agric. Eng.*, 31:15-20.

Owen, G.T., 1989. Force depth relationships in a pedogenetically compacted clay loam soil. *Applied Engineering in Agriculture*, 5(2): 185-191.

Owen, G.T., H.Drummond, L.Cobb and R.J.Godwin, 1987. An instrumentation system for deep tillage research. *Transactions of the ASAE*, 30(6): 1578-1582.

Ouwerkerk, C.V. and P.Schakel, 1965. An integrating reliefmeter for soil tillage experiments. *J.agric.Engg Res.*,10(3) :259-263.

Palmer, J. and C.A.Glasbey, 1990. Evaluation of load cycles generated on a fixed tine working in soil. *J.agric.Engg Res.*,45:295-311.

Palmer, A.L., 1992. Development of a three-point-linkage dynamometer for tillage research. *J.agric.Engg Res.*,52:157-167.

★ Payne, P.C.J., 1956. The relationship between mechanical properties of soil and the performance of simple cultivation implements. *J.agric.Engg Res.*, 1(1):23 reported by Payne and Tanner (1959).

Payne, P.C.J. and D.W.Tanner, 1959. The relationship between rake angle and the performance of simple cultivation implements. *J.agric.Engg Res.*,4(4):312-325.

Perumpral, J.V., R.D.Grisso and C.S.Desai, 1983. A soil-tool model based on limit equilibrium analysis. *Transactions of the ASAE*, 26(4): 991-995.

Perumpral, J.V., 1987. Cone penetrometer applications-A review *Transactions of the ASAE*,30(4): 939-944.

Plasse, R., G.S.V.Raghavan, and E.McKyes, 1985. Simulation of narrow blade performance in different soils. *Transactions of the ASAE*,28(4): 1007-1012.

Radhey Lal, 1959. Measurement of forces on mounted implements. *Transactions of the ASAE*, 2(1): 109-111.

Ram, D.N. and P.J.Zwerman, 1960. A convenient soil compaction indicator. *Agron.J.* 1960, 52(8): 484.

RNAM, 1983. Test codes and procedures for farm machinery, Technical series No.12.

Rajaram, G., 1990. Collapse failure in dry clay soils caused by tine implements. *J.Terramechanics*, 27(2): 69-78.

Rawitz,E., J.Morin, W.B.Hozmoed, M.Margolin and H.Etkin, 1983. Tillage practices for soil and water conservation in the semi-arid zone. Management fo fallow during the rainy season preceding cotton. *Soil Tillage Res.*, 3:211-231.

Rawitz, E. and M.Margolin, 1991. An economical hand-held recording penetrometer. *Soil Tillage Res.*, 19:67-75.

Reid,J. T., 1979. A system for measuring tractor fuel use on small plots. *Transactions of the ASAE*, 22(1): 57-58, 62.

Reid,J. T., L.M.Carter, and R.L.Clark, 1985. Draft measurements with a three-point hitch dynamometer. *Transactions of the ASAE*,28(10): 89-93.

Riethmuller, P., D.G.Batchelder, and P.D.Bloome, 1983. A micro computer system for cone index measurement. *Transactions of the ASAE*,26(4): 996-998.

Rogers, I.C. and G.M.Johnston, 1955. Measuring the forces in tractor linkage. *Agricultural Engineering*, 34(8): 542-544,638.

Rowe, R.J. and K.K.Barnes, 1961. Influence of speed on elements of draft of a tillage tool. *Transactions of the ASAE*,4(1): 55-57.

Saveson, I.L. and Z.F.Lund, 1958. Deep tillage for crop production. *Transactions of the ASAE*, 2:40-42.

Sheruddin Bukhari, G.R.Mari, M.Zafarullah, J.M.Baloch and M.S.Panhwar, 1992. Effect of disc and tilt angle on field capacity and power requirements of mounted plough. *AMA*. 23(2): 9-13.

Siemens, J.C., J.A.Weber, and T.H.Thornburn, 1965. Mechanics of soil as influenced by model tillage tools. *Transactions of the ASAE*, 8(1): 1-7.

Smith, L.A. and W.T.Dumas. 1978. A recording soil penetrometer. *Transactions of the ASAE*,21(1): 12-19.

Smith, L.A. and G.L.Barker, 1982. Equipment to monitor field energy requirements. *Transactions of the ASAE*, 25(6): 1556-1559.

Smith, L.H. and J.R.Williford, 1988. Power requirements of conventional triplex, and parabolic subsoilers. *Transactions of the ASAE*, 31(6): 1685-1688.

Sokolovshi, V.V., 1965. Statics of soil media London: Butterworths, 1960. (Revised version, Pergamon press) Reported by Albuquerque and Hettiaratchi (1980).

Spoor, G. and R.J.Godwin, 1978. An experimental investigation into the deep loosening of soil by rigid tines. *J.agric.Engg Res.*,23:243-258.

Spoor, G. and R.K.Fry, 1983. Field performance of trenchless drainage tines and implications for drainage system efficiency. *J.agric.Engg Res.*,28:319-335.

Spoor, G. and R.K.Fry, 1985. Soil disturbance generated by deep working low rake angle narrow tines. *J.agric.Engg Res.*, 28:217-234.

★ Sprinkle, L.W., T.D.Langston, J.A. Weber and N.M.Sharov. 1970. A similitude study with static and dynamic parameters in artificial soil. *Transactions of the ASAE*, 13(5): 580-586.

Stafford, J. V. and D.W.Tanner, 1983. Effect of rate on soil shear strength and soil-metal friction. I.Shear strength. *Soil Tillage Res.*, 3: 245-260.

Stafford, J.V. and D.W.Tanner, 1983. Effrect of rate on soil shear strength and soil-metal friction. II Soil-metal friction. *Soil Tillage Res.*, 3:321-330.

Stafford, J.V., 1984. Force prediction models for brittle and flow failure of soil by draught tillage tools. *J.agric.Engg Res.*, 29:51-60.

Steinbruegge, G.W, (1969). Improved method of locating centres of gravity. *Transactions of the ASAE*,12(5): 681-684.

Summers, J.D., A.Khalilian, and D.G.Batchelder, 1986. Draft relationships for primary tillage in Oklahoma soils. zof the ASAE, 29(1): 37-39.

Swick, W.C. and J.V.Perumpral, 1988. A model for predicting soil-tool interaction. *J.Terramechanics*,25(1): 43-56.

★ Taylor, H.M. and H.R.Gardner. 1963. Penetration of cotton seedling tap root as influenced by bulk density, moisture content, and strength of soil. *Soil Sci.* 96(3): 153-156. Reported by Khalilian et al 1988.

Terry, C.W. and H.M.Wilson, 1952. The Cornell soil penetrometer. *Agricultural Engineering*, 32: 425.

Terzaghi, K, 1959. Theoretical soil mechanics. John Wiley and Sons, Inc. Newyork.

Tessier, S., R.I.Papendick, K.E.Saxton, and G.M.Hyde, 1989. Roughness meter to measure seed row geometry and soil disturbance. *Transactions of the ASAE*, 32(6): 1871-1873.

Thomson, N.P. and K.J.Shinners, 1989. A portable instrumentation system for measuring draft and speed. *Applied Engineering in Agriculture*, 15(2): 133-137.

Threadegill, E.D.E., 1982. Residual tillage effects as determined by cone index. *Transactions of the ASAE*, 25(4): 859-863, 867.

Upadhyaya, S.K., T.H.Williams, L.J.Kemble, and N.E.Collins, 1984. Energy requirements for chiseling in coastal plain soils. *Transactions of the ASAE*,27(6): 1643-1649.

Upadhyaya, S.K., L.J.Kemble, N.E.Collins, and F.A.Camargo Jr, 1985. Accuracy of mounted implement draft prediction using strain gages mounted directly on three-point linkage system. *Transactions of the ASAE*, 28(1): 40-46.

Venkateswarlu, J., 1987. Efficient resource management systems for drylands of India. *Advances in soil science*, 7:166-216.

Verma, B.P., and R.L.Schafer, 1971. A distorted-model theory for non-uniform soil strength profiles. *Transactions of the ASAE*,14: 359-362.

Vittal,K. P.R., K.Vijayalakshmi and V.M.B.Rao, 1983. Effect of deep tillage on dryland crop production in red soils of India. *Soil Tillage Res.*, 3: 377-384.

Wadhwa, D.S., 1980. Force prediction equation using distorted model as an amalog device. *J.Terramechanics*, 17(3): 119-130.

Wells, L.G., C.O.Lewis and R.J.Distler, 1982. Remote electronic acquisition of soil cone index measurement. *J.Terramechanics* 19: 201-207.

Wildman, W.E., C.A.Reaves and W.R.Gill, 1978. Effect of slip plow design on draft forces and soil loosening. *Transactions of the ASAE*, 21(3): 422- 426.

Willatt, S.T. and A.H.Willis, 1965. A study of the trough formed by the passage of tines through soil. *J.agric.Engg Res.*, 10(1): 1-4.

Wilford, J.R., O.B.Wooten and F.E.Fulgham, 1972. Tractor mounted cone penetrometer. *Transactions of the ASAE*, 15(2): 226-227.

Willcocks, T.J., 1981. Tillage of clod-forming sandy loam soils in the semi-arid climate of Botswana. *Soil Tillage Res.*, 1:323-350.

Wolf,D., and H.J.Luth, 1979. Tillage equipment for clod-forming soils. *Transactions of the ASAE*, 22(5): 1029-1032.

Wolf, D., T.H.Garner, and J.W.Davis, 1981. Tillage mechanical energy input and soil crop response. *Transactions of the ASAE*, 24(6): 1412-1419, 1425.

Yao, Y. and D.Zeng, 1991. Investigation on the relationship between soil shear strength and shear strain rate. *J.Terramechanics*,28(1): 1-10.

Yong, R.N.and A.W.Hanna, 1979. Finite element analysis of plane soil cutting. *J.Terramechanics*, 14:103-123.

Yusu, Y., and D.Zeng, 1990. Investigation of the relationship between soil-metal friction and sliding speed. *J.Terramechanics*, 27(4): 283-290.

Zoz, F.M., 1974. Optimum width and speed for least cost tillage. *Transactions of the ASAE*, 17: 845-850.

★ Original not seen.

ANNEXURES

APPENDIX A

PROGRAM LISTINGS

I GODWIN AND SPOOR MODEL

```
      PROGRAM GWIND
      IMPLICIT DOUBLE PRECISION (A-H,O-Z)
      DIMENSION ALPHA(8),DN(8),CN(8),AN(8),RATM(8)
      OPEN(1,FILE='GWIN.DAT',STATUS='OLD')
      DO 110 J=1,8,1
      READ(1,100)ALPHA(J),DN(J),CN(J),AN(J),RATM(J)
100   FORMAT(5F6.3)
110   CONTINUE
      CLOSE(1)
      OPEN(1,FILE='GWIND.DAT',STATUS='NEW')
      IA=2
      DO 310 J=1,8,1
      DO 300 K=5,40,5
      I=IA/10.
      CA=ACOS((1.0/TAN(ALPHA(J)))/RATM(J))
      SA=SIN(ALPHA(J)+.52)
      S1=RATM(J)*K*SIN(CA)
      W=2.*S1+I
      AREA=K*(S1+I)
      A=4.11*DN(J)*SIN(ALPHA(J)+.59)*RATM(J)*SIN(CA)
      B=2.*100.*CN(J)*RATM(J)*SIN(CA)*SA+2.74*DN(J)*SA*I-.3*1.37*I*600.
      C=(100.*CN(J)+8.6E-3*AN(J))*SA*I+8.6E-3*ICOS*(ALPHA(J))-I*100.*600.
      CDEP=((-1.0)*B+SQRT(B**2.-4.*A*C))/2.0*A
      WRITE(1,200)CDEP
200   FORMAT(2X,'CDEP= ',F7.2)
      IF(K.LT.CDEP)THEN
       TEMP=CDEP
      CDEP=K
      Q=0.0
      ELSE IF(K.GE.CDEP)THEN
      Q=I*100.*600.*(K-CDEP)+.2055*I*600.*(K**2.-CDEP**2.)
      END IF
      F=(1.37*CDEP**2.*DN(J)+110.*CDEP*CN(J))
```

```
      HA=F*(I+RATM(J)*CDEP*SIN(CA))*SA+(23.32*I*CDEP*
      1(AN(J)*SA+COS(ALPHA(J))))
      V=(F*(I+RATM(J)*CDEP*CA)*COS(ALPHA(J)+.52)-23.32*I
      1*CDEP*(AN(J)*COS(ALPHA(J)+.52)-SIN(ALPHA(J))))/1000.
      H=HA/1000.
      WRITE (1,500)K,I,J
      WRITE(1,510)K,H,V,W,AREA
  510 FORMAT(2X,I2,2X,F8.2,2X,F8.2,2X,F8.2,2X,F8.2)
      WRITE(*,*)'FIRST LOOP IN PROGRESS...',K,J,I
  300 CONTINUE
      WRITE(*,*)'SECOND LOOP IN PROGRESS...',J,I
      WRITE(1,*)' '
  310 CONTINUE
      WRITE(*,*)'THIRD LOOP IN PROGRESS....',I
      WRITE(1,*)' '
      WRITE(1,*)' '
  320 CONTINUE
      STOP
      END
```

II McKEYES AND ALI MODEL

```
      PROGRAM MEKD
      IMPLICIT DOUBLE PRECISION (A-H,O-Z)
      OPEN(1,FILE='MEKD.DAT',STATUS='NEW')
      IA=20
      DO 520 MA=15,155,20
      DO 510 J=5,40,5
      ALPHA=MA/100.
      IF (ALPHA.LE.0.79)THEN
      DEL=0.52
      ELSE IF (ALPHA.GT.0.79)THEN
      DEL=0.88-0.45*ALPHA
      END IF
      B=IA/10.
      IF (ALPHA.GT.0.79) GOTO 100
   50 DEL=0.590
```

```
      CALL MINIM (ALPHA,DEL,BETA,J,B,RAD,ROWD,DN,CN)
      H=(B/1000.)*(1.37*J**2*DN+110*J*CN)
      V=H*(1.0/TAN(ALPHA+DEL))
      S=RAD*SIN(ROWD)
      W=2.*S+B
      A=(B+S)*J
      WRITE (*,*)DN,CN
      GOTO 600
100   ALPHA1=0.79
      DEL1=0.78
      CALL MINIM (ALPHA1,DEL1,BETA1,J,B,RAD,ROWD,DNS,CNS)
      TETA=(1.19-ALPHA)
      DENA=((1.0/TAN(ALPHA+DEL))+(1.0/TAN(TETA+.78)))
      DEPH=(J*0.713/SIN(ALPHA))*(SIN(ALPHA+.78)+(COS(ALPHA+.78)*
     1TAN(.414-ALPHA)))
      DNN=(0.5*(DEPH/J)*(0.983-(1.0/TAN(ALPHA))+2.0*(DEPH/J)*
     1DNS*(1.0/TAN(TETA+0.78))))/DENA
      CNN=(1.0-(2.0*DEPH/J)-(((2.0*DEPH*0.983/J)-(1.0/TAN(ALPHA)))*
     1(1.0/TAN(TETA+0.78)))+(DEPH*CNS*(1.0/TAN(TETA+0.78))/J))/DENA
      CALL MINIM(ALPHA,DEL,BETA2,RAD,ROWD,DN,CN)
      DEL2=0.00
      CALL MINIM(ALPHA1,DEL2,BETA,J,B,RAD,ROWD,DNDO,CNDO)
      250   DNND=DNDO*(DNN/DNDO)**(DEL/0.78)
      CNND=CNDO*(CNN/CNDO)**(DEL/0.78)
      RADN=DEPH*(0.98+(1.0/TAN(BETA1)))
      ROWDN=ACOS(DEPH*0.98/RADN)
      S=RADN*SIN(ROWDN)
      W=2.*S+B
      A=(B+S)*J
      H=(B/1000.0)*(1.37*DEPH**2*DNND+110*DEPH*CNND)
      V=H*(1.0/TAN(ALPHA+DEL))
600   WRITE(1,710)J,H,V,W,A
710   FORMAT(2X,I2,2X,F6.1,2X,F6.1,2X,F6.1,2X,F6.1)
      WRITE(*,*)'FIRST LOOP IN PROGRESS'
510   CONTINUE
      WRITE(1,*)' '
      WRITE(*,*)'SECOND LOOP IN PROGRESS'
520   CONTINUE
      STOP
      END
```

```
      SUBROUTINE MINIM (ALPHA,DEL,BETA,J,B,RAD,ROWD,DNA,CNA)
      IMPLICIT DOUBLE PRECISION (A-H,O-Z)
      DIMENSION DN(3)
      BETA=0.2
300   DO 320 K=1,2
      RAD=J*((1.0/TAN(ALPHA))+(1.0/TAN(BETA)))
      ROWD=ACOS(J*(1./TAN(ALPHA))/RAD)
      DEN=((1.0/TAN(ALPHA+DEL))+(1.0/TAN(BETA+0.78)))
      DN(K)=((RAD/(2*J))*(1.0+(2.0*RAD*J*SIN(ROWD)/(3*J*B))))/DEN
      BETA=BETA+0.05
320   CONTINUE
      PD=DN(1)-DN(2)
      IF(PD.GT.0) GOTO 300
      DNA=DN(2)
      CNA=((1.0+((1.0/TAN(BETA))*(1.0/TAN(BETA+0.78))))
     1*(1.0+(RAD*SIN(ROWD)/B)))/DEN
      RETURN
      END
```

III PERUMPRAL MODEL

```
      PROGRAM PPRLD
      REAL NDPO,NAPO,NCPO
      INTEGER BA,D
      DIMENSION PO(3)
      OPEN(1,FILE='PPRLD.DAT',STATUS='NEW')
      BA=20
      DO 310 MA=15,155,20
      DO 300 D=5,40,5
      B=BA/10.
      ALPHA=MA/100.0
      IF(ALPHA.LE.0.79)THEN
      DEL=0.52
      ELSE IF(ALPHA.GT.0.79)THEN
      DEL=0.88-0.45*ALPHA
      END IF
      BETA=.2
20    Z=D/3.0
      DO 50 J=1,2
```

```
      A=0.5*D**2*((1./TAN(ALPHA)+(1./TAN(BETA))))
      NDPO=(A/(B*D**2))*((0.4466*Z*SIN(0.78))+(B*SIN(0.78+BETA)))
      1/SIN(BETA+ALPHA+.78+DEL)
      NCPO=.711*(((2.*A)/(B*D))+(1./SIN(BETA)))
      1/(SIN(BETA+ALPHA+.78+DEL))
      NAPO=(-1.)*COS(BETA+ALPHA+.78)
      1/((SIN(BETA+ALPHA+.77+DEL))*(SIN(ALPHA)))
      PO(J)=(1.38*B*D**2*NDPO+110*B*D*NCPO+23.32*B*D*NAPO)/1000.
      BETA=BETA+.05
50    CONTINUE
      PD=PO(1)-PO(2)
      IF (PD .GT. 0)GO TO 20
      BETA=BETA-.05
      V=PO(1)*COS(ALPHA+DEL)
      H=PO(1)*SIN(ALPHA+DEL)
      WRITE(*,*)B,D,ALPHA
      WRITE(*,*)BETA,NDPO,NCPO,NAPO
      WRITE(1,530)D,PO(1),H,V
      WRITE(*,*)'FIRST LOOP IN PROGRESS'
300   CONTINUE
305   WRITE(1,*)' '
      WRITE(*,*)'SECOND LOOP IN PROGRESS.....'
310   CONTINUE
530   FORMAT (2X,I2,2X,F7.1,2X,F7.1,2X,F7.1)
      STOP
      END
```

IV SWICK AND PERUMPRAL MODEL

```
      PROGRAM SWICKD
      IMPLICIT DOUBLE PRECISION (A-H,O-Z)
      DIMENSION P(3)
      OPEN (1,FILE='SWICKD.DAT',STATUS='NEW')
      I=0
      JA=20
      DO 310 L=15,155,20
      DO 300 K=5,40,5
      J=JA/10.
      ALPHA=L/100.
      IF(ALPHA.LE.0.79)THEN
```

```
      DEL=0.52
      ELSE IF (ALPHA.GT.0.79)THEN
      DEL=0.88-0.45* ALPHA
      END IF
      BETA=.2
   10 DO 50 M=1,2
      RAD=K*((1/TAN(ALPHA))+(1/TAN(BETA)))
      ROWD=ACOS((K/RAD)*(1/TAN(ALPHA)))
      S=RAD*SIN(ROWD)
      ADF=23.32*J*K/SIN(ALPHA)
      W1=0.685*J*K*RAD
      W2=0.2283*K*RAD**2
      FA1=1.396E-3*J*K*I**2*SIN(ALPHA)/SIN (ALPHA+BETA)
      FA2=.698E-3*K*RAD*I**2*SIN(ALPHA)/SIN (ALPHA+BETA)
      CF1=110*J*K/SIN(BETA)
      CF2=55*K*RAD/SIN(BETA)
      P1=(-1.0*ADF*COS(ALPHA+.78+BETA)+W1*SIN (.78+BETA)
      1+(CF1+FA1)*.7132)
      1/SIN(ALPHA+.78+BETA+DEL)
      P2=(W2*SIN(.78+BETA)*SIN(ROWD)+FA2*.7132*((ROWD/2)
      1+(0.25*SIN(2.*ROWD)))+CF2*.7132*SIN(ROWD))/
      1SIN(ALPHA+.78+BETA+DEL)
      P(M)=(P1+2*P2)/1000.
      BETA=BETA+.05
   50 CONTINUE
      PD=P(1)-P(2)
      IF (PD.GT.0)GOTO 10
      BETA=BETA-.05
      H=P(1)*SIN(ALPHA+DEL)
      V=P(1)*COS(ALPHA+DEL)
      W=2*S+J
      A=(J+S)*K
      WRITE (1,220)K,H,V,W,A
      220 FORMAT(2X,I2,2X,F7.1,2X,F7.1,2X,F5.1,2X,F6.1)
      WRITE(*,*)'FIRST LOOP IN PROGRESS....',I,J,K,L
  300 CONTINUE
      WRITE(*,*)'SECOND LOOP IN PROGRESS...',I,J,K
      WRITE(1,*)' '
  310 CONTINUE
      STOP
      END
```

APPENDIX B

CALIBRATION RECORDINGS FOR TILLAGE DYNOMOMETER

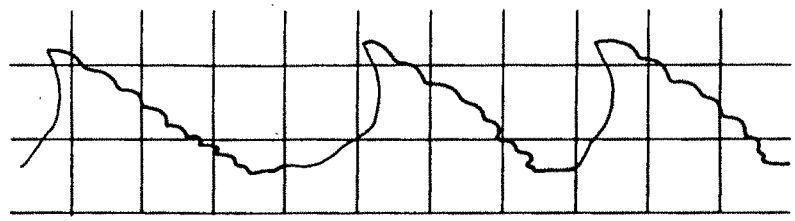

L_1

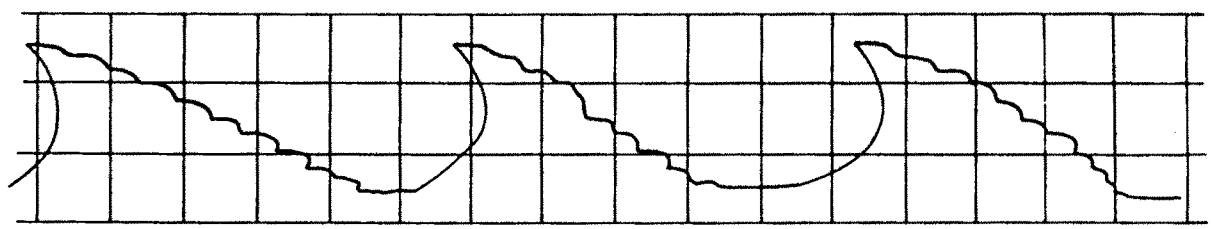

L_2

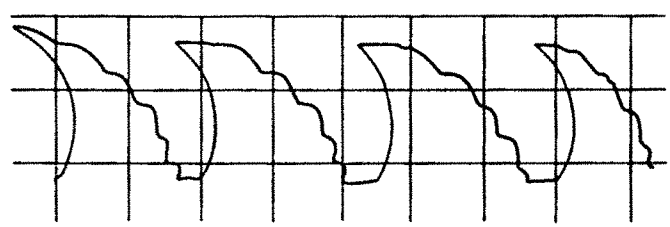

S

V_1

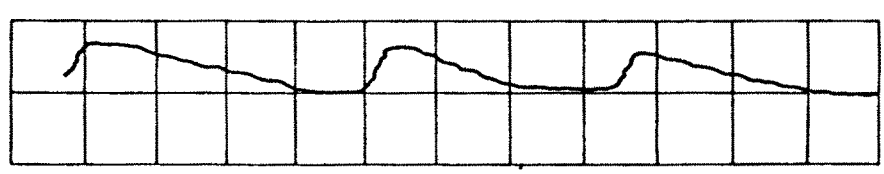

V_2

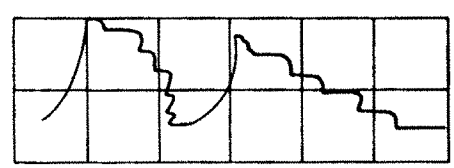

V_3

APPENDIX C
MODEL CALCULATION

The methodology adopted to calculate the forces acting on share from the recordings obtained from the tillage dynamometer was as follows. Fig.1 shows the recordings obtained for the share of size 30x100 mm. The marked segments represent recordings obtained in the treatment 13/40/1. The conversion of chart recordings into force values is illustrated by taking observation No.10 as an example. Refering Fig.2, The calculation for each value is as tabulated below.

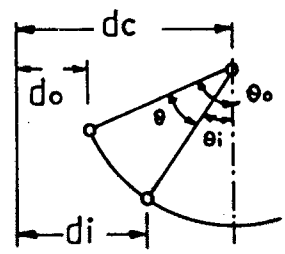

		L_1	V_1	V_2
1.	Distance read from chart (di), cm	19.5	13.4	8.4
2.	Null reading for each recording (do), cm	10.1	10.9	1.5
3.	Centre distance of pen arm (dc), cm	17.5	17.5	7.5
4.	Radius of pen arm(r),cm	7.4	7.0	7.0
	Pen angle at zero load, ZZ_0 $\sin ZZ_0 = (d_c - d_0)/r$	90.0	71.0	59.0
	Pen angle at under load, ZZi $\sin ZZ_i = (dc - di)/r$ $(di < dc)$	16.0	37.0	7.0
	$\mathrm{Sin}ZZ_i = (dc - di)/r$ $(di < dc)$ Angular deflection of pen ZZ	106.0	34.0	52.0

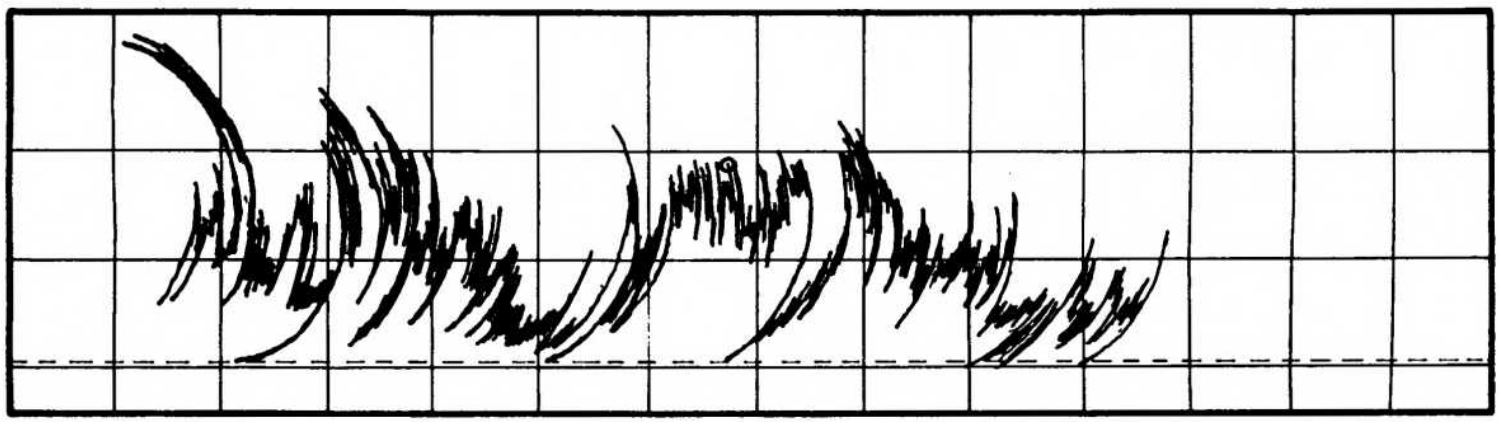

L_1

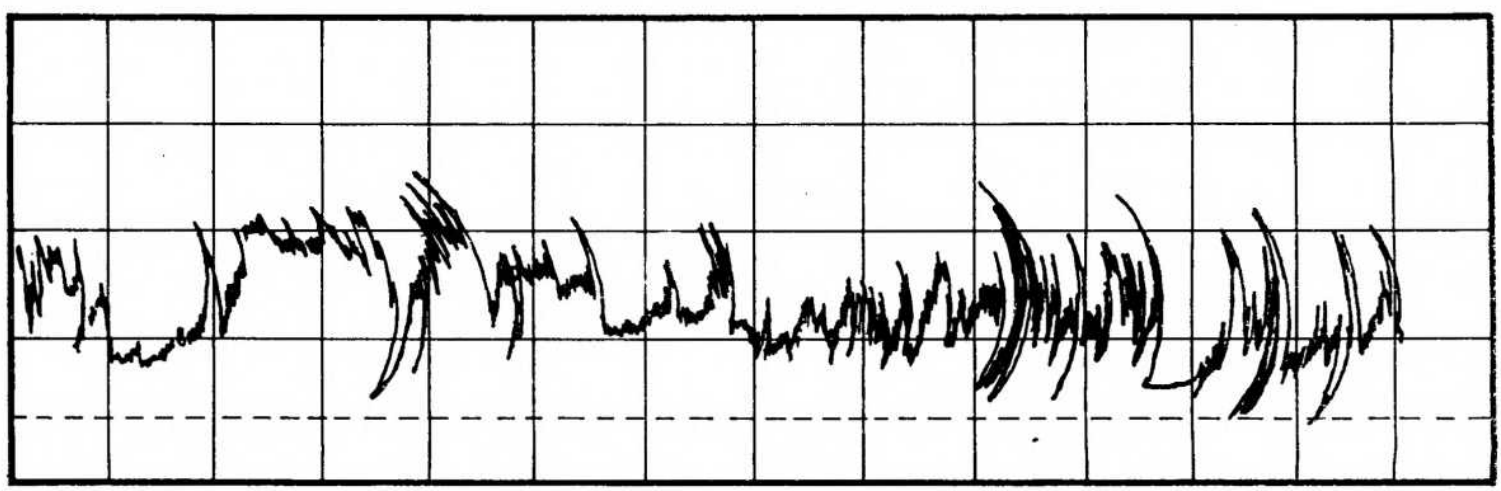

V_2

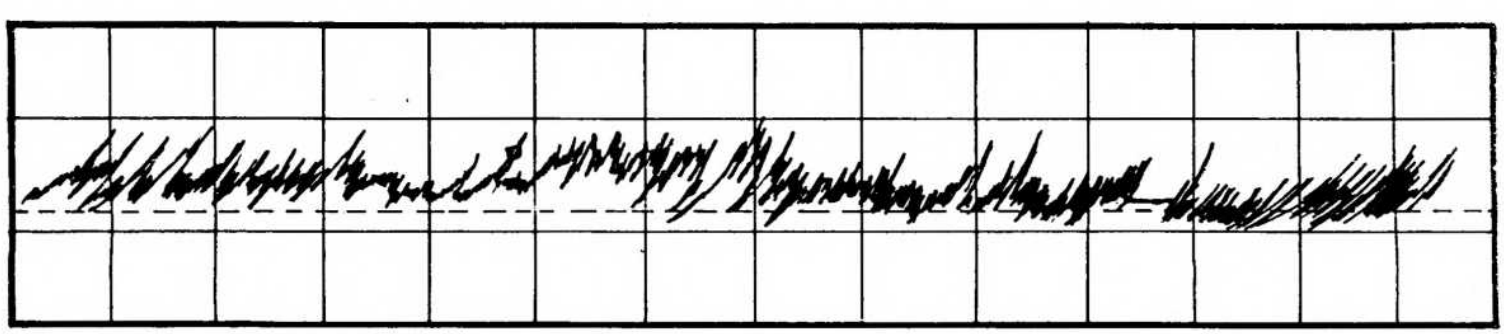

V_1

Fig. 1. DYNAMOMETER RECORDINGS

$ZZ = ZZi - ZZo$ (di < dc)

$ZZ = ZZi + ZZo$ (di > dc)

5. Conversion of angular deflection to load using calibration chart

$ZZ = -7.2 + 0.375L_1$	301.7		
$ZZ = 1.86 + 0.24\ V_1$		134.0	
$ZZ = -3.39 + 0.13\ V_2$			427.0

6. Correction for dead weight -

$2V_1$	V_2
+49.0	-33.0
= 317.0	= 394.0

7. Calculated forces

$L = 2L_1 = 603.4$ Kg

$V = V_2 - 2V_1$

$= 394 - 317$ Kg $= 77$ Kg

$ZZ = \tan^{-1}(V/L) = 14.31°$

$Rh = \_L^2 + V^2 = 608.3$ Kg

Location of resultant below V_2 dynamometer,

$x = 2V_1 \times 75/L$, cm $= 39.4$

APPENDIX D

FORCES ON SHARES

Table 1. Results of field trials - average values of soil reaction, its orientation and location for 25 mm x 150 mm share

S.No.	Depth cm	Speed m/s	L Kg	σ_L Kg	V Kg	σ_V Kg	θ rad	RV Kg	x cm
1.	18	0.44	395.9	84.6	36.00	49.6	0.11	401.46	94.72
2.	27	0.44	584.4	102.5	35.09	93.4	0.06	592.71	51.93
3.	23	0.44	511.8	73.2	72.92	67.6	0.14	521.47	53.46
4.	26	0.44	624.2	54.3	80.72	77.3	0.12	633.86	49.32
5.	30	0.44	712.4	39.3	135.56	44.3	0.19	726.66	43.08
6.	18	0.55	478.2	58.0	60.00	97.4	0.14	491.98	54.40
7.	21	0.55	485.5	134.4	128.32	114.4	0.27	516.10	49.32
8.	21	0.55	460.6	53.5	73.54	57.2	0.16	470.15	53.37
9.	28	0.55	693.5	97.7	83.33	47.2	0.12	700.31	46.73
10.	27	0.55	618.1	62.3	138.05	95.8	0.21	639.45	44.11
11.	18	0.67	505.5	83.6	123.38	168.8	0.21	541.64	51.17
12.	19	0.67	423.3	52.3	29.48	36.6	0.07	425.83	56.69
13.	26	0.67	630.9	76.4	43.87	57.7	0.07	635.14	54.37
14.	27	0.67	633.9	73.3	95.14	85.5	0.14	646.34	47.63
15.	12	1.00	307.9	61.4	74.80	36.3	0.25	319.75	56.81
16.	15	1.00	408.9	44.6	28.56	32.0	0.07	411.15	59.38
17.	24	1.00	689.9	110.4	139.53	141.6	0.19	716.63	50.43
18.	28	1.00	838.7	63.6	101.72	66.8	0.12	847.18	47.03
19.	30	1.00	834.3	58.9	229.85	131.3	0.26	874.08	43.14
20.	17	0.90	425.0	59.4	63.28	54.2	0.15	432.86	53.20
21.	21	0.90	539.6	156.1	70.64	94.8	0.13	549.97	57.86
22.	21	0.90	557.6	85.5	54.81	104.1	0.10	570.70	54.66
23.	28	0.90	775.1	84.1	85.38	112.6	0.11	787.75	46.77
24.	27	0.90	786.8	46.7	126.73	150.4	0.16	810.52	50.94

L - Mean Values of longitudinal reaction
σ - Standard deviation of L
$\bar{V}$ - Mean value of vertical reaction
σ_v - Standard deviation of V
θ^v - Mean Angle of resultant
RV - Mean value of resultant reaction
x - Distance of Rv below V2

Table 2. Results of field trials - average values of soil reaction, its orientation and location for 20 mm x 100 mm share

S.No.	Depth cm	Speed m/s	L Kg	σ_L Kg	V Kg	σ_V Kg	θ rad	RV Kg	x cm
1.	19	0.44	309.69	48.39	43.13	33.2	0.13	314.12	52.96
2.	13	0.44	187.32	43.73	35.75	17.9	0.20	191.72	57.62
3.	15	0.44	223.68	73.85	40.55	24.4	0.20	229.07	56.68
4.	15	0.44	215.29	42.99	24.73	43.7	0.14	222.03	53.84
5.	19	0.44	310.28	35.30	42.53	22.7	0.14	314.05	54.50
6.	34	0.44	474.96	57.15	114.87	34.6	0.24	490.55	33.31
7.	19	0.55	335.31	31.75	126.90	57.3	0.35	362.05	48.94
8.	9	0.55	179.00	55.61	43.78	8.3	0.27	185.14	58.95
9.	15	0.55	259.80	61.10	51.71	40.1	0.22	269.02	54.09
10.	17	0.55	267.16	50.56	39.45	40.8	0.16	273.69	50.97
11.	19	0.55	346.14	67.82	45.47	33.0	0.14	350.97	56.24
12.	24	0.55	442.95	59.17	52.25	93.6	0.12	456.11	44.50
13.	18	0.67	279.16	50.78	123.45	64.4	0.39	309.48	38.38
14.	16	0.67	246.67	71.10	33.89	58.32	0.19	257.08	55.65
15.	19	0.67	278.89	33.01	46.40	36.1	0.16	284.93	51.95
16.	24	0.67	310.27	41.86	53.04	38.6	0.18	317.59	55.08
17.	19	0.67	466.47	43.47	83.32	45.7	0.17	475.52	46.39
18.	19	0.70	323.28	82.85	82.38	30.9	0.27	336.13	54.42
19.	16	0.70	283.36	51.75	59.41	52.8	0.22	294.55	51.60
20.	15	0.70	255.16	52.90	30.35	43.4	0.13	261.05	55.47
21.	19	0.70	346.35	50.31	52.47	20.0	0.15	350.96	52.70
22.	22	0.70	430.96	56.42	72.34	35.3	0.17	438.56	54.09
23.	7	0.76	139.28	52.30	20.70		0.17	141.07	66.98
24.	15	0.76	202.28	65.14	51.35	39.7	0.25	212.15	55.57
25.	13	0.76	229.34	51.79	69.43	50.1	0.31	246.32	60.22
26.	17	0.76	313.78	40.55	57.34	39.0	0.19	321.71	54.19
27.	19	0.76	398.94	97.10	71.84	60.5	0.19	410.91	54.64
28.	24	0.76	573.14	129.69	106.83	36.9	0.19	584.29	44.06

L - Mean Values of longitudinal reaction
σ_x - Standard deviation of L
V - Mean value of vertical reaction
σ_v - Standard deviation of V
θ - Mean Angle of resultant
RV - Mean value of resultant reaction
x - Distance of Rv below V2

Table 3. Results of field trials - average values of soil reaction, its orientation and location for 40 mm x 200 mm share

S.No.	Depth cm	Speed m/s	L Kg	σ_L Kg	V Kg	σ_V Kg	θ rad	RV Kg	x cm
1.	19	0.27	241.21	47.79	28.72	45.9	0.10	246. 27	55.52
2.	16	0.27	147.71	43.75	22.07	15.3	0.16	150.20	55.53
3.	20.5	0.27	210.89	66.32	30.59	33.2	0.19	219.16	68.96
4.	21	0.27	261.40	26.02	41.63	30.9	0.16	266.40	46.37
5.	22.5	0.27	285.11	44.09	63.16	31.2	0.22	293.76	43.34
6.	28	0.27	508.50	32.61	129.28	37.6	0.25	525.89	45.10
7.	13.5	0.44	178.62	16.53	34.00	0.0	0.19	181.85	52.09
8.	16	0.44	209.22	42.97	31.52	27.8	0.15	213.27	52.01
9.	20.5	0.44	246.77	71.50	54.33	17.5	0.24	253.74	48.05
10.	21	0.44	283.14	70.87	54.24	29.0	0.20	290.01	48.23
11.	22.5	0.44	346.42	24.81	92.01	18.1	0.26	359.03	46.21
12.	28	0.44	486.59	28.06	128.10	17.3	0.26	503.53	46.99
13.	13.5	0.51	173.11	44.03	126.11	13.0	0.65	216.87	54.09
14.	16	0.51	305.89	42.44	47.98	24.7	0.16	310.87	53.24
15.	17	0.51	228.64	77.61	31.64	39.0	0.18	235.09	55.17
16.	21	0.51	326.35	59.85	46.61	25.1	0.14	330.53	64.02
17.	22	0.51	417.47	57.87	-0.46	26.0	0.00	418.27	54.88
18.	28	0.51	630.34	159.76	119.98	49.3	0.19	644.00	48.99
19.	13.5	0.67	170.29	56.37	18.37	41.8	0.15	176.99	58.03
20.	16	0.67	242.94	42.63	31.01	23.4	0.14	246.58	56.16
21.	15	0.67	194.84	44.66	32.60	3.2	0.17	197.68	55.86
22.	21	0.67	355.41	67.63	71.57	33.7	0.21	364.92	48.63
23.	22.5	0.67	428.57	38.00	72.70	31.2	0.17	435.39	69.58
24.	10.5	0.60	112.20	42.96	20.00	6.0	0.20	114.45	56.83
25.	12	0.60	125.23	48.42	20.33	6.8	0.21	127.66	69.65
26.	18	0.60	260.13	117.28	39.12	33.3	0.18	265.71	59.40
27.	21	0.60	337.55	49.84	75.66	32.7	0.23	347.82	52.40
28.	24	0.60	385.52	63.39	45.80	35.1	0.12	389.86	59.46

L - Mean Values of longitudinal reaction
σ - Standard deviation of L
V^x - Mean value of vertical reaction
σ_v - Standard deviation of V
θ^v - Mean Angle of resultant
RV - Mean value of resultant reaction
x - Distance of Rv below V2

Table 4. Results of field trials - average values of soil reaction, its orientation and location for 30 mm x 150 mm share

S.No.	Depth cm	Speed m/s	L Kg	σ_L Kg	V Kg	σ_V Kg	θ rad	RV Kg	x cm
1.	14	0.36	164.40	38.50	130.86	30.7	0.69	214.17	63.28
2.	26	0.36	374.80	34.10	33.71	47.9	0.09	379.34	49.48
3.	21	0.36	341.90	29.00	29.83	68.4	0.08	349.57	81.05
4.	28	0.36	443.10	65.60	66.57	35.0	0.15	449.44	54.70
5.	34	0.36	580.00	128.80	128.29	127.6	0.21	605.82	35.35
6.	13	0.49	161.80	18.60	7.81	26.9	0.05	164.04	57.88
7.	26	0.49	520.60	43.90	56.16	56.6	0.11	526.86	51.91
8.	21	0.49	423.10	69.70	25.24	49.8	0.07	427.23	50.92
9.	28	0.49	507.40	46.30	45.28	39.5	0.09	510.92	44.08
10.	34	0.49	668.50	124.50	93.93	68.4	0.15	679.06	39.32
11.	13	0.59	167.70	18.10	2.10		0.01	167.70	59.63
12.	26	0.59	465.60	54.80	31.48	74.0	0.06	472.63	52.61
13.	21	0.59	354.40	16.90	20.92	47.1	0.06	358.12	50.88
14.	28	0.59	568.50	94.20	74.33	45.7	0.13	574.77	45.66
15.	34	0.59	794.90	81.50	119.96	79.4	0.15	807.24	39.86
16.	13	0.81	147.60	13.60	4.10	0.0	0.03	147.68	58.92
17.	26	0.81	489.70	88.80	34.14	74.6	0.07	497.08	53.59
18.	21	0.81	551.80	54.40	141.94	47.0	0.38	382.32	50.15
19.	28	0.81	550.00	168.50	98.93	64.1	0.18	561.46	40.90
20.	34	0.81	836.50	80.00	100.33	76.8	0.11	845.62	39.32
21.	13	0.67	247.90	80.50	12.62	29.3	0.06	249.74	60.76
22.	22	0.67	364.90	50.00	46.75	57.1	0.13	372.65	52.86
23.	20	0.67	358.20	62.20	76.38	31.2	0.21	367.57	51.12
24.	34	0.67	870.33	260.80	93.72	179.6	0.08	892.32	34.20

L - Mean Values of longitudinal reaction
σ - Standard deviation of L
V^x - Mean value of vertical reaction
σ_v - Standard deviation of V
θ - Mean Angle of resultant
RV - Mean value of resultant reaction
x - Distance of Rv below V2

Table 5. Results of field trials - average values of soil reaction, its orientation and location for 30 mm x 200 mm share

S.No.	Depth cm	Speed m/s	L Kg	σ_L Kg	V Kg	σ_V Kg	θ rad	RV Kg	x cm
1.	31	0.27	775.3	214.7	173.29	140.4	0.22	803.79	67.52
2.	30	0.27	761.8	106.9	153.88	51.9	0.20	778.29	47.40
3.	30	0.27	816.8	58.2	251.83	103.7	0.29	859.95	41.10
4.	33	0.27	828.3	91.3	124.87	83.6	0.15	841.79	39.00
5.	33	0.27	836.1	89.7	108.70	111.6	0.13	850.40	38.92
6.	31	0.30	823.0	103.2	191.75	166.9	0.23	861.44	44.31
7.	30	0.30	785.3	109.6	199.83	100.8	0.25	815.74	44.92
8.	25	0.30	656.3	103.1	133.03	66.4	0.20	672.35	45.32
9.	31	0.30	825.5	115.5	192.96	114.9	0.22	854.15	38.40
10.	28	0.30	725.6	132.5	86.67	156.8	0.15	748.73	40.57
11.	18	0.76	498.3	42.5	106.63	41.7	0.21	510.96	47.00
12.	30	0.76	809.9	126.5	188.89	109.5	0.24	839.74	45.26
13.	32	0.76	851.9	72.9	119.86	74.5	0.14	863.58	40.87
14.	28	0.76	839.7	70.6	117.58	138.1	0.14	859.42	51.17
15.	30	0.76	872.2	51.3	148.79	99.6	0.17	890.90	41.72
16.	18	0.97	528.2	127.4	74.00	45.0	0.14	535.25	47.20
17.	30	0.97	830.3	73.6	220.42	119.3	0.26	867.22	43.00
18.	26	0.97	720.6	104.7	94.02	67.4	0.13	729.44	43.33
19.	28	0.97	869.6	80.9	155.99	131.1	0.18	892.99	39.93
20.	30	0.97	882.5	36.4	106.90	214.0	0.12	914.48	36.90
21.	18	1.20	486.9	41.7	98.56	43.2	0.20	498.30	46.78
22.	30	1.20	861.8	80.0	200.93	148.1	0.21	895.97	40.35
23.	18	1.20	673.7	117.0	163.62	103.5	0.24	701.12	39.57
24.	28	1.20	883.8	45.8	169.28	103.2	0.19	905.70	39.64
25.	30.5	1.20	888.0	22.6	88.26	98.5	0.10	897.97	42.41

L - Mean Values of longitudinal reaction
σ_x - Standard deviation of L
$\bar{V}$ - Mean value of vertical reaction
σ_v - Standard deviation of V
$\bar{\theta}$ - Mean Angle of resultant
RV - Mean value of resultant reaction
x - Distance of Rv below V2

Table 6. Results of field trials - average values of soil reaction, its orientation and location for 50 mm x 200 mm share

S.No.	Depth cm	Speed m/s	L Kg	σ_L Kg	V Kg	σ_V Kg	θ rad	RV Kg	x cm
1.	13	0.35	200.1	54.8	6.15	10.5	0.04	200.53	62.26
2.	16	0.35	319.4	37.0	90.84	50.7	0.27	334.71	50.56
3.	23	0.35	464.5	73.8	67.68	110.3	0.16	482.13	56.18
4.	23	0.35	405.8	42.7	142.90	34.2	0.34	431.14	51.50
5.	27	0.35	671.1	44.3	189.18	37.4	0.27	698.12	58.91
6.	13	0.44	265.9	69.6	72.11	42.2	0.27	279.45	53.98
7.	16	0.44	311.0	36.0	103.79	34.4	0.32	329.46	48.13
8.	23	0.44	411.9	71.0	106.57	38.7	0.25	426.61	54.50
9.	23	0.44	493.4	18.0	94.21	51.7	0.19	505.16	40.62
10.	27	0.44	711.4	92.9	143.76	53.7	0.20	728.07	37.70
11.	13	0.50	324.0	63.0	38.81	29.5	0.11	327.54	59.50
12.	16	0.50	305.9	40.2	78.21	57.4	0.24	320.44	50.96
13.	18	0.50	367.3	37.8	102.61	73.0	0.26	386.80	62.44
14.	20	0.50	423.4	6.7	106.93	47.1	0.24	439.04	76.28
15.	27	0.50	655.5	73.3	169.06	63.6	0.25	679.21	54.70
16.	13	0.67	232.7	44.7	35.36	30.8	0.16	237.76	57.95
17.	10	0.67	194.3	58.0	87.68	20.6	0.45	215.41	106.83
18.	23	0.67	591.3	61.1	163.55	41.5	0.27	615.15	34.82
19.	26	0.67	642.9	85.7	164.44	46.6	0.25	664.87	46.45
20.	27	0.67	736.4	89.0	172.21	82.63	0.23	760.38	42.30
21.	10	0.78	195.3	22.9	94.28	32.4	0.45	219.59	46.05
22.	16	0.78	410.1	60.1	122.42	35.5	0.29	429.50	58.57
23.	20	0.78	508.9	85.1	143.90	33.4	0.28	530.39	51.08
24.	23	0.78	571.1	93.3	104.93	53.9	0.18	582.87	62.08
25.	27	0.78	742.0	231.0	250.40	47.8	0.96	797.15	115.25

L - Mean Values of longitudinal reaction
σ_x - Standard deviation of L
V - Mean value of vertical reaction
σ_v - Standard deviation of V
θ - Mean Angle of resultant
RV - Mean value of resultant reaction
x - Distance of Rv below V2

Table 7. Results of field trials - average values of soil reaction, its orientation and location for 25 mm x 100 mm share

S.No.	Depth cm	Speed m/s	L Kg	σ_L Kg	V Kg	σ_V Kg	θ rad	RV Kg	x cm
1.	16	0.27	273.2	42.7	40.97	31.4	0.14	277.75	53.93
2.	20	0.27	382.4	37.0	42.24	44.8	0.10	386.58	49.68
3.	22	0.27	524.5	77.4	41.26	59.8	0.08	530.01	53.09
4.	25	0.27	560.1	90.8	78.67	38.1	0.14	567.05	48.71
5.	23	0.27	438.7	64.4	84.27	45.8	0.19	449.32	46.57
6.	16	0.55	334.0	66.9	43.34	54.6	0.11	339.75	54.20
7.	16	0.55	334.7	25.9	20.24	49.2	0.05	338.83	54.10
8.	22	0.55	516.0	97.3	92.72	61.7	0.17	527.20	50.22
9.	25	0.55	763.5	226.5	98.75	65.4	0.13	772.19	49.99
10.	22	0.55	502.3	66.1	97.35	47.2	0.19	514.05	54.10
11.	16	0.76	371.3	54.2	71.24	51.2	0.18	381.00	50.31
12.	20	0.76	417.3	71.1	33.06	44.3	0.08	421.13	58.69
13.	32	0.76	509.3	95.3	81.24	79.3	0.14	521.07	42.49
14.	26	0.76	858.6	198.7	137.47	59.7	0.17	873.03	47.11
15.	23	0.76	594.5	76.9	125.45	26.1	0.21	608.33	45.46
16.	17	0.97	398.9	38.3	60.90	42.7	0.15	405.81	50.95
17.	16	0.97	392.9	36.9	27.05	53.3	0.06	369.99	55.36
18.	20	0.97	480.1	68.5	56.42	61.3	0.11	486.80	52.68
19.	22	0.97	599.6	100.5	90.36	60.6	0.15	609.35	49.84
20.	21	0.97	517.1	42.8	99.21	40.5	0.19	528.16	49.06
21.	17	0.30	365.9	69.4	61.21	49.3	0.16	373.93	50.43
22.	18	0.30	392.5	32.4	20.45	50.2	0.05	396.19	53.75
23.	20	0.30	508.1	84.7	76.23	61.1	0.15	517.46	51.93
24.	19	0.30	466.2	33.8	46.63	109.7	0.09	479.47	53.75
25.	21	0.30	559.3	97.7	101.36	43.3	0.18	569.74	50.02

L - Mean Values of longitudinal reaction
σ - Standard deviation of L
V - Mean value of vertical reaction
σ_v - Standard deviation of V
θ - Mean Angle of resultant
RV - Mean value of resultant reaction
x - Distance of Rv below V2

Table 8. Results of field trials - average values of soil reaction, its orientation and location for 40 mm x 100 mm share

S.No.	Depth cm	Speed m/s	L Kg	σ_L Kg	V Kg	σ_V Kg	θ rad	RV Kg	x cm
1.	21	0.27	280.8	28.4	51.03	40.4	0.17	287.74	43.98
2.	25	0.27	292.3	69.4	74.31	36.2	0.25	303.99	51.16
3.	26	0.27	402.6	44.5	65.49	45.2	0.15	409.66	45.18
4.	27	0.27	469.5	70.6	90.01	41.1	0.18	480.05	45.72
5.	28	0.27	473.3	79.6	120.39	47.8	0.25	491.01	48.15
6.	24	0.55	333.6	56.6	53.77	45.4	0.16	341.54	49.05
7.	25	0.55	352.6	43.8	77.76	27.5	0.22	362.50	43.03
8.	27	0.55	519.3	46.2	138.27	47.0	0.25	538.68	41.92
9.	28	0.55	545.3	51.4	65.77	48.2	0.12	553.31	47.33
10.	28	0.55	509.5	36.3	107.94	61.1	0.20	523.59	37.03
11.	24	0.76	323.7	16.1	42.25	53.1	0.13	330.48	47.72
12.	25	0.76	348.2	74.3	96.29	63.4	0.27	366.83	42.40
13.	26	0.76	475.7	91.3	81.12	71.3	0.16	486.37	46.46
14.	24	0.76	404.5	36.8	81.82	50.1	0.19	415.04	47.03
15.	28	0.76	594.4	90.3	101.27	43.2	0.17	605.61	42.46
16.	24	0.97	408.6	67.9	90.57	49.1	0.21	421.04	43.51
17.	26	0.97	448.8	68.5	114.45	83.1	0.26	472.16	43.81
18.	27	0.97	532.2	111.9	91.60	25.9	0.18	541.04	42.95
19.	27	0.97	543.9	46.5	126.85	89.9	0.22	565.24	52.59
20.	28	0.97	545.4	19.5	64.20	80.2	0.11	554.41	43.93
21.	24	0.83	424.3	96.9	108.16	50.9	0.25	439.55	44.90
22.	25	0.83	433.8	73.4	110.83	91.0	0.24	454.52	42.95
23.	26	0.83	555.6	81.5	152.86	51.4	0.26	577.41	41.40
24.	27	0.83	547.5	84.0	109.51	59.6	0.20	562.25	44.99
25.	28	0.83	652.9	98.1	92.02	36.2	0.14	660.47	46.50

L - Mean Values of longitudinal reaction
σ - Standard deviation of L
$\bar{V}$ - Mean value of vertical reaction
σ_v - Standard deviation of V
$\bar{\theta}$ - Mean Angle of resultant
RV - Mean value of resultant reaction
x - Distance of Rv below V2

Table 9. Results of field trials - average values of soil reaction, its orientation and location for 20 mm x 200 mm share

S.No.	Depth cm	Speed m/s	L Kg	σ_L Kg	V Kg	σ_V Kg	θ rad	RV Kg	x cm
1.	19	0.27	301.7	0.0	202.30	21.7	0.59	363.71	32.81
2.	20	0.27	400.2	0.0	246.26	80.3	0.54	474.01	29.80
3.	25	0.27	531.7	96.1	296.84	58.8	0.52	613.09	32.80
4.	25	0.27	543.8	96.4	297.50	60.3	0.50	621.35	32.08
5.	32	0.27	682.1	101.0	417.89	110.4	0.54	803.24	32.04
6.	19	0.50	328.5	0.0	175.09	31.3	0.49	373.26	36.94
7.	15	0.50	272.5	0.0	198.00	35.0	0.62	338.06	30.83
8.	25	0.50	500.0	39.5	272.23	79.3	0.49	571.60	35.24
9.	26	0.50	577.5	48.2	330.10	108.5	0.51	670.90	43.86
10.	38	0.50	613.8	45.9	393.16	41.9	0.57	729.08	33.08
11.	19	0.66	312.4	40.8	236.93	50.7	0.65	394.57	30.55
12.	20	0.66	366.4	39.2	234.23	96.2	0.54	441.75	32.00
13.	25	0.66	478.9	49.2	293.46	81.3	0.54	564.29	27.24
14.	27	0.66	690.0	118.8	331.41	40.3	0.45	767.59	35.98
15.	30	0.66	632.9	41.5	370.34	48.4	0.53	734.72	26.75
16.	19	0.89	443.1	72.3	282.63	81.0	0.56	526.74	32.07
17.	20	0.89	496.1	10.3	310.70	28.7	0.56	585.67	37.04
18.	25	0.89	578.5	74.6	403.54	60.3	0.61	709.89	28.63
19.	26	0.89	654.4	44.8	267.26	24.4	0.39	707.85	35.06
20.	32	0.89	780.8	105.1	330.13	75.1	0.40	850.41	36.61
21.	19	1.07	408.3	76.5	285.37	45.7	0.62	500.86	32.65
22.	20	1.07	484.9	59.5	271.51	83.7	0.50	559.29	31.90
23.	25	1.07	598.2	95.0	319.04	36.5	0.47	705.70	37.61
24.	27	1.07	628.9	78.7	319.04	36.5	0.47	705.70	37.61
25.	25	1.07	685.3	72.5	383.85	97.3	0.50	789.06	32.97

L - Mean Values of longitudinal reaction
σ_x - Standard deviation of L
V - Mean value of vertical reaction
σ_v - Standard deviation of V
θ - Mean Angle of resultant
RV - Mean value of resultant reaction
x - Distance of Rv below V2

Table 10. Results of field trials - average values of soil reaction, its orientation and location for 40 mm x 150 mm share

S.No.	Depth cm	Speed m/s	L Kg	σ_L Kg	V Kg	σ_V Kg	θ rad	RV Kg	x cm
1.	14	0.27	224.4	0.0	15.35	4.8	0.07	224.97	52.77
2.	20	0.27	389.9	9.1	58.51	40.0	0.15	396.22	46.81
3.	25	0.27	508.0	110.6	91.84	93.6	0.17	523.33	42.30
4.	27	0.27	570.3	67.4	145.15	71.2	0.25	593.39	76.30
5.	30	0.27	737.0	167.9	96.46	42.7	0.14	744.82	41.22
6.	15	0.55	283.5	61.4	30.67	30.7	0.10	286.43	52.21
7.	19	0.55	368.4	53.0	75.58	141.0	0.19	402.00	50.12
8.	20	0.55	439.4	18.0	57.04	53.1	0.13	446.08	50.93
9.	22	0.55	473.0	3.6	105.25	67.6	0.21	489.00	43.88
10.	24	0.55	499.0	13.6	89.82	48.4	0.18	509.27	46.05
11.	19	0.76	386.0	25.7	57.33	25.9	0.15	390.99	49.18
12.	22	0.76	512.7	46.5	62.44	90.1	0.11	523.21	44.77
13.	20	0.76	397.1	15.7	56.15	69.0	0.13	406.11	49.03
14.	22	0.76	454.2	41.5	139.48	77.9	0.29	481.17	40.68
15.	22	0.76	459.0	14.1	147. 30	75.6	0.30	486.90	41.86
16.	15	0.97	355.0	6.1	71.97	102.1	0.18	374.91	52.86
17.	15	0.97	344.5	3.7	38.20	43.7	0.11	349.29	49.90
18.	20	0.97	467.0	76.4	61.62	67.0	0.14	475.34	47.82
19.	27	0.97	602.5	83.8	122.08	83.0	0.22	622.56	37.25
20.	30	0.97	698.0	87.6	76.50	0.0	0.11	702.24	43.67
21.	19	0.83	446.7	81.5	91.35	77.0	0.19	461.50	51.88
22.	14	0.83	335.5	7.5	50.42	53.6	0.14	343.25	49.96
23.	27	0.83	677.1	157.4	115.68	96.5	0.15	692.39	40.70
24.	25	0.83	604.3	27.3	134.41	128.0	0.21	630.73	39.44

L - Mean Values of longitudinal reaction
σ - Standard deviation of L
V - Mean value of vertical reaction
σ_v - Standard deviation of V
θ - Mean Angle of resultant
RV - Mean value of resultant reaction
x - Distance of Rv below V2

Table 11. Results of field trials - average values of soil reaction, its orientation and location for 50 mm x 150 mm share

S.No.	Depth cm	Speed m/s	L Kg	σ_L Kg	V Kg	σ_V Kg	θ rad	RV Kg	x cm
1.	20	0.20	403.8	75.0	86.09	84.6	0.21	421.16	44.07
2.	23	0.20	491.4	93.5	136.72	85.2	0.26	514.59	44.53
3.	23	0.20	414.1	65.6	132.79	93.2	0.29	441.06	40.73
4.	32	0.20	684.9	212.8	146.41	84.1	0.29	709.87	46.20
5.	26	0.20	622.86	68.9	206.18	65.7	0.32	659.40	43.65
6.	18	0.45	375.3	47.7	36.75	27.0	0.10	378.10	46.66
7.	13	0.45	241.7	21.3	72.43	18.5	0.29	253.25	44.72
8.	23	0.45	467.9	46.5	154.73	109.3	0.30	504.02	40.46
9.	26	0.45	642.9	71.0	220.54	57.7	0.33	681.70	52.34
10.	23	0.45	533.7	79.9				562.00	42.11
11.	13	0.40	274.5	40.6	36.53	19.5	0.14	277.86	49.52
12.	12	0.40	254.2	22.0	101.37	36.8	0.38	276.55	44.54
13.	18	0.40	415.8	80.7	109.29	145.1	0.21	446.18	43.73
14.	23	0.40	501.2	123.4	116.94	71.8	0.22	517.47	51.85
15.	26	0.40	637.0	141.1	217.97	56.5	0.33	675.86	44.84
16.	13	0.89	247.0	65.9	63.78	18.8	0.27	256.48	47.95
17.	15	0.89	346.4	33.7	121.42	35.3	0.34	368.56	41.16
18.	18	0.89	451.4	124.6	153.70	77.5	0.33	482.11	41.87
19.	32	0.89	928.9	346.4	370.60		0.38	1000.10	27.97
20.	23	0.89	617.8	93.3	218.36	88.7	0.33	659.97	44.30
21.	12	0.80	228.3	3.9	69.70	4.3	0.30	238.68	45.95
22.	15	0.80	390.0	52.8	141.37	78.5	0.33	420.63	40.92
23.	15	0.80	324.2	43.5	117.62	35.3	0.35	347.39	56.01
24.	23	0.80	654.3	141.1	308.14	48.0	0.45	727.52	42.69
25.	25	0.80	700.2	149.6	216.31	58.9	0.31	737.11	40.00

L - Mean Values of longitudinal reaction
σ_L - Standard deviation of L
$\bar{V}$ - Mean value of vertical reaction
σ_v - Standard deviation of V
$\bar{\theta}$ - Mean Angle of resultant
RV - Mean value of resultant reaction
x - Distance of Rv below V2

Table 12. Results of field trials - average values of soil reaction, its orientation and location for 20 mm x 150 mm share

S.No.	Depth cm	Speed m/s	L Kg	σ_L Kg	V Kg	σ_V Kg	θ rad	RV Kg	x cm
1.	13	0.26	180.4	46.1	23.02	39.3	0.11	185.98	65.51
2.	20	0.26	271.1	43.9	88.42	29.1	0.32	286.86	39.59
3.	24	0.26	391.6	58.1	160.17	93.6	0.36	428.81	48.72
4.	28	0.26	416.1	67.0	142.26	42.3	0.34	422.63	40.23
5.	23	0.26	588.8	99.5	361.55	66.1	0.56	695.04	34.78
6.	10	0.45	123.5	43.1	-0.15	29.6	0.00	127.36	66.58
7.	13	0.45	196.9	29.8	66.59	7.2	0.33	208.30	63.35
8.	20	0.45	336.1	33.2	122.77	71.7	0.34	362.74	42.32
9.	26	0.45	529.4	117.1	303.57	106.2	0.53	621.91	40.72
10.	25	0.45	490.2	83.3	314.72	73.0	0.57	586.37	42.80
11.	10	0.40	131.9	57.5	2.20	42.1	0.06	139.26	64.09
12.	20	0.40	353.5	108.9	129.15	69.9	0.34	379.27	44.52
13.	23	0.40	406.6	95.2	82.72	140.3	0.16	432.54	43.58
14.	25	0.40	462.0	106.6	103.47	82.1	0.22	478.42	44.09
15.	25	0.40	492.1	71.1	288.72	100.0	0.53	580.17	51.82
16.	13	0.44	229.3	61.2	4.61	44.9	-0.01	233.44	62.35
17.	20	0.44	330.7	75.1	116.31	79.9	0.30	355.08	37.84
18.	23	0.44	391.5	106.3	272.47	56.3	0.62	479.50	40.73
19.	24	0.44	466.5	116.6	190.46	51.2	0.39	505.74	48.72
20.	25	0.44	479.3	286.2	202.82	67.93	0.58	550.11	28.62
21.	13	0.80	201.4	56.8	8.66	46.2	0.03	206.64	63.93
22.	26	0.80	539.2	188.7	166.03	80.9	0.33	572.49	39.29
23.	20	0.80	390.5	64.6	119.72	72.6	0.29	413.07	50.93
24.	26	0.80	584.6	102.1	268.92	155.8	0.42	664.75	49.33
25.	25	0.80	531.4	96.8	296.46	72.2	0.51	612.58	42.12

L - Mean Values of longitudinal reaction
σ_x - Standard deviation of L
$\bar{V}$ - Mean value of vertical reaction
σ_v - Standard deviation of V
$\bar{\theta}$ - Mean Angle of resultant
RV - Mean value of resultant reaction
x - Distance of Rv below V2

Table 13. Results of field trials - average values of soil reaction, its orientation and location for 30 mm x 100 mm share

S.No.	Depth cm	Speed m/s	L Kg	σ_L Kg	V Kg	σ_V Kg	θ rad	RV Kg	x cm
1.	16	0.27	256.2	29.0	-49.82	19.0	-0.19	261.78	60.45
2.	17	0.27	229.7	40.6	16.38	31.7	0.07	232.40	52.37
3.	23	0.27	397.1	61.2	38.33	77.9	0.08	405.07	43.53
4.	21	0.27	425.4	75.8	37.86	54.5	0.09	430.45	46.50
5.	26	0.27	596.5	54.5	89.74	53.9	0.15	605.73	44.92
6.	16	0.55	257.5	27.2	-13.32	37.5	-0.05	260.29	55.10
7.	17	0.55	255.0	41.6	37.73	30.3	0.14	259.26	44.68
8.	29	0.55	435.5	87.5	65.03	32.2	0.14	440.97	41.25
9.	22	0.55	449.2	105.7	8.59	46.5	0.02	451.66	48.20
10.	23	0.55	456.1	119.8	9.20	45.5	0.01	458.30	39.96
11.	16	0.76	253.5	43.6	-16.11	32.9	-0.07	256.12	60.46
12.	17	0.76	278.8	84.1	-8.88	24.5	-0.03	279.81	53.50
13.	22	0.76	453.2	98.3	50.32	72.5	0.10	460.97	42.63
14.	24	0.76	588.4	109.5	40.45	73.6	0.06	593.55	47.49
15.	26	0.76	655.9	109.3	119.07	44.2	0.18	667.71	42.51
16.	16	0.97	259.9	30.0	14.73	40.7	0.05	263.39	51.94
17.	19	0.97	344.3	68.5	-7.21	85.4	-0.03	353.53	45.89
18.	23	0.97	599.9	68.6	90.43	46.9	0.15	609.14	47.78
19.	26	0.97	678.3	41.5	158.06	48.8	0.23	698.06	36.91
20.	26	0.97	874.2	68.1	159.02	42.13	0.18	889.34	36.11
21.	14	1.20	213.2	82.9	33.37	29.6	0.18	218.17	56.78
22.	19	1.20	342.3	57.7	13.43	36.3	0.03	344.42	45.05
23.	22	1.20	501.0	124.0	101.06	130.4	0.17	522.68	40.42
24.	24	1.20	693.5	106.2	147.08	78.6	0.20	711.92	42.34
25.	26	1.20	739.6	128.3	96.34	70.4	0.12	748.15	38.81

L - Mean Values of longitudinal reaction
σ_L - Standard deviation of L
V^x - Mean value of vertical reaction
σ_v - Standard deviation of V
θ^v - Mean Angle of resultant
RV - Mean value of resultant reaction
x - Distance of Rv below V2

Table 14. Results of field trials - average values of soil reaction, its orientation and location for 25 mm x 200 mm share

S.No.	Depth cm	Speed m/s	L Kg	σ_L Kg	V Kg	σ_V Kg	θ rad	RV Kg	x cm
1.	22	0.27	219.6	57.4	56.00	40.5	0.25	230.00	50.71
2.	21	0.27	270.2	61.2	76.93	54.9	0.31	286.93	38.77
3.	26	0.27	578.5	123.1	146.32	72.8	0.25	600.45	49.37
4.	30	0.27	680.7	67.9	224.94	65.2	0.32	719.78	44.17
5.	32	0.27	742.2	84.8	180.98	53.1	0.24	766.20	47.31
6.	20	0.37	204.7	51.2	19.93	27.6	0.09	207.17	55.31
7.	22	0.37	235.8	27.3	62.10		0.26	243.99	47.41
8.	30	0.37	623.7	106.1	185.72	95.4	0.25	712.07	41.39
9.	32	0.37	794.7	74.8	228.62	95.8	0.28	832.49	40.93
10.	30	0.37	642.7	139.4	194.21	74.3	0.31	677.53	47.23
11.	21	0.88	279.6	67.3	48.68	72.5	0.18	291.62	49.54
12.	25	0.88	246.5	39.6	67.84	35.6	0.27	257.85	48.34
13.	30	0.88	707.1	102.6	258.37	92.3	0.35	756.95	34.20
14.	31	0.88	792.7	138.4	271.57	20.3	0.34	839.85	39.90
15.	30	0.88	740.7	99.5	211.62	58.6	0.28	772.90	44.20
16.	20	0.97	227.6	50.2	21.70	51.6	0.13	234.61	46.79
17.	21	0.97	294.4	74.1	74.83	24.3	0.25	304.60	47.55
18.	26	0.97	639.2	146.2	141.36	103.1	0.20	660.85	39.53
19.	28	0.97	697.3	27.5	245.85	90.3	0.33	743.91	39.87
20.	29	0.97	687.0	99.6	204.08	96.7	0.29	723.86	42.12
21.	20	1.20	227.8	73.3	52.41	92.5	0.19	246.57	49.98
22.	21	1.20	370.7	90.8	93.70	55.6	0.25	387.19	48.17
23.	26	1.20	489.3	107.1	119.10	47.7	0.25	506.49	47.85
24.	28	1.20	681.7	105.5	255.88	67.4	0.36	731.26	40.65
25.	30	1.20	738.4	128.3	236.20	32.2	0.32	776.56	50.96

L - Mean Values of longitudinal reaction
σ_L - Standard deviation of L
$\bar{V}$ - Mean value of vertical reaction
σ_V - Standard deviation of V
$\bar{\theta}$ - Mean Angle of resultant
RV - Mean value of resultant reaction
x - Distance of Rv below V2

Table 15. Results of field trials - average values of soil reaction, its orientation and location for 50 mm x 100 mm share

S.No.	Depth cm	Speed m/s	L Kg	σ_L Kg	V Kg	σ_V Kg	θ rad	RV Kg	x cm
1.	13	0.25	200.3	26.0	3.54	35.0	0.02	203.40	52.57
2.	22	0.25	466.0	98.1	163.90	79.9	0.33	496.78	48.21
3.	23	0.25	512.2	60.0	222.90	67.1	0.40	560.76	39.96
4.	26	0.25	670.8	101.3	214.49	61.7	0.31	707.53	44.61
5.	27	0.25	612.9	144.7	266.23	75.7	0.43	675.59	52.82
6.	13	0.55	209.1	42.3	-7.00	38.2	-0.02	212.48	57.89
7.	15	0.55	268.5	83.3	125.63	59.2	0.45	301.19	42.18
8.	23	0.55	583.1	125.1	267.11	119.2	0.42	648.71	48.13
9.	23	0.55	528.5	118.2	168.76	89.3	0.31	562.47	50.43
10.	27	0.55	722.0	108.3	254.49	111.6	0.34	773.95	38.82
11.	13	0.76	217.4	37.2	0.11	28.6	-0.01	219.34	59.74
12.	15	0.76	251.2	73.2	108.94	34.6	0.42	276.10	44.53
13.	26	0.76	696.3	53.9	260.60	83.9	0.35	746.98	37.45
14.	20	0.76	449.3	85.0	113.94	122.5	0.22	475.78	49.46
15.	27	0.76	712.9	117.7	197.31	118.6	0.28	751.81	45.03
16.	13	0.97	246.3		32.00	00.00	0.13	248.3	757.86
17.	15	0.97	285.4	95.2	124.05	41.0	0.44	316.55	41.85
18.	26	0.97	717.7	148.5	216.12	121.9	0.31	763.44	37.95
19.	22	0.97	519.6	76.2	183.35	132.4	0.32	564.59	44.31
20.	23	0.97	579.2	85.5	198.03	97.4	0.32	617.50	36.75
21.	13	1.20	312.3	46.5	79.57	80.9	0.25	331.88	51.91
22.	15	1.20	320.8	57.5	43.72	38.3	0.13	325.95	26.39
23.	18	1.20	388.5	67.4	142.66	50.9	0.35	416.39	38.09
24.	18	1.20	397.8	42.1	135.86	41.0	0.33	422.04	41.10
25.	23	1.20	583.6	115.8	236.46	68.4	0.39	633.55	46.70

L - Mean Values of longitudinal reaction
σ_x - Standard deviation of L
V - Mean value of vertical reaction
σ_v - Standard deviation of V
θ - Mean Angle of resultant
RV - Mean value of resultant reaction
x - Distance of Rv below V2

APPENDIX - E

FURROW GEOMETRY

S.No.	Depth cm	Furrow area cm^2	Furrow width cm	S.No.	Depth cm	Furrow area cm^2	Furrow width cm
Share size 20 x 100				Share size 30 x 100			
1.	0	0	0	1.	0	0	0
2.	12	200	34	2.	13	174	28
3.	20	386	42	3.	17	340	63
4.	12	210	33	4.	18	331	44
5.	19	340	31	5.	25	392	34
6.	17	338	40	6.	16	234	33
7.	13	158	20	7.	17	340	35
8.	17	206	26	8.	27	612	64
9.	21	480	57	9.	22	457	49
10.	19	365	46	10.	26	616	48
11.	19	304	30	11.	26	665	54
12.	23	546	51				
13.	24	376	29				
Share size 25 x 100				Share size 40 x 100			
1.	0	0	0	1.	0	0	0
2.	16	169	36	2.	20	326	41
3.	17	360	58	3.	14	165	33
4.	21	498	59	4.	19	321	36
5.	17	343	57	5.	17	207	33
6.	21	320	37	6.	21	290	34
7.	21	390	47	7.	19	281	45
8.	19	457	54	8.	17	335	42
9.	21	490	56	9.	21	395	44
10.	22	492	56	10.	22	460	52
11.	23	510	57	11.	20	320	45
12.	25	595	57	12.	22	430	49
13.	25	530	53	13.	21	380	54
14.	24	524	54	14.	19	360	51
15.	22	392	59	15.	24	423	43
16.	24	543	49				
17.	23	416	46				

S.No.	Depth cm	Furrow area cm^2	Furrow width cm	S.No.	Depth cm	Furrow area cm^2	Furrow width cm
Share size 50 x 100				Share size 20 x 150			
1.	0	0	0	1.	0	0	0
2.	22	286	29	2.	13	184	42
3.	14	175	39	3.	21	515	64
4.	17	320	41	4.	20	311	44
5.	17	253	33	5.	21	417	64
6.	22	472	47	6.	20	378	52
7.	25	450	41	7.	20	540	63
8.	24	522	53	8.	22	635	62
9.	24	691	63	9.	25	570	50
10.	27	571	61	10.	25	655	63
11.	26	478	39	11.	27	611	63
12.	28	732	60				
Share size 25 x 150				Share size 30 x 150			
1.	0	0	0	1.	0	0	0
2.	18	287	30	2.	14	200	40
3.	17	373	33	3.	20	312	43
4.	19	410	47	4.	14	282	47
5.	21	522	44	5.	19	200	40
6.	24	573	44	6.	22	440	54
7.	21	535	44	7.	29	420	53
8.	26	668	50	8.	25	525	54
9.	30	765	46	9.	24	585	51
10.	30	660	47	10.	21	635	47
11.	21	410	35				
12.	20	400	56				
13.	32	620	48				
14.	20	300	51				
15.	25	525	55				
16.	28	795	53				
17.	26	676	59				
18.	29	716	60				

S.No.	Depth cm	Furrow area cm^2	Furrow width cm	S.No.	Depth cm	Furrow area cm^2	Furrow width cm
Share size 40 x 150				Share size 50 x 150			
1.	0	0	0	1.	0	0	0
2.	15	402	58	2.	14	183	30
3.	19	417	52	3.	13	218	48
4.	20	400	51	4.	24	541	51
5.	20	362	44	5.	15	311	49
6.	20	438	60	6.	23	380	44
7.	22	434	40	7.	22	422	38
8.	28	571	61	8.	27	485	47
9.	29	710	61	9.	33	703	61
10.	29	588	54	10.	24	721	52
11.	30	806	60				
Share size 20 x 200				Share size 25 x 200			
1.	0	0	0	1.	0	0	0
2.	20	330	50	2.	23	500	55
3.	21	413	46	3.	22	391	52
4.	23	460	50	4.	21	363	39
5.	19	277	36	5.	22	461	41
6.	26	592	59	6.	27	720	56
7.	26	594	58	7.	26	724	62
8.	32	522	40	8.	29	729	61
9.	26	522	52	9.	32	965	59
10.	33	711	55	10.	33	878	60
11.	22	384	38				

S.No.	Depth cm	Furrow area cm^2	Furrow width cm	S.No.	Depth cm	Furrow area cm^2	Furrow width cm
Share size 30 x 200				Share size 40 x 200			
1.	0	0	0	1.	0	0	0
2.	23	440	36	2.	14	135	32
3.	21	465	56	3.	14	246	43
4.	21	570	61	4.	17	255	38
5.	23	546	60	5.	16	278	40
6.	30	718	62	6.	19	265	32
7.	28	560	57	7.	21	217	39
8.	29	756	55	8.	19	393	38
9.	27	709	58	9.	22	375	39
10.	29	608	60	10.	23	527	52
11.	28	655	61	11.	19	256	40
12.	28	607	62	12.	25	646	60
13.	33	897	62	13.	23	553	60
14.	28	535	60	14.	27	745	62
Share size 50 x 200							
1.	0	0	0				
2.	16	180	27				
3.	14	293	40				
4.	14	300	45				
5.	25	555	60				
6.	18	290	43				
7.	21	470	59				
8.	26	654	60				
9.	31	718	62				
10.	27	715	56				
11.	26	583	48				
12.	28	664	51				
13.	28	594	59				
14.	24	555	61				
15.	25	564	62				
16.	27	724	59				
17.	24	500	46				
18.	30	730	63				

APPENDIX F

COST OF OPERATION

a. Fixed cost

Equipment (capital cost)	Tractor (Rs. 1,80,000)	Chisel plough (Rs. 5,000)	Disc plough (Rs. 15,000)
Interest @18%	Rs. 32,400	Rs. 900	Rs. 2700
Depreciation	Rs. 16,200	Rs. 450	Rs. 1,350
Taxes	Rs. 1,800	–	–
Repair and Maintenance	Rs. 8,100	Rs. 300	Rs. 500
Total	Rs. 58,500	Rs. 1,650	Rs. 4,500
Yearly use in hr.	1,000	200	500
Fixed cost/hr	Rs. 58.5	Rs. 8.25	Rs. 9.1

b. Hourly cost of operation	Chisel plough	Disc plough
Fixed cost	66.75	67.60
Wages @ Rs. 80/8hrs.	10.00	10.00
Cost of fuel @ Rs. 8/l.	33.60	43.68
Total	110.35	121.28

c. Cost of operation	Chisel plough	Disc plough
Coverage	0.42 ha/hr	0.167 ha/hr.
Cost of operation	Rs. 265/ha	Rs. 725/ha